Activation of Kv7.4 in the cochlea as a therapeutic approach in a mouse model of age-related hearing loss

Dissertation

der Mathematisch-Naturwissenschaftlichen Fakultät

der Eberhard-Karls-Universität Tübingen

zur Erlangung des Grades eines

Doktors der Naturwissenschaften

(Dr. rer. nat.)

vorgelegt von

Eva Barbara Peixoto Pinheiro

aus Stuttgart

Tübingen

2022

Gedruckt mit Genehmigung der Mathematisch-Naturwissenschaftlichen Fakultät der Eberhard Karls Universität Tübingen.

Tag der mündlichen Qualifikation:	19.01.2023
Dekan:	Prof. Dr. Thilo Stehle
1. Berichterstatter/-in:	Prof. Dr. Andreas Nieder
2. Berichterstatter/-in:	Prof. Dr. Hubert Löwenheim

Acknowledgements

An erster Stelle möchte ich mich bei Prof. Dr. Hubert Löwenheim herzlich bedanken für die Möglichkeit an diesem Projekt arbeiten zu dürfen, für die anregenden Diskussionen und die vielfältige Unterstützung.

Bei Prof. Marlies Knipper und Prof. Lukas Rüttiger möchte ich mich sehr herzlich für die immense Unterstützung und die stets offenen Türen bedanken.

Mein besonderer Dank geht an Dr. Marcus Müller und Dr. Michael Bös, die leider das Ende dieses Projektes nicht mehr miterleben konnten. Ich danke ihnen für die Möglichkeit an diesem Projekt mitwirken zu dürfen, für das geduldige Einarbeiten in die Methoden, die hervorragende Betreuung und die enorme Unterstützung bei Experimenten und Analysen.

Auch möchte ich mich besonders bei den derzeitigen und ehemaligen Mitgliedern der Arbeitsgruppe bedanken, vor allem bei Karina, Andrea, Stefan und Barbara. Danke, dass ihr immer ein offenes Ohr für mich hattet, für all die Gespräche, für den Rückenwind und die immense Unterstützung.

Ein großer Dank geht auch an die Mitarbeiter der Tierhaltung, die mir jederzeit tatkräftig zur Seite standen und mir einige Wochenenddienste erspart haben

Bei Karin möchte ich mich ganz herzlich für die enorme Unterstützung bei den Präparationen der Ohren, deren histologischen Aufarbeitung bedanken und natürlich auch für die Versorgung mit Süßem während der langen Wartezeiten am Mikroskop.

Vor allem möchte ich mich bei Philine und Alisha fürs gemeinsame Lachen und Weinen, unsere Kaffeepausen, die vielen aufmunternden Telefonanrufe und die immense Unterstützung bedanken.

Lieber Youssef – als Mitglieder der GFST Gruppe haben wir einiges durchgemacht. Und auch wenn du in Arbeit versunken bist, konnte ich jedes Mal bei dir ins Büro reinstampfen und meinen Frust, meine Freude, und alles Sonstige, dass mir durch den Kopf schwirrte bei dir rauslassen. Danke für alles! Ohne dich wäre diese Arbeit in dieser Form nicht zustande gekommen!

Ganz herzlich möchte ich mich auch bei meinen Eltern, meiner Schwester, Freunden und Thomas bedanken, die eine unfassbare Geduld aufgebracht haben und mich zu jedem Zeitpunkt meiner Promotion unterstützt haben.

Table of Contents

Abbreviations

ABR	auditory brainstem response
ARHL	age-related hearing loss
AUC	area under the curve
BK	large-conductance calcium-activated K^+ channel
BLB	brain-blood barrier
BMS-204352	Maxipost
Ca^{2+}	calcium ion
CAP	compound action potential
CSF	cerebrospinal fluid
DFNA2	deafness-associated autosomal locus 2
EC_{50}	half maximal effective concentration
EP	endocochlear potential
IHC	inner hair cells
$I_{K,n}$	K^+ conductance
K^+	potassium ions
KCNE1	potassium voltage-gated channel subfamily E member 1
KO	knock-out
$K_V7.1$	voltage-gated potassium channel of subfamily q, member 1, KCNQ1
$K_V7.4$	voltage-gated potassium channel of subfamily q, member 4, KCNQ4
LC-MS/MS	liquid chromatography with tandem mass spectrometry
LLOQ	lower limit of quantification
Na^+	sodium ions
OC	organ of corti
OHC	outer hair cells
postT	post-treatment
preT	pre-treatment
ROS	reactive oxygen species
RTG	retigabine
RWM	round window membrane
SAMP8	senescence accelerated mouse prone strain 8
SAMR1	senescence accelerated mouse resistant strain 1
SG	spiral ganglion
SGN	spiral ganglion neurons
SV	stria vascularis
TM	tympanic membrane
w/v	weight per volume
ZnP	zinc phyrithione

Summary

Age-related hearing loss (ARHL) is the largest contributor to the substantial hearing loss prevalence and is recognized as a significant factor in psychological and medical morbidity. There is thus a tremendous need for a safe and effective pharmacological treatment. The loss of auditory hair cells, consisting of outer hair cells (OHCs) and inner hair cells (IHCs), has been described as the major cochlear pathology of ARHL. The OHC physiology depends largely on functional potassium ion (K^+) recycling in the cochlea. One major component of the K^+ recycling circuit is the voltage-gated potassium channel of subfamily q, member 1 ($K_V7.1$), which is localized in the stria vascularis (SV). Loss of $K_V7.1$ has been associated with congenital deafness caused by impaired K^+ secretion. Furthermore, OHC survival is linked to the voltage-gated potassium channel of subfamily q, member 4 ($K_V7.4$), which dominantly determines their membrane potential. Impaired surface expression of $K_V7.4$ leads to functional impairment and has also been associated with ARHL. Although multiple chemical K_V7 channel openers have been developed as a therapeutic approach, their applicability has not yet been demonstrated in an *in vivo* model. The aim of the present study was to investigate the effect of pharmacological $K_V7.4$ channel activation in the senescence-accelerated mouse prone strain 8 (SAMP8) model as a novel therapeutic approach against ARHL. Surprisingly, we observed a significant threshold variability in the auditory decline of SAMP8 mice over age. In search of an underlying cause, age-related OHC loss could not be linked to this threshold variability. However, an altered $K_V7.4$ expression in OHCs was linked to the SAMP8 auditory threshold variability over age, preceding OHC loss. Pharmacological $K_V7.4$ channel activation by novel, small-molecule $K_V7.4$ agonists was then investigated in SAMP8 mice using different routes of administration: ACOU085 was locally via transtympanic application and ACOU082 was systemically administered via topical application. We demonstrated that the locally administered ACOU085 readily diffused into the cochlea and was able to significantly reduce age-related auditory threshold shifts as well as OHC loss in SAMP8 mice. Our findings in an *in-vivo* mouse model suggest that pharmacological activation of $K_V7.4$ is a promising approach to prevent and decelerate age-related decline of auditory function and morphological OHC loss linked to ARHL.

Zusammenfassung

Altersbedingte Schwerhörigkeit (ARHL) trägt am meisten zur hohen Prävalenz von Hörverlusten bei und wird als bedeutender Faktor für psychologische und medizinische Morbidität angesehen. Es besteht daher ein enormer Bedarf an einer sicheren und wirksamen pharmakologischen Behandlung. Der Verlust von Hörhaarzellen, bestehend aus äußeren Haarzellen (ÄHZ) und inneren Haarzellen (IHZ), wurde wiederholt als die wesentlichste Pathologie der Cochlea bei ARHL beschrieben. Die Physiologie der ÄHZ hängt weitgehend von einem funktionierenden Recycling der Kaliumionen (K^+) ab. Eine wichtige Komponente des K^+-Recyclingkreislaufs ist der spannungsabhängige Kaliumkanal der Unterfamilie q, Mitglied 1 ($K_V7.1$), der in der Stria vascularis (SV) lokalisiert ist. Ein Verlust von $K_V7.1$ wird mit angeborener Taubheit in Verbindung gebracht, die auf eine gestörte K^+-Sekretion zurückzuführen ist. Darüber hinaus wurde das Überleben der ÄHZ mit dem spannungsabhängigen Kaliumkanal der Unterfamilie q, Mitglied 4 ($K_V7.4$) in Verbindung gebracht, der ihr Membranpotenzial maßgeblich bestimmt. Eine gestörte Oberflächenexpression von $K_V7.4$ führt zu funktionellen Beeinträchtigungen und wurde auch mit ARHL in Verbindung gebracht. Obwohl bereits mehrere chemische K_V7-Kanalöffner entwickelt wurden, konnten deren Anwendbarkeit als Behandlungsansatz noch nicht in einem *in-vivo* Modell nachgewiesen werden. Das Ziel der vorliegenden Studie war es, die Wirkung einer pharmakologischen Aktivierung des $K_V7.4$-Kanals im Modell des seneszenzbeschleunigten Mäusestamms 8 (SAMP8) als neuen therapeutischen Ansatz für ARHL zu untersuchen. Überraschenderweise beobachteten wir eine signifikante Schwellenvariabilität im Hörverlust von SAMP8-Mäusen mit zunehmendem Alter. Auf der Suche nach einer zugrunde liegenden Ursache konnte der altersbedingte ÄHZ Verlust nicht mit dieser Schwellenvariabilität in Verbindung gebracht werden. Allerdings wurde eine veränderte $K_V7.4$-Expression in ÄHZ mit der altersbedingten Schwellenvariabilität der SAMP8-Mäuse in Verbindung gebracht, die dem ÄHZ Verlust vorausging. Die pharmakologische Aktivierung des $K_V7.4$-Kanals durch neuartige, niedermolekulare $K_V7.4$-Agonisten wurde dann in SAMP8-Mäusen auf verschiedenen Verabreichungswegen untersucht: ACOU085 wurde lokal über eine transtympanische Applikation und ACOU082 systemisch über eine topische Applikation verabreicht. Wir konnten zeigen, dass das lokal verabreichte ACOU085 leicht in die Cochlea diffundierte und in der Lage war, altersbedingte Hörschwellenverschiebungen sowie den ÄHZ Verlust bei SAMP8-Mäusen deutlich zu

reduzieren. Unsere Ergebnisse in einem *in-vivo* Mausmodell deuten darauf hin, dass die pharmakologische Aktivierung von $K_V7.4$ ein vielversprechender Ansatz ist, um den altersbedingten Rückgang der Hörfunktion und den morphologischen ÄHZ Verlust im Zusammenhang mit ARHL zu verhindern und zu verlangsamen.

List of Publications in the Thesis

a.) Accepted Papers

Peixoto Pinheiro, B., Vona, B., Löwenheim, H., Rüttiger, L., Knipper, M., Adel, Y. Age-related hearing loss pertaining to potassium ion channels in the cochlea and auditory pathway. *Pflügers Archive.* 2020 May, 473(5):823-840. (Review)

Peixoto Pinheiro, B., Adel, Y., Knipper, M., Müller, M., Löwenheim, H. Auditory Threshold Variability in the SAMP8 Mouse Model of Age-Related Hearing Loss: Functional Loss and Phenotypic Change Precede Outer Hair Cell Loss. *Frontiers in Aging Neuroscience.* 2021 Aug, 13:708190.

Peixoto Pinheiro, B., Müller, M. Bös, M., Guezguez J., Burnet, M., Tornincasa, M., Rizzetto, R., Rolland, J.-F., Liberati, C., Lohmer, S., Adel, Y.*, Löwenheim, H.*. 2022. A potassium channel agonist protects hearing function and promotes outer hair cell survival in a mouse model for age-related hearing loss. *Cell Death and Disease.* 2022.

**equal contribution*

Personal Contribution

In this section, I state my personal contributions to the publications presented in this thesis:

Peixoto Pinheiro, B., Vona, B., Lowenheim, H., Rüttiger, L., Knipper, M., Adel, Y. **Age-related hearing loss pertaining to potassium ion channels in the cochlea and auditory pathway**. *Pflügers Archive.* 2020 May, 473(5):823-840. (Review article)

Peixoto Pinheiro, B: My contribution to this work was to assist in the conception of the manuscript. Additionally, I performed the literature research, created and edited figures and contributed to the writing and editing of the manuscript.
Vona, B.: Contributed to the writing and editing of the manuscript.

Löwenheim, H.: Participated in the writing and editing of the manuscript.

Rüttiger, L.: Contributed to the writing and editing of the manuscript.

Knipper, M.: Devised the project and the main conceptual ideas and participated in the writing and editing of the manuscript.

Adel, Y: Assisted in the conception of the manuscript, participated in the creation and editing of figures and contributed to the writing and editing of the manuscript.

Peixoto Pinheiro, B., Adel, Y., Knipper, M., Müller, M., Löwenheim, H. **Auditory Threshold Variability in the SAMP8 Mouse Model of Age-Related Hearing Loss: Functional Loss and Phenotypic Change Precede Outer Hair Cell Loss**. *Frontiers in Aging Neuroscience.* 2021 Aug, 13:708190.

Peixoto Pinheiro, B: My contribution for this work was to assist in the study design and to review the technical requirements for the experiments. Furthermore, I performed measurements of auditory brainstem responses (ABRs) in all senescence-accelerated mouse prone 8 (SAMP8) mice at all ages and the corresponding statistical analysis. For the histological experiments, I extracted the cochlea and initiated preparations for whole-mount dissection and cochlear cross-section. Whole-mount preparation and generation of cochlear cross-sections, as well as staining, was accomplished with the assistance of technical assistants. I performed data analysis with the supervision and guidance of Dr. Youssef Adel and Prof. Hubert Löwenheim, such as threshold detection, hair cell counting and generation of cytochochleograms. Additionally, I

created and edited the figures and contributed to the writing and editing of the manuscript.

Adel, Y: Assisted in the study design and revision of the technical requirements for the experiments. YA supervised the study, was involved in statistical analyses, and helped creating and editing figures as well as writing and editing the manuscript.

Knipper, M: Helped with microscopic analysis of cochlear cross-sections, participated in research design and contributed to the writing of the manuscript.

Müller, M: Supervised conducting ABR measurements and histological experiments and participated in the research design.

Löwenheim, H: Participated in study design and supervised the data analysis of electrophysiological and histological experiments. HL contributed to writing the manuscript.

Peixoto Pinheiro, B**.**, Müller, M. Bös, M., Guezguez J., Burnet, M., Tornincasa, M., Rizzetto, R., Rolland, J.-F., Liberati, C., Lohmer, S., Adel, Y.*, Löwenheim, H*. **A potassium channel agonist protects hearing function and promotes outer hair cell survival in a mouse model for age-related hearing loss**. *Cell Death and Disease.* 2022.

Peixoto Pinheiro, B: My part in this work was to assist in the study design and to review the technical requirements for the experiments. Furthermore, I performed the measurements of ABRs and the administration of the compounds in all SAMP8 mice at all ages. For the histological experiments, I extracted the cochlea and initiated preparations for whole-mount dissection. Whole-mount preparation and staining were accomplished with the support of technical assistants. I performed data analysis with the supervision and guidance of Dr. Youssef Adel and Prof. Hubert Löwenheim, such as threshold detection, hair cell counting and generation of cytochochleograms. Additionally, I created and edited the figures and contributed to the writing and editing of the manuscript.

Müller, M: Conducted the experiments, performed data and statistical analyses, and contributed to the supervision and interpretation of the data.

Bös, M: Contributed to the supervision and interpretation of data.

Guezguez, J: Conducted the LC-MS/MS analysis in the pharmacokinetic study and contributed to the writing and editing of the manuscript.

Burnet, M: Conducted the LC-MS/MS analysis in the pharmacokinetic study and contributed to the revision and editing of the manuscript.

Tornincasa, M: Performed the in-vitro pharmacodynamic experiments and conducted the corresponding data analysis.

Rizzetto, R: Participated in the in-vitro pharmacodynamic experiments and conducted the corresponding data analysis.

Rolland, J-F: Assisted the in-vitro pharmacodynamic experiments and conducted the corresponding data analysis.

Liberati, C: Contributed to conceptualization of the study design and writing of the manuscript.

Lohmer, S: Participated in research design and contributed to conceptualization and writing of the manuscript

Adel, Y: Participated in the study design and revision of the technical requirements for the experiments. YA supervised the study, helped conduct the experiments, was involved in statistical analyses, and contributed to the creation and editing of figures as well as writing and editing the manuscript.

Löwenheim, H: Contributed to conceptualization and writing, supervised the experiments and data analyses. HL participated in the interpretation of the data and the writing, reviewing and editing of the manuscript.

1. Introduction

Hearing loss is the most prevalent form of sensory impairment in humans with over 1.57 billion affected individuals worldwide. According to the Global Burden of Disease study, it is the third largest contributor to years lived with disability, with age-related hearing loss (ARHL) ascertained as the leading impairment in the population older than 70 years compared with all other impairments (GBD Hearing Loss Collaborators, 2019). In industrialized countries, noise-induced acoustic trauma tends to be one of the main risk factors for hearing loss, however, a more prominent contributing factor continues to be aging. The underlying causes of ARHL include several environmental and polygenic factors that create a complex disorder (Géléoc and Holt, 2014; Wu et al., 2020). Almost everyone will develop some degree of hearing loss during their lifetime, and at least 50% will have moderate to profound hearing loss that requires intervention (GBD Hearing Loss Collaborators, 2019). Current treatment of ARHL is limited to prostheses (hearing aids) and implants (cochlear implants) that attempt to compensate for hearing loss. However, to date, a pharmacological treatment that enhances hearing function or delays the progression of hearing impairment in ARHL does not exist, so there remains a significant need for an appropriate causal treatment approach.

1.1 Age-related hearing loss

ARHL, also known as presbycusis, is the progressive loss of hearing sensitivity associated with aging and results from the cumulative effects of environmental and polygenetic factors on the auditory system (Bowl and Dawson, 2019). This complex disorder is defined as progressive, bilateral, symmetrical sensorineural hearing loss, particularly affecting the high frequencies (Bowl and Dawson, 2019). Due to its high prevalence, ARHL is a widespread social and healthcare problem. It is accompanied by impaired sound localization, reduced speech discrimination and decelerated central processing and (Frisina and Frisina, 1997; Frisina, 2001; Merchant and Nadol, 2010). Although ARHL is not life threatening, it is a key contributor to significant psychological and medical morbidity, including social isolation, cognitive decline and depression (Lin et al., 2011a; Lin et al., 2013; Kamil et al., 2016; Goman and Lin, 2018; Rutherford et al., 2018; Bowl and Dawson, 2019; GBD Hearing Loss Collaborators, 2019). In addition, it has also been identified as the single largest risk factor for dementia (Livingston et al., 2017; Chern and Golub, 2019; Livingston et al., 2020).

ARHL occurs in most mammals, including humans, with considerable variations in the age of onset, grade of hearing loss, magnitude and localization of cellular degeneration in the cochlea and the auditory pathway (Merchant and Nadol, 2010). ARHL arises in the cochlea (Keithley, 2019; Fischer et al., 2020; Tawfik et al., 2020) where the complex process of hearing takes place involving the transmission of sound through the middle ear to the cochlea, transduction of mechanical sound stimuli into electrical neuronal signals as well as transfer and process of this information to higher stages of the auditory pathway (Fettiplace and Hackney, 2006; Ashmore, 2008). The mammalian cochlea contains two categories of sensory hair cells arranged in rows along the organ of Corti (OC, Dallos, 1966; Pickles, 1988; Schwander et al., 2010). Inner hair cells (IHCs) are the primary sensory cells and transmit rapidly acoustic information via multiple ribbon synapses to the auditory neurons in the spiral ganglion (SG), whereas outer hair cells (OHCs) play an important role for amplification and frequency tuning. This sensory epithelium in the cochlea is mechanically tuned to high frequencies at the basal end and to low frequencies at the cochlear apex. Many forms of hearing loss, including ARHL, primarily affect the cochlear amplifier, including OHCs. Its nonlinear properties allow the inner ear to react to an extraordinarily wide range of sound intensities while preserving excellent frequency specificity (Gates and Mills, 2005). Patients suffering from ARHL primarily present a high-frequency hearing loss, which has adverse effects in communications, especially in noisy environments. With a progressive decline in hearing, the ability to detect, localize and identify sounds is impacted. At later stages of ARHL, hearing loss progresses to the low-frequency range, increasingly affecting speech understanding (Schuknecht and Gacek, 1993; Gates and Mills, 2005). ARHL is a complex disease composed of endogenous factors (Gates et al., 1999) as well as exogenous factors, primarily noise exposure that accumulates throughout life in modern societies (see chapter 1.1.1, Helzner et al., 2005; Wu et al., 2021). Device-related treatment including hearing aids and cochlear implants have the potential to ameliorate the symptoms but are not able to restore normal hearing (GBD Hearing Loss Collaborators, 2019). These devices have significant limitations for hearing rehabilitation, such as limited speech perception in noise, and thus, the development of new causal treatment strategies is of utmost importance.

1.1.1 Otopathology of age-related hearing loss

Otopathologic studies of postmortem human temporal bones have described different histopathologic features of ARHL. These features have been categorized into different types of ARHL, also known as the Schuhknecht typology. These categories were derived from quantitative otopathologic studies in serial histological sections of postmortem human temporal bones over a span of more than five decades that were correlated to life-time audiological measurements (Schuknecht, 1955; 1964; 1974; 1993; Schuknecht and Gacek, 1993; Merchant and Nadol, 2010). For the purpose of understanding the otopathology of presbycusis, a set of criteria has been established by Schuknecht and Gacek (1993) to categorize patterns of the multiple age-related changes of cellular cochlear elements and to classify them as distinct types of presbycusis. According to this model, presbycusis has been classified into sensory, strial, and neural presbycusis, or a combination thereof which is termed mixed presbycusis (Merchant and Nadol, 2010).

Sensory presbycusis

The loss of auditory hair cells, especially in the basal turn, has been repeatedly described as the major cochlear pathology of aging in humans (Crowe et al., 1934; Bredberg, 1967; Schuknecht and Gacek, 1993) and in various animal models (Bohne et al., 1990; Ohlemiller, 2004). The predominant pattern is loss of sensory auditory hair cells beginning in the basal turn of the cochlea. This pattern of hair cell loss correlates with a typical high-frequency hearing loss. A gradual reduction in outer hair cell density can be observed with age both in the base and to a lesser extent in the apex of the cochlea. The cellular loss in the apical turn apparently occurs at a later stage above the age of 70 years. For inner hair cells, the degenerative pattern is similar, although the quantitative decline is less pronounced (Wright et al., 1987). A recent comprehensive reanalysis of human temporal bones from the archival Schuknecht temporal bone collection based on a novel microscopic technique allowing for enhanced cellular resolution demonstrated that ARHL is best predicted by OHC and IHC loss, suggesting sensory presbycusis as the predominant type of ARHL in humans (Wu et al., 2020). In addition to sensory hair cell loss, other age-related yet unidentified factors may also contribute to ARHL (Wu et al., 2020). These factors are believed to impact the function of the cochlea at the cellular level before cytological evidence becomes apparent.

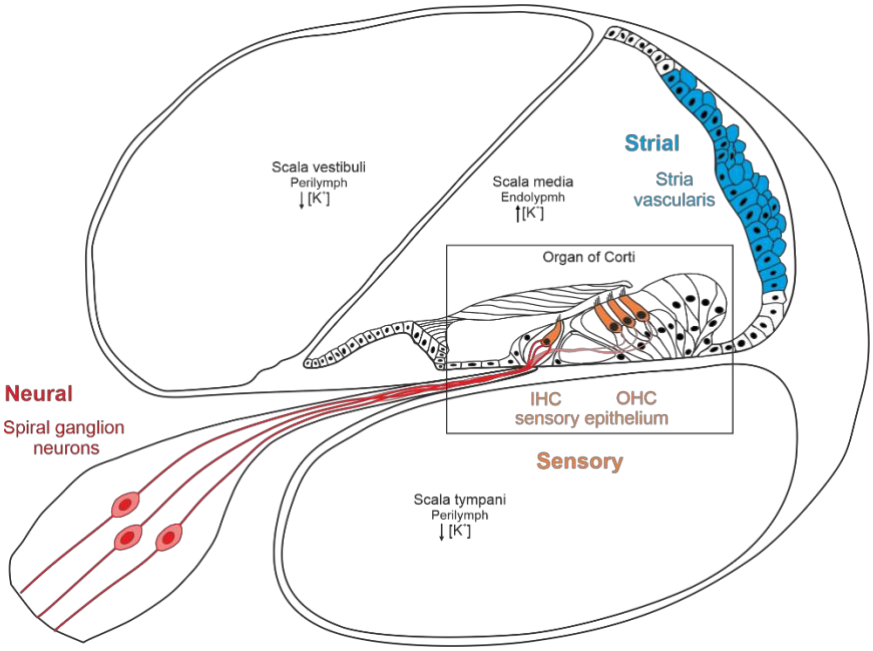

Figure 1: Schematic representation of a cochlear cross-section through a single coil of the cochlea spiral to show the main tissue areas of potential cellular degeneration in the aging cochlea (sensory, strial, neural). ARHL has been classified into sensory, strial, and neural presbycusis, or a combination of thereof is termed mixed presbycusis. The **sensory type** of ARHL was described as the loss of auditory hair cells primarily in the basal turn of the cochlea. The **strial type** of ARHL is characterized by cellular loss in the stria vascularis primarily in the apical turn. The **neural type** of ARHL has been described based on the loss of neuronal cell bodies in the spiral ganglion above the norm of spontaneous degeneration that occurs in this cell type.

Strial presbycusis

The stria vascularis (SV) is located in the lateral wall of the cochlear duct and plays an important role in ion transport, especially in releasing potassium (K^+) ions into the endolymphatic space. The cells of the SV generate the endocochlear potential (EP), which serves as an energy source for the hair cell conductance current and cochlear amplifier (Salt et al., 1987; Wangemann, 2006). The EP drives current into the hair cells once their transduction channels are mechanically opened by sound waves propagating through the cochlear fluid. Pathological degeneration of the SV has been observed and quantified in human temporal bones and represents a frequent pathology in ARHL (Schuknecht, 1974; Schuknecht and Gacek, 1993; Suzuki et al., 2006; Ishiyama et al., 2007; Kurata et al., 2016). In experimental models of ARHL cellular loss or functional inhibition of SV has been observed in human temporal bones and represents a major pathology, also termed metabolic presbycusis, with the

preceding cause being a reduction in the EP (Schulte and Schmiedt, 1992; Gratton et al., 1996; Schmiedt, 2010). The hair cell conductance current is carried by K^+ ions that are constantly recycled back to the SV after their passage through the hair cells (Spicer and Schulte, 1991; Schulte and Steel, 1994; Spicer and Schulte, 1996). The loss of the conduction current and the EP has the greatest effect on high-frequency hearing due to the reduced cochlear amplification which is driven by OHCs.

Neural presbycusis

Another common pathology of the aged inner ear is neural degeneration, both in humans (Johnsson and Hawkins, 1972; Schuknecht and Gacek, 1993; Felder and Schrott-Fischer, 1995) and in animals (Henry and Chole, 1980; Ohlemiller and Gagnon, 2004; Chen et al., 2006). In fact, the magnitude of neuronal loss exceeds that of IHC loss in humans and animals (Keithley and Feldman, 1979; Chen et al., 2006; Viana et al., 2015; Wu et al., 2019). In the mature mammalian cochlea, both IHCs and OHCs are afferently innervated by primary auditory neurons, termed spiral ganglion neurons (SGNs). However, the majority (> 90 %) of SGNs (Type I neurons) send a single peripheral axon to the IHCs through a single unmyelinated terminal dendrite (Liberman, 1980; Liberman et al., 1990; Stamataki et al., 2006). The remaining SGN population (Type II neurons) extend thin, unmyelinated fibers to innervate numerous OHCs. In the noise-damaged and aging ear, the connections between SGNs and IHCs, termed synaptic ribbons, degenerate first, rather than the IHCs themselves (Kujawa and Liberman, 2006). This noise-induced and age-related loss of synaptic connections between the afferent auditory-nerve fibers and IHCs has been established in animal models, but also found in human otopathology. In the aging human ear, a large number of auditory neurons are disconnected from the inner hair cell. Furthermore, Wu et al. (2019) have demonstrated that in humans neural loss greatly exceeds IHC loss by a relation of almost 3:1. This observation implies that neuronal degeneration is the primary event, while IHC loss remains secondary (Wu et al., 2019). This primary neural degeneration has a negligible effect on hearing thresholds until it exceeds 80% (Lobarinas et al., 2013). However, this deafferentation of IHCs, also known as “hidden hearing loss”, is suggested to compromise hearing ability in complex listening environments (Badri et al., 2011; Vermiglio et al., 2012; Wu et al., 2019).

1.1.2 Potential factors causing age-related hearing loss

ARHL is sometimes considered to be a part of the natural aging process, however, the decline in hearing is not similar in all humans. This indicates that cumulative effects of extrinsic environmental factors, such as noise exposure, and intrinsic factors, such as genetic predisposition or oxidative stress, can modulate the progression of ARHL (Yamasoba et al., 2013; Yang et al., 2015). Pure-tone audiograms of individuals suffering from ARHL initially present hearing loss in the high frequencies, which are processed in the basal turn of the cochlea. As presbycusis progresses, hearing loss spreads further to the low frequencies, toward the apical turn of the cochlea. Aging and noise exposure have been associated with the development of hearing loss in the elderly population (World Health Organization, 2021). Previous studies have even reported that noise exposure during aging can result in an acceleration of ARHL (Gates and Mills, 2005; Kujawa and Liberman, 2006; Bielefeld et al., 2010; Fetoni et al., 2011; Fernandez et al., 2015; Fetoni et al., 2022). Animal studies found that animals raised in quiet environments still display OHC loss in the basal turn, however, to a lesser magnitude (Liberman and Kiang, 1978; Keithley and Feldman, 1982; Tarnowski et al., 1991). Kujawa and Liberman (2006) discovered that noise exposure at young ages resulted in an increased hearing loss at older ages accompanied by synaptic damage (synaptopathy) at the synaptic terminal between IHC and SGNs, causing a loss of peripheral processes and neuronal cell bodies despite the absence of IHC degeneration (Kujawa and Liberman, 2006; 2009; Lin et al., 2011a; Sergeyenko et al., 2013; Valero et al., 2017). This phenomenon has been termed “hidden hearing loss”. The experimental data in laboratory mammals, and human temporal bone findings (Viana et al., 2015; Wu et al., 2019), support the interpretation that noise exposure at young age has the potential to damage the IHC synapse and potentially accelerate the progression of ARHL.

Heritability studies suggest that a genetic predisposition to ARHL provides an explanation for the observed variability regarding age of onset or grade of hearing loss (Trpchevska et al., 2022). The Framingham Heart Study concluded that approximately 55% of the variance in auditory thresholds in aged siblings and parent-child relations have a genetic association (Gates et al., 1999). Evaluation of mouse studies support the notion of genetic predisposition to ARHL (Erway et al., 1993; Johnson et al., 1997; Zheng and Johnson, 2001; Noben-Trauth et al., 2003; Keithley et al., 2004). Most of the candidate genes involved in ARHL in animal studies have been linked to defects

in hair bundle formation (e.g. tip-link component cadherin 23, Johnson et al., 1997), hair cell maintenance (e.g., potassium channels) and sensory transduction (e.g., transmembrane channel-like 1, (e.g. transmembrane channel-like 1, Kawashima et al., 2011; Beurg et al., 2021). The various combinations of inner ear pathologies, each with a potentially different etiology and genetic component, make it difficult to pinpoint a combination or relevant pathogenic variants in potentially numerous genes that account for the susceptibility to ARHL (Lewis et al., 2018). Twin studies for ARHL have estimated the heritability of ARHL or the importance of a genetic component (Van Eyken et al., 2006) and found that twin similarity of monozygotic twins decreased with age and dizygotic twins increased with age (Karlsson et al., 1997). This suggests that environmental factors also have a significant role in the development of ARHL.

Research to date points to mitochondrial dysfunction and oxidative stress as major contributors to age-related cellular degeneration in the cochlea (McFadden et al., 1999a; Ohlemiller et al., 2000; Keithley et al., 2005; Benkafadar et al., 2019). The inner ear needs energy to maintain the EP, which is essential for the motility of OHCs, the function of IHCs and SGNs. All cellular structures involved in the transduction process correspondingly contain a high number of mitochondria (Spoendlin, 1981; Nakazawa et al., 1995; Spicer and Schulte, 2002). Hair cells have a high demand for energy and are, therefore, highly dependent on energy supply (Shin et al., 2007). This energy is provided through cellular respiration in the mitochondria. However, mitochondria are also the source of reactive oxygen species (ROS), which can damage DNA and lead to apoptosis (Ames, 2006; Lee and Wei, 2012). It has been widely considered that aging is the process of accumulated oxidative stress caused by ROS (Harman, 1956; Beckman and Ames, 1998). Several studies have proposed that the imbalance between the cellular production of ROS and antioxidant enzymes, also referred to as oxidative stress, is one of the major risk factors for ARHL (Halliwell, 1992; Menardo et al., 2012; Han and Someya, 2013; Benkafadar et al., 2019). The accumulation of ROS and impaired antioxidant defenses cause cellular dysfunction, such as lipid peroxidation and enzyme inactivation, leading to permanent apoptotic cell degeneration initiating the process of cochlear senescence (Harman, 1956; Beckman and Ames, 1998; Baker and Staecker, 2012; Fujimoto and Yamasoba, 2019). The induced modifications of, e.g. ion channels, can alter channel activity or channel gene expression and consequently induce metabolic stress to the cochlea, cause mitochondrial dysfunction and an associated decrease in energy production (Matalon

et al., 2003; Balaban et al., 2005; Henderson et al., 2006; Lin and Beal, 2006). The function of K^+ channels requires a high energy supply, which can be severely challenged by the accumulation of ROS (Peixoto Pinheiro et al., 2020). Studies in mouse models with deficient or absent antioxidant enzymes resulted in hearing loss and loss of auditory neurons and hair cells compared to the control strain (McFadden et al., 1999b; Ohlemiller et al., 2000; Keithley et al., 2005). Interventions increasing antioxidant activity or decreasing ROS production may provide effective therapeutic approaches to decelerate or even prevent ARHL. Interestingly, voltage-gated K^+ channels have also been shown to be altered by oxidants both *in vivo* in C. elegans and *in vitro* (Ruppersberg et al., 1991; Cai and Sesti, 2009). A recent study even demonstrated that voltage-gated potassium channel of subfamily q, member 4 (K_V7.4 or KCNQ4) are also expressed in neuronal mitochondria, where they are presumably responsible for the regulation of membrane potential, calcium (Ca^{2+}) uptake, and ROS production (Paventi et al., 2022), indicating that pharmacological activation of K_V7.4 might counteract the detrimental mechanisms leading to cellular degeneration.

1.2 The potential role of K_V7 potassium channels in ARHL

Any restriction of metabolic supply, e.g., due to oxidative stress after acoustic trauma, ototoxic insults or aging, endangers vulnerable cochlear structures that require a high energy supply or are susceptible to ROS. Indeed, ROS contribute to the aging process in all organs by decreasing mitochondrial activity and increasing oxidative damage and also negatively affects hearing with age (Han and Someya, 2013). Selected K^+ channels in the cochlea and ascending auditory pathway are known to rely on continuous intracellular recycling processes for proper surface expression and are vulnerable early targets for energy supply limitations. K^+ channels exhibit extreme genetic heterogeneity and functional diversity unmatched by other types of ion channels and have been suggested as a major target of excess ROS. Moreover, there is strong evidence that ROS-mediated oxidation of K^+ channels is a relevant pathogenic factor in the aging nervous system and plays an important role in certain neuropathies (Cai and Sesti, 2009).

1.2.1 Impaired function of K_V7 as a primary step for hearing loss

The apical part of hair cells is specialized for mechanotransduction and bathes in endolymph, consisting of high K^+ and low sodium (Na^+) concentrations, while the basolateral part of the hair cells is surrounded by perilymph with low K^+ and high Na^+

concentrations (Dallos, 1966). The influx of K^+ through apical mechanosensitive channels depolarizes the membrane potential and drives the contraction of OHCs by the motor protein prestin. The speed of this action depends on the capacitance and conductance of the OHC at resting membrane potential, which in turn critically depend on the K^+ efflux current $I_{K,n}$ (Marcotti and Kros, 1999). However, essential to functional hair cells is the EP, a positive extracellular potential in the scala media generated by an extraordinarily high concentration of K^+ (Smith, 1954). The high K^+ concentration in the scala media and the positive potential are generated by specialized cells in the SV, which requires almost no additional metabolic energy (Zdebik et al., 2009; Patuzzi, 2011). To maintain the EP, K^+ ions entering hair cells are recycled back to the stria to complete the cycle of secretion back into the scala media. This recycling system requires specific cochlear cell types as well as selective ion channels (Zdebik et al., 2009; Adachi et al., 2013). As a component of K^+ circulation, voltage-gated potassium channel of subfamily q, member 1 (K_V7.1 or KCNQ1), which is located in the SV, is responsible for the secretion of K^+ to the endolymph and thereby generates the EP (Wangemann et al., 1995; Vetter et al., 1996). K_V7.1 is expressed throughout the body, including the lungs, liver and cochlea (Barhanin et al., 1996; Sanguinetti et al., 1996a; Sanguinetti et al., 1996b; Neyroud et al., 1997). In the inner ear, K_V7.1 modulates the kinetics by combining with potassium voltage-gated channel subfamily E member 1 KCNE1 to form a heteromeric channel (Neyroud et al., 1997). This drastically slows down channel activation, shifts the voltage activation threshold in a positive direction and avoids inactivation (Barhanin et al., 1996). Any reduction in EP affects cochlear amplification by causing a reduction in OHC depolarization. Therefore, it is not surprising that previous studies have shown that loss of K_V7.1 induces disruption of K^+ secretion into the endolymph, consequently disrupting the EP. In humans, pathogenic mutations in K_V7.1 and KCNE1 are associated with autosomal-recessive syndromic hearing loss in Jevell & Lange-Nielson Syndrome 1 (Neyroud et al., 1997) and 2 (Schulze-Bahr et al., 1997).

Furthermore, the physiology of OHCs depends on K^+ channels at the basolateral membrane. In particular, one type of K^+ channel is the main determinant responsible for the OHC resting membrane potential. The K_V7.4 channel is involved in K^+ efflux and mediates the predominant voltage-dependent K^+ conductance, $I_{K,n,}$ which is fully active at the OHC resting potential (Housley and Ashmore, 1992; Mammano and Ashmore, 1996; Nenov et al., 1997; Marcotti and Kros, 1999; Holt et al., 2007).

Expression of $K_V7.4$ is restricted to the basal pole of OHCs (Boettger et al., 2002; Winter et al., 2006), suggesting that $K_V7.4$ is responsible for the excretion of K^+ ions entering OHCs via apical mechanosensitive channels (Housley and Ashmore, 1992; Mammano and Ashmore, 1996; Kharkovets et al., 2000; Holt et al., 2007). Furthermore, $K_V7.4$ expression is also evident in IHCs (Beisel et al., 2000; Oliver et al., 2003), SGNs, and several nuclei along the auditory pathway, e.g., in the cochlear nucleus and inferior colliculus (Beisel et al., 2000; Kharkovets et al., 2000). Impaired surface expression or reduced activity of $K_V7.4$ leads to functional impairment and has been associated with age-related (Van Eyken et al., 2006; Van Eyken et al., 2007; Peixoto Pinheiro et al., 2020; Peixoto Pinheiro et al., 2021; Rim et al., 2021), noise-induced (Van Laer et al., 2006; Jaumann et al., 2012; Marchetta et al., 2020; Rim et al., 2021; Wang et al., 2021), and ototoxic hearing loss (Leitner et al., 2011). In humans, autosomal-dominant hereditary hearing loss DFNA2, is based on pathogenic mutations in $K_V7.4$ (Coucke et al., 1999; Kubisch et al., 1999; Van Hauwe et al., 2000). In a transgenic mouse model, the knock-out (KO) of $K_V7.4$ caused a slow loss of OHCs at the juvenile age of 3 weeks and then progressed to IHCs and SGNs after 6 months of age (Carignano et al., 2019). The loss of $K_V7.4$ has been linked to chronic depolarization, possibly increasing Ca^{2+} influx and causing chronic cellular stress resulting in the degeneration of OHCs (Rüttiger et al., 2004). Basal OHCs with the strongest $K_V7.4$ expression and largest $I_{K,n}$ current amplitudes are most susceptible to degeneration, whereas apical OHCs with the smallest $I_{K,n}$ currents remain less affected (Housley and Ashmore, 1992; Kubisch et al., 1999; Beisel et al., 2000; Nouvian et al., 2003; Kharkovets et al., 2006). This phenomenon is intriguing since this susceptibility of OHCs correlates with the high-frequency hearing loss as seen in ARHL.

In summary, the efflux of K^+ ions following the opening of K_V7 channels in the sensory hair cells of the inner ear is a fundamental physiological mechanism involving the maintenance or restoration of the resting potential, shaping the responses of sensory hair cells and neurons (Housley and Ashmore, 1992; Santos-Sacchi, 1993; Kros et al., 1998), synaptic inhibition in hair cells (Fuchs and Murrow, 1992; Oliver et al., 2000), and the generation of the EP by the SV (Wangemann, 2002). These findings suggest that pharmacological activation of K_V7 channels may preserve hearing function in ARHL, and possibly other forms of hearing loss related to compromised K_V7 functions.

1.2.2 Potassium channel K_V7 agonists as a potential therapeutic approach

Extensive studies of K^+ channel physiology have led to the appreciation that the gating of K^+ channels can be influenced by multiple factors, including pharmacological small-molecule ligands (Rim et al., 2021). To date, multiple chemical K_V7 channel openers have been developed, with some having reached clinical application in the treatment of neurological disorders (Miceli et al., 2008; Wulff et al., 2009).

One of the best characterized agonists of K_V7 channels is retigabine (RTG), which was originally developed for epilepsy rescuing channel function of epileptogenic $K_V7.2$ mutants (Rostock et al., 1996; Xiong et al., 2008). Furthermore, anxiolytic (Korsgaard et al., 2005) and neuroprotective properties (Rundfeldt, 1997) have been demonstrated for this compound. RTG is known to cause a shift in the hyperpolarizing direction of K_V7 voltage dependence. Leitner et al. (2012) showed for the first time *in vitro* that a combined administration of zync phyrithione (ZnP) and RTG and functionally rescue $K_V7.4$ currents in DFNA2-causing mutations in cell lines expressing the $K_V7.4$ channel. Moreover, RTG and ZnP were able to enhance the native $K_V7.4$-mediated $I_{K,n}$ current in native OHCs. These findings created the foundation for a new potential approach for the treatment of DFNA2 and other hearing impairment related to compromised $K_V7.4$ channel function (Leitner et al., 2012). RTG has been clinically approved as an anti-seizure drug; however, its administration has been associated with adverse side effects, such as blue skin discoloration and retinal abnormalities (Clark et al., 2015). ZnP has previously been shown to activate K_V7 channels by increasing the opening probability rather than altering the single channel conductance (Schroder et al., 2001; Xiong et al., 2007; Shin et al., 2019). Although ZnP was shown to be ineffective for $K_V7.4$ channels with mutations in the pore region (Leitner et al., 2012), it was able to rescue the reduced channel activity of $K_V7.4$ carrying a mutation at the cytoplasmic N-terminus (Shin et al., 2019). This indicates that ZnP, and presumably other K_V openers, primarily modify channel gating by stabilizing the open configuration of K_V7 channels. Interestingly, some K_V7 openers, e.g., BMS-204352 (Maxipost), are also able to enhance the activity of the large-conductance calcium-activated K^+ channel BK (Schroder et al., 2001; Gribkoff, 2003). Maxipost was initially used for the control of convulsions and stroke before being suggested as a therapeutic approach for hearing loss (Hewawasam et al., 2002). Shin et al. (2019) found that Maxipost was able to reverse the decreased activity and fast-deactivation kinetics in cells expressing mutant $K_V7.4$ channels. In contrast, the prospects for a therapeutic application in hearing loss

remained limited as Maxipost failed to enhance $I_{K,n}$ (Leitner et al., 2012). Besides these *in vitro* investigations, only one *in vivo* study has been performed involving the $K_V7.4$ agonists RTG and Maxipost in a rat model of tinnitus. Interestingly, in the study a sodium salicylate induced reduction of the compound action potential (CAP) amplitudes were reversed at high frequencies by Maxipost and at low frequencies by RTG, suggesting that Maxipost and RTG can protect against sodium salicylate induced peripheral damage (Sheppard et al., 2015). On the other hand, both $K_V7.4$ activators were unable to reverse the reduced distortion-product otoacoustic emissions, thus implying that protection was possibly not mediated at the OHC level. In addition, another compound designated ML-213 was reported to activate $K_V7.4$. This K_V7 channel modulator was found to be a potent activator with a unique selectivity for $K_V7.2$ and $K_V7.4$ (Yu et al., 2011), inducing a hyperpolarizing shift of the activation curve. To date, it has not been reported whether ML-213 is able to activate the native $I_{K,n}$ currents of OHCs.

The development of K_V7 channel targeting compounds to treat hearing impairments has been proposed as a strategy for over a decade (Wulff et al., 2009; Leitner et al., 2011; Leitner et al., 2012; Borgini et al., 2021; Rim et al., 2021). However, the lack of selective and potent compounds and the difficulties involved in the use appropriate animal models have inhibited further advances in the field. While voltage-gated K^+ channels offer tremendous opportunities for use in genetic, age-related, and noise-induced hearing loss, the variability of ARHL models and the necessary long-term application have complicated a potential *in vivo* experimental design to investigate their protective effect.

1.3 SAMP8 as an animal model for age-related hearing loss

Mice remain the most prominent model organism for hearing research and thus have been used to elucidate various mechanisms of ARHL. Mouse models have also become a reliable tool for age-related hearing research due to the ability to strictly control both intrinsic and extrinsic factors (Vanhooren and Libert, 2013; Bowl and Dawson, 2015). Although most inbred strains display some degree of ARHL, the age of onset, grade of hearing loss and magnitude of cochlear degeneration are known to vary considerably (Zheng et al., 1999; Merchant and Nadol, 2010). The most frequently used strain for ARHL is the C57BL6/J mouse, which exhibits premature progressive hearing loss, especially at high frequencies accompanied by a broad degeneration of

cochlear structures (Ison et al., 2007). At 2 months of age, this strain already shows significant hearing loss in the high-frequency range, whereas deterioration in the low-frequency range is not noticeable until 6 months of age (Li and Borg, 1991). These functional deficits are strongly associated with degenerative histopathological changes. The classic ARHL pattern, resembling that of humans, manifests in this strain at 10-15 months of age (Hunter and Willott, 1987; Zheng et al., 1999). C57BL6/J mouse strain is known to carry a specific mutation in the cadherin 23 gene (Cdh23), which encodes a component required for stereocilium bundle formation and has been identified as the underlying cause of accelerated ARHL progression (Johnson et al., 1997; Noben-Trauth et al., 2003; Keithley et al., 2004). Other studies of ARHL use inbred strains displaying normal aging, such as the CBA/J mouse. This mouse strain is characterized by a late onset of hearing loss due to an *Ahl* resistant allele. A significant threshold shift in the high frequencies occurs around the age of 12 months, progressing to lower frequencies until 26 months (Zheng et al., 1999; Frisina and Zhu, 2010; Ohlemiller et al., 2010). This functional loss is accompanied by a decrease in cell density at 18 months involving mainly the OHCs with a modest loss of IHCs at the basal turn (Ohlemiller et al., 2010). Despite the human-like course of ARHL, it should be noted that the age-related hearing loss in the C57BL6/J and CBA/J mice is due to predisposing genetic variants and therefore may not reflect biological aging.

Given the increasing evidence that oxidative stress is a key contributor to ARHL (Someya and Prolla, 2010; Menardo et al., 2012; Han and Someya, 2013; Roth, 2015; Rivas-Chacón et al., 2021), senescence-accelerated mouse strain 8 (SAMP8) may prove to be a more suitable model for ARHL. The SAMP8 mouse strain was developed through phenotypic selection toward senescence from the AKR/J strain (Takeda et al., 1981). SAMP8 mice have been shown to exhibit age-dependent hearing loss (Marie et al., 2017) together with other phenotypes, such as reduced anxiety behaviour (Miyamoto, 1997), learning and memory deficits (Yagi et al., 1988; Flood and Morley, 1998), and a reduced lifespan (Morley, 2002). Therefore, SAMP8 mice have been identified as a suitable model in gerontological research, including Alzheimer's disease, senile amyloidosis, cataracts, osteoporosis and brain atrophy (Akiguchi et al., 2017; Karuppagounder et al., 2017; Folch et al., 2018; Grinan-Ferre et al., 2018). Menardo et al. (2012) provided strong evidence that the accelerated progression of ARHL in SAMP8 mice occurs as a result of ROS accumulation and altered levels of antioxidant enzymes causing chronic inflammation and apoptotic cell death. The

overall progression of age-related threshold loss in SAMP8 mice is similar to that in other mouse models, although it occurs over a much shorter time frame, which facilitates the design of otoprotective studies (Fetoni et al., 2011; Marie et al., 2017). In addition to early functional age-dependent hearing loss starting at 1 month of age (Marie et al., 2017), SAMP8 mice also displayed a sequential degeneration and loss of OHCs, SGNs, SV and IHCs (Menardo et al., 2012; Fujimoto and Yamasoba, 2014; Benkafadar et al., 2019), which generally mimics human presbycusis, as observed in histopathological studies (Wu et al., 2020).

The requirements of ARHL animal models include simulating the human otopathology of ARHL, with normal hearing at a young age followed by progressive decline of hearing function in older adulthood. Although this cannot be perfectly replicated by any animal model, the accelerated aging process, earlier onset, and more rapid progression of age-related pathological phenotypes make the SAMP8 strain a useful model for studying the effects of aging on biological processes, particularly regarding the pathophysiology of ARHL (Menardo et al., 2012; Han and Someya, 2013; Benkafadar et al., 2019).

2. Objectives

The primary objective of this work was to investigate the effect of pharmacological activation of a K^+ channel as a novel therapeutic approach for ARHL in a suitable mouse model. K^+ channels are known to play an essential role in the auditory function of the inner ear, contributing to K^+ recycling and homeostasis maintenance. Furthermore, they show a distinctive vulnerability to age-dependent energy deprivation, which is required for continuous recycling and sustained surface expression (**Peixoto Pinheiro et al. 2020**). Based on these observations, small compounds activating $K_V7.4$, one of the most essential K^+ channels in the inner ear and specifically the OHCs, appears a promising approach to decelerate the progression of ARHL in the SAMP8 mouse model.

1. Variability of age-related hearing loss in SAMP8 mice

The aim of this study was to investigate the extent of functional variability and the relation to the pattern of cellular degeneration in the cochlea as a potential underlying cause. First, we characterized the hearing performance of SAMP8 mice by assessing the auditory function in different age groups using auditory brainstem responses (ABRs). Together with molecular markers of cochlear hair cell integrity and K^+ channel markers, in particular, the altered expression levels of $K_V7.4$ and $K_V7.1$, were investigated as the potential underlying cause of the observed threshold variability in SAMP8 mice (**Peixoto Pinheiro et al. 2021**).

2. Local administration of a small-molecule $K_V7.4$ agonist as an otoprotective treatment for ARHL in SAMP8 mice

$K_V7.4$ activation studies (Leitner et al., 2012) as well as $K_V7.4$ KO models (Kharkovets et al., 2006; Carignano et al., 2019) implied that the application of $K_V7.4$ activators has a therapeutic potential for ARHL. However, the administration of available $K_V7.4$ activators remains restricted, especially due to their insufficient *in vivo* efficacy (Rim et al., 2021). Therefore, in this second study, we aimed to investigate the effect of a novel, potent small-molecule $K_V7.4$ agonist developed by Acousia Therapeutics GmbH, Tübingen (Bös, 2018) on ARHL in the SAMP8 mouse model. A pharmacokinetic study provided information on the distribution of the $K_V7.4$ agonist ACOU085 from a sustained release formulation in the cochlea by sampling cochlear perilymph and tissue after a single application via transtympanic injection into the middle ear. The pharmacodynamic effect of ACOU085 on ARHL in the SAMP8 model was investigated

in two groups of mice that received repeated transtympanic injections of ACOU085 in two doses (0.6% w/v or 6.0% w/v) or vehicle as a control. To evaluate the effect of cochlear $K_V7.4$ enhancement *in vivo*, auditory function was assessed using ABRs, and quantitative cytohistological analysis was conducted (**Peixoto Pinheiro et al. 2022**).

3. Topical administration of a small-molecule $K_V7.4$ agonist as a treatment for ARHL in SAMP8 mice (not published)

Drug delivery to the inner ear is usually obtained locally via transtympanic injection (see study II) through the tympanic membrane (TM) into the middle ear both in the experimental setting and in clinical applications. However, due to a number of limitations such as scarring of the TM by repeated perforations and the presumed need for a life-long treatment in patients, local drug delivery to the inner ear via transtympanic injection is constrained. To address this limitation, this third study tested a non-invasive, systemic approach of drug delivery to the inner using a $K_V7.4$ agonist. For this purpose, a further novel, small-molecule $K_V7.4$ agonist, ACOU082, developed by Acousia Therapeutics GmbH, Tübingen (Bös, 2018) was delivered systemically via repeated topical administrations into the external ear canal of SAMP8 mice. To evaluate the effect of the $K_V7.4$ agonist ACOU082 of the cochlea in SAMP8 mice, auditory function was assessed using ABRs, and quantitative histological analysis was conducted.

3. Results

3.1 Variability of age-related hearing loss in SAMP8 mice

In this study, we investigated the auditory performance of SAMP8 mice. Hearing function was assessed using ABR in SAMP8 mice of different ages. SAMP8 mice exhibit a large variability in the decline of auditory function. Using molecular markers of cochlear hair cell integrity and K^+ channel markers, particularly the altered expression levels of $K_V7.4$ and $K_V7.1$, we investigated the underlying cause of this observed threshold variability in SAMP8 mice (**Peixoto Pinheiro et al. 2021**).

3.1.1 Progression of auditory functional decline

The SAMP8 strain has been identified as a suitable model to study age-dependent disorders, including ARHL (Menardo et al., 2012; Marie et al., 2017; Bös, 2018; Benkafadar et al., 2019). SAMP8 mouse model has been shown to develop an early progressive, age-related decline in hearing function associated with sensory, neural and strial cellular degeneration (Menardo et al., 2012; Fujimoto and Yamasoba, 2014; Benkafadar et al., 2019). One aim of this study was to phenotypically characterize the auditory performance of SAMP8 mice. First, we monitored hearing function of SAMP8 mice that were divided into three age groups: juvenile (average age of 6 weeks), young adult (average age of 12 weeks), and adult (average age of 24 weeks) to confirm premature and accelerated hearing decline in a SAMP8 reference cohort (Figure 2a, Peixoto Pinheiro et al. 2021). Hearing thresholds were assessed by pure-tone stimulus evoked ABR showing a progressive and significant increase in hearing loss, starting in the high-frequency range (> 8 kHz) between juvenile and young adult stages and further progressing toward the low-frequency range (≤ 8 kHz) in the adult stages (Figure 2b, Peixoto Pinheiro et al. 2021). This reference cohort of SAMP8 mice shows an early progressive, age-related increase in ABR thresholds, starting primarily in the high-frequency range and later extending to all frequencies at an adult age.

3.1.2 Variability in ABR threshold progression independent of hair cell loss

Analyzing ABR thresholds across age groups, it became apparent that this SAMP8 cohort also presented a large variability in the age-related decline of auditory function. We thereby observed an increase in variability with age (Figure 2a, Peixoto Pinheiro et al. 2021). Therefore, in a next step, we investigated the extent of this functional variability and the pattern of cellular degeneration as a potential underlying cause. We

first hypothesized a bifurcation into subgroups with slow or fast progression of ABR threshold increase over age, presumably entailing threshold variability between age groups. To identify the threshold distribution within SAMP8 subgroups, a new cohort of SAMP8 mice was compared with the interquartile range (between the 25th and 75th percentiles) of the reference cohort at the same reference ages. Based on the progression of age-related ABR threshold loss, we were able to select mice below the 25th percentile (lower quartile) showing a relatively slow progression (n = 3) of ABR threshold loss over age and mice above the 75th percentile (upper quartile) with a relatively fast progression (n = 3, Figure 3, Peixoto Pinheiro et al. 2021). Mice allocated to the normal-hearing subgroup (normal, n = 4) adhered to the progression found in the reference cohort. Overall, no correlations were found between these subgroups and the sex of the mice. Moreover, hearing loss between both ears for each mouse was shown to be symmetrical. At the juvenile age, SAMP8 mice allocated to the upper quartile demonstrated elevated ABR thresholds for all frequencies compared to normal hearing (mean shift 11 ± 5 dB) and mice allocated to the lower quartile (mean shift 16 ± 4 dB). This finding suggests that SAMP8 mice exhibit subgroups with different progressions of age-related hearing loss that already becomes apparent at the juvenile age.

Previous studies have shown that OHCs contribute to cochlear amplification, thus playing an essential role in cochlear sensitivity (Liberman and Kiang, 1978; Liberman and Beil, 1979; Dallos, 2008). Based on Wu et al. (2020), the primary histopathological predictor of ABR thresholds is OHC survival. For this reason, investigating OHC survival may provide insight regarding the observed diverging threshold shifts in the upper and lower quartiles of SAMP8 mouse. OHC survival was analyzed by performing cytocochleograms obtained from OC whole-mount preparations of SAMP8 mice at the respective ages (Figure 4, Peixoto Pinheiro et al. 2021). Cytocochleograms are cartographic representations that demonstrate hair cell number and distribution along the cochlear length (Viberg and Canlon, 2004; Müller et al., 2005; Carignano et al., 2019). Present or missing OHCs and IHCs were counted and allocated to 5% bins along the normalized spiral length of the OC. Ratio between missing hair cells and the sum of present and missing hair cells, i.e., percentage of hair cell loss in each bin are presented in cytocochleograms (Figure 5, Peixoto Pinheiro et al. 2021). To allow a more accurate quantification and comparability of ABR threshold shifts and OHC loss over age, a mouse place-frequency map (Viberg and Canlon, 2004) was used to

convert the relative distance from apex to the corresponding frequencies along the whole cochlear length. Cytocochleograms as well as ABR threshold shifts were divided into low- (≤ 8 kHz) and high-frequency (> 8 kHz) ranges in accordance with the progressive OHC loss observed in the middle and basal regions (> 40% distance from apex, Figure 6, Peixoto Pinheiro et al. 2021). Examining the overall number of OHCs, the most severe loss was detected in the basal region of young adult and adult mice, usually starting at a 40% distance from the apex. Although OHC survival was previously reported as the primary histopathological predictor of ABR thresholds (Wu et al., 2020), we could not confirm this observation, as no differences in OHC loss were found between mice in the lower and upper quartiles. In the SAMP8 mice, age-related OHC loss was not significant in the low-frequency range but showed a significant loss in the high-frequency range. These results confirm OHC loss as one predictor of age-related ABR threshold loss in SAMP8 mice. However, the observed threshold variability was not fully explained by OHC loss alone (Figure 6a, Peixoto Pinheiro et al. 2021). Interestingly, mice in the lower and upper quartiles exhibit the same progression of age-related ABR threshold loss. Both groups demonstrate comparable slopes of the linear regression models in the high-frequency range, with a threshold increase of 8.5 dB per 50 days in the lower quartile and 8.0 dB per 50 days in the upper quartile. In other words, even though the lower and upper quartiles indicate different time points for the onset of hearing loss, the rate of progression thereafter remains similar. Given that functional impairment, as measured by the progressive increase in ABR thresholds, preceded OHC loss in both the lower and upper quartiles, it is hypothesized that OHC loss is a predictor of the increase in ABR thresholds secondary to a functional age-related factor that is not apparent at the cellular level. As pointed out above, such an age-related factor without any correlation at the cellular histopathological level is also seen in the human otopathology of ARHL (Wu et al., 2020).

3.1.3 Altered K^+ channel related OHC and SV phenotypes as potential predictors for functional variability

K^+ is the major charge carrier for signal transduction, and its recirculation is essential for maintaining cochlear homeostasis (Konishi et al., 1978; Zidanic and Brownell, 1990; Wangemann et al., 1995; Kikuchi et al., 2000; Wangemann, 2006). In particular, $K_V7.4$ in the OHCs and $K_V7.1$ in the SV are crucial components in the K^+ recycling circuit. Therefore, we hypothesized that phenotypic variances preceding OHC loss may be linked to altered levels of membrane expression of $K_V7.4$ in OHCs or $K_V7.1$ in the SV.

For each age group, quantative assessment of $K_V7.4$ and $K_V7.1$ membrane expression in the cochleae of mice allocated to the lower and upper quartiles was carried out. Therefore, fluorescence images of mid-modiolar cochlear cross-sections were processed and pixel intensity in the respective regions of interest, in the OHCs and the SV, were evaluated (Figure 7, Peixoto Pinheiro et al 2021). To obtain the average $K_V7.4$ intensity per OHC and the average $K_V7.1$ intensity per SV width, pixel intensity profiles for $K_V7.4$ and $K_V7.1$ were integrated to obtain the area under the curve (AUC) and then normalized by the number of OHCs or SV length, respectively (Figure 7b, c, Peixoto Pinheiro et al. 2021). Mice allocated to the lower quartiles presented a generally higher $K_V7.4$ expression over age compared to mice allocated to the upper quartiles (Figure 8a, Peixoto Pinheiro et al. 2021); however, no significant differences were detected between these quartiles. A similar observation was made for $K_V7.1$ expression in the SV (Figure 8b, Peixoto Pinheiro et al. 2021). To examine the membrane expression in each turn, a scatterplot of the normalized AUC of $K_V7.4$ and $K_V7.1$ immunofluorescence as a function of age was calculated. Across age, mice allocated to the lower quartile showed relevant negative correlations between $K_V7.4$ expression and age that reached significance ($r = -0.71$, $p = 0.014$) for the middle turn. Besides, relevant linear regression was also apparent in the midbasal turns corresponding to the high-frequency region of the cochlea (> 8 kHz, Figure 9a, Peixoto Pinheiro et al. 2021). Regarding $K_V7.1$ expression in SV, mice assigned to either quartile generally showed no significant correlations between $K_V7.1$ expression and age, although a difference across age is observed between the lower and upper quartiles in the midbasal turn (Figure 9b, Peixoto Pinheiro et al. 2021).

Taken together, a generally decreased $K_V7.4$ and $K_V7.1$ membrane expression was observed in same aged mice allocated to the upper quartiles, a finding consistent with the higher ABR thresholds in the low- and high-frequency ranges. Therefore, we propose altered OHC and SV phenotypes as potential predictors of the observed ABR threshold differences, feasibly preceding OHC loss over age.

3.1.4 Summary

The large variability of age-related auditory threshold loss observed in SAMP8 mice was investigated by a bifurcation into two subgroups, in which SAMP8 mice were allocated to the lower and upper quartiles of the threshold distribution in a reference population. To identify the underlying cause of the observed threshold variability, OHC

survival was investigated as a potential predictor given that it was reported as a histopathological predictor for ARHL (Wu et al., 2020). The age-related progression of ABR threshold loss in the two groups was not related to an equitable loss of OHCs. An altered OHC phenotype related to an age-related decline in $K_V7.4$ membrane expression as well as a possible altered phenotype of SV linked to $K_V7.1$ appeared to precede OHC loss and correlated with the functional decline as observed in ABR threshold shifts. Based on these findings, the present study suggests that the integrity of $K_V7.4$ channel expression in the OHCs is a potentially critical step for the elevated hearing thresholds in SAMP8 mice preceding OHC loss. This leads to the hypothesis that declining levels of $K_V7.4$ channel expression may be functionally compensated by channel activation as an otoprotective measure, which in turn may delay the progression of ARHL.

3.2 Local administration of a small-molecule $K_V7.4$ agonist as an otoprotective treatment modality for ARHL in SAMP8 mice

The aim of this study was to investigate the effect of a novel, potent small molecule $K_V7.4$ agonist ACOU085 developed by Acousia Therapeutics GmbH, Tübingen (Bös, 2018) on ARHL in the SAMP8 model. Modulation of $K_V7.4$ by small molecule activators as a potential treatment strategy for various types of hearing loss, including ARHL, has been suggested in the literature for over a decade (Wulff et al., 2009; Leitner et al., 2011; Leitner et al., 2012; Rim et al., 2021). Consequently, the pharmacological modulation of $K_V7.4$ as a potential drug target in the context of hearing loss has been investigated with available, but nonselective, small-molecule activators in cell lines and native OHCs *in vitro* (Leitner et al., 2011; Leitner et al., 2012). To date *in vivo* investigations to test this hypothesis are missing, possibly due to the lack of potent and selective $K_V7.4$ agonists and suitable animal models. For this second study, a novel and potent $K_V7.4$ agonist was investigated for its pharmacokinetic and pharmacodynamic properties in the SAMP8 model established as a suitable model of ARHL in study I. A pharmacokinetic study was performed to provide information about the cochlear distribution of the $K_V7.4$ agonist ACOU085 from a sustained-release formulation applied to the middle ear via transtympanic injection. Cochlear perilymph and tissue were sampled after a single application of ACOU085 in a sustained-release formulation by transtympanic injection into the middle ear and analyzed via liquid chromatography with tandem mass spectrometry (LC-MS/MS). To study the pharmacodynamic effect of ACOU085 on ARHL in the SAMP8 model, groups of mice

received repeated transtympanic injections of ACOU085 at two doses (0.6% w/v or 6.0% w/v) or vehicle as a control. The *in vivo* effect of local drug treatment with the $K_V7.4$ agonist ACOU085 was examined by assessing auditory function using ABRs and correlating this to post-mortem cytohistological analysis (**Peixoto Pinheiro et al. 2022**).

3.2.1 $K_V7.4$ agonist reduces age-related ABR threshold shifts in SAMP8 mice

To ensure relevant pharmacokinetic drug distribution to the cochlea we investigated the concentrations of the $K_V7.4$ activator ACOU085 from the formulation administered by sampling cochlear perilymph and tissue at different timepoints after a single transtympanic injection of 0.6% w/v (n = 14) or 6.0% w/v (n = 24) formulations in SAMP8 mice (Figure 1a, Peixoto Pinheiro et al. 2022). This pharmacokinetic study confirmed that ACOU085 readily diffused into the cochlear perilymph and tissue from the sustained release formulation into the middle ear cavity after a single local transtympanic administration. In cochlear tissue as well as in perilymph, concentrations of 6.0% w/v formulation were at least an order of magnitude higher compared to the 0.6% w/v formulation, confirming a dose-dependent uptake into the cochlea (Salt and Plontke, 2018). Furthermore, given an EC_{50} in the nanomolar range (Bös, 2018), we may assume that therapeutically relevant concentrations of ACOU085 were available in the cochlea at 7 to 14 days after a single administration, with higher concentrations and a presumably longer time window for the 6.0% w/v dose (Supplementary Figure 1, Peixoto Pinheiro et al., 2022).

To determine the pharmacodynamic efficacy of $K_V7.4$ in the ARHL mouse model, two groups of SAMP8 mice received three consecutive, unilateral transtympanic injections of ACOU085 in intervals of one month. The injections were applied in 0.6% w/v (n = 10) or 6.0% w/v (n = 8) doses, denoted as 0.6% or 6.0% groups, respectively. Contralateral ears served as controls receiving equivalent volumes of the vehicle formulation. ABR measurements were determined before treatment (pre-treatment, preT) and at consecutive monthly timepoints until 3 months post-treatment (postT). One month after the third and last injection final ABR measurements were performed and animals were sacrificed for histologic analysis (Figure 2a, Peixoto Pinheiro et al. 2022).

Comparing the progression of hearing loss of vehicle-treated ears between the two dose groups, it is apparent that the 6.0% group demonstrates a relatively faster progression of hearing loss than the 0.6% group (Figures 3a, b, Peixoto Pinheiro et al.

2022). In both groups no statistically significant within-subject differences in ABR thresholds were seen between the ACOU085-treated and the vehicle-treated ears prior to initiation of treatment (Figures. 2b, c, Peixoto Pinheiro et al. 2022). Although the 0.6% group generally had lower ABR thresholds than the 6.0% group (mean difference 7.4 ± 2.6 dB for all frequencies), this did not affect within-subject comparisons.

Click-evoked ABR threshold shifts of the 0.6% group did not show a significant effect of ACOU085 treatment for all postT intervals (Figure 3a, Peixoto Pinheiro et al. 2022). However, an effect of treatment was observed in the 3-month post-treatment interval in the 6.0% group (p = 0.029, Figure 3b, Peixoto Pinheiro et al. 2022). This observation can be attributed to the initially higher thresholds as well as to the variability of age-related ABR threshold loss in SAMP8 mice investigated in the second study, presumably reflecting underlying phenotypic differences (see chapter 3.1). Tone burst-evoked ABR threshold shifts were calculated with respect to the mean for each dose group, 0.6% and 6.0%, separately. ACOU085-treated ears presented significantly decreased ABR threshold shifts in the 0.6% group at 3 months postT compared to vehicle-treated ears (Figure 4a, Peixoto Pinheiro et al. 2022). Similarly, the 6.0% group showed a main effect of treatment (tested with a two-way repeated-measures ANOVA) just above significance (Figure 4b, Peixoto Pinheiro et al. 2022).

Taken together, the reduced ABR threshold shifts for click- and tone-burst evoked ABRs demonstrate that repeated treatments with the $K_V7.4$ agonist protected a decline of hearing function in the ARHL mouse model SAMP8 in both the low and high dose groups.

3.2.2 $K_V7.4$ agonist reduces age-related OHC loss in SAMP8 mice

To determine the degree of OHC survival, which is attributable to $K_V7.4$ function (Kharkovets et al., 2006; Carignano et al., 2019), the effect of local $K_V7.4$ agonist treatment on OHC survival was compared in ACOU085-treated and vehicle-treated ears. This comparison was based on a quantitative analysis of cytocochleograms covering the whole cochlea as previously described (Peixoto Pinheiro et al., 2021). The analysis was performed for the 0.6% and 6.0% groups after the final ABR measurement at 3 months postT (Figure 5, Peixoto Pinheiro et al. 2022). In both treatment groups, IHC loss remained negligible below 7% (Figure 4, Peixoto Pinheiro et al. 2022), confirming our previous histological observation (Peixoto Pinheiro et al., 2021). Although an OHC loss of more than 10% was observed in the 0.6% group at a

distance of 37.5% from the apex, there were no significant differences between the ACOU085 treated and the vehicle treated ears in this 0.6% dose group (Figure 5b, Peixoto Pinheiro et al. 2022). In contrast, in the 6.0% dose group OHC loss was considerably reduced in the ACOU085 treated ears compared to the vehicle treated ears (Figure 5b, Peixoto Pinheiro et al. 2022).

To further quantify age-related ABR threshold shifts and OHC loss over age, a mouse place-frequency map was implemented (Viberg and Canlon, 2004). In accordance with the previously shown progressive OHC loss in SAMP8 mice observed in the mid- and basal regions (> 40% distance from the apex, Figure 4, Peixoto Pinheiro et al. 2021), the mouse place-frequency map was applied to divide the cytocochleograms into low-frequency (≤ 8 kHz) and high-frequency (>8 kHz) regions. Treatment with 0.6% ACOU085 showed a significant main effect in tone burst-evoked ABR threshold shifts at 3 months postT; however, this difference could not be observed in the cytocochleogram analysis (Figure 6a, Peixoto Pinheiro et al. 2022). In the 6.0% group, the main effect of treatment was just above the significance level comparable to the analysis for each frequency. Furthermore, a significant reduction in OHC loss in the high frequency range of ACOU085-treated ears was present compared with the vehicle-treated ears (Figure 6b, Peixoto Pinheiro et al. 2022). Overall, administration of the $K_V7.4$ agonist ACOU085 over a period of three months was shown to significantly reduce age-related OHC loss in the high frequency range for the higher dose group.

3.2.3 Summary

The findings presented in this study show that the novel small-molecule $K_V7.4$ agonist ACOU085 significantly reduced age-related ABR threshold shifts as well as OHC loss in the SAMP8 mouse model of ARHL. These findings suggest that pharmacological activation of $K_V7.4$ appears to be a promising approach to prevent and decelerate age-related decline of auditory function and morphological loss of OHCs. Note that this frequency range-specific effect of treatment with reduced OHC loss is consistent with the significant reduction in click-evoked ABR threshold shifts at 3 months postT.

3.3 Systemic administration of a small-molecule $K_V7.4$ agonist as an otoprotective treatment modality for ARHL in SAMP8 mice (not published)

The most common drug delivery approach to the inner ear is local drug delivery via transtympanic injection through the TM into the middle ear. Systemic drug delivery via

transdermal or oral routes have not been approached due to the small size of the inner ear, the blood-labyrinth barrier (BLB) and potential systemic side effects. On the other hand, local transtympanic inner ear drug administration has its own limitations such as the rapid loss of the drug from the middle ear via the eustachian tube or scarring of the TM caused by repeated perforation. These limitations may inhibit clinical development in the context of a repeated long-term treatment as required in ARHL (Figure 2a). To overcome these limitations and to allow a prolonged frequency of drug administration, a novel route of transdermal, topical application via the skin of the outer ear canal was tested in this study. For this study a further novel, potent small molecule $K_V7.4$ agonist, ACOU082 (Bös, 2018), with different chemical properties from ACOU085, was repeatedly administered by topical transdermal delivery into the external auditory canal of SAMP8 mice. The *in vivo* effect of topical, transdermal drug treatment with the $K_V7.4$ agonist ACOU082 was examined by assessing auditory function using ABRs and correlating this to post-mortem cytohistological analysis as previously described (Peixoto Pinheiro et al, 2022).

3.3.1 Study design

The $K_V7.4$ agonist ACOU082 was repeatedly administered via systemic, topical application into the external auditory canal of SAMP8 mice of both sexes. The experimental group (n = 10) received topical treatments with ACOU082 at 17% w/v concentration, and a control group treated in parallel received comparable treatment with vehicle as control (Figure 2b). With a temporal delay of 6 months, an additional experimental group (n = 10) was treated with 27.5% w/v ACOU082 without a parallel control group (Figure 2b). Treatment groups are hereafter referred to as 17% or 27.5% group and the vehicle treated control group is referred to as vehicle group. A pharmacokinetic study performed by Synovo (Tübingen) provided information on the distribution of the $K_V7.4$ agonist ACOU082 in the cochlea by sampling cochlear perilymph and tissue after a single administration to the external ear canal (data not shown). Concentration of ACOU082 was found to decline below the lower limit of quantification (LLOQ) within 84 hours. Therefore, each treatment group received an administration volume of 4 µl per ear of the respective compound into each external auditory canal via droplets every 84 hours (twice a week). The magnitude of hearing loss was determined by measuring acoustically evoked ABRs. At 45 days of age, ABR thresholds were determined for each mouse before treatment, followed by the first topical treatment for each group (ACOU082 or vehicle). Post-treatment ABR

measurements were performed at 1-month intervals, followed by biweekly treatments until the last ABR measurement at 5 months postT. After the final ABR measurements at 5 months postT (195 days), SAMP8 mice were sacrificed, cochleae were extracted and hair cell loss was quantified using immunohistochemical cochlear whole-mount analysis for the generation of cytocochleograms as previously described (Peixoto Pinheiro et al. 2021).

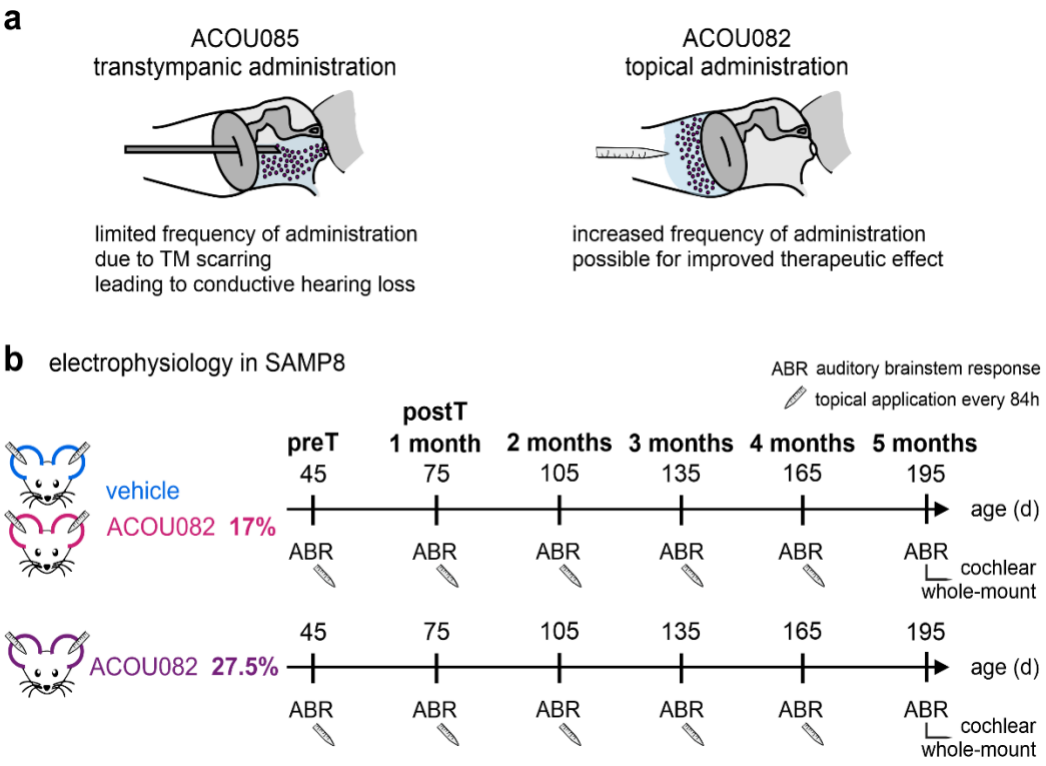

Figure 2: Schematic representation of the drug delivery approach and study design. (a) Transtympanic drug delivery into the middle ear compared to transdermal topical administration into the external auditory canal. (b) The effect of repeated bilateral administrations via topical application of ACOU082 or vehicle was investigated in the SAMP8 mouse model. ACOU082 was tested in two dose groups 17% w/v with a parallel control group and 27.5% w/v without a parallel control group. Treatments with 4 µl treatment solution were performed biweekly every 84 hours into each external auditory canal. Auditory function was assessed at 1-month intervals from 45 days of age (pre-treatment, preT) to 195 days (5-months post-treatment, postT) by determining auditory brainstem response (ABR) thresholds. After the final measurement at 5 months, mice were sacrificed and their cochlea were extracted for cochlear whole-mount analysis and the generation of cytocochleograms.

3.3.2 Effect of $K_V7.4$ agonist ACOU082 on age-related threshold shifts in SAMP8 mice

For all groups, ABR threshold shifts were calculated as the difference between averaged thresholds (two ears per mouse) and the corresponding averaged baseline measurement at 45 days of age. Comparing click-evoked thresholds at preT, vehicle-

treated group presented mean threshold shifts of 19.9 ± 3.5 dB in contrast to a 25.4 ± 7.7 dB threshold shift for the 17% group and 23.5 ± 5.4 dB threshold shift for the 27.5% group (data not shown). Although the vehicle group appeared to have a smaller threshold loss than the 17% group, no significant differences between drug treated groups and the vehicle group was found for the click-evoked ABR threshold shifts. In general, the 17%, 27.5% and vehicle control groups presented a similar progression of hearing loss throughout the study, and no significant differences were detected at any postT interval. The peak therapeutic effect was expected at the end of the treatment period of 5 months; however, since a similar progression of hearing loss occurred in all groups, no significant differences were seen in the click-evoked threshold shift of mice treated with 17% w/v ACOU082 or 27.5% w/v ACOU082 compared to the control group. Tone burst-evoked ABR also showed a similar outcome for both dose groups and the control group across all frequencies (Figure 3a). To allow frequency range-specific comparisons, ABR threshold shifts at 5 months postT were averaged over the low- (≤ 8 kHz) and high-frequency (> 8 kHz) ranges for each treatment (Figure 3b). However, no significant differences were evident in ABR threshold shifts between the treatment and vehicle groups.

3.3.3 Effect of $K_V7.4$ agonist ACOU082 on OHC loss in SAMP8 mice

To determine the effect of treatment on the degree of hair cell survival, cochleae were extracted for immunohistochemical analysis after the final ABR measurement at 5 months postT. Note that due to whole-mount preparation damage, three mice had to be excluded from the 27.5% ACOU082 group at the 5-month postT intervals. One mouse in the vehicle group met humane endpoint criteria and was therefore excluded from the experiment at 4 months postT. Cytocochleograms were generated from OC whole-mount preparations, counting both present and absent OHCs and IHCs along the normalized spiral length of the OC as described previously (Peixoto Pinheiro et al., 2021). The ratio of absent hair cells to the sum of present and absent hair cells was visualized in cytocochleograms (Figure 3c). To facilitate comparison with ABR data, a mouse place-frequency map was implemented (Viberg and Canlon, 2004). Cytochleograms were divided into low (≤ 8 kHz) and high frequency (> 8 kHz) ranges to correspond to the progressive OHC loss previously shown in SAMP8 mice in the mid and basal regions (> 40% distance from the apex). Consistent with previous findings, IHC loss remained negligible below 7% for both the treatment group and the control group (Peixoto Pinheiro et al., 2021; Peixoto Pinheiro et al., 2022). A mean

OHC loss of up to 36% was observed in the high frequency range of vehicle-treated ears, starting at a distance of 30-40% from the apex (Figure 3d). However, OHC loss showed no relevant differences between ACOU082- and vehicle-treated mice.

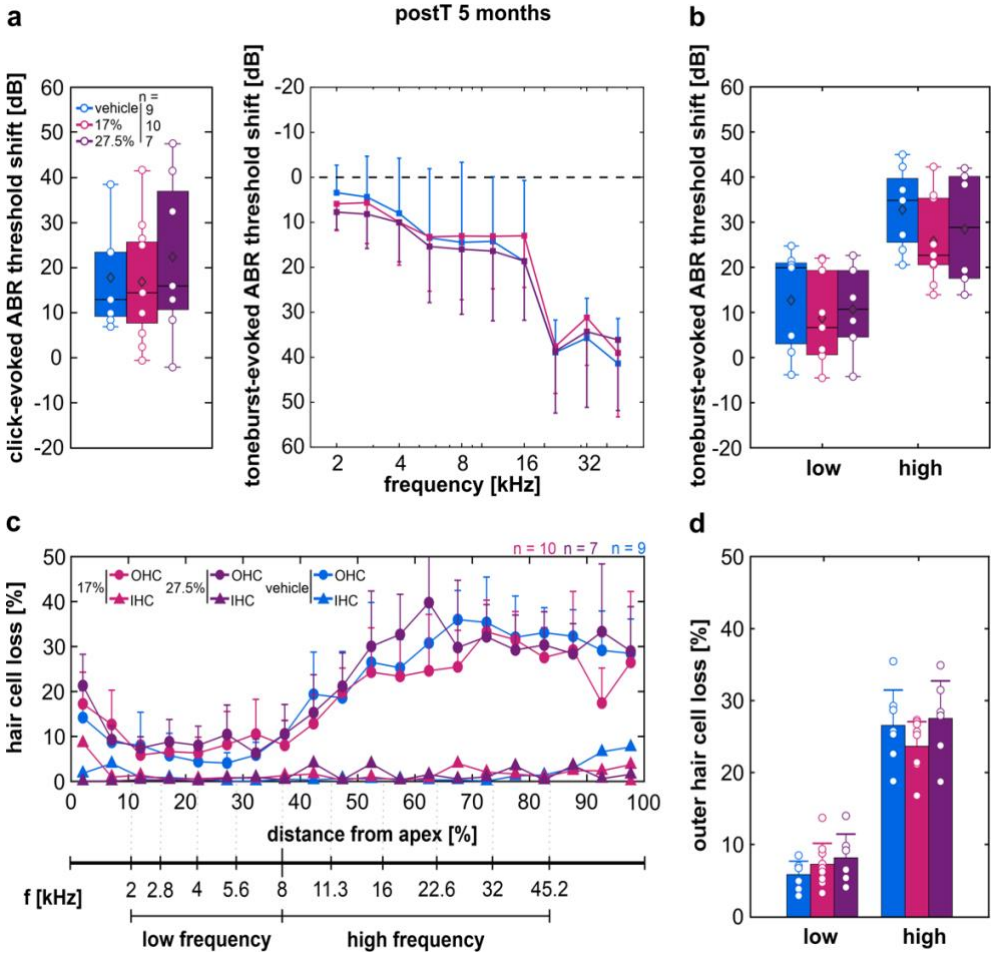

Figure 3: Effect of repeated treatments with $K_V7.4$ agonist on age-related click- and toneburst-evoked ABR threshold shifts and age-related hair cell loss. (a) Means (diamonds), box plots and individual (circles) click-evoked threshold shifts measured at 5 months post-treatment (postT, 195 days of age) are shown for SAMP8 mice treated bilaterally with either 17% w/v (n = 10), 27.5% w/v ACOU082 (n= 7) or vehicle control (n= 9). Toneburst-evoked ABR threshold shifts are shown as mean and standard deviation for each treatment group measured at 5 months postT. Toneburst-evoked ABR threshold shifts were calculated as the difference between individual thresholds (for each ear) and the population mean at preT (n = 36, two ears per mouse). (b) To allow frequency range-specific comparisons, ABR threshold shifts at 5 months postT were averaged over the low- (≤ 8 kHz) and high-frequency (> 8 kHz) ranges for each treatment. Means (diamonds), box plots and individual (circles) tone-evoked threshold shifts are shown for SAMP8 mice. (c) Degree of outer and inner hair cell loss (OHC, IHC, respectively) were determined at 5 months postT by generating cytocochloegrams for either 17%, 27.5% w/v ACOU082 or vehicle control. Cytocochleograms present mean and standard error of the mean OHC and IHC loss in percent, which are calculated as the ratio of absent hair cells to the sum of present and absent hair cells within 5% bins of distance from apex for each treatment group. For reference, a frequency (f) axis is depicted with respect to the relative distance from apex. (d) A mouse place-frequency map was used to divide the cytocochleograms into low- (< 8 kHz) and high-frequency (> 8 kHz) ranges to determine OHC loss.

3.3.4 Summary

In the present study, a $K_V7.4$ agonist, ACOU082, was administered via topical administration into the external ear canal of SAMP8 mice, which offers many advantages compared to transtympanic application. Our findings, however, could not verify that the systemic administration of ACOU082 had a protective effect on ABR threshold shifts or OHC survival. Still, some methodological limitations may have hindered the detection of a protective effect akin to that of ACOU085, which will be discussed in the following section.

4. Discussion

Presbycusis is a general term that refers to hearing loss in elderly individuals, representing lifetime insults to the auditory system. Decreased hearing sensitivity and speech understanding in noisy environments, slowed central processing of acoustic information, and impaired localization of sound sources are hallmarks of presbycusis (Gates and Mills, 2005). Considering the increasing life expectancy of the population, the impact of hearing loss on the general health and well-being of individuals during this prolonged lifespan has a significant clinical and economic impact (Stevens et al., 2013). However, understanding the multifaceted causes of ARHL faces several major challenges, including the high complexity of the auditory system. For this reason, the necessity of appropriate animal models for the characterization of ARHL is of paramount importance. At present, only prosthetic treatment for ARHL is available; thus, finding a suitable animal model would facilitate the search for a causal treatment.

Previously, SAMP8 mice have been reported to be a promising and suitable mouse model for ARHL due to their accelerated aging and similarity to many aspects of human ARHL (Marie et al., 2017). By analyzing the age-related decline in hearing sensitivity of SAMP8 mice in the first study, a significant increase in threshold variability was observed over age. A surprising finding was that the large variability of threshold loss did not conclusively correlate to a loss of OHCs. Attempting to find a sensitive phenotypic marker for this age-related loss of function, it was hypothesized that decreased expression levels of $K_V7.4$, a K^+ channel critical for OHC survival, and $K_V7.1$, a key channel for K^+ circulation and secretion into the endolymph, represent potential candidates for a K^+ channel related phenotypic alteration preceding OHC loss and possibly accounting for the observed threshold variability. Membrane expression levels of $K_V7.4$ were found to be decreased in mice with ABR thresholds allocated to the upper quartile compared with those in the lower quartile; in particular, differences in $K_V7.4$ expression were found to be congruent with the persistent ABR threshold differences between these groups. Based on these observations, we suggest that diminished expression levels of $K_V7.4$ in OHCs may be causative for auditory threshold variability and threshold progression of SAMP8 mice (Peixoto Pinheiro et al., 2021).

Dysfunctional or reduced activity of $K_V7.4$ has previously been associated with genetic, noise-induced, and age-related hearing loss (Van Eyken et al., 2007; Marchetta et al., 2020; Wang et al., 2021); thus, maintaining $K_V7.4$ expression in OHCs may provide a

novel therapeutic approach to treat ARHL and provide a proof-of-concept in the SAMP8 mouse model. Questioning the therapeutic potential of $K_V7.4$, we analyzed the hearing function of SAMP8 mice treated with a novel small-molecule $K_V7.4$ agonist termed ACOU085. Our results indicate an otoprotective effect of the $K_V7.4$ agonist that seems to delay age-related ABR threshold shifts and may protect from age-related OHC loss following repeated local administration in the SAMP8 mouse model of ARHL (Peixoto Pinheiro et al., 2022). This indicates that pharmaceutical targeting of $K_V7.4$ channels is a promising approach to decelerate or prevent ARHL before the progression of hair cell loss.

4.1 Variability in auditory functional decline of SAMP8 mice

Due to the similarities in auditory structure and physiology between mice and humans, the close evolutionary relationship of the genomes, genetic standardization, and relatively low husbandry costs, the mouse has been established as a useful and important model system for the study of the auditory system (Petit, 2006; Friedman et al., 2007; Brown et al., 2008; Bowl and Dawson, 2015). The SAMP8 strain is a commonly used mouse model to study several aging disorders, such as osteoporosis, cataracts, senile amyloidosis and brain atrophy (Akiguchi et al., 2017; Karuppagounder et al., 2017; Folch et al., 2018; Grinan-Ferre et al., 2018). Recently, SAMP8 mice have also been described as a suitable model to study ARHL due to their premature aging of the cochlea and their early progressive age-related decline in hearing thresholds (Menardo et al., 2012; Akiguchi et al., 2017; Marie et al., 2017; Peixoto Pinheiro et al., 2021).

In concordance with previous studies, in the presented study SAMP8 mice also showed a significant ABR threshold increase from juvenile to young adult and adult age (Figure 2, Peixoto Pinheiro et al. 2021). Benkafadar et al. (2019) compared the progression of ABR threshold increases in SAMP8 mice. They reported that SAMP8 mice developed ARHL after 1 month of age with a fast threshold progression increasing 5.0 dB per month over all frequencies compared to their senescence-accelerated mouse resistant 1 (SAMR1) control group (2.8 dB per month). Similar progressions have also been reported for the compound action potential (CAP) evoked by tone bursts at 20 kHz (Menardo et al., 2012). In the present study, a threshold increase of 3.6 dB per month was determined across all frequencies, which is 1.4 dB less as compared to previously reported progressions. Surprisingly, we also observed an age-

dependent increase in threshold variability for each age group, representing an early bifurcation of thresholds concluding a highly variable progression of age-related hearing loss (Figure 3, Peixoto Pinheiro et al. 2021). This observation confirmed previous findings by Benkafadar et al. (2019) and is reminiscent of the high variability in the progression of the ABR threshold found in, e.g., the SAMR1 strain, which represents normal senescence (Takeda et al., 1981). Focusing on thresholds at 1 month of age across all frequencies, Benkafadar et al. (2019) reported a mean ABR threshold range in SAMP8 mice of approximately 34 dB, which increased to 59 dB at 6 months of age. In comparison, in the present study, we observed a larger mean ABR threshold range of 63 dB in juvenile mice (1.5 months) in contrast to a smaller range of 45 dB in adult mice (6 months). Despite these differences, the variance in ABR thresholds within age groups proved comparable, e.g., at 8 and 16 kHz, the mean standard deviation of ABR thresholds was estimated to be 18.7 dB (n = 14, Benkafadar et al., 2019) compared to 19.8 dB (n = 22, Peixoto Pinheiro et al. 2021) in the present study. Unfortunately, further comparisons with data in the literature were not possible due to a limited number of studies describing age-related auditory function in SAMP8 mice or due to insufficient statistical reporting (Marie et al., 2017). Previous and current data underline the functional variability in the SAMP8 strain, which needs to be considered in the experimental design of future studies. Consequently, predictive biomarkers should be investigated to develop prognostic criteria to allow better selection of experimental SAMP8 groups.

The premature senescence of SAMP8 was previously linked to altered levels of antioxidant enzymes and an accumulation of ROS (Menardo et al., 2012). Mitochondria have been described as a source of ROS, which can cause DNA damage and apoptosis. On the other hand, the cellular respiratory function of mitochondria provides the cells with energy (Ames, 2006; Lee and Wei, 2012). This energy enables the inner ear to maintain the EP, assist motility in OHCs, perform synaptic activity and maintain spontaneous and sound-driven discharges of the auditory neurons in the spiral ganglion. Hair cells have a high demand for energy and therefore depend on efficient energy supply (Shin et al., 2007). In particular, K^+ channel require a high energy supply, which can be severely challenged by the accumulation of ROS (Peixoto Pinheiro et al., 2020). Previous studies have reported that voltage-gated K^+ channels are altered by oxidants both *in vivo* and *in vitro* (Ruppersberg et al., 1991; Cai and Sesti, 2009). Specifically, $K_V7.4$ known as the major conductance of OHCs is also

expressed in neuronal mitochondria, possibly regulating membrane potential and ROS production (Paventi et al., 2022). These observations suggest that, in parallel with OHC loss, decreased membrane expression of $K_V7.4$ channels in hair cells caused by ROS can serve as a potential predictor of the observed ABR threshold variability. Proceeding one step further, a possible pharmacological activation of these $K_V7.4$ channels may serve as a therapeutic approach and counteract cellular degeneration in the cochlea.

4.1.1 Degeneration of sensory hair cells is not an exclusive underlying factor of auditory threshold variability

Given the essential role of OHCs in the lower dynamic range of the cochlear amplifier, OHC loss is considered a major determinant of age-related threshold shifts (Liberman and Kiang, 1978; Liberman and Beil, 1979; Dallos, 2008). Hair cell ablation experiments in rats using the ototoxic industrial solvent styrene demonstrated that increasing OHCs loss resulted in a CAP threshold shift of up to 40 dB with a permanent increase of approximately 6 dB per 10% OHC loss (Chen et al., 2008). This observation is consistent with the results obtained in the present study, showing an increase in threshold shifts in the high-frequency range of approximately 7.5 dB per 10% OHC loss (Figure 5, Peixoto Pinheiro et al. 2021). In addition, mean cytocochleograms of SAMP8 mice showed the typical progression of age-related OHC loss, with an initial loss observed in the middle turn of young adult mice followed by a progression toward the basal region (Figure 5, Peixoto Pinheiro et al. 2021). As age increased, a further progression of OHC loss of up to 40% was observed. This observation confirms OHC loss as an important predictor of age-related ABR threshold loss. However, despite the persisting ABR threshold difference between mice allocated to the lower and upper quartiles (Figure 6a, Peixoto Pinheiro et al. 2021), OHC loss was comparable between these groups (Figure 6b, Peixoto Pinheiro et al. 2021). Therefore, in addition to OHC loss further factors need to be considered to explain the observed threshold variability in SAMP8 mice. Indeed, IHC loss has been demonstrated as another important histologic predictor of human ARHL in both high- and low-frequency regions (Wu et al., 2020). However, in the SAMP8 mouse, IHC loss did not appear as a predictor of age-related ABR threshold loss, as the quantification of IHC loss remained rather negligible for all age groups (Figure 6B, Peixoto Pinheiro et al. 2021). This observation confirmed previous findings of Menardo et al. (2012) as they did not observe IHC loss at least until 7 months of age in SAMP8 mice. In addition,

several previous studies in other animal models such as in chinchillas report that even a selective loss of 70% of IHCs did not significantly change ABR thresholds (Jock et al., 1996; El-Badry and McFadden, 2009). Furthermore, Lobarinas et al. (2013) found that after treatment with carboplatin, an ototoxic drug that selectively damages the IHC along the entire cochlear length, a negligible increase in threshold shift was observed until the IHC loss exceeded 80%. These findings indicate that in the SAMP8 model ABR thresholds are not influenced by the relatively low amount of IHC loss (< 10%). Within the last decades, afferent synapses have been suggested as a highly vulnerable structure. Loss of the afferent synapse has been shown to precede IHC loss in various pathogenic insults (Stamataki et al., 2006; Sergeyenko et al., 2013; Wu et al., 2019). Consequently affecting the ability to understand speech in noise (Badri et al., 2011; Vermiglio et al., 2012). Nonetheless, the effect of afferent fiber loss on ABR thresholds in mouse and guinea pig models was insignificant, as no changes were observed in ABR thresholds despite a significant loss of approximately 50% of afferent fibers (Kujawa and Liberman, 2009; Lin et al., 2011b).

Even though OHC loss in the SAMP8 mice of the present study has been confirmed as an important predictor for the age-related ABR threshold loss, further age-related factors may contribute to the observed threshold variability. Thus, damage to other structures or phenotypic changes could influence the progression of ABR threshold variability in SAMP8 mice.

4.1.2 Altered $K_V7.4$ and $K_V7.1$ expression as potential predictors of ARHL

While the loss of both OHC and IHC has been identified as the most relevant human otopathological predictor of ARHL in both high- and low-frequency regions, other age-related factors are needed to fully explain the functional decline in human ARHL (Wu et al., 2020). These unconsidered effects may be found, for example, in the phenotype of the surviving sensory hair cells or in other functionally relevant structures such as the SV.

K^+ channels are essential to function and survival of OHCs since the hair cell conductance current is carried by K^+ ions (Spicer and Schulte, 1991; Schulte and Steel, 1994; Spicer and Schulte, 1996). This current drives the electromotility of OHCs (Ashmore and Gale, 2004), with $K_V7.4$ maintaining the OHC receptor potential (Kubisch et al., 1999; Beisel et al., 2000; Kharkovets et al., 2000; Nouvian et al., 2003; Oliver et al., 2003; Holt et al., 2007). Although $K_V7.4$ has been reported to be expressed

in IHCs (Oliver et al., 2003), this was not demonstrated in this study. Previous studies have shown that impaired membrane expression of $K_V7.4$ in OHCs leads to progressive hearing loss (Jentsch, 2000; Kharkovets et al., 2006; Gao et al., 2013; Carignano et al., 2019). $K_V7.4$ KO mice have been shown to suffer from progressive degeneration of OHCs and progressive hearing loss (Kharkovets et al., 2006; Carignano et al., 2019). Based on these previous observations, diminished levels of $K_V7.4$ expression in OHCs may be an underlying cause of the observed ABR threshold variability in SAMP8 mice. Interestingly, $K_V7.4$ membrane expression appeared to be reduced in mice with ABR thresholds allocated to the upper quartile (Figure 8A, Peixoto Pinheiro et al. 2021). Moreover, the persistent ABR threshold difference over age between the lower and upper quartiles (Figure 6a, Peixoto Pinheiro et al. 2021) was found to be congruent with the persistent and increasing differences between these groups in $K_V7.4$ expression over age, with larger differences in the middle and midbasal turns (Figure 9a, Peixoto Pinheiro et al. 2021).

Another essential factor for maintaining auditory function is the recycling of K^+ from OHCs to the endolymph. K^+ is the main charge carrier for sensory transduction and facilitates the electromotility of OHCs (Wangemann, 2006; Nin et al., 2016). Marginal cells of the SV are responsible for the secretion of K^+ to the endolymph. The major component of this conductive pathway in the K^+ recycling circuit is the voltage-dependent K^+ channel $K_V7.1$ located in the apical cell membrane of the marginal cells. $K_V7.1$ mediated secretion of K^+ into the endolymph generates and maintains the EP (Wangemann et al., 1995; Wangemann, 2006). Dysfunction or loss of $K_V7.1$ has been shown to impair K^+ secretion into the endolymph, leading to a defect in endolymph production accompanied by a collapse of Reissner's membrane and a collapse of the endolymphatic space (Casimiro et al., 2001). Mice with a decrease in $K_V7.1$ membrane expression presented SV atrophy accompanied by profound sensorineural hearing loss (Yang et al., 2013). Taking these previous studies into account, $K_V7.1$ membrane expression in the SV of SAMP8 mice was hypothesized to be another potential underlying cause of the observed ABR threshold variability. However, no correlation between $K_V7.1$ expression and age was observed in mice assigned to either quartile (Figure 9B, Peixoto Pinheiro et al. 2021).

Many K^+ channels, including voltage-gated channels such as $K_V7.4$ and $K_V7.1$ have a high energy demand to maintain the continuous recycling processes to ensure proper membrane expression. This energy demand makes K^+ channels vulnerable to

oxidative stress and primary targets of ROS accumulation (Peixoto Pinheiro et al., 2020). Interaction of ROS with K^+ channels can cause modifications of membrane currents, thereby inducing alterations of signaling mechanisms causing changes in channel activity or gene expression (Ruppersberg et al., 1991; Matalon et al., 2003; Cai and Sesti, 2009). Given that the premature senescence of SAMP8 was previously linked to altered levels of antioxidant enzymes and an accumulation of ROS (Menardo et al., 2012), reduced membrane expression of $K_V7.4$ and $K_V7.1$ caused by ROS accumulation may be potential predictors of the observed ABR threshold variability in SAMP8 mice, preceding the observed age-related OHC loss. For this reason, compromised membrane expression of these two K^+ channels, in particular $K_V7.4$, is a potential predictor of the observed ABR threshold variability in SAMP8 mice, possibly preceding age-related OHC loss.

The loss of sensory hair cells and auditory function in ARHL are not attributable to a single cause; therefore, the possibility that other cellular or subcellular predictors may have an impact on the progression of ABR threshold variability in SAMP8 mice cannot be excluded. Degeneration of SGNs can be observed both in human and animal models of ARHL and have a potential role in the prediction of auditory threshold loss. Previous studies have shown that neuronal loss precedes the degeneration of IHCs (Viana et al., 2015; Wu et al., 2019). Furthermore, Menardo et al. (2012) reported an SGN loss of approximately 20% by 6 months of age in SAMP8 mice. However, it was previously reported that neuronal loss in this magnitude did not lead to elevated ABR thresholds (Schuknecht and Woellner, 1955; Kujawa and Liberman, 2009). Even a significant loss of 50% of SGNs does not affect ABR thresholds in mice and guinea pigs (Kujawa and Liberman, 2009; Lin et al., 2011b). Therefore, SGN loss does not predict ABR threshold elevation in animal models or audiometric thresholds in humans but very likely contributes to a significant decrease in speech discrimination, especially in noisy environments (Schuknecht and Woellner, 1955; Kujawa and Liberman, 2009; Wu et al., 2019).

Furthermore, an underlying genetic divergence would also be a possible cause for the observed variability of ABR thresholds. Attempting to investigate this, DNA samples were collected from SAMP8 mice allocated to the lower quartile and upper quartile (data not shown). After sequencing and initial analysis by QBiC (Center for Quantitative Biology, Tübingen), genetic differences were analyzed between these two groups. To exclude sequencing errors, strain-specific genes were detected. However, no apparent

sequence differences were found between the lower or upper quartiles for ARHL susceptibility genes or other known genetic candidate genes for hearing loss. Other genomic differences cannot be excluded but were beyond the scope of this project.

Although age-related predictors may exist the integrity of voltage-gated K^+ channels, particularly $K_V7.4$, should be considered as a phenotypic marker for elevated thresholds in SAMP8 preceding OHC loss. The observed $K_V7.4$ related OHC phenotype might be explained by the accumulated metabolic challenges, such as a decrease in antioxidant levels or an increase in ROS production which is a typical feature of SAMP8 mice. Therefore, balancing the generation of ROS and antioxidant defense mechanisms or pharmaceutical targeting of $K_V7.4$ might be a promising approach to slow or prevent ARHL before the inevitable loss of hair cells.

4.2 Drug delivery of a $K_V7.4$ agonist as an inner ear therapeutic

Dysfunctional $K_V7.4$ causes progressive degeneration of OHCs and hearing loss (Kharkovets et al., 2006; Carignano et al., 2019; Noh et al., 2022). Interestingly, Kharkovets et al. (2006) showed that residual $I_{K,n}$ currents in a mouse model with a heterozygous $K_V7.4$ mutation were sufficient to significantly delay hair cell degeneration and hearing loss. Furthermore, *in vivo* outer hair cell gene editing ameliorated progressive hearing loss in a dominant-negative KCNQ4 mouse model with a mutant allele carrying a common pathogenic human DFNA2 mutation (Noh et al., 2022). However, loss of OHC was not sufficiently prevented and protection of auditory thresholds was only partial (Noh et al., 2022). Nevertheless, this study provides an important proof-of-concept that enhancing $K_V7.4$ channel activity can restore hearing function in a murine model of compromised $K_V7.4$ function. In this regard, treatment with $K_V7.4$ agonists may potentiate moderate $I_{K,n}$ currents, potentially alleviating functional hearing loss and OHC loss related to compromised function of $K_V7.4$ (Leitner et al., 2012). One objective of the present study was to investigate the effects of $K_V7.4$ activation on age-related decline of hearing thresholds and OHC loss in the SAMP8 model. Inner ear therapeutics targeting the cochlea for protecting or enhancing hearing face many obstacles, such as the route of administration. Therefore, two different approaches of administration were investigated, with ACOU085 administered locally via transtympanic application and ACOU082 applied systemically via topical application.

4.2.1 Limitations of drug delivery to the cochlear

The development of inner ear therapeutics is undergoing tremendous progress with a wide range of different delivery methods. The spiral organization of the cochlea establishes an additional challenge for drug delivery because equal distribution of therapeutics cannot be assumed. Salt and Plontke (2005) have previously shown that the distribution of a drug along the cochlea is dominated by passive diffusion, resulting in a large longitudinal gradient from base to apex as the drug enters the cochlea through the round window. Therefore, the concentration of the drug is highest in the basal turn of the cochlea (high-frequency region) and probably does not reach the apical turn (low-frequency region). Computer modelling of drug pharmacokinetics with single injection strategies shows drug clearance into the middle ear and steep concentration gradients of the drug in the inner ear, resulting in rapid clearance of the drug from the basal turns of the cochlea (Plontke and Salt, 2006). Drug removal from the cochlear compartments can occur through several routes, such as through the Eustachian tube, via the vasculature, or via the lymphatics. In the present study, we not only observed a successful diffusion of ACOU085 into the cochlea but also an increase in ACOU085 concentration in the cochlear perilymph and cochlear tissue depending on the administered dose. The ability of small molecules to passively pass biological membranes has been shown to strongly depend on the lipid solubility and polar properties of the molecule (Egan et al., 2000). A greater lipophilicity generally correlated with a greater ability to cross cell membranes but also resulted in more rapid removal from the blood (Salt and Plontke, 2005; Nyberg et al., 2019). These factors may account for the temporal differences observed in the therapeutic window between 0.6% and 6.0% w/v concentrations. Compared to previous pharmacokinetic studies aspirating perilymph from the basal turn of the scala tympani, in this study, perilymph was sampled through the RWM. Salt et al. (2003) showed that perilymph samples taken through the RWM are highly contaminated with cerebrospinal fluid (CSF) and thus influence the sample concentration. However, it was also shown that samples with a volume of 1 µl taken through the RWM contained approximately 80% perilymph (Salt et al., 2003), and a greater volume than 2 µl contained more CSF than perilymph. In the present study, only a maximum of 2 µl of perilymph was taken, meaning that the contamination with CSF remained small. Furthermore, samples were taken postmortem and outside of the temporal bone, and leakage due to CSF pressure was minimal and therefore did not influence the drug concentration.

It has previously been shown that administration of a drug solution through TM into the middle ear allows drugs to reach and influence the function of the inner ear (Ersner et al., 1951; Salt and Hirose, 2018), even though this minimally invasive application relies on diffusion through the RWM. However, this method also presents some limitations, such as the lack of control of drug concentration reaching RWM as well as the duration of contact of the drug with the RWM, which are important factors in determining the drug level achieved in the cochlea (Salt and Plontke, 2005). Another limitation of transtympanic injection is perforation of the TM, which can cause scarring that results in conductive hearing loss. To avoid this, an administration interval of 1 month was chosen in the electrophysiological study to potentially minimize the effects of TM scarring (Pannu et al., 2011; Gupta et al., 2019). Therefore, the estimated therapeutic window within a 7- to 14-day time frame was less than or equal to half of the 1-month treatment interval. As a result, this pharmacokinetic limitation presented an additional challenge to the investigated effects of $K_V7.4$ activation on age-related decline in the SAMP8 model. Compared to oral administration, this drug delivery approach has the advantage of reducing systemic side effects in long-term applications. In a clinical trial, the drug concentration and delivery method will likely substantially differ from those demonstrated in experimental animals. As drug concentrations in the inner ear fluids depend on dispersal by diffusion, they are influenced by the different scala lengths and volumes of the inner ear in different species (Salt and Plontke, 2005).

Systemic approaches offer the advantages of ease of drug delivery and the potential for repeated dosing to enhance therapeutic benefit. However, the challenges include potentially lower drug penetration due to the presence of the BLB separating the inner ear from systemic circulation (Jahnke, 1980) and therefore not reaching its intended target cells in the cochlea in an effective concentration. In addition to the water solubility of the substance or carrier, lipophilicity must be present to ensure distribution in the blood as well as transport through the cell membranes (Mannhold, 2005; Nyberg et al., 2019). However, greater lipophilicity results in more rapid clearance of the compound from blood (Salt and Plontke, 2005). This limitation can be counteracted by increasing the frequency of applications. In the ACOU082 study, the pharmacokinetic study performed by Synovo (Tübingen) showed a decline of ACOU082 concentration below the LLOQ within 84 hours. Consequently, the frequency of administration of ACOU082, compared to ACOU085, was increased to a biweekly administration into the external ear canal to ensure an effective target engagement. Nevertheless,

systemic drug administration can cause off-target side effects, such as an exacerbation of hearing loss instead of its amelioration, especially if high doses are needed to provide protection (Rybak et al., 2019). However, this was not observed in the course of this study.

Overall, limited access to the inner ear presents one of the greatest challenges for inner ear drug delivery. Local drug delivery routes for inner ear disorders involve a perforation procedure that is invasive and can potentially result in persistent or transient hearing loss. However, to date, the bioavailability of the drug demonstrates higher success with local delivery than with traditional systemic delivery.

4.2.2 K_V7.4 agonist as a therapeutic approach against age-related hearing loss

Small-molecule K_V7.4 agonists have been suggested as potential treatment strategy for hearing loss for over a decade (Wulff et al., 2009; Rim et al., 2021). To the best of our knowledge, we have demonstrated for the first time that a novel small-molecule K_V7.4 agonist can functionally protect hearing function and OHC loss in an *in vivo* model of ARHL. A significant protective effect at the functional and morphological levels was found in the SAMP8 mouse model after 3 administrations of ACOU085 at the 6.0% w/v dose (Figure 3 and 5, Peixoto Pinheiro et al. 2022). Significant reductions in click-evoked ABR threshold shifts were evident in the higher dose group compared to the vehicle-treated ears (Figure 3d, Peixoto Pinheiro et al. 2022). A preliminary analysis of ABR input–output functions showed no additional suprathreshold effects on wave latency or function slope but only differences in thresholds. This suggests that OHCs were the main target of treatment, which maintained their function and increased their survival rate over age. In line with these electrophysiological data, cytocochleograms showed reduced OHC loss for ACOU085-treated ears compared with vehicle controls, which was mainly observed in the high frequency range (> 8 kHz).

Previously, we observed threshold variability between SAMP8 mice, which was not explained by OHC loss alone (Peixoto Pinheiro et al., 2021). Therefore, the reduction in OHC loss in the present within-subject study can largely be attributed to ACOU085 treatment, which most likely counteracted the negative effects of oxidative stress in SAMP8 mice on OHC survival. Furthermore, the therapeutic window was estimated to be between 7 and 14 days after a single application (Figure 1, Peixoto Pinheiro et al. 2022), while SAMP8 mice received ACOU085 at 1-month intervals, i.e., the therapeutic

window was not sustained during the experimental period of 3 months. Inner ear drug delivery research has been focusing on local drug delivery methods, but in the case of transtympanic application, there are some limitations, such as TM perforation for each administration that could confound the study results. Due to solubility issues, ACOU085 at 6.0% w/v had to be applied using a syringe with a diameter that was an order of magnitude larger than that for the contralateral vehicle application, resulting in greater perforation of the tympanic membrane. Previous studies have shown that the size of the perforation is directly related to the degree of conductive hearing loss (Pannu et al., 2011; Gupta et al., 2019). Considering the pharmacokinetic restriction reducing drug exposure to half or less than half of the experimental time, the perforation of the TM causing scarring and the large variability in age-related auditory decline of the SAMP8 model, the observed protective effects appear very encouraging and have considerable potential for further improvement, e.g., by a different drug delivery route.

To determine whether a different approach of drug delivery was able to overcome these challenges, the $K_V7.4$ agonist ACOU082 was applied via topical administration into the external auditory canal of SAMP8 mice. In a pharmacokinetic study, the concentration of ACOU082 was found to decline below the LLOQ within 84 hours. Therefore, ACOU082 or vehicle was administered bilaterally into the external auditory canal of SAMP8 mice twice per week. Despite the increased frequency of administration and the modified formulation to allow topical administration, no significant functional or morphological protection of OHCs could be observed. As mentioned before, a large variability in age-related decline was reported in SAMP8 mice (Peixoto Pinheiro et al., 2021), which could be one of the contributing factors to the nonsignificant group differences in the ACOU082 study. When comparing click-evoked ABR threshold shifts at 45 days of age (preT) of both treatment groups and the vehicle control group, more elevated mean threshold shifts were detected in the 17% and 27.5% groups. This difference could also be observed in the toneburst-evoked threshold shifts. Note that due to planning issues, the experiments of the 17% and vehicle groups were conducted at a different time and presumably with a different litter than the 27.5% group, which may have introduced some confounding variables to between-subject comparisons. Furthermore, a pharmacokinetic study after 5 months would have been necessary to reach conclusions about the concentration of ACOU082 in the cochlear perilymph and cochlear tissue as well as potential drug accumulation

over the course of treatment in other tissues. Finally, functional data analysis averaged ABR thresholds from two ears for each mouse, since the bilateral topical application and the lack of between-ear bias at baseline did not justify a choice of ear. Further analysis of within- and between-subject comparisons depending on the choice of ear may, however, reveal potential trends in the effect of treatment. And considering the large variability in age-related decline of SAMP8 mice, a larger sample size would probably have been required to reach sufficient statistical power given the potentially large variance of drug exposure due to the administration route. While the topical administration facilitated a systemic drug delivery and prevented damage to the TM, the current data could not verify the protection of OHCs functionally or morphologically. Still, the aforementioned methodological limitations may have hindered the detection of a protective effect akin to that of ACOU085.

Taken together, this study showed that the local administration of the novel small-molecule $K_V7.4$ agonist ACOU085 significantly reduced age-related ABR threshold shifts as well as OHC loss in the ARHL mouse model SAMP8. Thus, these findings suggest that pharmacological activation of $K_V7.4$ appears to be a promising approach to prevent and decelerate age-related decline of auditory function and morphological loss of OHCs.

4.3 Conclusion

The work presented here uncovered new insights into the novel ARHL mouse model SAMP8 as well as a potential therapeutic approach for ARHL. First, we confirmed that SAMP8 mice presented the typical progression of ARHL but concomitantly exhibited a large variability in age-related decline. Loss of OHC in SAMP8 mice could be confirmed as an important predictor for the age-related ABR threshold loss. However, the progression of ABR threshold variability in SAMP8 mice might be influenced by damage to other structures or phenotypic changes. We suggest that the integrity of voltage-gated K^+ channels, particularly $K_V7.4$, should be considered as phenotypic marker for elevated thresholds in SAMP8 preceding OHC loss (Peixoto Pinheiro et al. 2021). Therefore, pharmaceutical targeting of $K_V7.4$ might be a promising approach to prevent or decelerate ARHL. However, limited access to the inner ear presents one of the greatest challenges for inner ear drug delivery. For the first time *in vivo*, we were able to demonstrate that transtympanic administration of a novel, small molecule $K_V7.4$ agonist ACOU085 was able to functionally and morphologically protect OHCs against

age-related degeneration in the SAMP8 mouse model of ARHL (Peixoto Pinheiro et al. 2022). Due to the limitations of local drug delivery routes for inner ear disorders involving an invasive perforation procedure, which potentially results in conductive hearing loss and confound study results, drug delivery using systemic approaches may be an attractive option. However, in the present study, topical administration of the small molecule $K_V7.4$ agonist ACOU082 could not show functional or morphological protection of OHCs, but these findings may be limited by methodological caveats. Overall, the present findings provide a promising approach to decelerating age-related auditory decline by pharmacologically activating the $K_V7.4$ channel and thereby protecting OHCs. Targeting K^+ channels pharmaceutically to enable rapid recycling by activators thus has the potential to slow or even prevent ARHL before the inevitable progression of cell and structural degeneration.

5. References

Adachi, N., Yoshida, T., Nin, F., Ogata, G., Yamaguchi, S., Suzuki, T., et al. (2013). The mechanism underlying maintenance of the endocochlear potential by the K+ transport system in fibrocytes of the inner ear. *J Physiol* 591(18), 4459-4472. doi: 10.1113/jphysiol.2013.258046.

Akiguchi, I., Pallas, M., Budka, H., Akiyama, H., Ueno, M., Han, J., et al. (2017). SAMP8 mice as a neuropathological model of accelerated brain aging and dementia: Toshio Takeda's legacy and future directions. *Neuropathology* 37(4), 293-305. doi: 10.1111/neup.12373.

Ames, B.N. (2006). Delaying the Mitochondrial Decay of Aging. *Ann N Y Acad Sci* 1019, 406-411.

Ashmore, J. (2008). Cochlear outer hair cell motility. *Physiol Rev* 88(1), 173-210. doi: 10.1152/physrev.00044.2006.

Ashmore, J., and Gale, J. (2004). The cochlear amplifier. *Curr Biol* 14(11), 403-404. doi: 10.1016/j.cub.2004.05.025.

Badri, R., Siegel, J.H., and Wright, B.A. (2011). Auditory filter shapes and high-frequency hearing in adults who have impaired speech in noise performance despite clinically normal audiograms. *J Acoust Soc Am* 129(2), 852-863. doi: 10.1121/1.3523476.

Baker, K., and Staecker, H. (2012). Low dose oxidative stress induces mitochondrial damage in hair cells. *Anat Rec (Hoboken)* 295(11), 1868-1876. doi: 10.1002/ar.22594.

Balaban, R.S., Nemoto, S., and Finkel, T. (2005). Mitochondria, oxidants, and aging. *Cell* 120(4), 483-495. doi: 10.1016/j.cell.2005.02.001.

Barhanin, J., Lesage, F., Guillemare, E., Fink, M., Lazdunski, M., and Romey, G. (1996). K(V)LQT1 and lsK (minK) proteins associate to form the I(Ks) cardiac potassium current. *Nature* 384(6604), 78-80. doi: 10.1038/384078a0.

Beckman, K.B., and Ames, B.N. (1998). The Free Radical Theory of Aging Matures. *Phys Review* 78.

Beisel, K.W., Nelson, N.C., Delimont, D.C., and Fritzsch (2000). Longitudinal gradients of KCNQ4 expression in spiral ganglion and cochlear hair cells correlate with progressive hearing loss in DFNA2.

Benkafadar, N., Francois, F., Affortit, C., Casas, F., Ceccato, J.C., Menardo, J., et al. (2019). ROS-Induced Activation of DNA Damage Responses Drives Senescence-Like State in Postmitotic Cochlear Cells: Implication for Hearing Preservation. *Mol Neurobiol* 56(8), 5950-5969. doi: 10.1007/s12035-019-1493-6.

Beurg, M., Schimmenti, L.A., Koleilat, A., Amr, S.S., Oza, A., Barlow, A.J., et al. (2021). New Tmc1 Deafness Mutations Impact Mechanotransduction in Auditory Hair Cells. *J Neurosci* 41(20), 4378-4391. doi: 10.1523/JNEUROSCI.2537-20.2021.

Bielefeld, E.C., Tanaka, C., Chen, G.D., and Henderson, D. (2010). Age-related hearing loss: is it a preventable condition? *Hear Res* 264(1-2), 98-107. doi: 10.1016/j.heares.2009.09.001.

Boettger, T., Hübner, C.A., Maier, H., Rust, M.B., Beck, F.X., and Jentsch, T.J. (2002). Deafness and renal tubular acidosis in mice lacking the K-Cl co-transporter Kcc4. *Nature* 416**,** 874-878.

Bohne, B.A., Gruner, M.M., and Harding, G.W. (1990). Morphological correlates of aging in the chinchilla cochlea. *Hearing research* 48(1-2)**,** 79-91.

Borgini, M., Mondal, P., Liu, R., and Wipf, P. (2021). Chemical modulation of Kv7 potassium channels. *RSC Med Chem* 12(4)**,** 483-537. doi: 10.1039/d0md00328j.

Bös, M. (2018). *Cyclic amides, acetamides and ureas useful as potassium channel openers*. DE patent application.

Bowl, M.R., and Dawson, S.J. (2015). The mouse as a model for age-related hearing loss - a mini-review. *Gerontology* 61(2)**,** 149-157. doi: 10.1159/000368399.

Bowl, M.R., and Dawson, S.J. (2019). Age-Related Hearing Loss. *Cold Spring Harb Perspect Med* 9(8). doi: 10.1101/cshperspect.a033217.

Bredberg, G. (1967). The human cochlea during development and ageing. *The Journal of Laryngology & Otology* 81(7)**,** 739-758.

Brown, S.D., Hardisty-Hughes, R.E., and Mburu, P. (2008). Quiet as a mouse: dissecting the molecular and genetic basis of hearing. *Nat Rev Genet* 9(4)**,** 277-290. doi: 10.1038/nrg2309.

Cai, S.Q., and Sesti, F. (2009). Oxidation of a potassium channel causes progressive sensory function loss during aging. *Nat Neurosci* 12(5)**,** 611-617. doi: 10.1038/nn.2291.

Carignano, C., Barila, E.P., Rias, E.I., Dionisio, L., Aztiria, E., and Spitzmaul, G. (2019). Inner Hair Cell and Neuron Degeneration Contribute to Hearing Loss in a DFNA2-Like Mouse Model. *Neuroscience* 410**,** 202-216. doi: 10.1016/j.neuroscience.2019.05.012.

Casimiro, M.C., Knollmann, B.C., Ebert, S.N., Vary, J.C., Jr., Greene, A.E., Franz, M.R., et al. (2001). Targeted disruption of the Kcnq1 gene produces a mouse model of Jervell and Lange-Nielsen Syndrome. *Proc Natl Acad Sci U S A* 98(5)**,** 2526-2531. doi: 10.1073/pnas.041398998.

Chen, G.D., Tanaka, C., and Henderson, D. (2008). Relation between outer hair cell loss and hearing loss in rats exposed to styrene. *Hear Res* 243(1-2)**,** 28-34. doi: 10.1016/j.heares.2008.05.008.

Chen, M.A., Webster, P., Yang, E., and Linthicum Jr, F.H. (2006). Presbycusic neuritic degeneration within the osseous spiral lamina. *Otology & Neurotology* 27(3)**,** 316-322.

Chern, A., and Golub, J.S. (2019). Age-related Hearing Loss and Dementia. *Alzheimer Dis Assoc Disord* 33(3)**,** 285-290. doi: 10.1097/WAD.0000000000000325.

Clark, S., Antell, A., and Kaufman, K. (2015). New antiepileptic medication linked to blue discoloration of the skin and eyes. *Ther Adv Drug Saf* 6(1)**,** 15-19. doi: 10.1177/2042098614560736.

Coucke, P.J., Van Hauwe, P., Kelley, P.M., Kunst, H., Schatteman, I., Van Velzen, D., et al. (1999). Mutations in the KCNQ4 gene are responsible for autosomal dominant deafness in four DFNA2 families. *Hum Mol Genet* 8(7)**,** 1321-1328. doi: 10.1093/hmg/8.7.1321.

Crowe, S.J., Guild, S.R., and Polvogt, L.M. (1934). Observations on the pathology of high-tone deafness. *The Journal of Nervous and Mental Disease* 80(4), 480.

Dallos, P. (1966). Overview: cochlear neurobiology. *The cochlea*, 1-43.

Dallos, P. (2008). Cochlear amplification, outer hair cells and prestin. *Curr Opin Neurobiol* 18(4), 370-376. doi: 10.1016/j.conb.2008.08.016.

Egan, W.J., Merz, K.M., Jr., and Baldwin, J.J. (2000). Prediction of drug absorption using multivariate statistics. *J Med Chem* 43(21), 3867-3877. doi: 10.1021/jm000292e.

El-Badry, M.M., and McFadden, S.L. (2009). Evaluation of inner hair cell and nerve fiber loss as sufficient pathologies underlying auditory neuropathy. *Hear Res* 255(1-2), 84-90. doi: 10.1016/j.heares.2009.06.003.

Ersner, M.S., Spiegel, E.A., and Alexander, M.H. (1951). Transtympanic injection of anesthetics for the treatment of Menière's syndrome. *AMA Arch Otolaryngol.* 54(1), 43-52.

Erway, L.C., Willott, J.F., Archer, J.R., and Harrison, D.E. (1993). Genetics of age-related hearing loss in mice: I. Inbred and F1 hybrid strains. *Hear Res* 65, 125-132.

Felder, E., and Schrott-Fischer, A. (1995). Quantitative evaluation of myelinated nerve fibres and hair cells in cochleae of humans with age-related high-tone hearing loss. *Hearing research* 91(1-2), 19-32.

Fernandez, K.A., Jeffers, P.W., Lall, K., Liberman, M.C., and Kujawa, S.G. (2015). Aging after noise exposure: acceleration of cochlear synaptopathy in "recovered" ears. *Journal of Neuroscience* 35(19), 7509-7520.

Fetoni, A.R., Picciotti, P.M., Paludetti, G., and Troiani, D. (2011). Pathogenesis of presbycusis in animal models: a review. *Exp Gerontol* 46(6), 413-425. doi: 10.1016/j.exger.2010.12.003.

Fetoni, A.R., Pisani, A., Rolesi, R., Paciello, F., Viziano, A., Moleti, A., et al. (2022). Early Noise-Induced Hearing Loss Accelerates Presbycusis Altering Aging Processes in the Cochlea. *Front Aging Neurosci* 14, 803973. doi: 10.3389/fnagi.2022.803973.

Fettiplace, R., and Hackney, C.M. (2006). The sensory and motor roles of auditory hair cells. *Nat Rev Neurosci* 7(1), 19-29. doi: 10.1038/nrn1828.

Fischer, N., Johnson Chacko, L., Glueckert, R., and Schrott-Fischer, A. (2020). Age-Dependent Changes in the Cochlea. *Gerontology* 66(1), 33-39. doi: 10.1159/000499582.

Flood, J.F., and Morley, J.E. (1998). Learning and memory in the SAMP8 mouse. *Neurosci Biobehav Rev* 22(1), 1-20. doi: 10.1016/s0149-7634(96)00063-2.

Folch, J., Busquets, O., Ettcheto, M., Sanchez-Lopez, E., Pallas, M., Beas-Zarate, C., et al. (2018). Experimental Models for Aging and their Potential for Novel Drug Discovery. *Curr Neuropharmacol* 16(10), 1466-1483. doi: 10.2174/1570159X15666170707155345.

Friedman, L.M., Dror, A.A., and Avraham, K.B. (2007). Mouse models to study inner ear development and hereditary hearing loss. *Int J Dev Biol* 51(6-7), 609-631. doi: 10.1387/ijdb.072365lf.

Frisina, D.R. (2001). Subcortical neural coding mechanisms for auditory temporal processing. *Hear Res* 158(1-2), 1-27. doi: 10.1016/s0378-5955(01)00296-9.

Frisina, D.R., and Frisina, R.D. (1997). Speech recognition in noise and presbycusis: relations to possible neural mechanisms. *Hearing Research* 106(1-2), 95-104. doi: 10.1016/s0378-5955(97)00006-3.

Frisina, R.D., and Zhu, X. (2010). Auditory sensitivity and the outer hair cell system in the CBA mouse model of age-related hearing loss. *Open Access Anim Physiol* 2, 9-16. doi: 10.2147/oaap.S7202.

Fuchs, P.A., and Murrow, B.W. (1992). Cholinergic inhibition of short (outer) hair cells of the chick's cochlea *J Neurosci* 12(3), 800-809. doi: 10.1523/JNEUROSCI.12-03-00800.1992.

Fujimoto, C., and Yamasoba, T. (2014). Oxidative stresses and mitochondrial dysfunction in age-related hearing loss. *Oxid Med Cell Longev* 2014, 582849. doi: 10.1155/2014/582849.

Fujimoto, C., and Yamasoba, T. (2019). Mitochondria-Targeted Antioxidants for Treatment of Hearing Loss: A Systematic Review. *Antioxidants (Basel)* 8(4). doi: 10.3390/antiox8040109.

Gao, Y., Yechikov, S., Vazquez, A.E., Chen, D., and Nie, L. (2013). Impaired surface expression and conductance of the KCNQ4 channel lead to sensorineural hearing loss. *J Cell Mol Med* 17(7), 889-900. doi: 10.1111/jcmm.12080.

Gates, G.A., Couropmitree, N., and Myers, R.H. (1999). Genetic Associations in Age-Related Hearing Thresholds. *Arch Otolaryngol Head Neck Surg* 125, 654-659.

Gates, G.A., and Mills, J.H. (2005). Presbycusis. *The Lancet* 366(9491), 1111-1120. doi: 10.1016/s0140-6736(05)67423-5.

GBD Hearing Loss Collaborators (2019). Hearing loss prevalence and years lived with disability, 1990-2019: findings from the Global Burden of Disease Study 2019. *Lancet* 397(10278), 996-1009. doi: 10.1016/S0140-6736(21)00516-X.

Géléoc, G.S., and Holt, J.R. (2014). Sound strategies for hearing restoration. *Science* 344(6184), 1241062. doi: 10.1126/science.1241062.

Goman, A.M., and Lin, F.R. (2018). Hearing loss in older adults - From epidemiological insights to national initiatives. *Hear Res* 369, 29-32. doi: 10.1016/j.heares.2018.03.031.

Gratton, M., Schmiedt, R., and Schulte, B. (1996). Age-related decreases in endocochlear potential are associated with vascular abnormalities in the stria vascularis. *Hearing research* 102(1-2), 181-190.

Gribkoff, V.K. (2003). The therapeutic potential of neuronal KCNQ channel modulators. *Expert Opin Ther Targets* 7(6), 737-748. doi: 10.1517/14728222.7.6.737.

Grinan-Ferre, C., Corpas, R., Puigoriol-Illamola, D., Palomera-Avalos, V., Sanfeliu, C., and Pallas, M. (2018). Understanding Epigenetics in the Neurodegeneration of Alzheimer's Disease: SAMP8 Mouse Model. *J Alzheimers Dis* 62(3), 943-963. doi: 10.3233/JAD-170664.

Gupta, S., Harshvardhan, R., and Samdani, S. (2019). To Study the Association of the Size and Site of Tympanic Membrane Perforation with the Degree of Hearing Loss. *Indian*

J Otolaryngol Head Neck Surg 71(Suppl 2), 1047-1052. doi: 10.1007/s12070-017-1102-9.

Halliwell, B. (1992). Reactive Oxygen Species and the Central Nervous System. *J Neurochem* 49(5).

Han, C., and Someya, S. (2013). Mouse models of age-related mitochondrial neurosensory hearing loss. *Mol Cell Neurosci* 55, 95-100. doi: 10.1016/j.mcn.2012.07.004.

Harman, D. (1956). Aging: a theory based on free radical and radiation chemistry. *J Gerontol*.

Helzner, E.P., Cauley, J.A., Pratt, S.R., Wisniewski, S.R., Zmuda, J.M., Talbott, E.O., et al. (2005). Race and sex differences in age-related hearing loss: the Health, Aging and Body Composition Study. *J Am Geriatr Soc* 53(12), 2119-2127. doi: 10.1111/j.1532-5415.2005.00525.x.

Henderson, D., Bielefeld, E.C., Harris, K.C., and Hu, B.H. (2006). The role of oxidative stress in noise-induced hearing loss. *Ear Hear* 27(1), 1-19. doi: 10.1097/01.aud.0000191942.36672.f3.

Henry, K.R., and Chole, R.A. (1980). Genotypic differences in behavioral, physiological and anatomical expressions of age-related hearing loss in the laboratory mouse: original papers travaux originaux. *Audiology* 19(5), 369-383.

Hewawasam, P., Gribkoff, V.K., Pendri, Y., Dworetzky, S.I., Meanwell, N.A., Martinez, E., et al. (2002). The synthesis and characterization of BMS-204352 (MaxiPost™) and related 3-fluorooxindoles as openers of maxi-K potassium channels. *Bioorganic & medicinal chemistry letters* 12(7), 1023-1026.

Holt, J.R., Stauffer, E.A., Abraham, D., and Geleoc, G.S. (2007). Dominant-negative inhibition of M-like potassium conductances in hair cells of the mouse inner ear. *J Neurosci* 27(33), 8940-8951. doi: 10.1523/JNEUROSCI.2085-07.2007.

Housley, G.D., and Ashmore, J.F. (1992). Ionic currents of outer hair cells isolated from the guinea-pig cochlea. *J Physiol* 448, 73-98. doi: DOI 10.1113/jphysiol.1992.sp019030.

Hunter, K.P., and Willott, J.F. (1987). Aging and the auditory brainstem response in mice with severe or minimal presbycusis. *Hear Res* 30(2-3), 207-218. doi: 10.1016/0378-5955(87)90137-7.

Ishiyama, G., Tokita, J., Lopez, I., Tang, Y., and Ishiyama, A. (2007). Unbiased stereological estimation of the spiral ligament and stria vascularis volumes in aging and Meniere's disease using archival human temporal bones. *J Assoc Res Otolaryngol* 8(1), 8-17. doi: 10.1007/s10162-006-0057-4.

Ison, J.R., Allen, P.D., and O'Neill, W.E. (2007). Age-related hearing loss in C57BL/6J mice has both frequency-specific and non-frequency-specific components that produce a hyperacusis-like exaggeration of the acoustic startle reflex. *J Assoc Res Otolaryngol* 8(4), 539-550. doi: 10.1007/s10162-007-0098-3.

Jahnke, K. (1980). The blood-perilymph barrier. *Arch Otorhinolaryngol* 228(1), 29-34. doi: 10.1007/bf00455891.

Jaumann, M., Dettling, J., Gubelt, M., Zimmermann, U., Gerling, A., Paquet-Durand, F., et al. (2012). cGMP-Prkg1 signaling and Pde5 inhibition shelter cochlear hair cells and hearing function. *Nat Med* 18(2), 252-259. doi: 10.1038/nm.2634.

Jentsch, T.J. (2000). Neuronal KCNQ potassium channels - physiology and role in disease *Nature Neuroscience* 1(1), 21-30. doi: Doi 10.1038/35036198.

Jock, B.M., Hamernik, R.P., Aldrich, L.G., Ahroon, W.A., Petriello, K.-L., and Johnson, A.R. (1996). Evoked-potential thresholds and cubic distortion product otoacoustic emissionsin the chinchilla following carboplatin treatment and noise exposure. *Hear Res* 96, 179-190.

Johnson, K.R., Erway, L.C., Cook, S.A., Willott, J.F., and Zheng, Q.Y. (1997). A major gene affecting age-related hearing loss in C57BL/6J mice. *Hear Res* 114, 83-92.

Johnsson, L.G., and Hawkins, J.E. (1972). Sensory and neural degeneration with aging, as seen in microdissections of the human inner ear. *Annals of Otology, Rhinology & Laryngology* 81(2), 179-193.

Kamil, R.J., Betz, J., Powers, B.B., Pratt, S., Kritchevsky, S., Ayonayon, H.N., et al. (2016). Association of Hearing Impairment With Incident Frailty and Falls in Older Adults. *J Aging Health* 28(4), 644-660. doi: 10.1177/0898264315608730.

Karlsson, K.K., Harris, J.R., and Svartengren, M. (1997). Description and Primary Results from an Audiometric Study of Male Twins. *Ear Hear* 18, 114-120.

Karuppagounder, V., Arumugam, S., Babu, S.S., Palaniyandi, S.S., Watanabe, K., Cooke, J.P., et al. (2017). The senescence accelerated mouse prone 8 (SAMP8): A novel murine model for cardiac aging. *Ageing Res Rev* 35, 291-296. doi: 10.1016/j.arr.2016.10.006.

Kawashima, Y., Geleoc, G.S., Kurima, K., Labay, V., Lelli, A., Asai, Y., et al. (2011). Mechanotransduction in mouse inner ear hair cells requires transmembrane channel-like genes. *J Clin Invest* 121(12), 4796-4809. doi: 10.1172/JCI60405.

Keithley, E.M. (2019). Pathology and mechanisms of cochlear aging. *J Neurosci Res* 98(9), 1674-1684. doi: 10.1002/jnr.24439.

Keithley, E.M., Canto, C., Zheng, Q.Y., Fischel-Ghodsian, N., and Johnson, K.R. (2004). Age-related hearing loss and the ahl locus in mice. *Hearing Research* 188(1-2), 21-28. doi: 10.1016/s0378-5955(03)00365-4.

Keithley, E.M., Canto, C., Zheng, Q.Y., Wang, X., Fischel-Ghodsian, N., and Johnson, K.R. (2005). Cu/Zn superoxide dismutase and age-related hearing loss. *Hear Res* 209(1-2), 76-85. doi: 10.1016/j.heares.2005.06.009.

Keithley, E.M., and Feldman, M.L. (1979). Spiral Ganglion Cell Counts in an Age-graded Series of Rat Cochleas. *J Comp Neurol* 188, 429-442.

Keithley, E.M., and Feldman, M.L. (1982). Hair cell counts in an age-graded series of rat cochleas. *Hear Res* 8, 249-262.

Kharkovets, T., Dedek, K., Maier, H., Schweizer, M., Khimich, D., Nouvian, R., et al. (2006). Mice with altered KCNQ4 K+ channels implicate sensory outer hair cells in human progressive deafness. *EMBO J* 25(3), 642-652. doi: 10.1038/sj.emboj.7600951.

Kharkovets, T., Hardelin, J.-P., Safieddine, S., Schweizer, M., El-Amraoui, A., Petit, C., et al. (2000). KCNQ4, a K+ channel mutated in a form of dominant deafness, is expressed in the inner ear and the central auditory pathway. *PNAS* 97(8), 4333-4338. doi: DOI 10.1073/pnas.97.8.4333.

Kikuchi, T., Adams, J.C., Miyabe, Y., So, E., and Kobayashi, T. (2000). Potassium ion recycling pathway via gap junction systems in the mammalian cochlea and its interruption in hereditary nonsyndromic deafness. *Med Electron Microsc* 33(2), 51-56. doi: 10.1007/s007950070001.

Konishi, T., Hamrick, P.E., and Walsh, P.J. (1978). Ion transport in guinea pig cochlea. I. Potassium and sodium transport. *Acta Otolaryngol* 86(1-2), 22-34. doi: 10.3109/00016487809124717.

Korsgaard, M.P., Hartz, B.P., Brown, W.D., Ahring, P.K., Strøbaek, D., and Mirza, N.R. (2005). Anxiolytic effects of Maxipost (BMS-204352) and retigabine via activation of neuronal Kv7 channels. *J Pharmacol Exp Ther* 314(1), 282-292. doi: 10.1124/jpet.105.083923.

Kros, C.J., Ruppersberg, J.P., and Rüsch, A. (1998). Expression of a potassium current in inner hair cells during development of hearing in mice. *Nature* 394(6690), 291-284. doi: 10.1038/28401.

Kubisch, C., Schroeder, B.C., El-Amraoui, A., Marlin, S., Petit, C., and Jentsch, T.J. (1999). KCNQ4, a Novel Potassium Channel Expressed in Sensory Outer Hair Cells, Is Mutated in Dominant Deafness. *Cell Press* 96, 437-446.

Kujawa, S.G., and Liberman, M.C. (2006). Acceleration of age-related hearing loss by early noise exposure: evidence of a misspent youth. *J Neurosci* 26(7), 2115-2123. doi: 10.1523/JNEUROSCI.4985-05.2006.

Kujawa, S.G., and Liberman, M.C. (2009). Adding insult to injury: cochlear nerve degeneration after "temporary" noise-induced hearing loss. *J Neurosci* 29(45), 14077-14085. doi: 10.1523/JNEUROSCI.2845-09.2009.

Kurata, N., Schachern, P.A., Paparella, M.M., and Cureoglu, S. (2016). Histopathologic Evaluation of Vascular Findings in the Cochlea in Patients With Presbycusis. *JAMA Otolaryngology–Head & Neck Surgery* 142(2), 173-178. doi: 10.1001/jamaoto.2015.3163.

Lee, H.C., and Wei, Y.H. (2012). Mitochondria and aging. *Adv Exp Med Biol* 942, 311-327. doi: 10.1007/978-94-007-2869-1_14.

Leitner, M.G., Feuer, A., Ebers, O., Schreiber, D.N., Halaszovich, C.R., and Oliver, D. (2012). Restoration of ion channel function in deafness-causing KCNQ4 mutants by synthetic channel openers. *Br J Pharmacol* 165(7), 2244-2259. doi: 10.1111/j.1476-5381.2011.01697.x.

Leitner, M.G., Halaszovich, C.R., and Oliver, D. (2011). Aminoglycosides inhibit KCNQ4 channels in cochlear outer hair cells via depletion of phosphatidylinositol(4,5)bisphosphate. *Mol Pharmacol* 79(1), 51-60. doi: 10.1124/mol.110.068130.

Lewis, M.A., Nolan, L.S., Cadge, B.A., Matthews, L.J., Schulte, B.A., Dubno, J.R., et al. (2018). Whole exome sequencing in adult-onset hearing loss reveals a high load of predicted pathogenic variants in known deafness-associated genes and identifies new candidate genes. *BMC Med Genomics* 11(1), 77. doi: 10.1186/s12920-018-0395-1.

Li, H.S., and Borg, E. (1991). Age-related loss of auditory sensitivity in two mouse genotypes. *Acta Otolaryngol* 111(5), 827-834. doi: 10.3109/00016489109138418.

Liberman, M. (1980). Morphological differences among radial afferent fibers in the cat cochlea: an electron-microscopic study of serial sections. *Hearing research* 3(1), 45-63.

Liberman, M.C., and Beil, D.G. (1979). Hair cell condition and auditory nerve response in normal and noise-damaged cochleas. *Acta Otolaryngol* 88(3-4), 161-176. doi: 10.3109/00016487909137156.

Liberman, M.C., Dodds, L.W., and Pierce, S. (1990). Afferent and efferent innervation of the cat cochlea: quantitative analysis with light and electron microscopy. *Journal of Comparative Neurology* 301(3), 443-460.

Liberman, M.C., and Kiang, N.Y. (1978). Acoustic trauma in cats. Cochlear pathology and auditory-nerve activity. *Acta Otolaryngol Suppl.* 358, 1-63.

Lin, F.R., Ferrucci, L., Metter, E.J., An, Y., Zonderman, A.B., and Resnick, S.M. (2011a). Hearing loss and cognition in the Baltimore Longitudinal Study of Aging. *Neuropsychology* 25(6), 763-770. doi: 10.1037/a0024238.

Lin, F.R., Yaffe, K., Xia, J., Xue, Q.L., Harris, T.B., Purchase-Helzner, E., et al. (2013). Hearing loss and cognitive decline in older adults. *JAMA Intern Med* 173(4), 293-299. doi: 10.1001/jamainternmed.2013.1868.

Lin, H.W., Furman, A.C., Kujawa, S.G., and Liberman, M.C. (2011b). Primary neural degeneration in the Guinea pig cochlea after reversible noise-induced threshold shift. *J Assoc Res Otolaryngol* 12(5), 605-616. doi: 10.1007/s10162-011-0277-0.

Lin, M.T., and Beal, M.F. (2006). Mitochondrial dysfunction and oxidative stress in neurodegenerative diseases. *Nature* 443(7113), 787-795. doi: 10.1038/nature05292.

Livingston, G., Huntley, J., Sommerlad, A., Ames, D., Ballard, C., Banerjee, S., et al. (2020). Dementia prevention, intervention, and care: 2020 report of the Lancet Commission. *Lancet* 396(10248), 413-446. doi: 10.1016/S0140-6736(20)30367-6.

Livingston, G., Sommerlad, A., Orgeta, V., Costafreda, S.G., Huntley, J., Ames, D., et al. (2017). Dementia prevention, intervention, and care. *Lancet* 390(10113), 2673-2734. doi: 10.1016/S0140-6736(17)31363-6.

Lobarinas, E., Salvi, R., and Ding, D. (2013). Insensitivity of the audiogram to carboplatin induced inner hair cell loss in chinchillas. *Hear Res* 302, 113-120. doi: 10.1016/j.heares.2013.03.012.

Mammano, F., and Ashmore, J. (1996). Differential expression of outer hair cell potassium currents in the isolated. *J Physiol* 496, 639-646.

Mannhold, R. (2005). The impact of lipophilicity in drug research: a case report on beta-blockers. *Mini Rev Med Chem* 5(2), 197-205. doi: 10.2174/1389557053402701.

Marchetta, P., Mohrle, D., Eckert, P., Reimann, K., Wolter, S., Tolone, A., et al. (2020). Guanylyl Cyclase A/cGMP Signaling Slows Hidden, Age- and Acoustic Trauma-Induced Hearing Loss. *Front Aging Neurosci* 12, 83. doi: 10.3389/fnagi.2020.00083.

Marcotti, W., and Kros, C.J. (1999). Developmental expression of the potassium current IK n contributes to maturation of mouse outer hair cells. *J Physiol* 520, 653-660.

Marie, A., Larroze-Chicot, P., Cosnier-Pucheu, S., and Gonzalez-Gonzalez, S. (2017). Senescence-accelerated mouse prone 8 (SAMP8) as a model of age-related hearing loss. *Neurosci Lett* 656, 138-143. doi: 10.1016/j.neulet.2017.07.037.

Matalon, S., Hardimann, K.M., Jain, L., Eaton, D.C., Kotlikoff, M., Eu, J.P., et al. (2003). Regulation of ion channel structure and function by reactive oxygen-nitrogen species. *Am J Physiol Lung Cell Mol Physiol* 285**,** 1184-1189.

McFadden, S.L., Ding, D., Burkard, R.F., Jiang, H., Reaume, A.G., Flood, D.G., et al. (1999a). Cu/Zn SOD deficiency potentiates hearing loss and cochlear pathology in aged 129,CD-1 mice. *J Comp Neurol* 413(1)**,** 101-112.

McFadden, S.L., Ding, D., Reaume, A.G., Flood, D.G., and Salvi, R.J. (1999b). Age-related cochlear hair cell loss is enhanced in mice lacking copper/zinc superoxide dismutase. *Neurobiol Aging* 20(1)**,** 1-8. doi: 10.1016/s0197-4580(99)00018-4.

Menardo, J., Tang, Y., Ladrech, S., Lenoir, M., Casas, F., Michel, C., et al. (2012). Oxidative stress, inflammation, and autophagic stress as the key mechanisms of premature age-related hearing loss in SAMP8 mouse Cochlea. *Antioxid Redox Signal* 16(3)**,** 263-274. doi: 10.1089/ars.2011.4037.

Merchant, S.N., and Nadol, J.B. (2010). *Schuknecht's Pathology of the Ear, 3rd Edition* People's Medical Publishing House-USA.

Miceli, F., Soldovieri, M.V., Martire, M., and Taglialatela, M. (2008). Molecular pharmacology and therapeutic potential of neuronal Kv7-modulating drugs. *Curr Opin Pharmacol* 8(1)**,** 65-74. doi: 10.1016/j.coph.2007.10.003.

Miyamoto, M. (1997). Characteristics of age-related behavioral changes in senescence-accelerated mouse SAMP8 and SAMP10. *Exp Gerontol* 32(1-2)**,** 139-148. doi: 10.1016/s0531-5565(96)00061-7.

Morley, J.E. (2002). The SAMP8 mouse: a model of Alzheimer disease? *Biogerontology* 3(1-2)**,** 57-60. doi: 10.1023/a:1015207429786.

Müller, M., von Hunerbein, K., Hoidis, S., and Smolders, J.W. (2005). A physiological place-frequency map of the cochlea in the CBA/J mouse. *Hear Res* 202(1-2)**,** 63-73. doi: 10.1016/j.heares.2004.08.011.

Nakazawa, K., Spicer, S.S., and Schulte, B.A. (1995). Ultrastructural Localization of Na,K-ATPase in the Gerbil Cochlea. *J Histochem Cytochem* 43**,** 981-991.

Nenov, A.P., Norris, C., and Bobbin, R.P. (1997). Outwardly rectifying currents in guinea pig outer hair cells. *Hear Res* 105**,** 146-158.

Neyroud, N., Tesson, F., Denjoy, I., Leibovici, M., Donger, C., Barhanin, J., et al. (1997). A novel mutation in the potassium channel gene KVLQT1 causes the Jervell and Lange-Nielsen cardioauditory syndrome. *Nat Genet* 15(2)**,** 186-189. doi: 10.1038/ng0297-186.

Nin, F., Yoshida, T., Sawamura, S., Ogata, G., Ota, T., Higuchi, T., et al. (2016). The unique electrical properties in an extracellular fluid of the mammalian cochlea; their functional roles, homeostatic processes, and pathological significance. *Pflugers Arch* 468(10)**,** 1637-1649. doi: 10.1007/s00424-016-1871-0.

Noben-Trauth, K., Zheng, Q.Y., and Johnson, K.R. (2003). Association of cadherin 23 with polygenic inheritance and genetic modification of sensorineural hearing loss. *Nat Genet* 35(1)**,** 21-23. doi: 10.1038/ng1226.

Noh, B., Rim, J.H., Gopalappa, R., Lin, H., Kim, K.M., Kang, M.J., et al. (2022). In vivo outer hair cell gene editing ameliorates progressive hearing loss in dominant-negative Kcnq4 murine model. *Theranostics* 12(5)**,** 2465-2482. doi: 10.7150/thno.67781.

Nouvian, R., Ruel, J., Wang, J., Guitton, M.J., Pujol, R., and Puel, J.-L. (2003). Degeneration of sensory outer hair cells following pharmacological blockade of cochlear KCNQ channels in the adult guinea pig. *European Journal of Neuroscience* 17(12), 2553-2562. doi: 10.1046/j.1460-9568.2003.02715.x.

Nyberg, S., Abbott, N.J., Shi, X., Steyger, P.S., and Dabdoub, A. (2019). Delivery of therapeutics to the inner ear: The challenge of the blood-labyrinth barrier. *Sci Transl Med* 11(482). doi: 10.1126/scitranslmed.aao0935.

Ohlemiller, K.K. (2004). Age-related hearing loss: the status of Schuknecht's typology. *Curr Opin Otolaryngol Head Neck Surg* 12, 439-443.

Ohlemiller, K.K., Dahl, A.R., and Gagnon, P.M. (2010). Divergent aging characteristics in CBA/J and CBA/CaJ mouse cochleae. *J Assoc Res Otolaryngol* 11(4), 605-623. doi: 10.1007/s10162-010-0228-1.

Ohlemiller, K.K., and Gagnon, P.M. (2004). Apical-to-basal gradients in age-related cochlear degeneration and their relationship to "primary" loss of cochlear neurons. *J Comp Neurol* 479(1), 103-116. doi: 10.1002/cne.20326.

Ohlemiller, K.K., McFadden, S.L., Ding, D.L., Lear, P.M., and Ho, Y.S. (2000). Targeted mutation of the gene for cellular glutathione peroxidase (Gpx1) increases noise-induced hearing loss in mice. *J Assoc Res Otolaryngol* 1(3), 243-254. doi: 10.1007/s101620010043.

Oliver, D., Klöcker, N., Baukrowitz, T., Ruppersberg, J.P., and Fakler, B. (2000). Gating of Ca2+-activated K+ channels controls fast inhibitory synaptic transmission at auditory outer hair cells *Neuron* 26(3), 595-601. doi: 10.1016/s0896-6273(00)81197-6.

Oliver, D., Knipper, M., Derst, C., and Fakler, B. (2003). Resting Potential and Submembrane Calcium Concentration of Inner Hair Cells in the Isolated Mouse Cochlea Are Set by KCNQ-Type Potassium Channels. *Journal of Neuroscience* 23(6), 2141-2149.

Pannu, K.K., Chadha, S., Kumar, D., and Preeti (2011). Evaluation of hearing loss in tympanic membrane perforation. *Indian J Otolaryngol Head Neck Surg* 63(3), 208-213. doi: 10.1007/s12070-011-0129-6.

Patuzzi, R. (2011). Ion flow in stria vascularis and the production and regulation of cochlear endolymph and the endolymphatic potential. *Hear Res* 277(1-2), 4-19. doi: 10.1016/j.heares.2011.01.010.

Paventi, G., Soldovieri, M.V., Servettini, I., Barrese, V., Miceli, F., Sisalli, M.J., et al. (2022). Kv7.4 channels regulate potassium permeability in neuronal mitochondria. *Biochem Pharmacol* 197, 114931. doi: 10.1016/j.bcp.2022.114931.

Peixoto Pinheiro, B., Adel, Y., Knipper, M., Müller, M., and Löwenheim, H. (2021). Auditory Threshold Variability in the SAMP8 Mouse Model of Age-Related Hearing Loss: Functional Loss and Phenotypic Change Precede Outer Hair Cell Loss. *Front Aging Neurosci* 13, 708190. doi: 10.3389/fnagi.2021.708190.

Peixoto Pinheiro, B., Müller, M., Bös, M., Guezguez, J., Burnet, M., Tornincasa, M., et al. (2022). A potassium channel agonist protects hearing function and promotes outer hair cell survival in a mouse model for age-related hearing loss. *Cell Death & Disease* 13(7). doi: 10.1038/s41419-022-04915-5.

Peixoto Pinheiro, B., Vona, B., Lowenheim, H., Ruttiger, L., Knipper, M., and Adel, Y. (2020). Age-related hearing loss pertaining to potassium ion channels in the cochlea and auditory pathway. *Pflugers Arch* 473(5), 823-840. doi: 10.1007/s00424-020-02496-w.

Petit, C. (2006). From deafness genes to hearing mechanisms: harmony and counterpoint. *Trends Mol Med* 12(2), 57-64. doi: 10.1016/j.molmed.2005.12.006.

Pickles, J.O. (1988). *An Introduction to the Physiology of Hearing.* Brill.

Plontke, S.K., and Salt, A. (2006). Simulation of Application Strategies for Local Drug Delivery to the Inner Ear. *ORL J Otorhinolaryngol Relat Spec* 68(6), 386-392.

Rim, J.H., Choi, J.Y., Jung, J., and Gee, H.Y. (2021). Activation of KCNQ4 as a Therapeutic Strategy to Treat Hearing Loss. *Int J Mol Sci* 22(5). doi: 10.3390/ijms22052510.

Rivas-Chacón, L.D.M., Martínez-Rodríguez, S., Madrid-García, R., Yanes-Díaz, J., Riestra-Ayora, J.I., Sanz-Fernández, R., et al. (2021). Role of Oxidative Stress in the Senescence Pattern of Auditory Cells in Age-Related Hearing Loss. *Antioxidants (Basel)* 10(9). doi: 10.3390/antiox10091497.

Rostock, A., Tober, C., Rundfeldt, C., Bartsch, R., Engel, J., Polymeropoulos, E.E., et al. (1996). D-23129: a new anticonvulsant with a broad spectrum activity in animal models of epileptic seizures. *Epilepsy Res* 23(3), 211-223. doi: 10.1016/0920-1211(95)00101-8.

Roth, T.N. (2015). Aging of the auditory system. *Handb Clin Neurol* 129, 357-373. doi: 10.1016/b978-0-444-62630-1.00020-2.

Rundfeldt, C. (1997). The new anticonvulsant retigabine (D-23129) acts as an opener of K+ channels in neuronal cells. *Eur J Pharmacol* 336(2-3), 243-249. doi: 10.1016/s0014-2999(97)01249-1.

Ruppersberg, J.P., Stocker, M., Pongs, O., Heinemann, S.H., Frank, R., and Koenen, M. (1991). Regulation of fast inactivation of cloned mammalian IK(A) channels by cysteine oxidation. *Nature* 352(6337), 711-714. doi: 10.1038/352711a0.

Rutherford, B.R., Brewster, K., Golub, J.S., Kim, A.H., and Roose, S.P. (2018). Sensation and Psychiatry: Linking Age-Related Hearing Loss to Late-Life Depression and Cognitive Decline. *Am J Psychiatry* 175(3), 215-224. doi: 10.1176/appi.ajp.2017.17040423.

Rüttiger, L., Sausbier, M., Zimmermann, U., Winter, H., Braig, C., Engel, J., et al. (2004). Deletion of the Ca2+-activated potassium (BK) alpha-subunit but not the BKbeta1-subunit leads to progressive hearing loss. *Proc Natl Acad Sci U S A* 101(35), 12922-12927. doi: 10.1073/pnas.0402660101.

Rybak, L.P., Dhukhwa, A., Mukherjea, D., and Ramkumar, V. (2019). Local Drug Delivery for Prevention of Hearing Loss. *Front Cell Neurosci* 13, 300. doi: 10.3389/fncel.2019.00300.

Salt, A.N., and Hirose, K. (2018). Communication pathways to and from the inner ear and their contributions to drug delivery. *Hear Res* 362, 25-37. doi: 10.1016/j.heares.2017.12.010.

Salt, A.N., Kellner, C., and Hale, S. (2003). Contamination of perilymph sampled from the basal cochlear turn with cerebrospinal fluid. *Hear Res* 182(1-2), 24-33. doi: 10.1016/s0378-5955(03)00137-0.

Salt, A.N., Mleichar, I., and Thalmann, R. (1987). Mechanisms of endocochlear potential generation by stria vascularis. *The Laryngoscope* 97(8), 984-991.

Salt, A.N., and Plontke, S.K. (2018). Pharmacokinetic principles in the inner ear: Influence of drug properties on intratympanic applications. *Hear Res* 368, 28-40. doi: 10.1016/j.heares.2018.03.002.

Salt, A.N., and Plontke, S.K.R. (2005). Local inner-ear drug delivery and pharmacokinetics. *Drug Discovery Today* 10(19), 1299-1306. doi: 10.1016/s1359-6446(05)03574-9.

Sanguinetti, M.C., Curran, M.E., Spector, P.S., and Keating, M.T. (1996a). Spectrum of HERG K+-channel dysfunction in an inherited cardiac arrhythmia. *Proc Natl Acad Sci USA* 93, 2208-2212.

Sanguinetti, M.C., Curran, M.E., Zou, A., Shen, J., Spector, P.S., Atkinson, D.L., et al. (1996b). Coassembly of K(V)LQT1 and minK (IsK) proteins to form cardiac I(Ks) potassium channel. *Nature* 384(6604), 80-83. doi: 10.1038/384080a0.

Santos-Sacchi, J. (1993). Voltage-dependent ionic conductances of type I spiral ganglion cells from the guinea pig inner ear. *J Neurosci* 13(8), 3599-3611. doi: 10.1523/JNEUROSCI.13-08-03599.1993.

Schmiedt, R.A. (2010). "The physiology of cochlear presbycusis," in *The aging auditory system*. Springer), 9-38.

Schroder, R.L., Jespersen, T., Christophersen, P., Strobak, D., Jensen, B.S., and Olesen, S.P. (2001). KCNQ4 channel activation by BMS-204352 and retigabine. *Neuropharmacology* 40, 888-898.

Schuknecht, H.F. (1955). Presbycusis. *Laryngoscope* 65, 402–419.

Schuknecht, H.F. (1964). Further observations on pathology of presbycusis. *Arch Otolaryngol* 80, 369-382.

Schuknecht, H.F. (1974). *Pathology of the Ear.* Harvard University Press.

Schuknecht, H.F. (1993). *Pathology of the Ear.* Lea and Febiger.

Schuknecht, H.F., and Gacek, M.R. (1993). Cochlear pathology in presbycusis. *Ann Otol Rhinol Laryngol* 102, 1–16.

Schuknecht, H.F., and Woellner, R.C. (1955). An experimental and clinical study of deafness from lesions of the cochlear nerve. *J Laryngol Otol* 69(2), 75-97. doi: 10.1017/s0022215100050465.

Schulte, B.A., and Schmiedt, R.A. (1992). Lateral wall Na, K-ATPase and endocochlear potentials decline with age in quiet-reared gerbils. *Hearing research* 61(1-2), 35-46.

Schulte, B.A., and Steel, K.P. (1994). Expression of α and β subunit isoforms of Na, K-ATPase in the mouse inner ear and changes with mutations at the Wv or Sld loci. *Hearing research* 78(1), 65-76.

Schulze-Bahr, E., Haverkamp, W., Wedekind, H., Rubie, C., Hördt, M., Borggrefe, M., et al. (1997). Autosomal recessive long-QT syndrome (Jervell Lange-Nielsen syndrome) is genetically heterogeneous. *Hum Genet* 100(5-6), 573-576. doi: 10.1007/s004390050554.

Schwander, M., Kachar, B., and Muller, U. (2010). Review series: The cell biology of hearing. *J Cell Biol* 190(1), 9-20. doi: 10.1083/jcb.201001138.

Sergeyenko, Y., Lall, K., Liberman, M.C., and Kujawa, S.G. (2013). Age-related cochlear synaptopathy: an early-onset contributor to auditory functional decline. *J Neurosci* 33(34), 13686-13694. doi: 10.1523/JNEUROSCI.1783-13.2013.

Sheppard, A.M., Chen, G.D., and Salvi, R. (2015). Potassium ion channel openers, Maxipost and Retigabine, protect against peripheral salicylate ototoxicity in rats. *Hear Res* 327, 1-8. doi: 10.1016/j.heares.2015.04.007.

Shin, D.H., Jung, J., Koh, Y.I., Rim, J.H., Lee, J.S., Choi, H.J., et al. (2019). A recurrent mutation in KCNQ4 in Korean families with nonsyndromic hearing loss and rescue of the channel activity by KCNQ activators. *Hum Mutat* 40(3), 335-346. doi: 10.1002/humu.23698.

Shin, J.-B., Streijger, F., Beynon, A., Peters, T., Gadzalla, L., McMillen, D., et al. (2007). Hair Bundles Are Specialized for ATP Delivery via Creatine Kinase. *Neuron* 53, 371-386.

Smith, C.A. (1954). Capillary areas of the membranous labyrinth. *Ann Otol Rhinol Laryngol* 63(2), 435-447. doi: 10.1177/000348945406300213.

Someya, S., and Prolla, T.A. (2010). Mitochondrial oxidative damage and apoptosis in age-related hearing loss. *Mech Ageing Dev* 131(7-8), 480-486. doi: 10.1016/j.mad.2010.04.006.

Spicer, S.S., and Schulte, B.A. (1991). Differentiation of inner ear fibrocytes according to their ion transport related activity. *Hearing research* 56(1-2), 53-64.

Spicer, S.S., and Schulte, B.A. (1996). The fine structure of spiral ligament cells relates to ion return to the stria and varies with place-frequency. *Hearing research* 100(1-2), 80-100.

Spicer, S.S., and Schulte, B.A. (2002). Spiral ligament pathology in quiet-aged gerbils. *Hear Res* 172, 172-185.

Spoendlin, H. (1981). Differentiation of cochlear afferent neurons. *Acta Otolaryngol* 91(5-6), 451-456. doi: 10.3109/00016488109138527.

Stamataki, S., Francis, H.W., Lehar, M., May, B.J., and Ryugo, D.K. (2006). Synaptic alterations at inner hair cells precede spiral ganglion cell loss in aging C57BL/6J mice. *Hear Res* 221(1-2), 104-118. doi: 10.1016/j.heares.2006.07.014.

Stevens, G., Flaxman, S., Brunskill, E., Mascarenhas, M., Mathers, C.D., and Finucane, M. (2013). Global and regional hearing impairment prevalence: an analysis of 42 studies in 29 countries. *Eur J Public Health* 23(1), 146-152. doi: 10.1093/eurpub/ckr176.

Suzuki, T., Nomoto, Y., Nakagawa, T., Kuwahata, N., Ogawa, H., Suzuki, Y., et al. (2006). Age-dependent degeneration of the stria vascularis in human cochleae. *The Laryngoscope* 116(10), 1846-1850.

Takeda, T., Hosokawa, M., Takeshita, S., Irino, M., Higuchi, K., Matsushita, T., et al. (1981). A new murine model of accelerated senescence. *Mech Ageing Dev* 17. doi: 10.1016/0047-6374(81)90084-1.

Tarnowski, B.I., Schmiedt, R.A., Hellstrom, L.I., Lee, F.S., and Adams, J.C. (1991). Age-related changes in cochleas of mongolian gerbils. *Hear Res* 54, 123-134.

Tawfik, K.O., Klepper, K., Saliba, J., and Friedman, R.A. (2020). Advances in understanding of presbycusis. *J Neurosci Res* 98(9), 1685-1697. doi: 10.1002/jnr.24426.

Trpchevska, N., Freidin, M.B., Broer, L., Oosterloo, B.C., Yao, S., Zhou, Y., et al. (2022). Genome-wide association meta-analysis identifies 48 risk variants and highlights the role of the stria vascularis in hearing loss. *Am J Hum Genet* 109(6), 1077-1091. doi: 10.1016/j.ajhg.2022.04.010.

Valero, M.D., Burton, J.A., Hauser, S.N., Hackett, T.A., Ramachandran, R., and Liberman, M.C. (2017). Noise-induced cochlear synaptopathy in rhesus monkeys (Macaca mulatta). *Hear Res* 353, 213-223. doi: 10.1016/j.heares.2017.07.003.

Van Eyken, E., Van Camp, G., and Van Laer, L. (2007). The complexity of age-related hearing impairment: contributing environmental and genetic factors. *Audiol Neurootol* 12(6), 345-358. doi: 10.1159/000106478.

Van Eyken, E., Van Laer, L., Fransen, E., Topsakal, V., Lemkens, N., Laureys, W., et al. (2006). KCNQ4: a gene for age-related hearing impairment? *Hum Mutat* 27(10), 1007-1016. doi: 10.1002/humu.20375.

Van Hauwe, P., Coucke, P.J., Ensink, R.J., Huygen, P., Cremers, C.W., and Van Camp, G. (2000). Mutations in the KCNQ4 K+ channel gene, responsible for autosomal dominant hearing loss, cluster in the channel pore region. *Am J Med Genet* 93(3), 184-187. doi: 10.1002/1096-8628(20000731)93:3<184::aid-ajmg4>3.0.co;2-5.

Van Laer, L., Carlsson, P.I., Ottschytsch, N., Bondeson, M.L., Konings, A., Vandevelde, A., et al. (2006). The contribution of genes involved in potassium-recycling in the inner ear to noise-induced hearing loss. *Hum Mutat* 27(8), 786-795. doi: 10.1002/humu.20360.

Vanhooren, V., and Libert, C. (2013). The mouse as a model organism in aging research: usefulness, pitfalls and possibilities. *Ageing Res Rev* 12(1), 8-21. doi: 10.1016/j.arr.2012.03.010.

Vermiglio, A.J., Soli, S.D., Freed, D.J., and Fisher, L.M. (2012). The relationship between high-frequency pure-tone hearing loss, hearing in noise test (HINT) thresholds, and the articulation index. *Journal of the American Academy of Audiology* 23(10), 779-788.

Vetter, D.E., Mann, J.R., Wangemann, P., Liu, J., McLaughlin, K.J., Lesage, F., et al. (1996). Inner ear defects induced by null mutation of the isk gene. *Neuron* 17(6), 1251-1264. doi: 10.1016/s0896-6273(00)80255-x.

Viana, L.M., O'Malley, J.T., Burgess, B.J., Jones, D.D., Oliveira, C.A., Santos, F., et al. (2015). Cochlear neuropathy in human presbycusis: Confocal analysis of hidden hearing loss in post-mortem tissue. *Hear Res* 327, 78-88. doi: 10.1016/j.heares.2015.04.014.

Viberg, A., and Canlon, B. (2004). The guide to plotting a cochleogram. *Hear Res* 197(1-2), 1-10. doi: 10.1016/j.heares.2004.04.016.

Wang, Q., Li, W., Cai, C., Hu, P., and Lai, R. (2021). miR-153/KCNQ4 axis contributes to noise-induced hearing loss in a mouse model. *J Physiol Sci* 71(1), 28. doi: 10.1186/s12576-021-00814-0.

Wangemann, P. (2002). K+ cycling and the endocochlear potential. *Hear Res* 165, 1-9.

Wangemann, P. (2006). Supporting sensory transduction: cochlear fluid homeostasis and the endocochlear potential. *J Physiol* 576(Pt 1), 11-21. doi: 10.1113/jphysiol.2006.112888.

Wangemann, P., Liu, J., and Marcus, D.C. (1995). Ion transport mechanisms responsible for K+ secretion and the transepithelial voltage across marginal cells of stria vascularis in vitro. *Hear Res* 84(1-2), 19-29. doi: Doi 10.1016/0378-5955(95)00009-S.

Winter, H., Braig, C., Zimmermann, U., Geisler, H.S., Franzer, J.T., Weber, T., et al. (2006). Thyroid hormone receptors TRalpha1 and TRbeta differentially regulate gene expression of Kcnq4 and prestin during final differentiation of outer hair cells. *J Cell Sci* 119(Pt 14), 2975-2984. doi: 10.1242/jcs.03013.

World Health Organization (2021). "World report on hearing.". (Geneva 2021: World Health Organization).

Wright, A., Davis, A., Bredberg, G., Ulehlova, L., and Spencer, H. (1987). Hair cell distributions in the normal human cochlea. *Acta oto-laryngologica. Supplementum* 444, 1-48.

Wu, P.Z., Liberman, L.D., Bennett, K., de Gruttola, V., O'Malley, J.T., and Liberman, M.C. (2019). Primary Neural Degeneration in the Human Cochlea: Evidence for Hidden Hearing Loss in the Aging Ear. *Neuroscience* 407, 8-20. doi: 10.1016/j.neuroscience.2018.07.053.

Wu, P.Z., O'Malley, J.T., de Gruttola, V., and Liberman, M.C. (2020). Age-Related Hearing Loss Is Dominated by Damage to Inner Ear Sensory Cells, Not the Cellular Battery That Powers Them. *J Neurosci* 40(33), 6357-6366. doi: 10.1523/JNEUROSCI.0937-20.2020.

Wu, P.Z., O'Malley, J.T., de Gruttola, V., and Liberman, M.C. (2021). Primary Neural Degeneration in Noise-Exposed Human Cochleas: Correlations with Outer Hair Cell Loss and Word-Discrimination Scores. *J Neurosci* 41(20), 4439-4447. doi: 10.1523/JNEUROSCI.3238-20.2021.

Wulff, H., Castle, N.A., and Pardo, L.A. (2009). Voltage-gated potassium channels as therapeutic targets. *Nat Rev Drug Discov* 8(12), 982-1001. doi: 10.1038/nrd2983.

Xiong, Q., Sun, H., and Li, M. (2007). Zinc pyrithione-mediated activation of voltage-gated KCNQ potassium channels rescues epileptogenic mutants. *Nat Chem Biol* 3(5), 287-296. doi: 10.1038/nchembio874.

Xiong, Q., Sun, H., Zhang, Y., Nan, F., and Li, M. (2008). Combinatorial augmentation of voltage-gated KCNQ potassium channels by chemical openers. *Proc Natl Acad Sci U S A* 105(8), 3128-3133. doi: 10.1073/pnas.0712256105.

Yagi, H., Katoh, S., Akiguchi, I., and Takeda, T. (1988). Age-related deterioration of ability of acquisition in memory and learning in senescence accelerated mouse: SAM-P/8 as an animal model of disturbances in recent memory. *Brain Res* 474(1), 86-93. doi: 10.1016/0006-8993(88)90671-3.

Yamasoba, T., Lin, F.R., Someya, S., Kashio, A., Sakamoto, T., and Kondo, K. (2013). Current concepts in age-related hearing loss: epidemiology and mechanistic pathways. *Hearing research* 303, 30-38.

Yang, H., Xiong, H., Huang, Q., Pang, J., Zheng, X., Chen, L., et al. (2013). Compromised potassium recycling in the cochlea contributes to conservation of endocochlear potential in a mouse model of age-related hearing loss. *Neurosci Lett* 555, 97-101. doi: 10.1016/j.neulet.2013.09.028.

Yang, S., Cai, Q., Bard, J., Jamison, J., Wang, J., Yang, W., et al. (2015). Variation analysis of transcriptome changes reveals cochlear genes and their associated functions in

cochlear susceptibility to acoustic overstimulation. *Hear Res* 330(Pt A), 78-89. doi: 10.1016/j.heares.2015.04.010.

Yu, H., Wu, M., Hopkins, C., Engers, J., Townsend, S., Lindsley, C., et al. (2011). A small molecule activator of KCNQ2 and KCNQ4 channels. *Probe Reports from the NIH Molecular Libraries Program*

Zdebik, A.A., Wangemann, P., and Jentsch, T.J. (2009). Potassium ion movement in the inner ear: insights from genetic disease and mouse models. *Physiology (Bethesda)* 24, 307-316. doi: 10.1152/physiol.00018.2009.

Zheng, Q.Y., and Johnson, K.R. (2001). Hearing loss associated with the modifier of deaf waddler (mdfw) locus corresponds with age-related hearing loss in 12 inbred strains of mice. *Hear Res* 154, 45-53.

Zheng, Q.Y., Johnson, K.R., and Erway, L.C. (1999). Assessment of hearing in 80 inbred strains of mice by ABR threshold analyses. *Hear Res* 130(1-2), 94-107. doi: 10.1016/s0378-5955(99)00003-9.

Zidanic, M., and Brownell, W.E. (1990). Fine structure of the intracochlear potential field. I. The silent current. *Biophys J* 57(6), 1253-1268. doi: 10.1016/s0006-3495(90)82644-8.

6. Appendix

a.) Accepted Papers

Peixoto Pinheiro, B., Vona, B., Löwenheim, H., Rüttiger, L., Knipper, M., Adel, Y. Age-related hearing loss pertaining to potassium ion channels in the cochlea and auditory pathway. *Pflügers Archive.* 2020 May, 473(5):823-840. (Review)

Peixoto Pinheiro, B., Adel, Y., Knipper, M., Müller, M., Löwenheim, H. Auditory Threshold Variability in the SAMP8 Mouse Model of Age-Related Hearing Loss: Functional Loss and Phenotypic Change Precede Outer Hair Cell Loss. *Frontiers in Aging Neuroscience.* 2021 Aug, 13:708190.

Peixoto Pinheiro, B., Müller, M. Bös, M., Guezguez J., Burnet, M., Tornincasa, M., Rizzetto, R., Rolland, J.-F., Liberati, C., Lohmer, S., Adel, Y.*, Löwenheim, H.*. 2022. A potassium channel agonist protects hearing function and promotes outer hair cell survival in a mouse model for age-related hearing loss. *Cell Death and Disease.* 2022.

*equal contribution

Pflügers Archiv - European Journal of Physiology (2021) 473:823–840
https://doi.org/10.1007/s00424-020-02496-w

INVITED REVIEW

Age-related hearing loss pertaining to potassium ion channels in the cochlea and auditory pathway

Barbara Peixoto Pinheiro[1] · Barbara Vona[1] · Hubert Löwenheim[1] · Lukas Rüttiger[2] · Marlies Knipper[2] · Youssef Adel[1]

Received: 24 September 2020 / Revised: 27 October 2020 / Accepted: 10 November 2020 / Published online: 17 December 2020

Abstract

Age-related hearing loss (ARHL) is the most prevalent sensory deficit in the elderly and constitutes the third highest risk factor for dementia. Lifetime noise exposure, genetic predispositions for degeneration, and metabolic stress are assumed to be the major causes of ARHL. Both noise-induced and hereditary progressive hearing have been linked to decreased cell surface expression and impaired conductance of the potassium ion channel $K_V7.4$ (KCNQ4) in outer hair cells, inspiring future therapies to maintain or prevent the decline of potassium ion channel surface expression to reduce ARHL. In concert with $K_V7.4$ in outer hair cells, $K_V7.1$ (KCNQ1) in the stria vascularis, calcium-activated potassium channels BK (KCNMA1) and SK2 (KCNN2) in hair cells and efferent fiber synapses, and $K_V3.1$ (KCNC1) in the spiral ganglia and ascending auditory circuits share an upregulated expression or subcellular targeting during final differentiation at hearing onset. They also share a distinctive fragility for noise exposure and age-dependent shortfalls in energy supply required for sustained surface expression. Here, we review and discuss the possible contribution of select potassium ion channels in the cochlea and auditory pathway to ARHL. We postulate genes, proteins, or modulators that contribute to sustained ion currents or proper surface expressions of potassium channels under challenging conditions as key for future therapies of ARHL.

Keywords Kv7.4 · Kv7.1 · BK · SK2 · Kv3.1 · Presbycusis

Introduction

Age-related hearing loss (ARHL), or presbycusis, is the most prevalent sensory deficit in the elderly [1]. Although it is not life-threatening, this condition is associated with significant psychological and medical morbidity, including social isolation, frailty, depression, and cognitive decline [2–5]. As a major risk factor for dementia [6], the prevention of hearing loss with age has been recently suggested as a foremost modifying factor to lower future dementia prevalence [7]. ARHL occurs in most mammals with variations in the age of onset, rate of decline, and magnitude of degeneration in the cochlea and the auditory pathway [8–11]. The affected cochlear structures include the stria vascularis and its vasculature, spiral ligament, sensory hair cells, and auditory neurons. Until recently, the dysfunction of the stria vascularis resulting in a reduced endocochlear potential (EP) was assumed to be a primary cause of ARHL [1, 12, 13]. However, new evidence from analyzing temporal bones of the elderly challenges this long-held view, showing that hair cell loss not only occurs in predominantly high-frequency regions but also extends to low-frequency regions in ARHL preceding stria vascularis degeneration [14]. Based on this observation, lifetime acoustic noise exposure was suggested as a primary cause of hearing loss with age, particularly due to outer hair cell (OHC) damage after acoustic overexposure, which is suggested to be the major contributor to ARHL [14]. Moreover, increasing evidence suggests that even in the absence of detectable loss of hearing sensitivity, neuronal degeneration of synaptic auditory fibers or ascending auditory projections can precede hearing

This article is part of the special issue on Aging Brain in Pflügers Archiv—European Journal of Physiology

✉ Marlies Knipper
marlies.knipper@uni-tuebingen.de

[1] Translational Hearing Research, Tübingen Hearing Research Center, Department of Otolaryngology, Head and Neck Surgery, University of Tübingen, 72076 Tübingen, Germany

[2] Molecular Physiology of Hearing, Tübingen Hearing Research Center, Department of Otolaryngology, Head and Neck Surgery, University of Tübingen, 72076 Tübingen, Germany

threshold loss and contribute as an additional hallmark of ARHL to difficulties in speech discrimination with advancing age, especially in noisy environments [15–17]. Thus, noise exposure as a major cause of ARHL affects not only OHC over age [14] but also age-related synaptopathies and neuropathies [8], gradually leading to degeneration of spiral ganglion neurons (SGNs) [16, 18] and central auditory processing deficits [19, 20]. Furthermore, independent of lifetime noise exposure being linked to damaged hair cells and neurons, individuals with cardiovascular risk factors, e.g., hypertension, diabetes, smoking, or increased serum cholesterol, exhibit a high risk of developing hearing impairment over age [21].

We hypothesize that any limits in metabolic supply, e.g., from oxidative stress after acoustic trauma or limitations during ischemic insults, endanger particularly sensitive stages that require high energy supply or exhibit vulnerability for radical oxygen species (ROS) as the precursor of ARHL. Indeed, ROS contribute through reduced mitochondrial activity and enhanced oxidative damage to aging processes in all organs, and thus negatively affect hearing with advancing age [22]. We postulate that select potassium ion (K^+) channels in the cochlea and ascending auditory pathway, which are known to critically depend on continuous recycling processes for proper surface expression, are vulnerable, early targets for limitations in energy supply. K^+ channels show extreme genetic heterogeneity and functional diversity unmatched by other types of ion channels, which suggests them as one of the primary targets of excess ROS. Moreover, strong evidence exists that ROS-mediated oxidation of K^+ channels is a recurring theme in the aging nervous system and is intrinsically involved in certain neuropathies [23]. Here, we focus on functionally relevant K^+ channels in the cochlea and auditory pathway, which share common temporal expression during the final differentiation stages of the organ of Corti prior to hearing function in rodents, hypothesizing that late differentiation stages are the ones affected early during aging, offering a therapeutic window that could allow functional restoration before cell death [24]. We discuss the following K^+ channels with functional expression during or after hearing onset, that is, around postnatal day (P) 12 in rodents, and around embryonic week (EW) 27 in humans (Fig. 1): (i) $K_V7.4$ (KCNQ4) maintains OHC receptor potential [25–30]; (ii) $K_V7.1$ (KCNQ1) is expressed in marginal cells of the stria vascularis [31–33]; (iii) calcium ion (Ca^{2+})-activated potassium channels BK (KCNMA1) and SK2 (KCNN2) are involved in repolarization of OHC and termination of Ca^{2+} action potential (AP) firing in medial olivocochlear (MOC) efferent fibers [34, 35]; and (iv) $K_V3.1$ (KCNC1) in SGNs and ascending auditory circuits [36] are shown to be involved in temporal precision of sound processing [37]. In this review, we first summarize the expression profiles and physiological functions of these K^+ channels, then discuss their individual roles in the context of age- and noise-dependent hearing loss, and the contribution of genetic predisposition to progressive hearing loss over age. Finally, we address respective possibilities and advantages in targeting K^+ channels for therapeutic intervention against ARHL.

K^+ channels in the auditory system

$K_V7.4$ (KCNQ4)

OHC provide the mammalian ear with fast electromechanical amplification, which is required for the dynamic range and speed of sound encoding by the cochlea [38]. A direct mechanical gating of mechanoelectrical transduction channels modulates the input current at cochlear locations of sound stimulus-specific frequencies. This influx of K^+ through apical mechanosensitive channels depolarizes the membrane and drives the contraction of OHC by the motor protein prestin [39]. The speed of this action depends on the capacitance and conductance of the OHC at resting membrane potential, which in turn critically depend on determinants of OHC conductance maintained through the efflux current $I_{K,n}$, mediated by the voltage-gated potassium channel subunit $K_V7.4$ [40].

While $K_V7.4$ expression [41, 42] and its current $I_{K,n}$ [40] are detected prior to hearing onset along the entire basolateral membrane of OHC in mice (Fig. 1a), $K_V7.4$ is redistributed after the onset of hearing (P12-14), becoming restricted solely to the basal pole (Fig. 1b) [43, 44]. This localization suggests that $K_V7.4$ serves to extrude K^+ ions that enter OHC through the apical mechanosensitive channels [28, 29, 45, 46]. $K_V7.4$ is also detected in inner hair cells (IHCs) [25, 26], SGNs, and several nuclei along the auditory pathway, e.g., cochlear nuclei and inferior colliculus [25, 29].

Impaired surface expression of $K_V7.4$ in hair cells has been shown to be a primary step of hearing loss [47–50]. In *Kcnq4* knock-out mice, Carignano et al. [49] showed that the number of OHC slowly decreased at a young age with increasing cell loss up to complete degeneration at oldest ages. Degeneration of IHCs was also observed, but only in the adult stage. The loss of this important K^+ channel in OHC results in a chronic depolarization, possibly increasing Ca^{2+} influx through voltage-gated Ca^{2+} channels and causing their subsequent degeneration due to chronic cellular stress [51].

$K_V7.1$ (KCNQ1)

The sensory cells of the inner ear are in contact with the fluids in the scala media which is filled with endolymph, the extracellular fluid with high K^+ concentration. K^+ is the major charge carrier for sensory transduction and its proper circulation is of great importance for the process of hearing. K^+ ions are secreted into the endolymph by the stria vascularis, enter the hair cells through apical mechanosensitive non-selective

cation channels, and exit these cells via their basolateral membrane, then migrate through supporting cells and fibrocytes towards the stria vascularis using a network of gap junctions where they are reabsorbed by strial marginal cells and released into the endolymph [52, 53]. $K_V7.1$ (KCNQ1) and its β-subunit KCNE1 form a channel complex that is expressed in the mature organ of Corti in the apical membrane of marginal cells of the stria vascularis where it mediates the slow delayed rectifier current $I_{K,s}$ [31–33, 54]. As components of K^+ circulation, $K_V7.1$ and KCNE1 are responsible for the secretion of potassium to the endolymph [55, 56], generating the EP [57, 58].

$K_V7.1$ is expressed throughout the body including the liver, lung, heart, and cochlea [31–33]. The homomeric form of $K_V7.1$ gives rise to a slowly activating and deactivating voltage-dependent potassium current [33]. However, in the inner ear, $K_V7.1$ modulates the kinetics by assembling to KCNE1 to form a heteromeric channel [32]. This results in a drastic slowdown in channel activation, a positive shift in voltage activation threshold, and an absence of inactivation [31]. During cochlear development, $K_V7.1$ was not detected at several embryonic stages in mice (Fig. 1a), indicating that its expression is first established during the postnatal stages (Fig. 1b) [59].

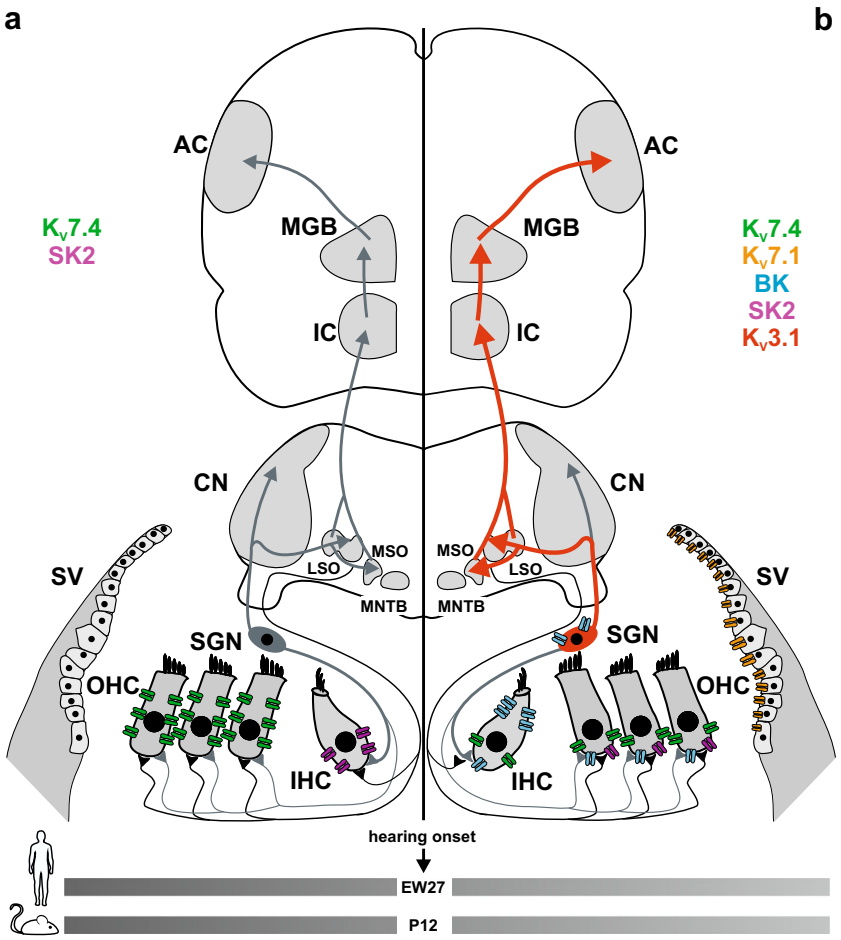

Fig. 1 K^+ expression along the ascending auditory pathway before and after hearing onset. **a** Before the onset of hearing, potassium ion (K^+) channels are mainly expressed in the organ of Corti. In the outer hair cells (OHC), $K_V7.4$ (KCNQ4, green) is found along the entire basolateral membrane, while the inner hair cells (IHCs) express the calcium-activated potassium channel SK2 (KCNN2, purple) before postnatal day (P) 12 in mice, corresponding to embryonic week (EW) 27 in humans. For reference, afferent (gray) and efferent (black) neural projections are shown. **b** In the mature organ of Corti, the endolymph of the scala media contains a high concentration of K^+, which is mediated by $K_V7.1$ (KCNQ1, orange) channels in the apical marginal cells of the stria vascularis (SV). During auditory stimulation, endolymphatic K^+ enter the OHC at the basolateral membrane, and leave the cell via $K_V7.4$, BK (KCNMA1, blue), and SK2 channels. In the IHC, K^+ exits the cell through $K_V7.4$ and BK channels. The expression of BK channels was identified at the lateral wall of IHC as well as in the cell bodies of spiral ganglion neurons (SGNs). The auditory signal is then transmitted from the cochlea to the cochlear nucleus (CN) via rapidly firing neurons containing $K_V3.1$ (KCNC1, red arrows) channels. From here, parvalbumin-positive interneurons project onto the lateral and medial superior olive (LSO and MSO, respectively) and the medial nucleus of the trapezoid body (MNTB), whose fibers also express $K_V3.1$. The inferior colliculus (IC) receives input from the contralateral (not shown) and ipsilateral superior olivary complex. The fibers from the IC project to the medial genicular body (MGB) and the signals are then transmitted to the auditory cortex (AC) via rapid firing, $K_V3.1$ expressing neurons

Loss of functional $K_V7.1$ or KCNE1 leads to Jervell and Lange-Nielsen syndrome which is characterized by cardiac arrhythmia [60–63] and associated with congenital deafness in humans [32, 62, 64, 65]. Potassium secretion into the endolymph is consequently disturbed causing a defect of endolymph production and a collapse of the Reissner membrane [66].

BK (KCNMA1) and SK2 (KCNN2)

Calcium-activated potassium channels are divided into two broad categories, small conductance calcium-activated SK channels and large conductance, voltage-gated, and calcium-sensitive BK channels [67]. SK channels have high Ca^{2+} affinity and long open times, while BK channels are distinguished by significant differences in voltage sensitivity, single-channel conductance, Ca^{2+} affinity, and gating kinetics [68]. These channels share the common functional role of coupling the increase in intracellular Ca^{2+} concentration to hyperpolarization of membrane potential, thus playing an important role in cellular excitability and maintaining K^+ homeostasis [69].

Calcium-activated K^+ conductance has been described in both OHC and IHCs [45, 70]. BK decreases membrane time constants and enables the fast repolarization of hair cell receptor potentials [46] and efferent fibers [71]. BK channels in hair cells appear to show tonotopic gradients of increasing expression from apical (low frequency) to basal (high frequency) regions [34, 35, 72]. The stronger expression in high-frequency regions suggests a contribution of BK channels to high-frequency hearing in mammals. Furthermore, application of acetylcholine, a major efferent neurotransmitter, has been shown to exclusively activate BK currents in high-frequency OHC as opposed to SK currents in the lower-frequency OHC [35], and has been shown to modify efferent inhibitory synaptic responses in high-frequency OHC [73].

In the developing mouse, SK2 channel expression in IHCs was demonstrated during the first two postnatal weeks with a peak around P9 (Fig. 1a), disappearing during hearing onset with decline of cholinergic axosomatic efferent IHC innervations (Fig. 1b) [74]. BK channel expression has been identified in the cell bodies of SGN as well as in inner and outer sensory hair cells at the onset of hearing around P12 (Fig. 1b) [75, 76]. The appearance of the fast BK current, $I_{K,f}$, in IHCs has been shown to coincide with the disappearance of spontaneous action potentials, transforming mature mammalian IHCs into high-frequency signal transducers [77, 78]. During the first four postnatal weeks, $BK\alpha^{-/-}$ mice surprisingly did not show any obvious hearing deficits [51]. High-frequency hearing loss developed in $BK\alpha^{-/-}$ mice only from approximately 8 weeks postnatally onward and was accompanied by a lack of distortion product otoacoustic emissions, suggesting OHC dysfunction.

$K_V3.1$ (KCNC1)

The *Kcnc1* gene yields two $K_V3.1$ subtypes (a and b) through alternative splicing [79], but $K_V3.1b$ has been shown to predominate in the adult rodent brain [80, 81]. Apart from the medial nucleus of the trapezoid body (MNTB) and anteroventral cochlear nucleus (AVCN), $K_V3.1$ is also expressed in neurons of the reticular thalamic nucleus and parvalbumin-positive (PV+) interneurons of the cortex and hypothalamus [81, 82]. $K_V3.1$ belongs to the delayed rectifier channel family and is located on presynaptic terminals [83–85]. Its high activation threshold and rapid activation and deactivation in response to voltage changes reduce the AP duration while simultaneously maximizing firing frequency [86]. This special characteristic of $K_V3.1$ for maximizing firing frequencies is related to its distinct expression profile in fast spiking interneurons [81, 82] and the important role it plays in the auditory system.

During auditory pathway maturation, $K_V3.1$ levels increase in SGNs between P4 and P8, reducing AP latencies and duration after hearing onset [87, 88]. The expression level of $K_V3.1$ rises dramatically near the onset of hearing along with the maturation of fast auditory processing as shown in the brainstem [89–91] and the inferior colliculus (Fig. 1b) [92, 93]. This expression profile in fast PV+ interneurons makes $K_V3.1$ a key contributor to the lowered threshold and shortened latency of cortical auditory responses, which can be measured after the sharpening of cortical receptive fields [94] at the end of the critical period after hearing onset. Thus, receptive field maturation coincides with the maturation of a network of fast-spiking GABAergic PV+ interneurons [95–98], predicted to mature in the auditory pathway with fast auditory processing after hearing onset [99]. Accordingly, given the optimal design of $K_V3.1$ for high-rate repetitive firing [100, 101], it has been identified as critical for fast-spiking PV+ interneurons [102]. Also, the key components in the auditory pathway required for auditory discrimination, the MNTB and AVCN, contain neurons that fire at very rapid rates, requiring the expression of $K_V3.1$ for rapid repolarization of AP during sound-induced activity [103–105]. MNTB neurons of $K_V3.1$ deficient mice were incapable of following high-rate stimulation or sustaining high-rate firing AP [37], demonstrating that $K_V3.1$ is essential for the rapid firing patterns. Given that hearing impairment can lead to a decline in $K_V3.1$ expression in the MNTB [36, 106], it is likely that the lack of $K_V3.1$ channels is a key contributor to deficits in fast auditory discrimination over age [107].

Noise exposure linked to ARHL

The driving mechanisms of hearing loss over age remain largely unclear. Already in rodent animal species that are

widely used as models for human hearing, the age-related loss of cochlear function is highly variable; different mouse lines display hearing loss as early as 5 weeks after birth, determined partly by species, strain, and animal history, but also partly by lifetime auditory exposure determined by noise intensity level, duration, predictability, exposure context, and other characteristics of the sound [108]. In healthy-aged Mongolian gerbils, auditory-evoked potentials show a decrease of responses before the loss of auditory sensitivity, which is attributed to age-related pathologies in the auditory periphery [109, 110]. Studies in quiet-aged gerbils suggest that loss of synapses is the earliest age-related degenerative event (reviewed in [111]), preceding strial dysfunction and other cochlear pathologies [112]. Functional studies on aging rats have confirmed this [113] and extended the functional consequences of the loss of synapses beyond hearing sensitivity towards the loss of central compensatory action of the brain to make use of the few remaining auditory signals. In the cochlea, aging in gerbils and rats is characterized by threshold increase and concurrent loss of normal OHC phenotype from the second third of their lifespan onwards, which is related to a reduced brain-derived neurotrophic factor (BDNF) expression levels in the auditory nerve [114].

In CD-1 mice, often used as a model for human hearing, the EP is already lost at the age of 9 months, and the sensory organ is completely degenerated [115]. CBA/CaJ mice are described to have normal EP and excellent hearing for a large portion of their lifespan. Nevertheless, they display a remarkable acceleration of ARHL when repeatedly exposed to "benign" noise during their lifespan [116, 117]. By contrast, 129/SvEv mice are exceptionally resistant to noise-induced hearing loss [118], but preexisting anomalies in substrains of 129/SvJ mice predispose the ear to degenerate prematurely when interacting with K^+ channel deletion [118]. Finally, ROS-induced activation of DNA damage in senescence-accelerated mouse-prone 8 (SAMP8) mice are discussed as the driver for ARHL [119]. ROS can be induced in the ear by exposure to moderate, nevertheless harmful, acoustic noise [120, 121] causing an accumulation of toxic noise events throughout lifetime (reviewed in [122]). We have to assume that even the early loss of synaptic contacts between sensory hair cells and SGNs or synaptopathy [17] can be traced back to cumulative excitotoxic injury events [123], the largest source of which is likely to be noise exposure [124, 125].

One of the earliest events following metabolic limitations during noise exposure is the impairment of membrane surface expression of distinct K^+ channels in the cochlea, a process that is here suggested to have a pivotal role in ARHL. Both $K_V7.4$ (KCNQ4) and BK (KCNMA1) channels are required for normal hearing and have been suggested to protect OHC in cochlear regions that register high frequencies from Ca^{2+} overload [47, 72]. Functional loss in OHC has been linked to the loss of $K_V7.4$ in the membrane of the OHC, preceding their degeneration in the middle- and high-frequency coding cochlear compartments [51, 126]. The loss of BKα led to a similar phenotype as by pharmacological blockage of $K_V7.4$ channels, suggesting that a loss of the *BK* gene increases susceptibility for progressive ARHL, similar to *KCNQ4* mutation [26, 47, 51, 78]. Consistent with that assumption, exposure to a low-frequency, non-traumatic sound has been found to not affect hearing sensitivity of wild-type mice, but mice with *BK*α gene deletion experienced a dramatic loss of hearing sensitivity within the stimulated low-frequency hearing range [72]. It is important to note that the affected low-frequency range was not part of the hearing range affected by accelerated ARHL in the young unexposed BKα deficient mice, thus confirming that the low-frequency cochlear compartments are rendered susceptible by the absence of BK. The low-frequency noise exposure extended the loss of KCNQ4 from OHC towards the low-frequency cochlear compartments affected by the noise exposure, confirming that the hearing loss resulted from the absence of KCNQ4 from hair cell plasma membrane [72]. The metabolic balance due to the fast repolarization of the receptor potential is a requirement for the healthy homeostasis of hair cells. Thus, the maintenance of KCNQ4 and BK in the OHC membrane is most critical to counteract a Ca^{2+} overload of hair cells, irrespective of whether induced through excitotoxic, ototoxic, or noise exposure events, all of which are challenges that accumulate over advancing age. The activity in MOC efferent fibers contacting OHC plays an important role to activate BK and SK2 channels through acetylcholine release. Therefore, any reduction in MOC efferent fibers, which were previously shown to decline with advancing age [127], is expected to increase susceptibility to noise-induced hearing loss over age, due to reduced potential to rapidly remove K^+ from OHC, as can be predicted from various studies [34, 51, 72, 128, 129].

Furthermore, the protective role of BK channels is not limited to the hearing organ. In the mammalian central nervous system, BK is expressed in the neuron soma, processes, and presynaptic terminals, where it drives the membrane potential towards the potassium equilibrium potential to re- and hyperpolarize the neuron [130]. To study the importance of central BK deletion in the brain, normal hearing mice are required. Fortunately, the F1 generation of a hybrid sv129/C547/Bl6 background of mice with genetic deletion of the BK channel has documented good hearing up to the age of 15 weeks [131], which again confirms the multifactorial nature of BK gene deletion-related progression of hearing disorder. Most strikingly, these mice nevertheless display slower learning capacity and no improvement of pre-pulse inhibition of the acoustic startle response over days [131]. This strongly suggests that besides the protective role of cochlear BK channels [51, 72], they further contribute to the integrity of central neuronal circuits that are essential to process environmental auditory information. Because the top-down modulation of cochlear hair

cells' excitability is assumed to play a critical role in adaptation to and avoiding damaging influences of environmental changes [132–134], the centrifugal control of neuronal excitability may be a major factor of K^+ channel-related ARHL.

SK2 (KCNN2) is expressed in OHC as a postsynaptic marker apposing synapses of MOC efferent fibers and required for Ca^{2+}-activated SK2 channel activation through MOC's cholinergic function [135]. The number of SK2-positive foci is remarkably reduced in mouse strains that exhibit fast progression of ARHL, such as the C57BL/6J [136], thus representing a general trait in the pathophysiological progression of ARHL. The protective role of MOC efferent fibers during aging and noise only recently received support through the discovery that loss of MOC efferent fibers is an early event of ARHL [127]. We may thus conclude that loss of BK, SK2, and KCNQ4 is likely to be early contributors to ARHL, with their dysfunction discussed as a primary event of OHC loss over age.

K_V7.1 (KCNQ1) is a major component of the K^+ circulation by the stria vascularis and is responsible for the secretion of potassium to the endolymph and maintaining the EP, to assist motility in OHC, perform synaptic activity, and maintain the spontaneous and evoked activity of SGNs. The cells of the stria vascularis contain high numbers of mitochondria [137, 138] and Na^+/K^+ATPase [139, 140]. In quiet-aged gerbils, the stria vascularis and spiral ligament showed a decrease in Na^+/K^+ATPase activity in these tissues [141], as well as degeneration of strial capillaries at both ends of the cochlear spiral [142] and decreased blood flow [143]. In aged CBA/CaJ mice, Na^+/K^+ATPase expression was largely reduced, and the stria vascularis was found to be atrophied [139]. However, it remains difficult to determine whether the lack of blood flow or the cellular dysfunction leads to the strial atrophy. As such, most of these studies did not specifically analyze membrane expression patterns of KCNQ1 during stria vascularis degeneration over age. Interestingly, 12-month-old C57BL/6 mice displayed notable hearing loss and morphological examination showed a significant OHC loss in the cochlear basal turn accompanied by atrophy of the stria vascularis, with immunohistochemical analysis revealing dramatically decreased KCNJ10 and KCNQ1 expression [144]. While these studies observed a conservation of the EP in these aging C57BL/6 mice, and suggested that the stria vascularis can generate a new balance for potassium influx and efflux at relatively low turnover [144], other studies found a clear requirement of adequate KCNQ1 recycling in marginal stria vascularis membranes for hearing and OHC cell survival [145]. On the whole, age-dependent decline of KCNQ1 from the marginal surface of the stria vascularis should be urgently reconsidered with regard to ARHL.

The expression of K_V3.1 (KCNC1) subtype b, which is predominant in the adult rodent brain [80, 81], has been shown to decrease in neurons of the MOC efferent system by middle age in CBA/CaJ mice, and these changes appeared to correlate with functional declines in efferent activity in both middle-aged CBA/CaJ mice and K_V3.1b knockout mice [106, 146], suggesting age-dependent decline of K_V3.1b as a possible cause of MOC efferent decline over age [127]. Also, C57BL/6 mice have been shown to lose sensory basal hair cells during early adulthood progressing towards the apex with age [147], which was linked to a concurrent decrease in levels of K_V3.1b in brainstem neurons [106]. In Sprague-Dawley rats, both the intensity of K_V3.1 immunostaining and number of K_V3.1-positive neurons have been shown to decline with age in the cochlear nucleus [148]. Age-dependent K_V3.1 modifications are expected to contribute to age-dependent temporal discrimination deficits [149]. This is particularly important when considering the special role K_V3.1 activity displays as a modulator for fast-spiking inhibitory PV+ interneurons, which control feedforward and feedback inhibitory modalities [150], suggested to be essential for fast auditory processing circuits [99]. Reduced PV expression levels have also been found in the auditory cortex in aged animal models [151], which implies a potential relation between the decline of K_V3.1 expression over age and PV-mediated processing deficits in ARHL.

Based on evidence from different animal models and from human temporal bones, it seems likely that aging or senescence alone is not necessarily a major risk factor for hearing impairment over advancing age. Convincing evidence that aging per se is not necessarily the main cause for ARHL comes from geriatric cats that have normal hearing sensitivity and auditory brainstem functions over the whole frequency range of hearing, developing ARHL only late in their lifespan [152]. The current evidence suggests that an accumulation of noise events may most likely be the origin of ARHL in humans (Fig. 2a), with excessive noise able to overstimulate sensory hair cells and requires fast and effective K^+ recycling within the inner ear. This suggests that ARHL may rather be an accumulation of damage from minor toxic events instead of an inevitable progressing loss of cells, structures, and the ability for regeneration.

Genetic predisposition to ARHL

The human genome contains roughly 70 K^+ channel-encoding genes [153]. Many of these genes play essential roles in normal physiological processes, including those involved in hearing, as evidenced by the clinical appearance of syndromic and/or non-syndromic hearing loss with genetic variation. As ARHL has a delayed onset and progressive nature, it is plausible to hypothesize that genetic variation may directly contribute to an inter-individual variability and susceptibility to ARHL or to other indirect processes of aging such as metabolic status. One way to test this is to perform statistical

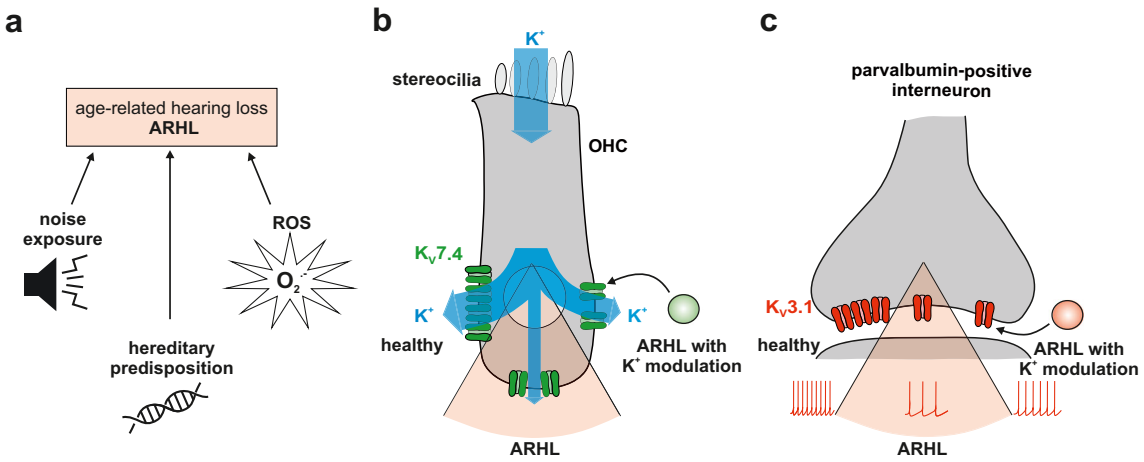

Fig. 2 **a** In the challenged auditory system leading to age-related hearing loss (ARHL), the key causing factors are postulated to be lifetime noise exposure, hereditary predisposition, and the accumulation of reactive oxygen species (ROS). **b** In a healthy outer hair cell (OHC), potassium ions (K^+) enter the cell through apical mechanosensitive channels and are then transported to the supporting cells through $K_V7.4$ (KCNQ4, green) channels on the basolateral membrane of OHC. However, in the challenged system, the expression of $K_V7.4$ is reduced, resulting in a poor K^+ efflux. This state can be influenced by the addition of K^+ channel modulators (green circle) in a way where cell surface expression remains stable but the efflux rate can be increased. **c** In fast-spiking, parvalbumin-positive interneurons, $K_V3.1$ (KCNC1, red) is required for the high-frequency repetitive firing. A decline in $K_V3.1$ cell surface expression leads to an incapacity of neurons to maintain high-frequency firing action potentials. Modulators that bind to $K_V3.1$ (red circle) may lower action potential latencies and duration and increase the firing pattern of these neurons

analyses in the form of association testing to identify genetic regions or variants, in either genes of interest or across the entire genome, to identify associations with ARHL. This type of analysis has not been performed for all of the genes encoding the channels discussed in this review. However, in the following section, we summarize the current body of genetics knowledge for our selected K^+ channels and make connections to ARHL.

The *KCNQ4* gene encodes the potassium voltage-gated channel subfamily Q member 4 protein ($K_V7.4$). Deleterious variants in *KCNQ4* cause autosomal dominant non-syndromic hearing loss (MIM* 603537) [30]. A significant association between *KCNQ4* and ARHL has been identified by Van Eyken et al. [154] in two independent populations. However, except for one single nucleotide polymorphism (SNP), i.e., SNP12 (rs2149034), different SNP spanning a 13-kb region of *KCNQ4* were positively associated in both populations. *KCNQ4* was regarded by the authors as a strong susceptibility gene for ARHL; however, replication studies have not reproduced this observation. *KCNQ4* expression increases with age, supporting a hypothesis that an increased defective protein load may lead to progressive cellular dysfunction [154, 155]. Van Laer et al. [156] also found significant differences between individuals susceptible and resistant to noise exposure for the allele, genotype, and haplotype frequencies for a *KCNQ4* SNP (rs34287852). A genome-wide association study (GWAS) meta-analysis from the Cohorts for Heart and Aging Research in Genomic Epidemiology or CHARGE Consortium was performed with the aim to identify genetic factors associated with overall mortality and healthy longevity [157]. This study identified 14 independent SNP that predicted risk of death and eight that predicted healthy longevity. Several of these SNP were located either in or near genes that are involved in neurological processes. A *KCNQ4* SNP (rs2769255) was significantly associated with both mortality and healthy longevity and is located approximately 4.4 kb upstream from the gene. The enrichment of SNP, either in or adjacent to genes involved in neurological processes, suggests the importance of these genes in regulating healthy aging and longevity.

The *KCNQ1* gene encodes the potassium voltage-gated channel subfamily Q member 1 protein ($K_V7.1$). *KCNQ1* variants have been associated with long QT syndrome, short QT syndrome, atrial fibrillation, and Jarvell and Lange-Nielsen syndrome (MIM* 607542) [158]. The same study by Van Laer et al. [156] also found one significant difference between noise susceptible and resistant individuals in one *KCNQ1* SNP (rs163171). The most interesting literature linking KCNQ1 to ARHL comes from the diabetes field, which constitutes a risk factor for ARHL [21]. With respect to a broader biological context, *KCNQ1* is also expressed in the heart, stomach, intestine, liver, kidney, and insulin-producing cells [159, 160]. Several GWAS have uncovered many independent intronic regions in *KCNQ1* that harbor type 2 diabetes mellitus risk alleles (rs231362, rs2283228, rs2237892, rs2237895, and rs2237897) in Europeans, East Asians, and Native Americans [161–164]. It is unclear if the SNP exert a functional effect and whether this would involve *KCNQ1* or the neighboring genes, *KCNQ1OT1*, or *CDKN1C*, a known regulator of pancreatic beta-cell development [163]. Neither

Kcnq1 null mice nor patients with deleterious variants show impaired hyperglycemia or glucose intolerance; therefore, it is thought that an increase in expression in pancreatic beta-cells may be linked to the development of type 2 diabetes [163]. Interestingly, *KCNQ1* resides on chromosome 11p15.5, a maternally imprinted region [161]. This means that maternally inherited variants in this imprinted region confer disease risk. There is compelling evidence that diabetes risk at the *KCNQ1* locus is medicated through a gene with imprinted gene expression that may be mediated by *KCNQ1* or neighboring genes (*KCNQ1OT1* or *CDKN1C*) [165]. The confirmation of so-called parent-of-origin effects that have been identified in every organ system of the human body so far except the auditory system would fundamentally re-shape the way the genomics field views genetic contributors of ARHL [166].

The *KCNMA1* (BK), *KCNN2* (SK2), and *KCNC1* (K_V3.1) genes presently do not have compelling evidence linking them to ARHL, but several already have gene-disease associations. The *KCNMA1* gene encodes the potassium calcium-activated channel subfamily M alpha 1 protein (BK). Deleterious *KCNMA1* variants are associated with paroxysmal nonkinesigenic dyskinesia with or without generalized epilepsy, Liang-Wang syndrome and cerebellar atrophy (MIM* 600150). Although no current genetic-based studies linking *KCNMA1* SNP to presbycusis and aging exist, BK channels appear to be sensitive to oxidative stress [167]. The *KCNN2* gene encodes the potassium calcium-activated channel subfamily N member 2 protein (SK2) and is currently not associated with any human phenotypes. The SK channel has been linked to neuroprotection in the form of mitochondrial resilience against neuronal death [168]. SK channels may involve attenuation of mitochondrial calcium uptake upon SK channel activation. Mitochondrial activation calcium uptake across the mitochondrial membrane is essential for the numerous calcium-sensitive processes required for mitochondrial metabolism and respiration [169]. Oxidative stress in neurons leads to a series of detrimental effects such as intracellular calcium overload that induces changes in mitochondrial metabolism such as alterations in ATP synthesis and NADP(H) oxidation that lead to an increase in ROS [168, 170]. Finally, the *KCNC1* gene encodes the potassium voltage-gated channel subfamily C member 1 protein (K_V3.1). It has been associated with autosomal-dominant progressive myoclonic epilepsy (MIM* 176258) [171] and intellectual disability without seizure or epilepsy [172].

On the whole, the current literature lacks conclusive human genetic evidence to link ARHL and *KCNQ1* (K_V7.1), *KCNMA1* (BK), *KCNN2* (SK2), and *KCNC1* (K_V3.1), but contains limited information to link it to *KCNQ4* (K_V7.4). These genes are still intriguing due to possible gene-environment interactions in processes such as aging and metabolism that are presently unknown (Fig. 2a). ARHL is a complex disorder with environmental, e.g., noise exposure, and genetic factors. Twin studies for ARHL have estimated the heritability of ARHL, or importance of a genetic component in a disease [154] and found that twin similarity of monozygotic twins decreased with age and dizygotic twins increased with age [173]. This suggests that environmental factors may become more prominent with age. Of note, SNP in K^+ channel genes have not been noted with significance in the more recent large-scale genomics studies [174, 175]. However, if K^+ channel genetic targets are identified with future ongoing studies, they have the potential to make excellent therapeutic targets.

K^+ channels as therapeutic targets against ARHL

Having given a comprehensive view about the role select potassium channels play in the cochlea and the ascending auditory pathway for ARHL in the context of noise exposure and genetic predispositions, we may next illuminate therapeutic intervention strategies with a potential to prevent or repair hearing dysfunction as future ARHL therapies. Provided that noise exposure, age-related synaptopathies and neuropathies, and cardiovascular risk factors are major contributors of ARHL [8, 14, 21], substantial evidence points to oxygen metabolism as one of the main culprits for K^+ channel dysfunctions with aging given that these dysfunctions are not only based on channel mutations. Numerous studies evidenced that ROS increases with age [176] and by statistical probability alone preferentially affects K^+ channels (Fig. 2a). The extreme genetic heterogeneity and functional diversity of K^+ channels are unparalleled to that of other types of channels [23]. ROS can indirectly modulate K^+ channel function by acting on cellular pathways that regulate gene transcription, trafficking, turnover, and proteasomal degradation [177]. On the other hand, direct age-related oxidation of particular voltage-dependent K^+ channels that include the aforementioned K_V7 channels, Ca^{2+}-activated BK and SK2, and K_V3.1 underlie a specific type of neuronal aging [23]. In the auditory system, several lines of evidence hint to the importance of these channels with respect to ARHL as discussed above.

KCNQ genes have a considerable physiological impact in many cell types. This reliance upon K_V7 channels for normal cellular function is evident by hereditary disorders caused by mutations in *KCNQ* genes, meaning that pharmacological targeting of these channels has broad appeal. Consequently, a plethora of chemical entities that modulate K_V7 channel activity has been developed. Moreover, K_V7 channels are influenced by many disparate intracellular mediators and trafficking processes, making upstream targeting an appealing prospect for therapeutic development to overcome deficits related to these channels [178]. Until now, however, modulation of K_V7 channels has been recognized mainly as a

potential to prevent neurodegenerative disorders linked to epilepsy and cognitive deficits [179]. Although efforts have not reached ARHL, pharmacological approaches in trials targeting $K_V7.2$ to $K_V7.5$ channels with the novel antiepileptic drug retigabine (or ezogabine) have been used to overcome hearing loss [180, 181]. Retigabine increases the probability of opening these K_V7 channels upon causing a negative 15-mV leftward shift in the voltage-dependence of activation and a decrease in the rate of deactivation (Fig. 2b) [178, 182–184].

Given a hereditary origin of progressive hearing loss through *KCNQ4* dysfunction, as it occurs in DFNA2 non-syndromic autosomal-dominant progressive high-frequency hearing loss [155, 157], genetic therapeutic approaches have been envisioned, e.g., those following heterologic expression of wild-type channels that could be combined with K_V7 channel openers such as retigabine [181]. Correspondingly, retigabine has already proven successful to rescue hearing deficits in Korean families with co-segregating *KCNQ4* pathogenic variants [180]. Also, a combination of zinc pyrithione plus retigabine has been used in Chinese hamster ovary cells either transfected with wild-type *Kcnq4* sequences or ones containing variants that encode mutated channels, evidencing a restoration of channel function that was dependent on the location of the DFNA2 mutation within the gene [185]. This further provides an interesting approach to rescue progressive ARHL linked with mutations of *KCNQ* genes on the personalized medicine level.

Undoubtedly, $K_V7.1$ (KCNQ1) expression decreases with advancing age in the stria vascularis [144], but, as previously highlighted, it may only contribute to ARHL in a secondary manner [14]. Hormone changes may be considered as contributors to the decline of $K_V7.1$ surface expression loss in the stria vascularis with age. Thus, throughout the lifespan, the steroid hormone estrogen (17β-oestradiol, E2) declines with age in females [186]. Estrogen decline has been suggested to induce $K_V7.1$ dysfunction through changes in estrogen-dependent control of its internalization from the plasma membrane by a clathrin-mediated endocytosis process [187]. Estrogen has been shown to modulate the association between $K_V7.1$ and the clathrin adaptor AP-2, required for endocytosis, rather than degrading the ion channel, and a biphasic recycling mechanism involving Rab4 and Rab11 is involved in this process, as shown in colon epithelium [187]. Modulators of $K_V7.1$ may thus contribute to overcome postmenopausal-related hearing loss reported to occur with aging [188].

Within this context, it may be interesting to note that a spatio-temporal correlation of the loss of KCNQ1 and KCNE1 surface expression and loss of hearing thresholds has been reported following loss of proteins involved in KCNQ1 recycling, such as SCARB2 [145]. Human SCARB2 is a key regulator of lysosome integrity, motility, and dynamics, and its loss has been shown to cause rupture of lysosome membranes and significantly shortened lifespan [189]. This may suggest any disturbance of proper membrane recycling or insufficient targeting of KCNQ1 and KCNE1 in the stria vascularis, might be a possible rationale for ARHL [190], and renders lysosomal enzymes that stimulate trafficking as potential candidates for targeting ARHL [191].

The Ca^{2+}-activated channels BK (KCNMA1) and SK2 (KCNN2) play an important role in noise-induced ARHL, counteracting noise-induced hyperpolarization of OHC. These may be particularly sensitive for age-dependent ROS damage, being both susceptible to redox modifications [23, 192]. The noise-induced rise in Ca^{2+} in OHC (i.e., Ca^{2+} overload) is expected to induce slow cellular after-hyperpolarizations for SK2 and fast ones for BK channels, both possibly contributing to the prevention of noise damage to OHC [34]. Within this context, the specific role of BK in IHCs, shown to rapidly and robustly shape IHC receptor potential [193], needs to be considered. An oligonucleotide antisense against SK channels was shown to compensate an age-related memory decline in mice, resulting from ROS-induced modification of SK channel function [194, 195], providing viral-mediated expression of SK2 channel as a potential means to target its deficits with advancing age. For BK channels, specific blockers have been shown to counteract the negative redox effects in the brain, indicating that ROS-signaling on BK channels leads more to active, rather than inactive, channels [196]. This would expectedly lead to reduced neuronal excitability of hair cells, through upregulation of K^+ channel activities as a hallmark of the aging process. This hypothesis for the aging cochlea awaits further studies and requires reflection in the context of age-dependent deficits of fast auditory processing [197, 198].

A-type voltage-gated potassium (K_V) channels, to which the $K_V3.1$ (KCNC1) channel belongs, are sensitive for age-dependent ROS changes [199], resulting through oxidation of channels in slowed inactivation and increased open channel currents, modifications that would dampen neuronal excitability as shown for the hippocampus [200, 201]. $K_V3.1$ has not only been shown as important for sustained temporally accurate firing, being susceptible to deprivation, but also to its deficits partially restored in animals by the compound AUT00063 (Fig. 2c) [197]. AUT00063 has also been shown to improve auditory synchronization and support more accurate decoding of temporal sound features in the inferior colliculus and auditory cortex in adult mice with a near-complete loss of auditory nerve afferent synapses in the contralateral ear [197], rendering $K_V3.1$ modulators an attractive candidate for pharmaceutical targeting against fast auditory processing deficits due to ARHL. Furthermore, antidepressants, such as p11, have been shown to control $K_V3.1$ expression level and intracellular localization in PV+ interneurons of

the hippocampus [202]. With reduced $K_V3.1$ levels, the capacity of PV+ interneurons to adapt to high-frequency firing is abolished [202], underscoring the crucial role that sustained expression levels of $K_V3.1$ may have over age for preserving temporal auditory processing and speech discrimination. Importantly, the high metabolic vulnerability of particular PV+ interneuron synapses [203] should be reconsidered in the context of required sustained $K_V3.1$ channels for its proper function in the ascending auditory pathway. $K_V3.1$ channel modulators have recently been shown to enable faster activating kinetics and increase firing frequency in fast-spiking GABAergic interneurons [204, 205]. This renders these modulators as promising candidate pharmaceutical drugs to overcome ARHL, with a potential to improve speech in noise deficits, especially with regard to the reconsidered role that maintained PV+ interneuron-mediated feedforward and feedback circuits have in fast auditory processing [99].

Outlook

In humans, the classification of various presbycusis profiles over age is manifold, but despite profound heterogeneity, most of the presbycusis profiles are characterized by a dominant loss of sensitivity to high-frequency tones [206]. Therefore, loss of auditory sensory function with age must be classified by the probable excessive noise exposure as a main contributor [14]. The current review suggests that noise-induced overstimulation of sensory hair cells and neurons most critically depends on fast and effective K^+ recycling in the cochlea, including sustained fast auditory processing that may be required for $K_V3.1$-driven, fast PV+ interneuron function over age. Pharmaceutical targeting of K^+ channels to enable fast recycling through stimulators, modulators, or activators has future potential to arrest or even prevent ARHL before the inevitable progression of loss of cells, structures, and degeneration.

An important caveat to consider with respect to different functional consequences of oxidation for the reviewed K^+ channels is the rationale against considering therapies based on generic anti-oxidants for the treatment of ARHL. Modes of interventions aimed at targeting more specific channel proteins or distinctly responsible ROS species, which is not a simple task, may be more likely to succeed. The ability to pharmacologically separate the impact of individual K^+ channel subunits needs further refinement, beginning with existing compounds and reinforcement with molecular interference techniques.

Although many clinicians inform patients that ARHL cannot be prevented, animal model studies provide insight and future prospects for clinical trials and even clinical interventions to prevent or slow the progression of ARHL.

Acknowledgements Open Access funding enabled and organized by Projekt DEAL.

Funding This work was supported by the German Research Foundation (DFG-KN316/12-1 to M.K.; DFG-RU713/3-2 to L.R.), Intramural Funding (*f*ortüne) at the University of Tübingen (2545-1-0 to B.V.), and the Ministry of Science, Research and Art, Baden-Württemberg (MWK RISC 2019 to B.V.). B.P. was supported by a scholarship for the promotion of young scientists from the Episcopal Foundation "Cusanuswerk" (Bonn, Germany).

Compliance with ethical standards

Conflict of interest The authors declare that they have no conflict of interest.

Ethics approval Not applicable.

Consent to participate Not applicable.

Consent for publication Not applicable.

Code availability Not applicable.

References

1. Bowl MR, Dawson SJ (2019) Age-related hearing loss. Cold Spring Harb Perspect Med:9. https://doi.org/10.1101/cshperspect.a033217
2. Lin FR, Yaffe K, Xia J, Xue QL, Harris TB, Purchase-Helzner E, Satterfield S, Ayonayon HN, Ferrucci L, Simonsick EM, Health ABCSG (2013) Hearing loss and cognitive decline in older adults. JAMA Intern Med 173:293–299. https://doi.org/10.1001/jamainternmed.2013.1868
3. Kamil RJ, Betz J, Powers BB, Pratt S, Kritchevsky S, Ayonayon HN, Harris TB, Helzner E, Deal JA, Martin K, Peterson M, Satterfield S, Simonsick EM, Lin FR, Health ABCs (2016) Association of hearing impairment with incident frailty and falls in older adults. J Aging Health 28:644–660. https://doi.org/10.1177/0898264315608730
4. Rutherford BR, Brewster K, Golub JS, Kim AH, Roose SP (2018) Sensation and psychiatry: linking age-related hearing loss to late-life depression and cognitive decline. Am J Psychiatry 175:215–224. https://doi.org/10.1176/appi.ajp.2017.17040423
5. Lin FR, Ferrucci L, Metter EJ, An Y, Zonderman AB, Resnick SM (2011) Hearing loss and cognition in the Baltimore Longitudinal Study of Aging. Neuropsychology 25:763–770. https://doi.org/10.1037/a0024238

6. Livingston G, Sommerlad A, Orgeta V, Costafreda SG, Huntley J, Ames D, Ballard C, Banerjee S, Burns A, Cohen-Mansfield J, Cooper C, Fox N, Gitlin LN, Howard R, Kales HC, Larson EB, Ritchie K, Rockwood K, Sampson EL, Samus Q, Schneider LS, Selbæk G, Teri L, Mukadam N (2017) Dementia prevention, intervention, and care. Lancet 390:2673–2734. https://doi.org/10.1016/s0140-6736(17)31363-6
7. Montero-Odasso M, Ismail Z, Livingston G (2020) One third of dementia cases can be prevented within the next 25 years by tackling risk factors. The case "for" and "against". Alzheimers Res Ther 12:81. https://doi.org/10.1186/s13195-020-00646-x
8. Fischer N, Johnson Chacko L, Glueckert R, Schrott-Fischer A (2020) Age-dependent changes in the cochlea. Gerontology 66:33–39. https://doi.org/10.1159/000499582
9. Frisina RD (2001) Subcortical neural coding mechanisms for auditory temporal processing. Hear Res 158:1–27. https://doi.org/10.1016/s0378-5955(01)00296-9
10. Frisina RD (2009) Age-related hearing loss: ear and brain mechanisms. Ann N Y Acad Sci 1170:708–717. https://doi.org/10.1111/j.1749-6632.2009.03931.x
11. Frisina RD, Frisina DR (2013) Physiological and neurobiological bases of age-related hearing loss: biotherapeutic implications. Am J Audiol 22:299–302. https://doi.org/10.1044/1059-0889(2013/13-0003)
12. Ohlemiller KK (2004) Age-related hearing loss: the status of Schuknecht's typology. Curr Opin Otolaryngol Head Neck Surg 12:439–443
13. Merchant SN, Nadol JB (2010) Schuknecht's pathology of the Ear. People's Medical Publishing House-USA
14. Wu PZ, O'Malley JT, de Gruttola V, Liberman MC (2020) Age-related hearing loss is dominated by damage to inner ear sensory cells, not the cellular battery that powers them. J Neurosci 40:6357–6366. https://doi.org/10.1523/JNEUROSCI.0937-20.2020
15. Plack CJ, Barker D, Prendergast G (2014) Perceptual consequences of "hidden" hearing loss. Trends Hear 18. https://doi.org/10.1177/2331216514550621
16. Kujawa SG, Liberman MC (2015) Synaptopathy in the noise-exposed and aging cochlea: primary neural degeneration in acquired sensorineural hearing loss. Hear Res 330:191–199. https://doi.org/10.1016/j.heares.2015.02.009
17. Wu PZ, Liberman LD, Bennett K, de Gruttola V, O'Malley JT, Liberman MC (2019) Primary neural degeneration in the human cochlea: evidence for hidden hearing loss in the aging ear. Neuroscience 407:8–20. https://doi.org/10.1016/j.neuroscience.2018.07.053
18. Viana LM, O'Malley JT, Burgess BJ, Jones DD, Oliveira CA, Santos F, Merchant SN, Liberman LD, Liberman MC (2015) Cochlear neuropathy in human presbycusis: confocal analysis of hidden hearing loss in post-mortem tissue. Hear Res 327:78–88. https://doi.org/10.1016/j.heares.2015.04.014
19. Muniak MA, Ayeni FE, Ryugo DK (2018) Hidden hearing loss and endbulbs of held: evidence for central pathology before detection of ABR threshold increases. Hear Res 364:104–117. https://doi.org/10.1016/j.heares.2018.03.021
20. Salvi R, Ding D, Jiang H, Chen GD, Greco A, Manohar S, Sun W, Ralli M (2018) Hidden age-related hearing loss and hearing disorders: current knowledge and future directions. Hearing Balance Commun 16:74–82. https://doi.org/10.1080/21695717.2018.1442282
21. Hong JW, Jeon JH, Ku CR, Noh JH, Yoo HJ, Kim DJ (2015) The prevalence and factors associated with hearing impairment in the Korean adults: the 2010-2012 Korea National Health and Nutrition Examination Survey (observational study). Medicine (Baltimore) 94:e611. https://doi.org/10.1097/MD.0000000000000611
22. Han C, Someya S (2013) Mouse models of age-related mitochondrial neurosensory hearing loss. Mol Cell Neurosci 55:95–100. https://doi.org/10.1016/j.mcn.2012.07.004
23. Cai SQ, Sesti F (2009) Oxidation of a potassium channel causes progressive sensory function loss during aging. Nat Neurosci 12:611–617. https://doi.org/10.1038/nn.2291
24. Knipper M (2014) Introduction to Compensation after injury: always for good? Neuroscience 283:1–3. https://doi.org/10.1016/j.neuroscience.2014.08.039
25. Beisel KW, Nelson NC, Delimont DC, Fritzsch (2000) Longitudinal gradients of KCNQ4 expression in spiral ganglion and cochlear hair cells correlate with progressive hearing loss in DFNA2
26. Oliver D, Knipper M, Derst C, Fakler B (2003) Resting potential and submembrane calcium concentration of inner hair cells in the isolated mouse cochlea are set by KCNQ-type potassium channels. J Neurosci 23:2141–2149
27. Nouvian R, Ruel J, Wang J, Guitton MJ, Pujol R, Puel J-L (2003) Degeneration of sensory outer hair cells following pharmacological blockade of cochlear KCNQ channels in the adult guinea pig. Eur J Neurosci 17:2553–2562. https://doi.org/10.1046/j.1460-9568.2003.02715.x
28. Holt JR, Stauffer EA, Abraham D, Geleoc GS (2007) Dominant-negative inhibition of M-like potassium conductances in hair cells of the mouse inner ear. J Neurosci 27:8940–8951. https://doi.org/10.1523/JNEUROSCI.2085-07.2007
29. Kharkovets T, Hardelin J-P, Safieddine S, Schweizer M, El-Amraoui A, Petit C, Jentsch TJ (2000) KCNQ4, a K+ channel mutated in a form of dominant deafness, is expressed in the inner ear and the central auditory pathway. PNAS 97:4333–4338. https://doi.org/10.1073/pnas.97.8.4333
30. Kubisch C, Schroeder BC, El-Amraoui A, Marlin S, Petit C, Jentsch TJ (1999) KCNQ4, a Novel Potassium Channel Expressed in Sensory Outer Hair Cells, Is Mutated in Dominant Deafness. Cell Press 96:437–446. https://doi.org/10.1016/S0092-8674(00)80556-5
31. Barhanin J, Lesage F, Guillemare E, Fink M, Lazdunski M, Romey G (1996) KvLQTl and lsK (minK) proteins associate to form the IKs cardiac potassium current. Nature 384:78–80
32. Neyroud N, Tesson F, Denjoy I, Leibovici M, Donger C, Barhanin J, Fauré S, Gary F, Coumel P, Petit C, Schwartz K, Guicheney P (1997) A novel mutation in the potassium channel gene KVLQT1 causes the Jervell and Lange-Nielsen cardioauditory syndrome. Nat Genet 15:186–189. https://doi.org/10.1038/ng0297-186
33. Sanguinetti MC, Curran ME, Zou A, Shen J, Spector PS, Atkinson DL, Keating MT (1996) Coassembly of KvLQT1 and minK {lsK} proteins to form cardiac fKs potassium channel. Nature 384:80–83
34. Maison SF, Pyott SJ, Meredith AL, Liberman MC (2013) Olivocochlear suppression of outer hair cells in vivo: evidence for combined action of BK and SK2 channels throughout the cochlea. J Neurophysiol 109:1525–1534. https://doi.org/10.1152/jn.00924.2012
35. Wersinger E, McLean WJ, Fuchs PA, Pyott SJ (2010) BK channels mediate cholinergic inhibition of high frequency cochlear hair cells. PLoS One 5:e13836. https://doi.org/10.1371/journal.pone.0013836
36. Schimmang T, Duran Alonso B, Zimmermann U, Knipper M (2014) Is there a relationship between brain-derived neurotrophic factor for driving neuronal auditory circuits with onset of auditory function and the changes following cochlear injury or during aging? Neuroscience 283:26–43. https://doi.org/10.1016/j.neuroscience.2014.07.025
37. Macica CM, von Hehn CA, Wang L-Y, Ho C-S, Yokoyama S, Joho RH, Kaczmarek LK (2003) Modulation of the Kv3.1b potassium channel isoform adjusts the fidelity of the firing pattern of auditory neurons. J Neurosci 23:1133–1141

38. Dallos P (2008) Cochlear amplification, outer hair cells and prestin. Curr Opin Neurobiol 18:370–376. https://doi.org/10.1016/j.conb.2008.08.016
39. Dallos P, Zheng J, Cheatham MA (2006) Prestin and the cochlear amplifier. J Physiol 576:37–42. https://doi.org/10.1113/jphysiol.2006.114652
40. Marcotti W, Kros CJ (1999) Developmental expression of the potassium current IK,n contributes to maturation of mouse outer hair cells. J Physiol 520(Pt 3):653–660. https://doi.org/10.1111/j.1469-7793.1999.00653.x
41. Fang Q, Giordimaina AM, Dolan DF, Camper SA, Mustapha M (2012) Genetic background of Prop1(df) mutants provides remarkable protection against hypothyroidism-induced hearing impairment. J Assoc Res Otolaryngol 13:173–184. https://doi.org/10.1007/s10162-011-0302-3
42. Winter H, Braig C, Zimmermann U, Geisler HS, Franzer JT, Weber T, Ley M, Engel J, Knirsch M, Bauer K, Christ S, Walsh EJ, McGee J, Kopschall I, Rohbock K, Knipper M (2006) Thyroid hormone receptors TRalpha1 and TRbeta differentially regulate gene expression of Kcnq4 and prestin during final differentiation of outer hair cells. J Cell Sci 119:2975–2984. https://doi.org/10.1242/jcs.03013
43. Winter H, Braig C, Zimmermann U, Engel J, Rohbock K, Knipper M (2007) Thyroid hormone receptor alpha1 is a critical regulator for the expression of ion channels during final differentiation of outer hair cells. Histochem Cell Biol 128:65–75. https://doi.org/10.1007/s00418-007-0294-6
44. Boettger T, Hubner CA, Maier H, Rust MB, Beck FX, Jentsch TJ (2002) Deafness and renal tubular acidosis in mice lacking the K-Cl co-transporter Kcc4. Nature 416:874–878. https://doi.org/10.1038/416874a
45. Housley GD, Ashmore JF (1992) Ionic currents of outer hair cells isolated from the guinea-pig cochlea. J Physiol 448:73–98. https://doi.org/10.1113/jphysiol.1992.sp019030
46. Mammano F, Ashmore JF (1996) Differential expression of outer hair cell potassium currents in the isolated cochlea of the guinea-pig. J Physiol 496(Pt 3):639–646. https://doi.org/10.1113/jphysiol.1996.sp021715
47. Kharkovets T, Dedek K, Maier H, Schweizer M, Khimich D, Nouvian R, Vardanyan V, Leuwer R, Moser T, Jentsch TJ (2006) Mice with altered KCNQ4 K+ channels implicate sensory outer hair cells in human progressive deafness. EMBO J 25:642–652. https://doi.org/10.1038/sj.emboj.7600951
48. Gao Y, Yechikov S, Vazquez AE, Chen D, Nie L (2013) Impaired surface expression and conductance of the KCNQ4 channel lead to sensorineural hearing loss. J Cell Mol Med 17:889–900. https://doi.org/10.1111/jcmm.12080
49. Carignano C, Barila EP, Rias EI, Dionisio L, Aztiria E, Spitzmaul G (2019) Inner hair cell and neuron degeneration contribute to hearing loss in a DFNA2-like mouse model. Neuroscience 410:202–216. https://doi.org/10.1016/j.neuroscience.2019.05.012
50. Jentsch TJ (2000) Neuronal KCNQ potassium channels - physiology and role in disease. Nat Neurosci 1:21–30. https://doi.org/10.1038/35036198
51. Ruttiger L, Sausbier M, Zimmermann U, Winter H, Braig C, Engel J, Knirsch M, Arntz C, Langer P, Hirt B, Muller M, Kopschall I, Pfister M, Munkner S, Rohbock K, Pfaff I, Rusch A, Ruth P, Knipper M (2004) Deletion of the Ca2+-activated potassium (BK) alpha-subunit but not the BKbeta1-subunit leads to progressive hearing loss. Proc Natl Acad Sci U S A 101:12922–12927. https://doi.org/10.1073/pnas.0402660101
52. Kikuchi T, Adams JC, Miyabe Y, So E, Kobayashi T (2000) Potassium ion recycling pathway via gap junction systems in the mammalian cochlea and its interruption in hereditary nonsyndromic deafness. Med Electron Microsc 33:51–56. https://doi.org/10.1007/s007950070001
53. Wangemann P (2006) Supporting sensory transduction: cochlear fluid homeostasis and the endocochlear potential. J Physiol 576:11–21. https://doi.org/10.1113/jphysiol.2006.112888
54. Shen Z, Marcus DC (1998) Divalent cations inhibit IsK/KvLQT1 channels in excised membrane patches of strial marginal cells. Hear Res 123:157–167. https://doi.org/10.1016/s0378-5955(98)00110-5
55. Vetter DE, Mann JR, Wangemann P, Liu J, McLaughlin KJ, Lesage F, Marcus DC, Lazdunski M, Heinemann SF, Barhanin J (1996) Inner ear defects induced by null mutation of the isk gene. Neuron 17:1251–1264. https://doi.org/10.1016/s0896-6273(00)80255-x
56. Wangemann P, Liu J, Marcus DC (1995) Ion transport mechanisms responsible for K+ secretion and the transepithelial voltage across marginal cells of stria vascularis in vitro. Hear Res 84:19–29. https://doi.org/10.1016/0378-5955(95)00009-S
57. Tasaki I, Spyropoulos CS (1959) Stria vascularis as source of endocochlear potential. J Neurophysiol 22:149–155. https://doi.org/10.1152/jn.1959.22.2.149
58. Nin F, Yoshida T, Sawamura S, Ogata G, Ota T, Higuchi T, Murakami S, Doi K, Kurachi Y, Hibino H (2016) The unique electrical properties in an extracellular fluid of the mammalian cochlea; their functional roles, homeostatic processes, and pathological significance. Pflugers Arch 468:1637–1649. https://doi.org/10.1007/s00424-016-1871-0
59. de Castro MP, Aranega A, Franco D (2006) Protein distribution of Kcnq1, Kcnh2, and Kcne3 potassium channel subunits during mouse embryonic development. Anat Rec A Discov Mol Cell Evol Biol 288:304–315. https://doi.org/10.1002/ar.a.20312
60. Wollnik B, Schroeder BC, Kubisch C, Esperer HD, Wieacker P, Jentsch TJ (1997) Pathophysiological mechanisms of dominant and recessive KVLQT1 K+ channel mutations found in inherited cardiac arrhythmias. Hum Mol Genet 6:1943–1949. https://doi.org/10.1093/hmg/6.11.1943
61. Splawski I, Tristani-Firouzi M, Lehmann MH, Sanguinetti MC, Keating MT (1997) Mutations in the hminK gene cause long QT syndrome and suppress IKs function. Nat Genet 17:338–340. https://doi.org/10.1038/ng1197-338
62. Chouabe C, Neyroud N, Guicheney P, Lazdunski M, Romey G, Barhanin J (1997) Properties of KvLQT1 K+ channel mutations in Romano-Ward and Jervell and Lange-Nielsen inherited cardiac arrhythmias. EMBO J 16:5472–5479. https://doi.org/10.1093/emboj/16.17.5472
63. Wang Q, Curran ME, Splawski I, Burn TC, Millholland JM, VanRaay TJ, Shen J, Timothy KW, Vincent GM, de Jager T, Schwartz PJ, Toubin JA, Moss AJ, Atkinson DL, Landes GM, Connors TD, Keating MT (1996) Positional cloning of a novel potassium channel gene: KVLQT1 mutations cause cardiac arrhythmias. Nat Genet 12:17–23. https://doi.org/10.1038/ng0196-17
64. Schulze-Bahr E, Wang Q, Wedekind H, Haverkamp W, Chen Q, Sun Y, Rubie C, Hördt M, Towbin JA, Borggrefe M, Assmann G, Qu X, Somberg JC, Breithardt G, Oberti C, Funke H (1997) KCNE1 mutations cause Jervell and Lange-Nielsen syndrome. Nat Genet 17:267–268
65. Tyson J, Tranebjerg L, Bellman S, Wren C, Taylor JFN, Bathen J, Aslaksen B, Sorland SJ, Lund O, Malcolm S, Pembrey M, Bhattacharya S, BitnerGlindzicz M (1997) IsK and KVLQT1: mutation in either of the two subunits of the slow component of the delayed rectifier potassium channel can cause Jervell and Lange-Nielsen syndrome. Hum Mol Genet 6:2179–2185. https://doi.org/10.1093/hmg/6.12.2179
66. Casimiro MC, Knollmann BC, Ebert SN, Vary JC Jr, Greene AE, Franz MR, Grinberg A, Huang SP, Pfeifer K (2001) Targeted disruption of the Kcnq1 gene produces a mouse model of Jervell

and Lange-Nielsen Syndrome. Proc Natl Acad Sci U S A 98: 2526–2531. https://doi.org/10.1073/pnas.041398998
67. Wei AD, Gutman GA, Aldrich R, Chandy KG, Grissmer S, Wulff H (2005) International Union of Pharmacology. LII. Nomenclature and molecular relationships of calcium-activated potassium channels. Pharmacol Rev 57:463–472. https://doi.org/10.1124/pr.57.4.9
68. Butler A, Tsunoda S, Mccobb DP, Wei A, Salkoff L (1993) Mslo, a complex mouse gene encoding maxi calcium-activated potassium channels. Science 261:221–224. https://doi.org/10.1126/science.7687074
69. Schumacher MA, Rivard AF, Bachinger HP, Adelman JP (2001) Structure of the gating domain of a Ca2+-activated K+ channel complexed with Ca2+/calmodulin. Nature 410:1120–1124. https://doi.org/10.1038/35074145
70. Dulon D, Sugasawa M, Blanchet C, Erostegui C (1995) Direct measurements of Ca(2+)-activated K+ currents in inner hair cells of the guinea-pig cochlea using photolabile Ca2+ chelators. Pflugers Arch 430:365–373. https://doi.org/10.1007/BF00373911
71. Wangemann P, Takeuchi S (1993) Maxi-K+ channel in single isolated cochlear efferent nerve terminals. Hear Res 66:123–129. https://doi.org/10.1016/0378-5955(93)90133-l
72. Engel J, Braig C, Ruttiger L, Kuhn S, Zimmermann U, Blin N, Sausbier M, Kalbacher H, Munkner S, Rohbock K, Ruth P, Winter H, Knipper M (2006) Two classes of outer hair cells along the tonotopic axis of the cochlea. Neuroscience 143:837–849. https://doi.org/10.1016/j.neuroscience.2006.08.060
73. Rohmann KN, Wersinger E, Braude JP, Pyott SJ, Fuchs PA (2015) Activation of BK and SK channels by efferent synapses on outer hair cells in high-frequency regions of the rodent cochlea. J Neurosci 35:1821–1830. https://doi.org/10.1523/JNEUROSCI.2790-14.2015
74. Katz E, Elgoyhen AB, Gomez-Casati ME, Knipper M, Vetter DE, Fuchs PA, Glowatzki E (2004) Developmental regulation of nicotinic synapses on cochlear inner hair cells. J Neurosci 24:7814–7820. https://doi.org/10.1523/JNEUROSCI.2102-04.2004
75. Hafidi A, Beurg M, Dulon D (2005) Localization and developmental expression of BK channels in mammalian cochlear hair cells. Neuroscience 130:475–484. https://doi.org/10.1016/j.neuroscience.2004.09.038
76. Skinner LJ, Enee V, Beurg M, Jung HH, Ryan AF, Hafidi A, Dulon D (2003) Contribution of BK Ca2+-activated K+ channels to auditory neurotransmission in the guinea pig cochlea. J Neurophysiol 90:320–332. https://doi.org/10.1152/jn.01155.2002
77. Kros CJ (2007) How to build an inner hair cell: challenges for regeneration. Hear Res 227:3–10. https://doi.org/10.1016/j.heares.2006.12.005
78. Marcotti W, Johnson SL, Holley MC, Kros CJ (2003) Developmental changes in the expression of potassium currents of embryonic, neonatal and mature mouse inner hair cells. J Physiol 548:383–400. https://doi.org/10.1113/jphysiol.2002.034801
79. Luneau CJ, Williams JB, Marshall J, Levitan ES, Oliva C, Smith JS, Antanavage J, Folander K, Stein RB, Swanson R et al (1991) Alternative splicing contributes to K+ channel diversity in the mammalian central nervous system. Proc Natl Acad Sci U S A 88:3932–3936. https://doi.org/10.1073/pnas.88.9.3932
80. Gan L, Kaczmarek LK (1998) When, where, and how much? Expression of the Kv3.1 potassium channel in high-frequency firing neurons. J Neurobiol 37:69–79. https://doi.org/10.1002/(sici)1097-4695(199810)37:1<69::Aid-neu6>3.0.Co;2-6
81. Perney TM, Marshall J, Martin KA, Hockfield S, Kaczmarek LK (1992) Expression of the mRNAs for the Kv3.1 potassium channel gene in the adult and developing rat brain. J Neurophysiol 68: 756–766. https://doi.org/10.1152/jn.1992.68.3.756
82. Weiser M, Bueno E, Sekirnjak C, Martone ME, Baker H, Hillman D, Chen S, Thornhill W, Ellisman M, Rudy B (1995) The potassium channel subunit Kv3.1b is localized to somatic and axonal membranes of specific populations of Cns neurons. J Neurosci 15: 4298–4314
83. Ishikawa T, Nakamura Y, Saitoh N, Li WB, Iwasaki S, Takahashi T (2003) Distinct roles of Kv1 and Kv3 potassium channels at the calyx of Held presynaptic terminal. J Neurosci 23:10445–10453
84. Meneses D, Vega AV, Torres-Cruz FM, Barral J (2016) KV1 and KV3 potassium channels identified at presynaptic terminals of the corticostriatal synapses in rat. Neural Plast 2016:8782518. https://doi.org/10.1155/2016/8782518
85. Parameshwaran S, Carr CE, Perney TM (2001) Expression of the Kv3.1 potassium channel in the avian auditory brainstem. J Neurosci 21:485–494
86. Kanemasa T, Gan L, Perney TM, Wang LY, Kaczmarek LK (1995) Electrophysiological and pharmacological characterization of a mammalian Shaw channel expressed in NIH 3T3 fibroblasts. J Neurophysiol 74:207–217. https://doi.org/10.1152/jn.1995.74.1.207
87. Adamson CL, Reid MA, Mo ZL, Bowne-English J, Davis RL (2002) Firing features and potassium channel content of murine spiral ganglion neurons vary with cochlear location. J Comp Neurol 447:331–350. https://doi.org/10.1002/cne.10244
88. Flores-Otero J, Xue HZ, Davis RL (2007) Reciprocal regulation of presynaptic and postsynaptic proteins in bipolar spiral ganglion neurons by neurotrophins. J Neurosci 27:14023–14034. https://doi.org/10.1523/JNEUROSCI.3219-07.2007
89. Friedland DR, Eernisse R, Popper P (2007) Potassium channel gene expression in the rat cochlear nucleus. Hear Res 228:31–43. https://doi.org/10.1016/j.heares.2007.01.024
90. Lu Y, Monsivais P, Tempel BL, Rubel EW (2004) Activity-dependent regulation of the potassium channel subunits Kv1.1 and Kv3.1. J Comp Neurol 470:93–106. https://doi.org/10.1002/cne.11037
91. Grigg JJ, Brew HM, Tempel BL (2000) Differential expression of voltage-gated potassium channel genes in auditory nuclei of the mouse brainstem. Hear Res 140:77–90. https://doi.org/10.1016/s0378-5955(99)00187-2
92. Liu SQ, Kaczmarek LK (1998) Depolarization selectively increases the expression of the Kv3.1 potassium channel in developing inferior colliculus neurons. J Neurosci 18:8758–8769
93. Elezgarai I, Díez J, Puente N, Azkue JJ, Benítez R, Bilbao A, Knöpfel T, Doñate-Oliver F, Grandes P (2003) Subcellular localization of the voltage-dependent potassium channel Kv3.1b in postnatal and adult rat medial nucleus of the trapezoid body. Neuroscience 118:889–898. https://doi.org/10.1016/s0306-4522(03)00068-x
94. de Villers-Sidani E, Chang EF, Bao S, Merzenich MM (2007) Critical period window for spectral tuning defined in the primary auditory cortex (A1) in the rat. J Neurosci 27:180–189. https://doi.org/10.1523/JNEUROSCI.3227-06.2007
95. Hong EJ, McCord AE, Greenberg ME (2008) A biological function for the neuronal activity-dependent component of Bdnf transcription in the development of cortical inhibition. Neuron 60: 610–624. https://doi.org/10.1016/j.neuron.2008.09.024
96. Lehmann K, Steinecke A, Bolz J (2012) GABA through the ages: regulation of cortical function and plasticity by inhibitory interneurons. Neural Plast 2012:892784. https://doi.org/10.1155/2012/892784
97. Xu H, Kotak VC, Sanes DH (2010) Normal hearing is required for the emergence of long-lasting inhibitory potentiation in cortex. J Neurosci 30:331–341. https://doi.org/10.1523/JNEUROSCI.4554-09.2010

98. Griffen TC, Maffei A (2014) GABAergic synapses: their plasticity and role in sensory cortex. Front Cell Neurosci 8:91. https://doi.org/10.3389/fncel.2014.00091
99. Knipper M, van Dijk P, Schulze H, Mazurek B, Krauss P, Scheper V, Warnecke A, Schlee W, Schwabe K, Singer W, Braun C, Delano PH, Fallgatter AJ, Ehlis AC, Searchfield GD, Munk MHJ, Baguley DM, Ruttiger L (2020) The neural bases of tinnitus: lessons from deafness and cochlear implants. J Neurosci 40:7190–7202. https://doi.org/10.1523/JNEUROSCI.1314-19.2020
100. Massengill JL, Smith MA, Son DI, ODowd DK (1997) Differential expression of K4-AP currents and Kv3.1 potassium channel transcripts in cortical neurons that develop distinct firing phenotypes. J Neurosci 17:3136–3147
101. Rudy B, McBain CJ (2001) Kv3 channels: voltage-gated K+ channels designed for high-frequency repetitive firing. Trends Neurosci 24:517–526. https://doi.org/10.1016/s0166-2236(00)01892-0
102. McBain CJ, Fisahn A (2001) Interneurons unbound. Nat Rev Neurosci 2:11–23. https://doi.org/10.1038/35049047
103. Brew HM, Forsythe ID (1995) Two voltage-dependent K+ conductances with complementary functions in postsynaptic integration at a central auditory synapse. J Neurosci 15:8011–8022
104. Perney TM, Kaczmarek LK (1997) Localization of a high threshold potassium channel in the rat cochlear nucleus. J Comp Neurol 386:178–202
105. Wang LY, Gan L, Forsythe ID, Kaczmarek LK (1998) Contribution of the Kv3.1 potassium channel to high-frequency firing in mouse auditory neurones. J Physiol 509(Pt 1):183–194. https://doi.org/10.1111/j.1469-7793.1998.183bo.x
106. von Hehn CA, Bhattacharjee A, Kaczmarek LK (2004) Loss of Kv3.1 tonotopicity and alterations in cAMP response element-binding protein signaling in central auditory neurons of hearing impaired mice. J Neurosci 24:1936–1940. https://doi.org/10.1523/JNEUROSCI.4554-03.2004
107. Keithley EM (2020) Pathology and mechanisms of cochlear aging. J Neurosci Res 98:1674–1684. https://doi.org/10.1002/jnr.24439
108. Turner JG, Parrish JL, Hughes LF, Toth LA, Caspary DM (2005) Hearing in laboratory animals: strain differences and nonauditory effects of noise. Comp Med 55:12–23
109. Boettcher FA, Mills JH, Norton BL (1993) Age-related changes in auditory evoked potentials of gerbils. I. Response amplitudes. Hear Res 71:137–145. https://doi.org/10.1016/0378-5955(93)90029-z
110. Boettcher FA, Mills JH, Norton BL, Schmiedt RA (1993) Age-related changes in auditory evoked potentials of gerbils. II. Response latencies. Hear Res 71:146–156. https://doi.org/10.1016/0378-5955(93)90030-5
111. Heeringa AN, Koppl C (2019) The aging cochlea: towards unraveling the functional contributions of strial dysfunction and synaptopathy. Hear Res 376:111–124. https://doi.org/10.1016/j.heares.2019.02.015
112. Gleich O, Semmler P, Strutz J (2016) Behavioral auditory thresholds and loss of ribbon synapses at inner hair cells in aged gerbils. Exp Gerontol 84:61–70. https://doi.org/10.1016/j.exger.2016.08.011
113. Mohrle D, Ni K, Varakina K, Bing D, Lee SC, Zimmermann U, Knipper M, Ruttiger L (2016) Loss of auditory sensitivity from inner hair cell synaptopathy can be centrally compensated in the young but not old brain. Neurobiol Aging 44:173–184. https://doi.org/10.1016/j.neurobiolaging.2016.05.001
114. Ruttiger L, Panford-Walsh R, Schimmang T, Tan J, Zimmermann U, Rohbock K, Kopschall I, Limberger A, Muller M, Fraenzer JT, Cimerman J, Knipper M (2007) BDNF mRNA expression and protein localization are changed in age-related hearing loss. Neurobiol Aging 28:586–601. https://doi.org/10.1016/j.neurobiolaging.2006.02.008
115. Wu T, Marcus DC (2003) Age-related changes in cochlear endolymphatic potassium and potential in CD-1 and CBA/CaJ mice. J Assoc Res Otolaryngol 4:353–362. https://doi.org/10.1007/s10162-002-3026-6
116. Kujawa SG, Liberman MC (2006) Acceleration of age-related hearing loss by early noise exposure: evidence of a misspent youth. J Neurosci 26:2115–2123. https://doi.org/10.1523/JNEUROSCI.4985-05.2006
117. Wang Y, Ren C (2012) Effects of repeated "benign" noise exposures in young CBA mice: shedding light on age-related hearing loss. J Assoc Res Otolaryngol 13:505–515. https://doi.org/10.1007/s10162-012-0329-0
118. Yoshida N, Hequembourg SJ, Atencio CA, Rosowski JJ, Liberman MC (2000) Acoustic injury in mice: 129/SvEv is exceptionally resistant to noise-induced hearing loss. Hear Res 141:97–106. https://doi.org/10.1016/S0378-5955(99)00210-5
119. Benkafadar N, Francois F, Affortit C, Casas F, Ceccato JC, Menardo J, Venail F, Malfroy-Camine B, Puel JL, Wang J (2019) ROS-induced activation of DNA damage responses drives senescence-like state in postmitotic cochlear cells: implication for hearing preservation. Mol Neurobiol 56:5950–5969. https://doi.org/10.1007/s12035-019-1493-6
120. Henderson D, Bielefeld EC, Harris KC, Hu BH (2006) The role of oxidative stress in noise-induced hearing loss. Ear Hear 27:1–19. https://doi.org/10.1097/01.aud.0000191942.36672.f3
121. Vlajkovic SM, Lin SC, Wong AC, Wackrow B, Thorne PR (2013) Noise-induced changes in expression levels of NADPH oxidases in the cochlea. Hear Res 304:145–152. https://doi.org/10.1016/j.heares.2013.07.012
122. Roth TN (2015) Aging of the auditory system. Handb Clin Neurol 129:357–373. https://doi.org/10.1016/B978-0-444-62630-1.00020-2
123. Han BR, Lin SC, Espinosa K, Thorne PR, Vlajkovic SM (2019) Inhibition of the adenosine A2A receptor mitigates excitotoxic injury in organotypic tissue cultures of the rat cochlea. Cells 8. https://doi.org/10.3390/cells8080877
124. Bures Z, Grecova J, Popelar J, Syka J (2010) Noise exposure during early development impairs the processing of sound intensity in adult rats. Eur J Neurosci 32:155–164. https://doi.org/10.1111/j.1460-9568.2010.07280.x
125. Grecova J, Bures Z, Popelar J, Suta D, Syka J (2009) Brief exposure of juvenile rats to noise impairs the development of the response properties of inferior colliculus neurons. Eur J Neurosci 29:1921–1930. https://doi.org/10.1111/j.1460-9568.2009.06739.x
126. Marchetta P, Mohrle D, Eckert P, Reimann K, Wolter S, Tolone A, Lang I, Wolters M, Feil R, Engel J, Paquet-Durand F, Kuhn M, Knipper M, Ruttiger L (2020) Guanylyl cyclase A/cGMP signaling slows hidden, age- and acoustic trauma-induced hearing loss. Front Aging Neurosci 12:83. https://doi.org/10.3389/fnagi.2020.00083
127. Liberman LD, Liberman MC (2019) Cochlear efferent innervation is sparse in humans and decreases with age. J Neurosci 39:9560–9569. https://doi.org/10.1523/JNEUROSCI.3004-18.2019
128. Maison SF, Luebke AE, Liberman MC, Zuo J (2002) Efferent protection from acoustic injury is mediated via α9 nicotinic acetylcholine receptors on outer hair cells. J Neurosci 22:10838–10846. https://doi.org/10.1523/jneurosci.22-24-10838.2002
129. Maison SF, Liberman MC (2000) Predicting vulnerability to acoustic injury with a noninvasive assay of olivocochlear reflex strength. J Neurosci 20:4701–4707
130. Vergara C, Latorre R, Marrion NV, Adelman JP (1998) Calcium-activated potassium channels. Curr Opin Neurobiol 8:321–329. https://doi.org/10.1016/s0959-4388(98)80056-1

131. Typlt M, Mirkowski M, Azzopardi E, Ruettiger L, Ruth P, Schmid S (2013) Mice with deficient BK channel function show impaired prepulse inhibition and spatial learning, but normal working and spatial reference memory. PLoS One 8:e81270. https://doi.org/10.1371/journal.pone.0081270
132. Knipper M, Panford-Walsh R, Singer W, Ruttiger L, Zimmermann U (2015) Specific synaptopathies diversify brain responses and hearing disorders: you lose the gain from early life. Cell Tissue Res 361:77–93. https://doi.org/10.1007/s00441-015-2168-x
133. Robertson D (2009) Centrifugal control in mammalian hearing. Clin Exp Pharmacol Physiol 36:603–611. https://doi.org/10.1111/j.1440-1681.2009.05185.x
134. Suga N, Gao E, Zhang Y, Ma X, Olsen JF (2000) The corticofugal system for hearing: recent progress. Proc Natl Acad Sci U S A 97:11807–11814. https://doi.org/10.1073/pnas.97.22.11807
135. Kong JH, Adelman JP, Fuchs PA (2008) Expression of the SK2 calcium-activated potassium channel is required for cholinergic function in mouse cochlear hair cells. J Physiol 586:5471–5485. https://doi.org/10.1113/jphysiol.2008.160077
136. Jeng JY, Johnson SL, Carlton AJ, De Tomasi L, Goodyear RJ, De Faveri F, Furness DN, Wells S, Brown SDM, Holley MC, Richardson GP, Mustapha M, Bowl MR, Marcotti W (2020) Age-related changes in the biophysical and morphological characteristics of mouse cochlear outer hair cells. J Physiol. https://doi.org/10.1113/JP279795
137. Nakazawa K, Spicer SS, Schulte BA (1995) Ultrastructural localization of Na,K-ATPase in the gerbil cochlea. J Histochem Cytochem 43:981–991. https://doi.org/10.1177/43.10.7560888
138. Spicer SS, Schulte BA (2002) Spiral ligament pathology in quiet-aged gerbils. Hear Res 172:172–185. https://doi.org/10.1016/s0378-5955(02)00581-6
139. Ding B, Walton JP, Zhu X, Frisina RD (2018) Age-related changes in Na, K-ATPase expression, subunit isoform selection and assembly in the stria vascularis lateral wall of mouse cochlea. Hear Res 367:59–73. https://doi.org/10.1016/j.heares.2018.07.006
140. Ryan AF, Watts AG (1991) Expression of mRNAs encoding alpha and beta subunit isoforms of the Na,K-ATPase in the rat cochlea. Mol Cell Neurosci 2:179–187. https://doi.org/10.1016/1044-7431(91)90011-c
141. Gratton MA, Smyth BJ, Lam CF, Boettcher FA, Schmiedt RA (1997) Decline in the endocochlear potential corresponds to decreased Na,K-ATPase activity in the lateral wall of quiet-aged gerbils. Hear Res 108:9–16. https://doi.org/10.1016/s0378-5955(97)00034-8
142. Gratton MA, Smyth BJ, Schulte BA, Vincent DA Jr (1995) Na,K-ATPase activity decreases in the cochlear lateral wall of quiet-aged gerbils. Hear Res 83:43–50. https://doi.org/10.1016/0378-5955(94)00188-v
143. Prazma J, Carrasco VN, Butler B, Waters G, Anderson T, Pillsbury HC (1990) Cochlear microcirculation in young and old gerbils. Arch Otolaryngol Head Neck Surg 116:932–936. https://doi.org/10.1001/archotol.1990.01870080054015
144. Yang H, Xiong H, Huang Q, Pang J, Zheng X, Chen L, Yu R, Zheng Y (2013) Compromised potassium recycling in the cochlea contributes to conservation of endocochlear potential in a mouse model of age-related hearing loss. Neurosci Lett 555:97–101. https://doi.org/10.1016/j.neulet.2013.09.028
145. Knipper M, Claussen C, Ruttiger L, Zimmermann U, Lullmann-Rauch R, Eskelinen EL, Schroder J, Schwake M, Saftig P (2006) Deafness in LIMP2-deficient mice due to early loss of the potassium channel KCNQ1/KCNE1 in marginal cells of the stria vascularis. J Physiol 576:73–86. https://doi.org/10.1113/jphysiol.2006.116889
146. Zettel ML, Zhu X, O'Neill WE, Frisina RD (2007) Age-related decline in Kv3.1b expression in the mouse auditory brainstem correlates with functional deficits in the medial olivocochlear efferent system. J Assoc Res Otolaryngol 8:280–293. https://doi.org/10.1007/s10162-007-0075-x
147. Spongr VP, Flood DG, Frisina RD, Salvi RJ (1997) Quantitative measures of hair cell loss in CBA and C57BL/6 mice throughout their life spans. J Acoust Soc Am 101:3546–3553. https://doi.org/10.1121/1.418315
148. Jung DK, Lee SY, Kim D, Joo KM, Cha CI, Yang HS, Lee WB, Chung YH (2005) Age-related changes in the distribution of Kv1.1 and Kv3.1 in rat cochlear nuclei. Neurol Res 27:436–440. https://doi.org/10.1179/016164105X22011
149. Costa M, Lepore F, Prevost F, Guillemot JP (2016) Effects of aging on peripheral and central auditory processing in rats. Eur J Neurosci 44:2084–2094. https://doi.org/10.1111/ejn.13302
150. Hu H, Gan J, Jonas P (2014) Interneurons. Fast-spiking, parvalbumin(+) GABAergic interneurons: from cellular design to microcircuit function. Science 345:1255263. https://doi.org/10.1126/science.1255263
151. Martin del Campo HN, Measor KR, Razak KA (2012) Parvalbumin immunoreactivity in the auditory cortex of a mouse model of presbycusis. Hear Res 294:31–39. https://doi.org/10.1016/j.heares.2012.08.017
152. Strain GM, McGee KA (2017) Distortion product otoacoustic emissions in young adult and geriatric cats. Vet J 221:34–37. https://doi.org/10.1016/j.tvjl.2017.01.019
153. Gonzalez C, Baez-Nieto D, Valencia I, Oyarzun I, Rojas P, Naranjo D, Latorre R (2012) K(+) channels: function-structural overview. Compr Physiol 2:2087–2149. https://doi.org/10.1002/cphy.c110047
154. Van Eyken E, Van Laer L, Fransen E, Topsakal V, Lemkens N, Laureys W, Nelissen N, Vandevelde A, Wienker T, Van De Heyning P, Van Camp G (2006) KCNQ4: a gene for age-related hearing impairment? Hum Mutat 27:1007–1016. https://doi.org/10.1002/humu.20375
155. Beisel KW, Rocha-Sanchez SM, Morris KA, Nie L, Feng F, Kachar B, Yamoah EN, Fritzsch B (2005) Differential expression of KCNQ4 in inner hair cells and sensory neurons is the basis of progressive high-frequency hearing loss. J Neurosci 25:9285–9293. https://doi.org/10.1523/JNEUROSCI.2110-05.2005
156. Van Laer L, Carlsson PI, Ottschytsch N, Bondeson ML, Konings A, Vandevelde A, Dieltjens N, Fransen E, Snyders D, Borg E, Raes A, Van Camp G (2006) The contribution of genes involved in potassium-recycling in the inner ear to noise-induced hearing loss. Hum Mutat 27:786–795. https://doi.org/10.1002/humu.20360
157. Walter S, Atzmon G, Demerath EW, Garcia ME, Kaplan RC, Kumari M, Lunetta KL, Milaneschi Y, Tanaka T, Tranah GJ, Volker U, Yu L, Arnold A, Benjamin EJ, Biffar R, Buchman AS, Boerwinkle E, Couper D, De Jager PL, Evans DA, Harris TB, Hoffmann W, Hofman A, Karasik D, Kiel DP, Kocher T, Kuningas M, Launer LJ, Lohman KK, Lutsey PL, Mackenbach J, Marciante K, Psaty BM, Reiman EM, Rotter JI, Seshadri S, Shardell MD, Smith AV, van Duijn C, Walston J, Zillikens MC, Bandinelli S, Baumeister SE, Bennett DA, Ferrucci L, Gudnason V, Kivimaki M, Liu Y, Murabito JM, Newman AB, Tiemeier H, Franceschini N (2011) A genome-wide association study of aging. Neurobiol Aging 32(2109):e2115–e2128. https://doi.org/10.1016/j.neurobiolaging.2011.05.026
158. Alders M, Bikker H, Christiaans I (2003) Long QT Syndrome. GeneReviews® [Internet]. University of Washington, Seattle, Seattle (WA)
159. Lee MP, Ravenel JD, Hu RJ, Lustig LR, Tomaselli G, Berger RD, Brandenburg SA, Litzi TJ, Bunton TE, Limb C, Francis H, Gorelikow M, Gu H, Washington K, Argani P, Goldenring JR,

Coffey RJ, Feinberg AP (2000) Targeted disruption of the Kvlqt1 gene causes deafness and gastric hyperplasia in mice. J Clin Invest 106:1447–1455. https://doi.org/10.1172/JCI10897

160. Ullrich S, Su J, Ranta F, Wittekindt OH, Ris F, Rosler M, Gerlach U, Heitzmann D, Warth R, Lang F (2005) Effects of I(Ks) channel inhibitors in insulin-secreting INS-1 cells. Pflugers Arch 451:428–436. https://doi.org/10.1007/s00424-005-1479-2
161. Hanson RL, Guo T, Muller YL, Fleming J, Knowler WC, Kobes S, Bogardus C, Baier LJ (2013) Strong parent-of-origin effects in the association of KCNQ1 variants with type 2 diabetes in American Indians. Diabetes 62:2984–2991. https://doi.org/10.2337/db12-1767
162. Li YY, Wang XM, Lu XZ (2014) KCNQ1 rs2237892 C–>T gene polymorphism and type 2 diabetes mellitus in the Asian population: a meta-analysis of 15,736 patients. J Cell Mol Med 18:274–282. https://doi.org/10.1111/jcmm.12185
163. Unoki H, Takahashi A, Kawaguchi T, Hara K, Horikoshi M, Andersen G, Ng DP, Holmkvist J, Borch-Johnsen K, Jorgensen T, Sandbaek A, Lauritzen T, Hansen T, Nurbaya S, Tsunoda T, Kubo M, Babazono T, Hirose H, Hayashi M, Iwamoto Y, Kashiwagi A, Kaku K, Kawamori R, Tai ES, Pedersen O, Kamatani N, Kadowaki T, Kikkawa R, Nakamura Y, Maeda S (2008) SNPs in KCNQ1 are associated with susceptibility to type 2 diabetes in East Asian and European populations. Nat Genet 40:1098–1102. https://doi.org/10.1038/ng.208
164. Voight BF, Scott LJ, Steinthorsdottir V, Morris AP, Dina C, Welch RP, Zeggini E, Huth C, Aulchenko YS, Thorleifsson G, McCulloch LJ, Ferreira T, Grallert H, Amin N, Wu G, Willer CJ, Raychaudhuri S, McCarroll SA, Langenberg C, Hofmann OM, Dupuis J, Qi L, Segre AV, van Hoek M, Navarro P, Ardlie K, Balkau B, Benediktsson R, Bennett AJ, Blagieva R, Boerwinkle E, Bonnycastle LL, Bengtsson Bostrom K, Bravenboer B, Bumpstead S, Burtt NP, Charpentier G, Chines PS, Cornelis M, Couper DJ, Crawford G, Doney AS, Elliott KS, Elliott AL, Erdos MR, Fox CS, Franklin CS, Ganser M, Gieger C, Grarup N, Green T, Griffin S, Groves CJ, Guiducci C, Hadjadj S, Hassanali N, Herder C, Isomaa B, Jackson AU, Johnson PR, Jorgensen T, Kao WH, Klopp N, Kong A, Kraft P, Kuusisto J, Lauritzen T, Li M, Lieverse A, Lindgren CM, Lyssenko V, Marre M, Meitinger T, Midthjell K, Morken MA, Narisu N, Nilsson P, Owen KR, Payne F, Perry JR, Petersen AK, Platou C, Proenca C, Prokopenko I, Rathmann W, Rayner NW, Robertson NR, Rocheleau G, Roden M, Sampson MJ, Saxena R, Shields BM, Shrader P, Sigurdsson G, Sparso T, Strassburger K, Stringham HM, Sun Q, Swift AJ, Thorand B, Tichet J, Tuomi T, van Dam RM, van Haeften TW, van Herpt T, van Vliet-Ostaptchouk JV, Walters GB, Weedon MN, Wijmenga C, Witteman J, Bergman RN, Cauchi S, Collins FS, Gloyn AL, Gyllensten U, Hansen T, Hide WA, Hitman GA, Hofman A, Hunter DJ, Hveem K, Laakso M, Mohlke KL, Morris AD, Palmer CN, Pramstaller PP, Rudan I, Sijbrands E, Stein LD, Tuomilehto J, Uitterlinden A, Walker M, Wareham NJ, Watanabe RM, Abecasis GR, Boehm BO, Campbell H, Daly MJ, Hattersley AT, Hu FB, Meigs JB, Pankow JS, Pedersen O, Wichmann HE, Barroso I, Florez JC, Frayling TM, Groop L, Sladek R, Thorsteinsdottir U, Wilson JF, Illig T, Froguel P, van Duijn CM, Stefansson K, Altshuler D, Boehnke M, McCarthy MI, investigators M, Consortium G (2010) Twelve type 2 diabetes susceptibility loci identified through large-scale association analysis. Nat Genet 42:579–589. https://doi.org/10.1038/ng.609
165. Kong A, Steinthorsdottir V, Masson G, Thorleifsson G, Sulem P, Besenbacher S, Jonasdottir A, Sigurdsson A, Kristinsson KT, Jonasdottir A, Frigge ML, Gylfason A, Olason PI, Gudjonsson SA, Sverrisson S, Stacey SN, Sigurgeirsson B, Benediktsdottir KR, Sigurdsson H, Jonsson T, Benediktsson R, Olafsson JH, Johannsson OT, Hreidarsson AB, Sigurdsson G, Consortium D, Ferguson-Smith AC, Gudbjartsson DF, Thorsteinsdottir U, Stefansson K (2009) Parental origin of sequence variants associated with complex diseases. Nature 462:868–874. https://doi.org/10.1038/nature08625
166. Provenzano MJ, Domann FE (2007) A role for epigenetics in hearing: establishment and maintenance of auditory specific gene expression patterns. Hear Res 233:1–13. https://doi.org/10.1016/j.heares.2007.07.002
167. Hermann A, Sitdikova GF, Weiger TM (2015) Oxidative stress and maxi calcium-activated potassium (BK) channels. Biomolecules 5:1870–1911. https://doi.org/10.3390/biom5031870
168. Honrath B, Matschke L, Meyer T, Magerhans L, Perocchi F, Ganjam GK, Zischka H, Krasel C, Gerding A, Bakker BM, Bunemann M, Strack S, Decher N, Culmsee C, Dolga AM (2017) SK2 channels regulate mitochondrial respiration and mitochondrial Ca(2+) uptake. Cell Death Differ 24:761–773. https://doi.org/10.1038/cdd.2017.2
169. Rizzuto R, De Stefani D, Raffaello A, Mammucari C (2012) Mitochondria as sensors and regulators of calcium signalling. Nat Rev Mol Cell Biol 13:566–578. https://doi.org/10.1038/nrm3412
170. Lemasters JJ, Theruvath TP, Zhong Z, Nieminen AL (2009) Mitochondrial calcium and the permeability transition in cell death. Biochim Biophys Acta 1787:1395–1401. https://doi.org/10.1016/j.bbabio.2009.06.009
171. Muona M, Berkovic SF, Dibbens LM, Oliver KL, Maljevic S, Bayly MA, Joensuu T, Canafoglia L, Franceschetti S, Michelucci R, Markkinen S, Heron SE, Hildebrand MS, Andermann E, Andermann F, Gambardella A, Tinuper P, Licchetta L, Scheffer IE, Criscuolo C, Filla A, Ferlazzo E, Ahmad J, Ahmad A, Baykan B, Said E, Topcu M, Riguzzi P, King MD, Ozkara C, Andrade DM, Engelsen BA, Crespel A, Lindenau M, Lohmann E, Saletti V, Massano J, Privitera M, Espay AJ, Kauffmann B, Duchowny M, Moller RS, Straussberg R, Afawi Z, Ben-Zeev B, Samocha KE, Daly MJ, Petrou S, Lerche H, Palotie A, Lehesjoki AE (2015) A recurrent de novo mutation in KCNC1 causes progressive myoclonus epilepsy. Nat Genet 47:39–46. https://doi.org/10.1038/ng.3144
172. Poirier K, Viot G, Lombardi L, Jauny C, Billuart P, Bienvenu T (2017) Loss of Function of KCNC1 is associated with intellectual disability without seizures. Eur J Hum Genet 25:560–564. https://doi.org/10.1038/ejhg.2017.3
173. Karlsson KK, Harris JR, Svartengren M (1997) Description and primary results from an audiometric study of male twins. Ear Hear 18:114–120. https://doi.org/10.1097/00003446-199704000-00003
174. Vuckovic D, Mezzavilla M, Cocca M, Morgan A, Brumat M, Catamo E, Concas MP, Biino G, Franze A, Ambrosetti U, Pirastu M, Gasparini P, Girotto G (2018) Whole-genome sequencing reveals new insights into age-related hearing loss: cumulative effects, pleiotropy and the role of selection. Eur J Hum Genet 26:1167–1179. https://doi.org/10.1038/s41431-018-0126-2
175. Wells HRR, Freidin MB, Zainul Abidin FN, Payton A, Dawes P, Munro KJ, Morton CC, Moore DR, Dawson SJ, Williams FMK (2019) GWAS identifies 44 independent associated genomic loci for self-reported adult hearing difficulty in UK Biobank. Am J Hum Genet 105:788–802. https://doi.org/10.1016/j.ajhg.2019.09.008
176. Serrano F, Klann E (2004) Reactive oxygen species and synaptic plasticity in the aging hippocampus. Ageing Res Rev 3:431–443. https://doi.org/10.1016/j.arr.2004.05.002

177. Matalon S, Hardimann KM, Jain L, Eaton DC, Kotlikoff M, Eu JP, Sun J, Meissner G, Stamler JS (2003) Regulation of ion channel structure and function by reactive oxygen-nitrogen species. Am J Phys Lung Cell Mol Phys 285:1184–1189. https://doi.org/10.1152/ajplung.00281.2003
178. Barrese V, Stott JB, Greenwood IA (2018) KCNQ-encoded potassium channels as therapeutic targets. Annu Rev Pharmacol Toxicol 58:625–648. https://doi.org/10.1146/annurev-pharmtox-010617-052912
179. Greene DL, Hoshi N (2017) Modulation of Kv7 channels and excitability in the brain. Cell Mol Life Sci 74:495–508. https://doi.org/10.1007/s00018-016-2359-y
180. Shin DH, Jung J, Koh YI, Rim JH, Lee JS, Choi HJ, Joo SY, Yu S, Cha DH, Lee SY, Lee JH, Lee MG, Choi JY, Gee HY (2019) A recurrent mutation in KCNQ4 in Korean families with nonsyndromic hearing loss and rescue of the channel activity by KCNQ activators. Hum Mutat 40:335–346. https://doi.org/10.1002/humu.23698
181. Xia X, Zhang Q, Jia Y, Shu Y, Yang J, Yang H, Yan Z (2020) Molecular basis and restoration of function deficiencies of Kv7.4 variants associated with inherited hearing loss. Hear Res 388:107884. https://doi.org/10.1016/j.heares.2020.107884
182. Lange W, Geissendorfer J, Schenzer A, Grotzinger J, Seebohm G, Friedrich T, Schwake M (2009) Refinement of the binding site and mode of action of the anticonvulsant Retigabine on KCNQ K+ channels. Mol Pharmacol 75:272–280. https://doi.org/10.1124/mol.108.052282
183. Schenzer A, Friedrich T, Pusch M, Saftig P, Jentsch TJ, Grotzinger J, Schwake M (2005) Molecular determinants of KCNQ (Kv7) K+ channel sensitivity to the anticonvulsant retigabine. J Neurosci 25:5051–5060. https://doi.org/10.1523/JNEUROSCI.0128-05.2005
184. Wuttke TV, Seebohm G, Bail S, Maljevic S, Lerche H (2005) The new anticonvulsant retigabine favors voltage-dependent opening of the Kv7.2 (KCNQ2) channel by binding to its activation gate. Mol Pharmacol 67:1009–1017. https://doi.org/10.1124/mol.104.010793
185. Leitner MG, Feuer A, Ebers O, Schreiber DN, Halaszovich CR, Oliver D (2012) Restoration of ion channel function in deafness-causing KCNQ4 mutants by synthetic channel openers. Br J Pharmacol 165:2244–2259. https://doi.org/10.1111/j.1476-5381.2011.01697.x
186. Cooke PS, Nanjappa MK, Ko C, Prins GS, Hess RA (2017) Estrogens in male physiology. Physiol Rev 97:995–1043. https://doi.org/10.1152/physrev.00018.2016
187. Rapetti-Mauss R, O'Mahony F, Sepulveda FV, Urbach V, Harvey BJ (2013) Oestrogen promotes KCNQ1 potassium channel endocytosis and postendocytic trafficking in colonic epithelium. J Physiol 591:2813–2831. https://doi.org/10.1113/jphysiol.2013.251678
188. Curhan SG, Eliassen AH, Eavey RD, Wang M, Lin BM, Curhan GC (2017) Menopause and postmenopausal hormone therapy and risk of hearing loss. Menopause 24:1049–1056. https://doi.org/10.1097/GME.0000000000000878
189. Li Y, Chen B, Zou W, Wang X, Wu Y, Zhao D, Sun Y, Liu Y, Chen L, Miao L, Yang C, Wang X (2016) The lysosomal membrane protein SCAV-3 maintains lysosome integrity and adult longevity. J Cell Biol 215:167–185. https://doi.org/10.1083/jcb.201602090
190. Patel R, McKinnon BJ (2018) Hearing loss in the elderly. Clin Geriatr Med 34:163–174. https://doi.org/10.1016/j.cger.2018.01.001
191. Ambrosi G, Ghezzi C, Zangaglia R, Levandis G, Pacchetti C, Blandini F (2015) Ambroxol-induced rescue of defective glucocerebrosidase is associated with increased LIMP-2 and saposin C levels in GBA1 mutant Parkinson's disease cells. Neurobiol Dis 82:235–242. https://doi.org/10.1016/j.nbd.2015.06.008
192. Zeng X-H, Xia X-M, Lingle CJ (2003) Redox-sensitive extracellular gates formed by auxiliary β subunits of calcium-activated potassium channels. Nat Struct Biol 10:448–454. https://doi.org/10.1038/nsb932
193. Lingle CJ, Martinez-Espinosa PL, Yang-Hood A, Boero LE, Payne S, Persic D, Babak VG, Xiao M, Zhou Y, Xia XM, Pyott SJ, Rutherford MA (2019) LRRC52 regulates BK channel function and localization in mouse cochlear inner hair cells. Proc Natl Acad Sci U S A 116:18397–18403. https://doi.org/10.1073/pnas.1907065116
194. Blank T, Nijholt I, Kye MJ, Radulovic J, Spiess J (2003) Small-conductance, Ca2+-activated K+ channel SK3 generates age-related memory and LTP deficits. Nat Neurosci 6:911–912. https://doi.org/10.1038/nn1101
195. Zhang WH, Liu WZ, He Y, You WJ, Zhang JY, Xu H, Tian XL, Li BM, Mei L, Holmes A, Pan BX (2019) Chronic stress causes projection-specific adaptation of amygdala neurons via small-conductance calcium-activated potassium channel downregulation. Biol Psychiatry 85:812–828. https://doi.org/10.1016/j.biopsych.2018.12.010
196. Coles B, Wilton LA, Good M, Chapman PF, Wann KT (2008) Potassium channels in hippocampal neurones are absent in a transgenic but not in a chemical model of Alzheimer's disease. Brain Res 1190:1–14. https://doi.org/10.1016/j.brainres.2007.10.071
197. Chambers AR, Pilati N, Balaram P, Large CH, Kaczmarek LK, Polley DB (2017) Pharmacological modulation of Kv3.1 mitigates auditory midbrain temporal processing deficits following auditory nerve damage. Sci Rep 7:17496. https://doi.org/10.1038/s41598-017-17406-x
198. Parthasarathy A, Cunningham PA, Bartlett EL (2010) Age-related differences in auditory processing as assessed by amplitude-modulation following responses in quiet and in noise. Front Aging Neurosci 2:152. https://doi.org/10.3389/fnagi.2010.00152
199. Abbott GW, Mercer EAJ, Miller RT, Ramesh B, Srai SKS (1998) Conformational changes in a mammalian voltage-dependent potassium channel inactivation peptide. Biochemistry 37:1640–1645. https://doi.org/10.1021/bi972350c
200. Duprat F, Guillemare E, Romey G, Fink M, Lesage F, Lazdunski M (1995) usceptibilityofclonedK+ channelstoreactiveoxygenspecies. Proc Natl Acad Sci USA 42:11796–11800
201. Pan Y, Weng J, Cao Y, Bhosle RC, Zhou M (2008) Functional coupling between the Kv1.1 channel and aldoketoreductase Kvbeta1. J Biol Chem 283:8634–8642. https://doi.org/10.1074/jbc.M709304200
202. Medrihan L, Umschweif G, Sinha A, Reed S, Lee J, Gindinova K, Sinha SC, Greengard P, Sagi Y (2020) Reduced Kv3.1 activity in dentate gyrus parvalbumin cells induces vulnerability to depression. Biol Psychiatry 88:405–414. https://doi.org/10.1016/j.biopsych.2020.02.1179
203. Kann O (2016) The interneuron energy hypothesis: Implications for brain disease. Neurobiol Dis 90:75–85. https://doi.org/10.1016/j.nbd.2015.08.005
204. Boddum K, Hougaard C, Xiao-Ying Lin J, von Schoubye NL, Jensen HS, Grunnet M, Jespersen T (2017) Kv3.1/Kv3.2 channel positive modulators enable faster activating kinetics and increase firing frequency in fast-spiking GABAergic interneurons. Neuropharmacology 118:102–112. https://doi.org/10.1016/j.neuropharm.2017.02.024
205. Brown MR, El-Hassar L, Zhang Y, Alvaro G, Large CH, Kaczmarek LK (2016) Physiological modulators of Kv3.1

channels adjust firing patterns of auditory brain stem neurons. J Neurophysiol 116:106–121. https://doi.org/10.1152/jn.00174.2016

206. Dubno JR, Eckert MA, Lee FS, Matthews LJ, Schmiedt RA (2013) Classifying human audiometric phenotypes of age-related hearing loss from animal models. J Assoc Res Otolaryngol 14:687–701. https://doi.org/10.1007/s10162-013-0396-x

frontiers in Aging Neuroscience

ORIGINAL RESEARCH
published: 02 August 2021
doi: 10.3389/fnagi.2021.708190

Auditory Threshold Variability in the SAMP8 Mouse Model of Age-Related Hearing Loss: Functional Loss and Phenotypic Change Precede Outer Hair Cell Loss

Barbara Peixoto Pinheiro[1], Youssef Adel[1], Marlies Knipper[2], Marcus Müller[1†] and Hubert Löwenheim[1]*

[1] Translational Hearing Research, Tübingen Hearing Research Center, Department of Otolaryngology, Head and Neck Surgery, University of Tübingen, Tübingen, Germany, [2] Molecular Physiology of Hearing, Tübingen Hearing Research Center, Department of Otolaryngology, Head and Neck Surgery, University of Tübingen, Tübingen, Germany

OPEN ACCESS

Edited by:
Tobias Kleinjung, University of Zurich, Switzerland

Reviewed by:
Michael Hoa, National Institute on Deafness and Other Communication Disorders (NIDCD), United States
Richard Altschuler, University of Michigan, United States

***Correspondence:**
Barbara Peixoto Pinheiro
barbara.peixoto-pinheiro@uni-tuebingen.de

† Deceased

Received: *11 May 2021*
Accepted: *09 July 2021*
Published: *02 August 2021*

Citation:
Peixoto Pinheiro B, Adel Y, Knipper M, Müller M and Löwenheim H (2021) Auditory Threshold Variability in the SAMP8 Mouse Model of Age-Related Hearing Loss: Functional Loss and Phenotypic Change Precede Outer Hair Cell Loss. Front. Aging Neurosci. 13:708190. doi: 10.3389/fnagi.2021.708190

Age-related hearing loss (ARHL) is the most common sensory deficit in aging society, which is accompanied by increased speech discrimination difficulties in noisy environments, social isolation, and cognitive decline. The audiometric degree of ARHL is largely correlated with sensory hair cell loss in addition to age-related factors not captured by histopathological analysis of the human cochlea. Previous studies have identified the senescence-accelerated mouse prone strain 8 (SAMP8) as a model for studying ARHL and age-related modifications of the cochlear redox environment. However, the SAMP8 population exhibits a large variability in auditory function decline over age, whose underlying cause remains unknown. In this study, we analyzed auditory function of SAMP8 mice by measuring auditory brainstem response (ABR) thresholds at the age of 6 weeks (juvenile), 12 weeks (young adult), and 24 weeks (adult). Consistent with previous studies, SAMP8 mice exhibit an early progressive, age-related decline of hearing acuity. However, a spatiotemporal cytohistological analysis showed that the significant increase in threshold variability was not concurrently reflected in outer hair cell (OHC) loss observed in the lower and upper quartiles of the ABR threshold distributions over age. This functional loss was found to precede OHC loss suggesting that age-related phenotypic changes may be contributing factors not represented in cytohistological analysis. The expression of potassium channels KCNQ4 ($K_V7.4$), which mediates the current $I_{K,n}$ crucial for the maintenance of OHC membrane potential, and KCNQ1 ($K_V7.1$), which is an essential component in potassium circulation and secretion into the endolymph generating the endocochlear potential, showed differences between these quartiles and age groups. This suggests that phenotypic changes in OHCs or the stria vascularis due to variable oxidative deficiencies in individual mice may be predictors

of the observed threshold variability in SAMP8 mice and their progressive ARHL. In future studies, further phenotypic predictors affected by accumulated metabolic challenges over age need to be investigated as potentially underlying causes of ARHL preceding irreversible OHC loss in the SAMP8 mouse model.

Keywords: SAMP8 strain, age-related hearing loss, auditory brainstem response, cytocochleogram, KCNQ4 (Kv7.4), KCNQ1 (Kv7.1)

INTRODUCTION

Age-related hearing loss (ARHL), or presbycusis, is the most common sensory impairment (Bowl and Dawson, 2019). According to the comprehensive Global Burden of Disease study, hearing loss is the third most common cause of years lived with disability, with ARHL ascertained as the leading impairment in the population older than 70 years (GBD Hearing Loss Collaborators, 2021). ARHL typically presents as a decline in hearing ability with aging that is symmetrical and pronounced in the high frequencies. There is considerable variation in the age of onset, the grade of hearing loss, and the progression of the disease (Merchant and Nadol, 2010). Age-dependent loss of hearing sensitivity is accompanied by reduced speech discrimination, decelerated central processing, and impaired sound localization (Frisina and Frisina, 1997; Frisina, 2001; Merchant and Nadol, 2010). Although this condition is not considered life-threatening, it can significantly degrade the quality of life and is associated with psychological and medical morbidity, including social isolation, depression, and cognitive decline (Lin et al., 2011a, 2013; Kamil et al., 2016; Goman and Lin, 2018; Rutherford et al., 2018; Bowl and Dawson, 2019; GBD Hearing Loss Collaborators, 2021).

ARHL has been suggested to result from age-related cochlear degeneration caused by cumulative environmental effects in industrialized societies, such as noise exposure, which are not present in ethnologically isolated populations (Hilke and Plester, 1955; Rosen et al., 1962, 1964). Controlling for population-specific genetic factors, true or intrinsic presbycusis was demonstrated in other non-industrial populations (Goycoolea et al., 1986). This supports observations that ARHL develops from the multifactorial interaction of environmental, monogenic, or polygenic factors that shape a complex disease situation (Van Eyken et al., 2007; Vuckovic et al., 2018). The classic human pathophysiological model of ARHL, also known as Schuknecht's typology (Ohlemiller, 2004), is derived from studies of audiometric tests and serial histological sections of post-mortem human temporal bones over a span of more than five decades (Schuknecht, 1955, 1964, 1974, 1993; Schuknecht and Gacek, 1993; Merchant and Nadol, 2010). According to this model, ARHL has been classified into sensory, strial, and neural presbycusis, or combinations thereof which are termed mixed presbycusis or an indeterminate type (Merchant and Nadol, 2010). A recent, modified re-analysis of human temporal bones from the same archival temporal bone collection showed that the degree of ARHL is best predicted by the loss of outer hair cells (OHCs) and inner hair cells (IHCs), strongly suggesting sensory presbycusis as the predominant type of ARHL in humans (Wu et al., 2020). This quantitative re-analysis of serial sections confirmed earlier findings using microdissected sensory epithelia that were analyzed using the surface specimen technique to generate cytocochleograms of the human cochlea (Engström et al., 1966). This technique demonstrated similar degeneration patterns of OHCs and IHCs pursuant to ARHL (Bredberg, 1968). However, in addition to sensory hair cell loss, it is proposed that other age-related detrimental effects causing phenotypic change of surviving hair cells can contribute to ARHL and which remain unexplained (Wu et al., 2020).

Increasing evidence proposes oxidative stress as one of the major risk factors for ARHL (Menardo et al., 2012; Han and Someya, 2013; Benkafadar et al., 2019). Oxidative stress refers to the imbalance between cellular production of reactive oxygen species (ROS) and antioxidant defenses (Halliwell, 1992). It can result in cell damage by oxidization of cellular components such as membrane lipids, proteins, and DNA (Serrano and Klann, 2004). Accumulation of ROS production and impaired antioxidant defense systems, e.g., due to aging stress or following noise overstimulation, are implicated to cause cellular dysfunction such as lipid peroxidation and enzyme inactivation, leading to permanent apoptotic cell degeneration and hence initiating the process of cochlear senescence (Harman, 1956; Beckman and Ames, 1998; Baker and Staecker, 2012; Fujimoto and Yamasoba, 2019). ROS-mediated modification of ion channels can also alter the activity of other signaling mechanisms leading to changes in channel activity or channel gene expression (Matalon et al., 2003). ROS overproduction can, therefore, metabolically stress the cochlea and induce mitochondrial dysfunction and an associated decrease of energy production (Balaban et al., 2005; Henderson et al., 2006; Lin and Beal, 2006). Consequently, sensitive stages that require high energy supply, e.g., potassium ion (K^+) channels, can be severely challenged by the accumulation of ROS.

K^+ channels are critically dependent on continuous recycling processes for proper membrane expression, suggesting them as one of the primary targets of ROS accumulation (Peixoto Pinheiro et al., 2020). In the inner ear, physiological functions of various K^+ channels involve the adjustment of the resting potential, shaping the responses of sensory hair cells and neurons (Housley and Ashmore, 1992; Santos-Sacchi, 1993; Kros et al., 1998), synaptic inhibition in hair cells (Fuchs and Murrow, 1992; Oliver et al., 2000), and the generation of the endocochlear potential (EP) by the stria vascularis (SV) establishing a high K^+ concentration in the endolymph (Wangemann, 2002). A number of K^+ channels, including voltage-gated (K_V) channels, have been shown to be modified both *in vivo* and *in vitro* by oxidants (Ruppersberg et al., 1991; Cai and Sesti, 2009). Interventions

intended to either increase antioxidant activity or decrease ROS production could, therefore, be effective therapeutic approaches to prevent or decelerate ARHL. In this endeavor, animal models have been used to investigate whether restoration of normal ROS balance with antioxidants may have therapeutic value (Ohinata et al., 2003; Hamernik et al., 2008; Fetoni et al., 2009; Fujimoto and Yamasoba, 2019). For example, a recent study showed that treatment with a synthetic superoxide dismutase/catalase-induced mitigation of excessive ROS could prevent accelerated ARHL and sensory hair cell loss in the senescence-accelerated mouse prone strain 8 (SAMP8) (Benkafadar et al., 2019), a mouse model which has been introduced for studying the pathophysiology of senescence in different systems.

The SAMP8 is a mouse strain established through phenotypic selection toward accelerated senescence from the AKR/J strain (Takeda et al., 1981). SAMP8 mice have been identified as a suitable model to study age-dependent disorders including senile amyloidosis, osteoporosis, cataracts, and brain atrophies (Akiguchi et al., 2017; Karuppagounder et al., 2017; Folch et al., 2018; Grinan-Ferre et al., 2018). Furthermore, the SAMP8 strain has previously shown to exhibit an early age-dependent hearing loss (Marie et al., 2017) associated with sensory, neural, and strial degeneration, which were primarily linked to oxidative stress (Menardo et al., 2012; Fujimoto and Yamasoba, 2014; Benkafadar et al., 2019). The premature SAMP8 senescence causing early presbycusis was linked to altered levels of antioxidant enzymes and decreased activity of complexes I, II, and IV, which in turn lead to chronic inflammation and triggering of apoptotic cell death pathways (Menardo et al., 2012). Even before the premature onset of hearing loss, SAMP8 cochleae already displayed an early increase in ROS levels and downregulation of antioxidant enzymes (Menardo et al., 2012; Benkafadar et al., 2019). The rapidly aging SAMP8 strain may provide a useful model for studying the effects of aging on biological processes, especially regarding ARHL pathophysiology. However, the SAMP8 population exhibits a large variability in their age-related decline of auditory function. The extent of this functional variability and the underlying cellular degeneration pattern have thus far not been systematically studied.

In the present study, the auditory function of SAMP8 mice was analyzed at the age of 6 weeks (juvenile), 12 weeks (young adult), and 24 weeks (adult; Wang et al., 2020) by measuring auditory brainstem response (ABR) thresholds. We observed a bifurcation into two subgroups, i.e., in lower and upper quartiles with respect to different progressions of age-related ABR threshold increase. We investigated the variability in auditory function by contrasting these two classifications in a spatiotemporal histological analysis. For each age group and subgroup, cytocochleograms were created, which cartographically represent the number of OHCs and IHCs along the cochlear length (Viberg and Canlon, 2004; Müller et al., 2005; Carignano et al., 2019). A frequency-place map was used to correlate functional changes measured by the ABR to morphological insults in the organ of Corti (OC). Here, OHC loss observed over age could not explain threshold variability within the age groups. Therefore, cochlear cross-sections were analyzed for membrane expression of KCNQ4 ($K_V7.4$) and KCNQ1 ($K_V7.1$). KCNQ4 is a K^+ channel expressed in the basal pole of mature OHCs and is responsible for their resting potential and $I_{K,n}$ current (Housley and Ashmore, 1992; Santos-Sacchi, 1993; Kros et al., 1998), which is critical for OHC function (Jentsch, 2000a,b; Kharkovets et al., 2006; Gao et al., 2013; Carignano et al., 2019). And KCNQ1 is expressed in marginal cells of the SV where it mediates the slow delayed rectifier current $I_{K,s}$ (Barhanin et al., 1996; Sanguinetti et al., 1996; Neyroud et al., 1997; Shen and Marcus, 1998) and forms an essential component in K^+ circulation and secretion into the endolymph, generating the EP. We hypothesize that diminished levels of KCNQ4 and KCNQ1 constitute possible candidates for phenotypic change preceding OHC apoptosis, which may account for the observed auditory threshold variability in SAMP8 mice.

MATERIALS AND METHODS

Animals and Experimental Design

Senescence-accelerated mouse prone strain 8/TaHsd mice of either sex were acquired from Envigo (Horst, Netherlands) at an age of 30 days and allowed to acclimatize for 7 days in an in-house animal facility. They were held in groups of one (only aggressive males) to five animals in a standard macrolon polycarbonate housing and were maintained on a 12-h light-dark cycle with access to food and water *ad libitum*. All animals were handled and housed according to the German (TierSchG) and European Union (directive 2010/63/EU) guidelines for the protection of animals used for experimental purposes, as reviewed and approved by the veterinary care unit of the University of Tübingen and by the regional Animal Care and Ethics Committee (Regierungspräsidium Tübingen).

The experimental design consisted of two cohorts of SAMP8 mice. In a **reference cohort** of 84 animals, ABR thresholds were collected from accumulated control groups that were divided into three age groups: juvenile (average age of 6 weeks), young adult (average age of 12 weeks), and adult (average age of 24 weeks). This cohort served as a reference for age-dependent development of ABR threshold distributions.

In the **experimental cohort** of 46 animals, ABR thresholds were measured for each age group (juvenile, young adult, or adult) and compared to the interquartile range (between the 25th and 75th percentile) of the age-respective distribution in the reference cohort. In order to correlate functional ABR threshold distributions with significant cellular changes in a cytohistologic analysis, mice were selected based on ABR thresholds below the 25th percentile (lower quartile) and above the 75th percentile (upper quartile). Following this classification for each age group, three (to four) mice from the lower or upper quartile of the respective reference cohort were sacrificed and their cochleae extracted for histologic analysis, with one cochlea used for the generation of cytocochleograms from surface whole-mount preparations and the other for cross-sectional analysis. In this experimental cohort, the total of 46 mice only underwent ABR measurements and 22 mice met the selection criteria and were thus included for histological analysis. An overview of the experimental design is shown in **Figure 1**.

Auditory Brainstem Response

Auditory brainstem response was recorded in response to pure-tones at frequencies 2.0–45.2 kHz in 2 steps per octave, with a duration of 3 ms and 1 ms rise and fall times. Stimuli were presented at levels 10–100 dB SPL in 3 dB steps in alternating condensation and rarefaction polarities. A multi-function I/O-card (National Instruments, Austin, TX, United States) was used to generate the stimulus waveforms and record the ABR signal. Acoustic stimuli were delivered in a calibrated open-field system using a dynamic loudspeaker placed lateral to the respective auricle of the animal. The sound pressure level was calibrated before each measurement block using a microphone probe (Brüel & Kjaer Types 4939 and 2670, Nærum, Denmark) placed near the entrance of the external auditory canal in line with the loudspeaker at 90° incidence. The ABR signal was recorded using a differential amplifier between silver-wire electrodes inserted subcutaneously on the vertex (positive terminal), on the mastoid of the respective ear (negative terminal) and on the back (ground), with a gain of 80 dB. Signals were filtered between 100 Hz and 5 kHz using sixth-order Butterworth low- and high-pass filters and then processed by the Audiology Lab software (Otoconsult, Frankfurt am Main, Germany) after analog-to-digital conversion at 50 kHz sampling frequency. ABR recordings were conducted in a soundproof chamber (IAC Acoustics, Niederkrüchten, Germany). ABR thresholds are defined as the sound pressure level at which a stimulus-related response was clearly identified by visual inspection of the ABR signal averaged from 128 stimulus repetitions for each polarity.

All animals were anesthetized during the ABR measurement by intraperitoneal injection of 0.05 mg/kg fentanyl (Fentadon, Dechra, Aulendorf, Germany), 0.5 mg/kg medetomidine hydrochloride (Dormilan, alfavet, Neumünster, Germany) and 2.5 mg/kg midazolam (Hameln Pharma plus GmbH, Hameln, Germany). To preserve eye moisture, an ointment (Bepanthen, Bayer AG, Leverkusen, Germany) was applied. Over the course of the measurement, electrocardiography was monitored and the animals were placed on a heating blanket to maintain their body temperature at approximately 37°C.

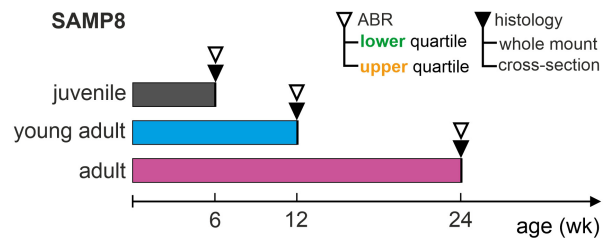

FIGURE 1 | Schematic representation of the experimental design. Auditory function over age was assessed in SAMP8 mice by determining auditory brainstem response (ABR) thresholds for each age group: juvenile (6 weeks), young adult (12 weeks), and adult (24 weeks). ABR thresholds were compared with respective reference distributions from accumulated controls for each age group (reference cohort), and then allocated to the lower (generally below the 25th percentile) or upper (generally above the 75th percentile) quartiles. Following this, mice in the lower or upper quartiles were sacrificed and their cochleae extracted for histology, using one cochlea for whole-mount and the other for cross-section analysis. This study included a total of 22 mice (out of 46 measured).

Histology

After the ABR measurement and allocation to the lower or upper quartile of the respective reference cohort, pre-anesthetized mice were sacrificed by intracardial injection of 600 mg/kg pentobarbital-natrium (Narcoren, Boehringer Ingelheim, Ingelheim am Rhein, Germany) followed by decapitation. Temporal bones were subsequently removed and the cochleae isolated, with one cochlea used for whole-mount and the other for cross-section analysis.

Cochlear Whole-Mount Preparation

To generate cochlear whole-mount preparations, temporal bones were dissected on ice, perfused with 4% formaldehyde and decalcified in 0.2 M EDTA for 27 h at 4°C. Once decalcification was completed, dissection of the cochlear sensory epithelium, i.e., the OC, was performed under a stereo microscope (Zeiss Stemi 200-C, Oberkochen, Germany). For OC extraction, the bony labyrinth was removed, followed by a detachment of the SV and a separation of the sensory epithelium from the spiral ganglion. The OC was divided into three segments designated as apical, middle, and basal segments. The three segments for each cochlea were transferred into one well of a 48-well plate filled with 500 µl of PBS.

For fluorescence and immunofluorescence labeling, the prepared whole-mount preparations were permeabilized using 0.2% Triton X-100 in PBS for 20 min at room temperature and immersed in a blocking buffer containing 0.2% Triton X-100 in PBS and 1% normal donkey serum (NDS) for 30 min at room temperature. Whole-mount preparations were incubated with anti-Myosin VIIa (1:400, rabbit, Developmental Studies Hybridoma Bank, Iowa City, IA, United States) and anti-CtBP2 (1:200, monoclonal mouse, BD Biosciences, San Jose, CA, United States) antibodies and visualized with an Alexa 488-conjugated anti-rabbit secondary antibody (1:400, Invitrogen, Paisley, United Kingdom) and an Alexa 647-conjugated anti-mouse secondary antibody (1:400, Invitrogen). All antibodies were diluted in PBS that had been supplemented with 0.2% Triton X-100 and 0.5% NDS. For nuclear and F-actin fluorescence staining, samples were incubated for 20 min at room temperature in DAPI (1:100, Sigma-Aldrich, St. Louis, MO, United States) and Phalloidin 568 (1:400, Invitrogen) and coverslipped using FluorSave mounting medium (Calbiochem, Merck, Darmstadt, Germany). Immunolabelled whole-mount preparations divided into apical, middle, and basal segments were imaged at 10× magnification using an epifluorescence microscope (Zeiss Axioplan 2 with an ApoTome.2 unit).

Cochlear Cross-Sections

For generation of cochlear cross-sections, isolated cochleae were fixed by immersion in 2% paraformaldehyde and 125 mM sucrose in 100 mM PBS (pH 7.4) for 2 h. After fixation, cochleae were decalcified for 45 min in RDO rapid decalcifier (Apex Engineering Products Corporation, Aurora, IL, United States). Cochleae were stored overnight at 4°C in 25% Sucrose-Hank's

solution and, on the following day, embedded in Tissue-tek (Sakura Finetek, AV, Netherlands). After embedding, cochleae were cryosectioned at 12 μm and mounted on SuperFrost Plus microscope slides (Thermo Fisher Scientific, Waltham, MA, United States) before storage at −20°C.

For fluorescence and immunofluorescence labeling of KCNQ4, microscope slides with mounted cochlear sections were permeabilized in 0.1% Triton-X 100 in PBS for 10 min and incubated for 30 min in a humidified chamber in blocking buffer containing 1% BSA in PBS. Cochlear sections were stained with antibodies against prestin (1:3000, rabbit, Squarix, Berlin, Germany) and KCNQ4 (1:50, mouse, StressMarq, Victoria, BC, Canada). For labeling of KCNQ1, microscope slides with mounted cochlear sections were permeabilized in 0.5% Triton-X 100 in PBS for 10 min and incubated for 30 min in blocking solution containing 4% normal goat serum (NGS) in PBS. Cochlear sections were stained with antibodies against KCNQ1 (1:200, rabbit, Alomone Labs, Jerusalem, Israel) and KCNJ10 (K_{ir}4.1, 1:50, mouse, Sigma-Aldrich). To detect primary antibodies, Cy3 anti-rabbit (1:1500, Jackson Immuno Research Laboratories, West Grove, PA, United States) and Alexa477-conjugated anti-mouse secondary antibodies (1:500, Invitrogen) were used. Antibodies against prestin, KCNQ4, and corresponding secondary antibodies were diluted in 0.5% BSA in PBS, whereas antibodies against KCNQ1, KCNJ10, and corresponding secondary antibodies were diluted in a reaction buffer containing 0.1% Triton-X 100 in PBS, 2% NaCl, and NGS. For nuclear staining, Vectashield mounting medium with DAPI (Vector Laboratories, Burlingame, CA, United States) was used to mount microscope slides with cochlear sections.

Sections were viewed using an Olympus BX61 microscope (Olympus, Hamburg, Germany) equipped with epifluorescence illumination and analyzed with cellSens Dimension software (OSIS GmbH, Münster, Germany). To increase spatial resolution, slices were imaged over a distance of 15 μm within an image-stack along the *z*-axis (z-stack) followed by three-dimensional deconvolution using cellSens Dimension's built-in algorithm.

Data Analysis

Cytocochleogram

Images of OC whole-mount preparations were analyzed using the ImageJ software (NIH, Bethesda, MD, United States) and cell counting was carried out manually by assigning different markers stored with their coordinates using the plug-in "Cellcounter." For each OC whole-mount segment (apical, middle, or basal), the length was measured along the clearly defined junction between the outer pillar cell and the first row of OHCs. The line was traced along the longitudinal axis of the OC across all three segments to determine the full spiral length. OHCs and IHCs were counted as present if co-staining of three cellular markers consisting of the cellular nucleus (DAPI), the stereocilia bundle (phalloidin), and the cellular cytoplasm (Myosin VIIa) were evident. Otherwise, if one of these markers was absent, hair cells were counted as missing. Each marker (present or missing OHCs and IHCs) was allocated to the nearest point on the spiral of the OC by calculating the minimum Euclidean distance. The total OC spiral length was determined by concatenating the three whole-mount segments. Then, the length was normalized to 100% and the count of present or missing OHCs and IHCs, respectively, was calculated as a function of the relative distance from the apex subdivided into 5% bins. Thereby, the extent and pattern of lost cells and the remaining intact cells along the cochlear length were mapped as a "cytocochleogram" (Engström et al., 1966; Viberg and Canlon, 2004; Müller et al., 2005; Carignano et al., 2019).

OHC and SV Phenotypes

For each age group and for either KCNQ4 or KCNQ1 analysis, pairs of cochlear cross-sections from two mice in the lower and upper quartiles, respectively, were stained on the same day using the same corresponding reagent solutions (see section "Histology"). Each pair was then imaged together using the same confocal acquisition parameters and exposure times. The presence of an OHC was verified if both the cell nucleus as well as the OHC-specific motor protein prestin were labeled, then KCNQ4 membrane expression at the basal pole of at least three OHCs was localized. The expression of KCNJ10 in the intermediate layer of the SV was used to delimit the marginal layer with KCNQ1 expression. Thereafter, a 100× oil immersion lens was used to image the OC and the SV, respectively, at an apical, middle, and midbasal position.

Quantitative analysis of KCNQ4 and KCNQ1 was performed in fluorescence images of cochlear cross-sections using the ImageJ software. For each magnified image, the background was reduced using the "rolling ball" algorithm (built-in ImageJ tool) with a radius of six pixels. The regions of interest (ROIs) used for quantification were delimited by circles with a diameter of 100 pixels around the basal pole of OHCs for the KCNQ4 staining, and by rectangles with a fixed width of 100 pixels along the marginal layer of the SV for the KCNQ1 staining. Subsequently, delimited ROIs were inserted onto a black background and the corresponding color channel (green for KCNQ4 and red for KCNQ1) was split and converted to an 8-bit grayscale image with a threshold of 75 pixel intensity to minimize contributions from background staining. Subsequently, pixel intensity was integrated over the processed images to obtain the area under the curve (AUC), then normalized by the number of OHCs to obtain a mean KCNQ4 intensity per OHC, or by the SV length to obtain a mean KCNQ1 intensity per SV width.

Statistics

Data are presented as mean with standard deviation (SD), or with standard error of the mean (SEM) for small sample sizes (n = 3 or 4) as an estimate of the deviation of the sample mean from the population mean. Data distributions were tested for normality by the Shapiro–Wilk test. Pairwise differences of means were compared for statistical significance using the Mann–Whitney-U for two samples or the Kruskal–Wallis test for more than two samples. Least-squares linear regressions were assessed by the coefficient of determination R^2. And linear correlations were determined by Pearson's correlation coefficient r. A p-value of less than 0.05 or less than 0.001 was considered statistically significant or highly significant, respectively. Statistical analysis

was performed using IBM SPSS Statistics 27 (IBM Corporation, Armonk, NY, United States).

RESULTS

SAMP8 Mice Develop Progressive Age-Related ABR Threshold Increase

ABR in SAMP8 mice were assessed over age by pure-tone stimulus-evoked ABR thresholds from accumulated control groups (reference cohort) that were divided into three age groups: juvenile (n = 84, mean 34 ± 6 days, range 25–45 days), young adult (n = 49, mean 80 ± 11 days, range 65–105 days), and adult (n = 22, mean 188 ± 14 days, range 170–210 days). Mean and SD of ABR thresholds for frequencies 2.0–45.2 kHz as well as corresponding mean age and age range are shown for each age group in **Figure 2A**. Comparison of the ABR thresholds across frequencies between age groups revealed a progressive increase in hearing loss starting in the high-frequency range (>8 kHz) between juvenile and young adult stages and further progressing toward the low-frequency range (≤8 kHz) in the adult stages. The significant differences between age groups from pairwise comparisons of ABR thresholds are indicated graphically in **Figure 2B** for each frequency, with young adult SAMP8 mice already exhibiting a significant increase of hearing thresholds for high frequencies (>8 kHz) compared with juvenile mice ($p < 0.05$). In adult mice, ABR thresholds were further elevated across all frequencies when compared with young adult mice, reaching statistical significance at 5.6 and 8 kHz ($p < 0.05$), and at 16–45.2 kHz ($p < 0.05$). When compared with juvenile mice, significantly elevated ABR thresholds were found in adult animals for all frequencies ($p < 0.05$). The mean increase in ABR threshold between juvenile and adult SAMP8 mice was 9.3 dB for the low-frequency range (≤8 kHz) and 26.5 dB for the high-frequency range (>8 kHz). SAMP8 mice thus show an early progressive, age-related increase in ABR thresholds, starting primarily in the high-frequency range and later extending to all frequencies at an adult age.

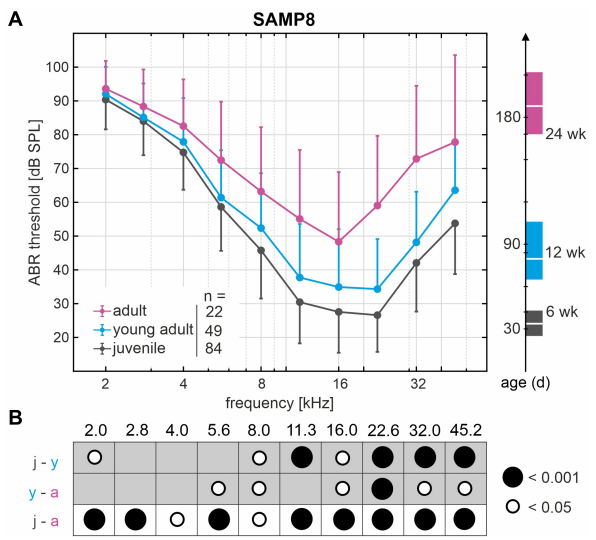

FIGURE 2 | Decline of hearing acuity over age in SAMP8 mice as assessed by auditory brainstem response (ABR) thresholds. **(A)** Mean and standard deviation of ABR thresholds from accumulated control groups (reference cohort) divided into three age groups: juvenile (black, n = 84), young adult (blue, n = 49), and adult (pink, n = 22). The right graph shows mean age and age range in days for each group: juvenile (black, mean 34 days, range 25–45 days), young adult (blue, mean 80 days, range 65–105 days), and adult (pink, mean 188 days, range 170–210 days). **(B)** Graphical representation of significant differences (white and black circles represent $p < 0.05$ and $p < 0.001$, respectively) from pairwise comparisons of ABR thresholds between age groups (j, juvenile; y, young adult; a, adult) for each frequency in kHz.

SAMP8 Mice Exhibit Variability in ABR Threshold Progression

Apart from the significantly progressive, age-related ABR threshold increase found in the SAMP8 reference cohort, the threshold variability for each age group–as represented by the SD–also appears to increase as a function of age (**Figure 2A**). In line with this observation, the mean SD of ABR thresholds over all frequencies in adult mice (18 ± 5 dB SPL) was significantly higher than in juvenile mice (12 ± 2 dB SPL, $p < 0.05$). We hypothesize a bifurcation into subgroups with slow or fast progression of ABR threshold increase over age, which presumably entails the significant increase in threshold variability between age groups. To identify the lower and upper ends of the threshold distribution within the SAMP8 subgroups, we compared the ABR threshold of a **monitoring cohort** of SAMP8 mice (n = 10, five males and five females) at juvenile (34 days), young adult (80 days), and adult age (195 days) with the interquartile range of the reference cohort for each age group. The monitoring cohort was then divided into subgroups (lower, normal, or upper) based on their progression of age-related ABR threshold increase. For each classification and age group, mean and SEM of ABR thresholds (one ear for each mouse) are shown in **Figure 3**. Mice in the lower quartile (lower, n = 3) showed a relatively slow progression of ABR threshold increase over age, tending toward a resistance against age-related decline. By contrast, mice in the upper quartile (upper, n = 3) showed a relatively fast progression. Finally, mice in the normal-hearing subgroup (normal, n = 4) adhered to the progression found in the reference cohort. No correlation was found between these classifications and the sex of the mice, and no relevant asymmetries were found between ears for each mouse. Note that at juvenile age, SAMP8 mice allocated to the upper quartile already showed elevated ABR thresholds for all frequencies when compared with either normal-hearing mice (mean shift 11 ± 5 dB) or mice in the lower quartile (mean shift 16 ± 4 dB). By contrast, normal-hearing mice and mice allocated to the lower quartile were initially comparable at juvenile age (mean shift 4 ± 6 dB), then progressively diverged up to the adult age (mean shift 18 ± 8 dB). In summary, the monitoring SAMP8 cohort confirmed an age-dependent bifurcation into subgroups with different progressions of age-related ABR threshold increase. In order to address related morphological

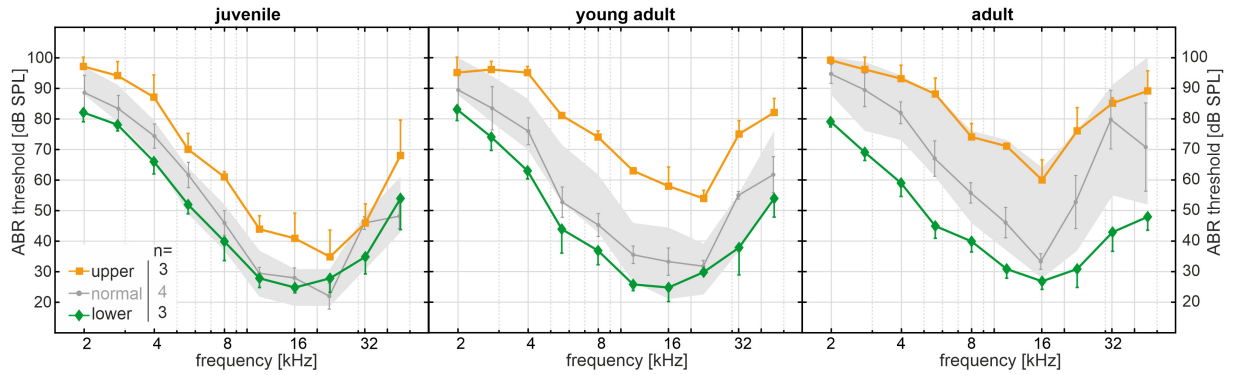

FIGURE 3 | Long-term SAMP8 monitoring cohort (n = 10) with auditory brainstem response (ABR) thresholds measured at juvenile (34 days), young adult (80 days), and adult age (195 days). ABR thresholds were compared with the interquartile range of the reference cohort for each age group (gray area, see **Figure 2**) and divided into subgroups in the lower quartile (green diamonds, n = 3), in the normal range (gray circles, n = 4), and in the upper quartile (orange squares, n = 3) based on their progression of age-related threshold increase over age. For each age group and subgroup, mean and standard error of the mean ABR thresholds are shown.

alterations, a spatiotemporal histological analysis was performed for the different age groups.

ABR Threshold Loss of SAMP8 Mice Partly Independent of Cochlear Hair Cell Loss

Outer hair cell survival were analyzed performing cytocochleograms obtained from OC whole-mount preparations of juvenile, young adult, and adult aged SAMP8 mice. According to the functional ABR threshold classification, SAMP8 mice were selected from the lower and upper quartiles as described above for each of the three age groups. The two functionally different groups were chosen to gain insight into potential cellular correlates of the observed diverging threshold losses. An illustrative example of analyzing OC whole-mount segments (apical, middle, and basal) is shown in **Figure 4A**. Present or missing OHCs and IHCs were counted and allocated to bins along the normalized spiral length of the OC. The mean length of the OC was 5.33 ± 0.36 mm (n = 19). In some cases, whole-mount segments were only partially intact due to preparation artifacts, e.g., in the 90–100% range of this illustrative example (**Figure 4B**). These were not included in the analysis while the length axis was maintained to allocate the hair cell count to the correct position along the total length of the OC. Cell counts of present or missing OHCs and IHCs as a function of the relative distance from apex in 5% bins are demonstrated in **Figure 4C**. Note that entire bins without valid hair cell markers were excluded from the analysis. However, bins with only partially valid markers due to preparation difficulties were included but showed generally lower cell counts.

In the following, cytocochleograms are presented as the ratio between missing hair cells and the sum of present and missing hair cells, i.e., percentage of hair cell loss, in each bin. Thereby, the limitation of only partially valid markers in a given bin was overcome and the comparison between relative OHC and IHC loss was facilitated. The mean age at the ABR measurement followed by cochlear extraction for mice in either quartile was 38 ± 4 days (juvenile), 97 ± 15 days (young adult), and 184 ± 16 days (adult). At juvenile age, mice in the upper quartile (n = 3) had elevated ABR thresholds across all frequencies compared with same-aged mice in the lower quartile (n = 3). The most pronounced difference was seen at 16 kHz (**Figure 5A**, dashed line). At this frequency, juvenile mice in the lower quartile had a mean threshold of 16 ± 3 dB SPL, whereas mice in the upper quartile had a mean threshold of 58 ± 3 dB SPL, i.e., the mean threshold difference at 16 kHz was 42 dB. At young adult age, the mean threshold difference was 35 dB between the respective mice in the lower (n = 3) and upper (n = 3) quartiles. And at adult age, the difference was 51 dB between the respective mice in the lower (n = 3) and upper (n = 4) quartiles. Note that at adult age, mice in the upper quartile had profound hearing loss with a mean threshold of 77 ± 6 dB SPL at 16 kHz. By contrast, the same-aged mice in the lower quartile had a mean threshold of 26 ± 1 dB SPL, which lies within the interquartile range of the reference cohort at juvenile age, i.e., they had a decelerated progression of ABR threshold increase over age. This is in line with the observations made in the SAMP8 monitoring cohort with continuous ABR measurements (see **Figure 3**).

Cytocochleograms corresponding to mice of the experimental cohort with ABR thresholds allocated to the lower or upper quartiles over age are plotted in **Figure 5B**. IHC loss remained below 5% for mice in either quartile, for all age groups. Surprisingly, no OHC loss was observed in both the lower and upper quartiles at all frequencies of the juvenile age group despite a mean threshold difference of 42 dB at 16 kHz. In young adult mice, OHC loss was found starting at an approximately 40% distance from apex, which corresponds to about 9 kHz as estimated by a mouse place-frequency map (Wang et al., 2002; Viberg and Canlon, 2004; Müller et al., 2005), and progressed toward the basal region. In adult mice, OHC loss further increased in the same regions. However, no consistent differences were found between respective mice in the lower and upper quartiles. At young adult age, for example, the distance from apex corresponding to 16 kHz (**Figure 5B**, dashed line) had a mean OHC loss of 7 ± 2% in the lower (n = 3) and 12 ± 2%

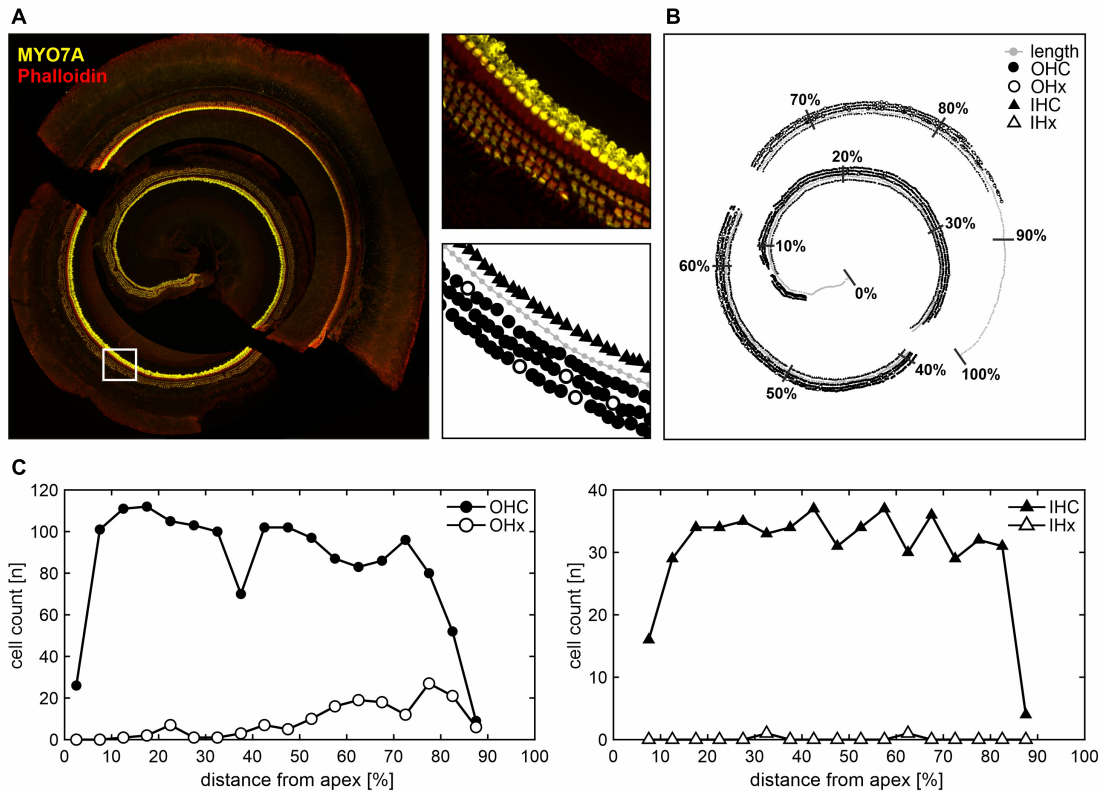

FIGURE 4 | Hair cell count along the cochlear spiral length in whole-mount histological analysis. **(A)** Illustrative example of apical, middle, and basal cochlear segments stained with MYO7A for hair cells and phalloidin for stereocilia (left panel). In the white-square delimited area, different marker assignments are illustrated (right panels): cochlear length axis (gray circles), present or missing outer hair cells (OHC as black circles, or OHx as white circles, respectively), and present or missing inner hair cells (IHC as black triangles, or IHx as white triangles, respectively). **(B)** The corresponding overview is shown with the cochlear length normalized to 100% distance from apex and subdivided into 10% bins. Due to preparation difficulties, some whole-mount segments were only partially intact, e.g., in the 90–100% range. These were not included in the analysis, i.e., no hair cell markers were assigned, whereas the length axis was still used to approximate the total cochlear spiral length. **(C)** Present or missing OHC (left panel) and IHC (right panel) counts are shown as a function of the relative distance from apex in 5% bins, with the cell count plotted in the middle of the respective bin. Note that entire bins without valid hair cell markers were excluded, while bins with only partially valid markers due to preparation difficulties were included, but showed generally lower cell counts.

in the upper (n = 3) quartiles, which is in contrast to a mean threshold difference of 35 dB between these groups. At adult age, the mean OHC loss was 21 ± 8% in the lower (n = 3) and 38 ± 9% in the upper (n = 4) quartiles. This presents a relatively larger difference between the two groups and functionally compares to a mean threshold difference of 51 dB. At more basal sites (70–90% distance from apex), young adult and adult mice in the respective upper quartiles showed less OHC loss than those in the respective lower quartiles, which appears contradictory to the ABR threshold difference at the same frequency locations between mice in the upper and lower quartiles.

To further quantify ABR threshold shifts and OHC loss over age, a mouse place-frequency map (Viberg and Canlon, 2004) was used to convert the relative distance from apex to corresponding frequencies. The cytocochleograms were then divided into low- (≤8 kHz) and high-frequency (>8 kHz) ranges in accordance with the progressive OHC loss observed in the middle and basal regions (>40% distance from apex) in contrast to the apical region (see **Figure 5B**). As an equivalent to relative hair cell loss, ABR threshold shifts were calculated for each mouse by subtracting the mean threshold of the reference cohort at juvenile age (see **Figure 2**) from each given threshold, at each given frequency. Thereby, a relative ABR threshold shift from the population mean with the juvenile age as reference could be compared between mice allocated to the lower or upper quartiles over age. Within each frequency range (low or high frequency) and for each classification (lower or upper quartile), scatterplots as a function of absolute age in days and corresponding linear regression models are shown for ABR threshold shifts in **Figure 6A** and for OHC or IHC losses in **Figure 6B**. The coefficient of determination (R^2) of the linear regression models is indicated graphically in **Figure 6C**. And corresponding correlation coefficients (Pearson's r, upper table) and their significance value (p, lower table) are indicated graphically in **Figure 6D**.

In the low-frequency range, only mice allocated to the lower quartile showed relevant linear regressions and had moderate positive correlations between age and ABR threshold shift (r = 0.42, p = 0.005) and OHC loss (r = 0.44, p = 0.002, see **Figures 6C,D**). In the high-frequency range, by contrast,

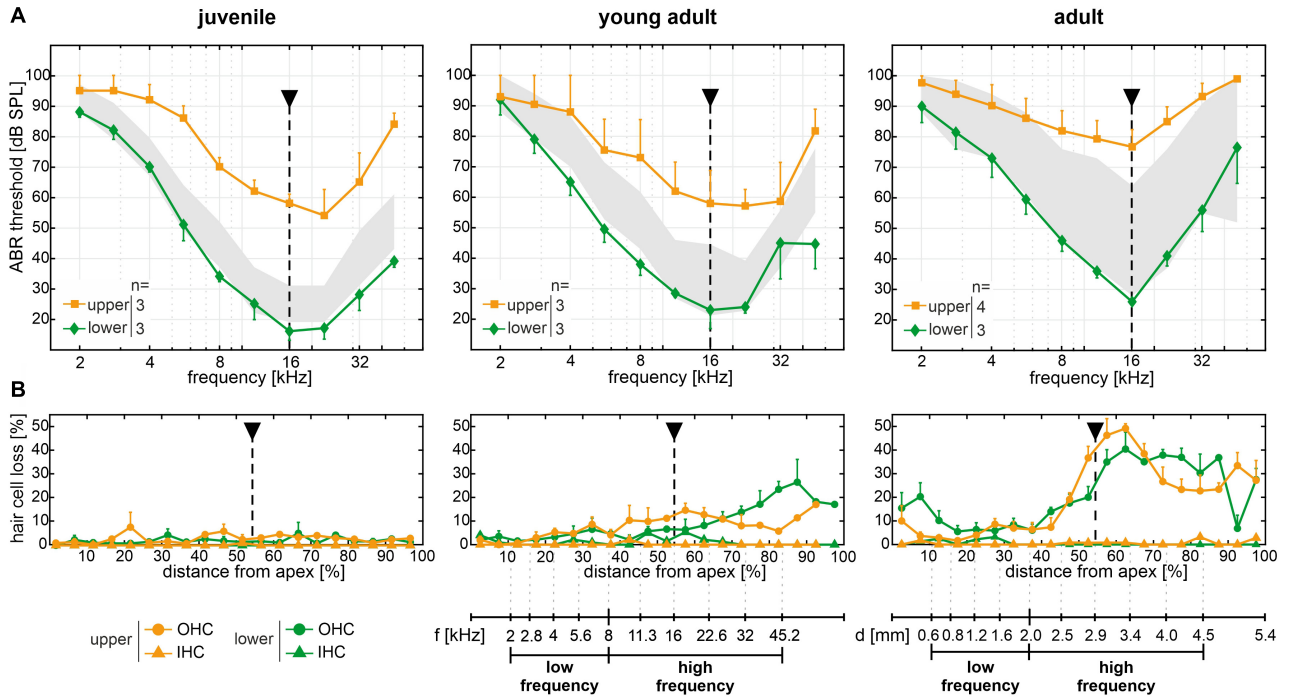

FIGURE 5 | Spatiotemporal analysis of cochlear hair cell loss over age of the experimental cohort. **(A)** Mean and SEM of auditory brainstem response (ABR) thresholds of ears corresponding to the whole-mount analysis for each mouse, for mice allocated to the lower (green diamonds) and upper (orange squares) quartiles in each age group (juvenile, young adult, and adult). The interquartile range of ABR thresholds of the reference cohort for each age group is shown for comparison (gray area, see **Figure 2**). **(B)** Cytocochleograms showing mean and SEM of outer and inner hair cell loss (OHC as circles and IHC as triangles, respectively) as a function of relative distance from apex, for mice with ABR thresholds allocated to the lower (green) and upper (orange) quartiles, respectively, in each age group. A mouse place-frequency map (Wang et al., 2002; Viberg and Canlon, 2004; Müller et al., 2005) was used to divide cytocochleograms into low- (≤8 kHz) and high-frequency (>8 kHz) ranges. For reference, frequency (f) and cochlear spiral length (d) axes are depicted with respect to the relative distance from apex. The dashed line highlights ABR thresholds and corresponding OHC and IHC loss at 16 kHz, for which the largest mean threshold difference was found in all age groups.

ABR threshold shift as well as OHC loss were well-described by linear regression ($R^2 > 0.4$) and had strong positive correlations with age ($r \geq 0.7$, $p < 0.001$) for either quartile. By contrast, IHC loss was not significant over age as shown above (see **Figure 5B**). In other words, the increase of ABR threshold over age was observed in the high-frequency range independent of quartile allocation, while thresholds at lower frequencies remained largely unchanged. These observations are in line with age-related OHC loss, showing little loss in the low-frequency range, but a significant loss in the high-frequency range over age. Although these results confirm OHC loss as one predictor of ABR threshold increase over age in SAMP8 mice, the observed threshold variability cannot be explained by OHC loss alone. While OHC loss is comparable between mice allocated to the lower and upper quartiles (see **Figure 6B**), this is in stark contrast to the ABR threshold difference in the high-frequency range between these groups ($\Delta = 38$ dB, see **Figure 6A**) which persists over age. Furthermore, the hypothesis that mice in the lower and upper quartiles exhibit slow and fast progression of age-related ABR threshold increase, respectively, is not supported by comparable slopes of the linear regression models in the high-frequency range, with a threshold increase of 8.5 dB per 50 days in the lower and 8.0 dB per 50 days in the upper quartile. This implies that lower and upper quartiles have different time points of hearing loss onset, but progress with the same rate thereafter. Despite the largely unchanged ABR thresholds over age in the low-frequency range, a persisting threshold difference between mice in the lower and upper quartiles was observed ($\Delta = 22$ dB). Based on these observations, it is suggested that OHC loss is a secondary predictor of ABR threshold increase over age in either quartile given that functional impairment, as measured by increase in ABR thresholds, preceded OHC loss in both lower and upper quartiles.

OHC and SV Phenotypic Differences of SAMP8 Mice Relate to ABR Threshold Variability

Given that OHC loss over age could not be linked to the observed variability of ABR thresholds between SAMP8 mice in the lower and upper quartiles, we hypothesized that potential sensitive phenotypic variances preceding OHC loss may be linked to altered levels of KCNQ4 ($K_V7.4$) membrane expression in OHCs or to altered levels of KCNQ1 ($K_V7.1$) in the SV. For each age group, three (juvenile) to four (young adult and adult) pairs of cochlear cross-sections of mice in the lower and upper quartiles, respectively, were analyzed for KCNQ4 (**Supplementary Figures 1–3**) and

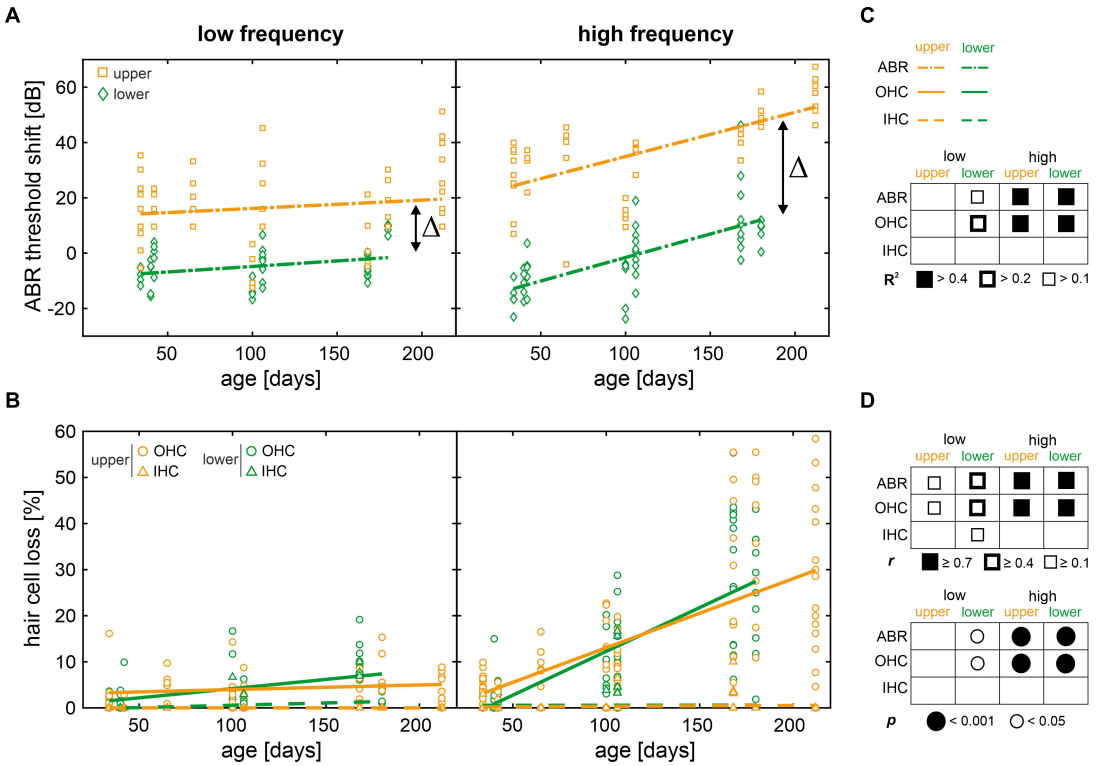

FIGURE 6 | Scatterplots of auditory brainstem response (ABR) threshold shifts and hair cell loss as a function of age with regression and correlation analysis. **(A)** Individual ABR threshold shifts over age for mice in the lower (green diamonds) and upper (orange squares) quartiles, in the low- (≤8 kHz) and high-frequency (>8 kHz) range, respectively. ABR threshold shifts were calculated for each mouse by subtracting the mean threshold of the reference cohort at juvenile age (see **Figure 2**) from each given threshold, at each given frequency. Fitted linear regression models (dash-dotted lines) are shown for mice in the lower (green) and upper (orange) quartiles, respectively. Δ indicates the difference of intercepts between models for mice in the lower and upper quartiles, for each frequency range. **(B)** Individual outer and inner hair cell loss (OHC as circles and IHC as triangles, respectively) over age for mice in the lower (green) and upper (orange) quartiles, in the low- and high-frequency range, respectively. Fitted linear regression models for OHC loss (solid lines) and for IHC loss (dashed lines) are shown for mice in the lower (green) and upper (orange) quartiles, respectively. **(C)** Graphical representation of the coefficient of determination (R^2) ranges of the linear regression models for each measure and for each condition. **(D)** Graphical representation of correlation coefficients (Pearson's *r*, upper table) and corresponding significance values (*p*, lower table) for each measure and for each condition.

KCNQ1 (**Supplementary Figures 4–6**) membrane expression. Quantitative analysis of KCNQ4 and KCNQ1 membrane expression was carried out by processing fluorescence images of cochlear cross-sections to reduce background and detect ROIs, then split the corresponding color channel, and evaluate the pixel intensity in 8-bit grayscale images (**Figures 7A,C**). The pixel intensity profiles for KCNQ4 (**Figure 7B**) and KCNQ1 (**Figure 7D**) were then integrated to obtain the AUC, then normalized by the number of OHCs to obtain a mean KCNQ4 intensity per OHC, or by the SV length to obtain a mean KCNQ1 intensity per SV width.

For each age group, normalized AUCs of KCNQ4 and KCNQ1 that were averaged from cochlear cross-sections in the apical, middle, and midbasal turns, for mice allocated to the lower and upper quartiles, respectively, are shown in **Figure 8**. Across age groups, KCNQ4 expression (**Figure 8A**) was generally higher in mice allocated to the lower quartiles than in mice allocated to the upper quartiles, with the ratio of mean KCNQ4 expression in the lower quartile to the upper quartile ranging from 1.14 to 3.16. However, no significant differences were found between these quartiles for each age group. This trend was similarly observed for KCNQ1 expression (**Figure 8B**), with the ratio of mean KCNQ1 expression in the lower quartile to the upper quartiles ranging from 1.15 to 1.98, but no significant differences were found. Still, the data suggest that KCNQ4 and KCNQ1 membrane expressions averaged over three cochlear turns were generally reduced in the age-matched mice allocated to the upper quartiles, which is in concordance with the higher ABR thresholds found in the low- and high-frequency ranges (see **Figure 6A**).

Scatterplots as a function of absolute age in days and corresponding linear regression models for normalized AUCs of KCNQ4 and KCNQ1 are shown in **Figures 9A,B**, respectively, for each quartile (lower or upper) and for each cochlear turn (apical, middle, or midbasal). The coefficients of determination (R^2) of the linear regression models and corresponding correlation coefficients (Pearson's *r*) are indicated graphically for KCNQ4 and KCNQ1 in **Figures 9C,D**, respectively. KCNQ4 expression in OHCs showed relevant linear regressions in the middle turn with negative correlations between KCNQ4 expression and age in mice allocated to the lower ($r = -0.71$, $p = 0.014$) and

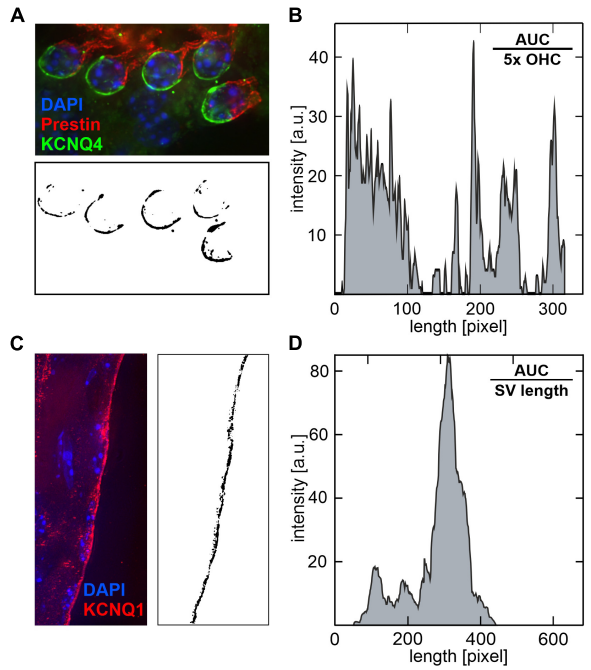

FIGURE 7 | Quantitative analysis of KCNQ4 and KCNQ1 pixel intensity profiles in cochlear cross-section fluorescence images. **(A)** Illustrative example of a cochlear cross-section stained with KCNQ4 (green), prestin (red) for the outer hair cell (OHC) motor protein, and DAPI (blue) for cell nuclei (upper panel). For each image, the regions of interest (ROIs) were delimited by circles around the basal pole of OHCs. The green channel (KCNQ4) was split and converted to an 8-bit grayscale image (lower panel). **(B)** The corresponding pixel intensity profile is shown. The pixel intensity was integrated over the processed image to obtain the area under the curve (AUC) and normalized by the number of OHCs, here 5×, to calculate a mean KCNQ4 intensity per OHC. **(C)** Illustrative example of a cochlear cross-section stained with KCNQ1 (red) in the stria vascularis (SV), and DAPI (blue, left panel). ROIs were delimited by rectangles with a fixed width along the marginal layer of the SV. The red channel (KCNQ1) was split and converted to an 8-bit grayscale image (right panel). **(D)** The corresponding pixel intensity profile is shown. The AUC was normalized by the SV length along the *y*-axis to calculate a mean KCNQ1 intensity per SV width.

upper quartiles, respectively ($r = -0.39$, $p > 0.05$, **Figure 9A**, middle). The persistent difference (Δ) between the lower and upper quartiles over age is congruent with the ABR threshold difference observed between these groups which also persists over age (see **Figure 6A**). Another relevant linear regression was found in the midbasal turn with a negative correlation between KCNQ4 expression and age in mice allocated to the upper quartile ($r = -0.55$, $p = 0.078$), while the expression in the lower quartile did not correlate with age (**Figure 9A**, midbasal). The apparent increase (ε) in expression difference between the lower and upper quartiles in the midbasal turn and the aforementioned, persistent difference (Δ) in the middle turn coincide with the larger ABR threshold difference observed in the high-frequency region (compare **Figures 6A**, **9A**). With regards to KCNQ1 expression in the SV, a relevant linear regression was solely found in the apical turn for mice allocated to the lower quartile with a moderate negative correlation between KCNQ1 expression and age ($r = -0.43$, $p > 0.05$, **Figure 9B**, apical). Although mice allocated to either quartile generally showed weak correlations between KCNQ1 expression and age, a persistent difference over age may be interpreted between the lower and upper quartiles in the midbasal turn (**Figure 9B**, midbasal). Based on these observations, it is suggested that altered OHC and SV phenotypes constitute potential predictors of the observed ABR threshold differences in SAMP8 mice, feasibly preceding OHC loss over age.

DISCUSSION

In the present study, we analyzed the auditory thresholds and sensory hair cell loss of SAMP8 mice as a function of age. Apart from the early progressive, age-related decline in hearing acuity, we observed a significant increase in threshold variability over age. We hypothesized that SAMP8 mice exhibit different progressions of age-related ABR threshold increase. In line with this hypothesis, we found that a monitoring cohort of SAMP8 presented a bifurcation into two subgroups, i.e., in lower and upper quartiles, with respect to ABR threshold distribution. Surprisingly, in the experimental cohort, the large variability of threshold loss between these quartiles did not conclusively correlate to a cellular loss of OHCs. In fact, functional loss as measured by ABR threshold increase was found to precede OHC loss. In search for sensitive phenotypic markers of this age-related functional loss, we hypothesized that diminished expression levels of KCNQ4 ($K_V7.4$), a K^+ channel crucial for OHC function and survival, and KCNQ1 ($K_V7.1$), an essential channel for K^+ circulation and secretion into the endolymph generating the EP, constitute possible candidates for phenotypic alteration preceding OHC loss and possibly accounting for the observed threshold variability. KCNQ4 and KCNQ1 membrane expressions were found to be decreased in mice with ABR thresholds allocated to the upper quartile compared with those in the lower quartile, with partly persistent or increasing differences between these quartiles and weak negative correlations between membrane expression and age. We thus propose that diminished expression levels of KCNQ4 in OHCs and KCNQ1 in the SV may be underlying causes of the variability in auditory threshold progression of SAMP8 mice. In the following sections, we discuss the implications of these results for the SAMP8 mouse model of ARHL, the ABR threshold increase in the context of OHC or IHC loss, i.e., sensory presbycusis, and KCNQ4 and KCNQ1 expressions as well as other potential predictors affected by accumulated metabolic challenges over age that need to be investigated as possible underlying causes of ARHL preceding irreversible OHC loss in the SAMP8 mouse model.

SAMP8 Mouse Model of ARHL

The SAMP8 strain is commonly used as a model to study several disorders observed in aging, such as senile amyloidosis, osteoporosis, cataracts, and brain atrophies (Akiguchi et al., 2017; Karuppagounder et al., 2017; Folch et al., 2018; Grinan-Ferre et al., 2018). Previously, SAMP8 mice were used to investigate premature cochlear aging and as a model of ARHL with an early progressive, age-related decline in hearing acuity (Menardo et al., 2012; Marie et al., 2017). In the present study,

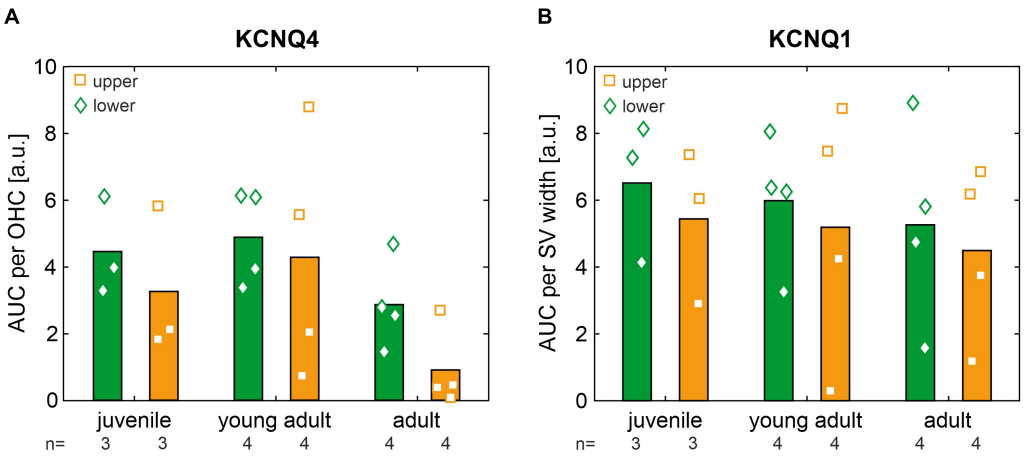

FIGURE 8 | (A) Area under the curve (AUC) of KCNQ4 immunofluorescence normalized per outer hair cell (OHC) and averaged from cochlear cross-sections in the apical, middle, and midbasal turns for mice allocated to the lower (green diamonds) and upper (orange squares) quartiles in each age group (juvenile, young adult, and adult). Grand means are shown as bar graphs. **(B)** Same as panel **(A)** for the AUC of KCNQ1 immunofluorescence normalized per stria vascularis (SV) width.

we confirmed these findings with our SAMP8 reference cohort showing significant ABR threshold increases from juvenile to young adult and adult age (see **Figure 2**). This age-related increase in ABR thresholds started in the high-frequency range and later extended to all frequencies, which closely mimics the typical audiometric progression in human ARHL, characterized by a greater deterioration of audiometric thresholds over age at high frequencies than at low frequencies (Gates and Mills, 2005; Gordon-Salant, 2005; Wu et al., 2020).

In addition to the significantly progressive age-related ABR threshold increase found in the SAMP8 population, we observed an age-dependent increase in threshold variability for each age group. The continuous ABR measurement in the monitoring cohort presented a bifurcation in thresholds showing a highly variable progression of ARHL in the SAMP8 model (see **Figure 3**). Previously, Benkafadar et al. (2019) compared the progression of ABR threshold increase over age between SAMP8 and the senescence-accelerated mouse resistant 1 (SAMR1) strain, which was typically used as a SAMP8 control representing normal senescence (Takeda et al., 1981). Benkafadar et al. (2019) confirmed that both strains develop ARHL after 1 month of age, but threshold progression was shown to be faster in the SAMP8 strain with a threshold increase over the frequencies 2–32 kHz of 5.0 dB/month versus 2.8 dB/month in the SAMR1. Similar progressions have also been previously reported for the compound action potential (CAP) evoked by tone bursts at 20 kHz (Menardo et al., 2012). For our SAMP8 reference cohort, we estimated a threshold increase of 3.6 dB/month over all frequencies, which seems to fall in between the progressions previously reported for the SAMP8 and SAMR1 strains.

Furthermore, individual data reported by Benkafadar et al. (2019) for either strain also presented a large ABR threshold variability as observed in the present study. Already at 1 month of age, they reported a mean ABR threshold range over all frequencies of approximately 34 dB (n = 14), and at 6 months of age, the range increased up to 59 dB (n = 14, Benkafadar et al., 2019). By comparison, in the considerably larger reference cohort of the present study, we observed a larger mean ABR threshold range of 63 dB in juvenile mice (1.5 months, n = 84) in contrast to a smaller range of 45 dB in adult mice (6 months, n = 22). The variance of ABR thresholds within age groups were found to be comparable, for example, at 8 and 16 kHz, mean SD of ABR threshold were estimated at 18.7 dB (n = 14, Benkafadar et al., 2019) compared with 19.8 dB (n = 22) in the present study. While further comparisons in the literature were limited due to the few studies describing age-related auditory function in the SAMP8 mice (Marie et al., 2017), previous and current data underline the functional variability in the SAMP8 strain, which needs to be taken into account in the experimental design, for example, for investigating age-related changes in auditory function or for evaluating therapeutic measures in long-term studies.

The overall progression of threshold loss over age in SAMP8 mice is comparable to other mouse models, but occurs within a shorter time scale (Fetoni et al., 2011). One of the most commonly used models is the C57BL/6J mouse, which presents a progressive high-frequency hearing loss from as early as 2 months of age (Li and Borg, 1991; Zheng et al., 1999) accompanied by broad degeneration of cochlear structures (Ison et al., 2007). While C57BL/6J mice already demonstrate a significant hearing loss in high frequencies (>20 kHz) starting at 2 months of age, low frequencies (≤8 kHz) first start to palpably deteriorate at 6 months of age with significant increase at 9–10 months of age (Li and Borg, 1991). Even though the audiometric progression in C57BL/6J mice also mimics the typical situation in human ARHL, this is observed over a course of 10 months or longer. By contrast, the SAMP8 strain exhibits a more rapidly progressing, significant hearing loss for a wide range of frequencies over the course of 6 months (see **Figure 2**). With regards to cytologic changes, an age-dependent progressive loss of both IHCs and OHCs was observed between 3 and 7 months of age in C57BL/6J, while loss

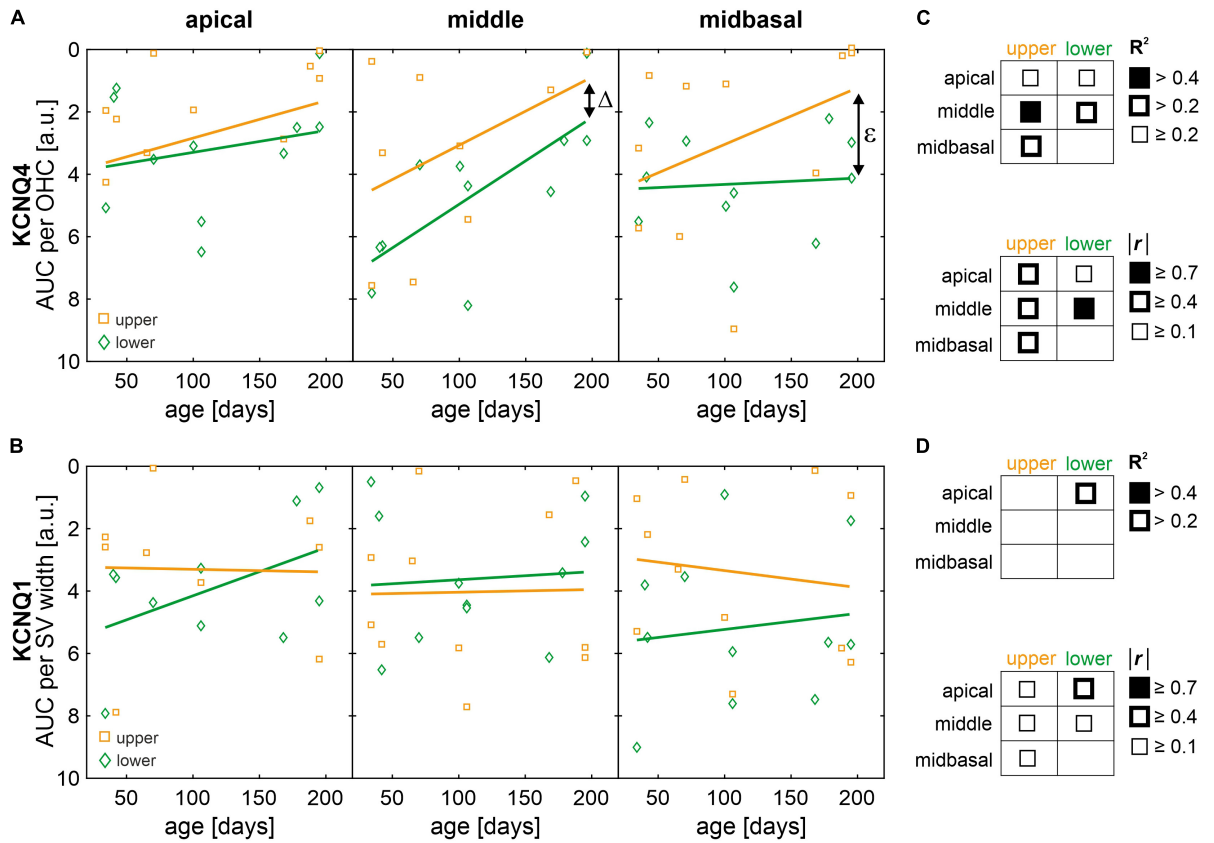

FIGURE 9 | Scatterplots of normalized areas under the curve (AUC) of KCNQ4 and KCNQ1 immunofluorescence as a function of age with regression and correlation analysis. **(A)** AUC of KCNQ4 immunofluorescence per outer hair cell (OHC) over age for mice in the lower (green diamonds) and upper (orange squares) quartiles, for the apical, middle, and midbasal turns, respectively. Fitted linear regression models (solid lines) are shown for mice in the lower (green) and upper (orange) quartiles, respectively. Δ indicates the difference of intercepts between models for mice in the lower and upper quartiles and ε indicates the increase in difference over age between the lower and upper quartiles. **(B)** AUC of KCNQ1 immunofluorescence per stria vascularis (SV) width over age for mice in the lower (green diamonds) and upper (orange squares) quartiles, for the apical, middle, and midbasal turns, respectively. Fitted linear regression models (solid lines) are shown for mice in the lower (green) and upper (orange) quartiles, respectively. **(C,D)** Graphical representations of the coefficient of determination (R^2, upper tables) ranges of the linear regression models and the modulus correlation coefficients (Pearson's *r*, lower tables) for KCNQ4 **(C)** and KCNQ1 **(D)**. Note that none of the correlation coefficients was significantly different from zero.

of spiral ganglion neurons (SGNs) was evident by 7 months of age (Hequembourg and Liberman, 2001). By comparison, loss of sensory hair cells in SAMP8 can be observed at 1 month of age and degeneration of SGNs occurs already by 3 months of age (Menardo et al., 2012). Furthermore, the underlying cause behind the early onset of ARHL in C57BL/6J has been pinpointed to a mutation in the cadherin 23 gene (*Cdh23*), which encodes a cell component of the hair cell tip link (Noben-Trauth et al., 2003; Keithley et al., 2004). Given that ARHL is presumably influenced by multiple factors, with growing evidence pointing to oxidative stress as one of the main risk factors (Someya and Prolla, 2010; Menardo et al., 2012; Han and Someya, 2013; Benkafadar et al., 2019), the SAMP8 strain may prove to be a more appropriate and less time-consuming model of ARHL for several study questions.

The normal aging CBA/J mouse strain carries an *Ahl* resistant allele and does not develop premature hearing loss. Until the age of 1 year, this animal model presents almost no change in auditory thresholds (Zheng et al., 1999; Frisina and Zhu, 2010; Ohlemiller et al., 2010). The hearing sensitivity starts to decline in the high frequency region at the age of 19 months with a parallel loss of OHCs in the apical half of the cochlea (Ohlemiller et al., 2010), which is comparable to human cochlear aging (Wu et al., 2020). Despite the longer time scale of hearing loss progression in the normal aging CBA/J mouse strain, the variance of ABR thresholds has been shown to noticeably increase with age for low and high frequencies in the range 3–48 kHz (Frisina and Zhu, 2010), which is consistent with our observations in the SAMP8 strain over a shorter time scale.

In summary, compared with the C57BL/6J or the CBA/J strain, an accelerated senescence process, shorter lifespan, earlier onset and more rapid progression of age-related pathological phenotypes arguably make the SAMP8 mouse a useful animal model to study ARHL pathophysiology in a time frame that is permissive to animal experimentation. The large variability observed in auditory function needs to be taken into account in

the experimental design and analysis. In future studies, predictive biomarkers should be investigated in order to allow better control and criteria selection of experimental SAMP8 groups.

Auditory Threshold Increase Due to OHC or IHC Loss Over Age

Auditory thresholds are known to provide a sensitive measure of OHC function given their essential role in the lower dynamic range of the cochlear amplifier (Liberman and Kiang, 1978; Liberman and Beil, 1979; Dallos, 2008). The loss of the cochlear amplification has been shown to result in a CAP threshold shift of up to 30–40 dB in rats exposed to the ototoxic agent styrene (Chen et al., 2008), whose primary target are the OHCs. Their results further suggested that the resulting permanent threshold shift increases by approximately 6 dB per 10% OHC loss (Chen et al., 2008). In the present study, mean cytocochleograms showed an OHC loss first observed in young adult mice starting in the middle region and progressing toward the basal region (see **Figure 5**). With advancing age, a further increased OHC loss up to 40% could be observed. Our results showed an increase of the threshold shift in the high-frequency range by approximately 7.5 dB per 10% OHC loss, which generally corresponds to the observation of Chen et al. (2008). Although these results confirm OHC loss as one predictor of ABR threshold increase over age in SAMP8 mice, the observed threshold variability could not be explained by OHC loss alone, since OHC loss was comparable between mice allocated to the lower and upper quartiles (see **Figure 6B**) despite the persisting ABR threshold difference between these groups (see **Figure 6A**).

Human ARHL is best predicted by the loss of OHCs and IHCs, strongly suggesting sensory presbycusis as the predominant type of ARHL in humans (Wu et al., 2020). While the observed OHC loss in the SAMP8 mouse appears to be one predictor for age-related ABR threshold increase, this could not be confirmed for IHC loss. Despite the ABR threshold difference between the lower and upper quartiles in the experimental cohort, the loss of IHCs remained rather negligible for all age groups (see **Figure 6B**). A recent report showed that the selective loss of 70% of IHCs in a chinchilla model did not significantly change ABR thresholds (Jock et al., 1996; El-Badry and McFadden, 2009). Furthermore, in chinchillas, the selective IHC damage reduced the amplitude of CAP but the thresholds obtained from the higher brain regions, e.g., the inferior colliculus attributed to generating the ABR wave IV (Melcher and Kiang, 1996), remained unaffected (El-Badry and McFadden, 2007). The treatment with carboplatin, an ototoxic drug that selectively damages the IHC along the entire cochlea length in chinchillas, presented a negligible increase in threshold shift until the IHC loss exceeded 80% (Lobarinas et al., 2013). These studies indicate that ABR threshold shifts may not be influenced by the loss of IHC. In the past decade, multiple studies have suggested that afferent synapses may be the most vulnerable structures demonstrating a degeneration of synaptic connections prior to IHC loss (Stamataki et al., 2006; Sergeyenko et al., 2013; Wu et al., 2019). This preceding degeneration of synapses, known as "hidden hearing loss," has been suggested to affect the ability to understand speech in noise (Badri et al., 2011; Vermiglio et al., 2012). The effect of afferent fiber loss on ABR thresholds has been previously shown to be negligible, e.g., in mice and guinea pigs no changes could be observed in ABR thresholds despite a significant loss of approximately 50% of afferent fibers (Kujawa and Liberman, 2009; Lin et al., 2011b).

In the SAMP8 model of ARHL, OHC loss has been previously shown to predominate age-related sensory degeneration (Menardo et al., 2012), which was confirmed in the present study as a secondary histopathological predictor for ABR thresholds. By contrast, IHC loss was not observed at least up to 7 months of age, while further progression of age can also lead to a delayed but progressive loss of IHCs (Menardo et al., 2012), which is similar to the human situation (Wu et al., 2020).

Altered KCNQ4 and KCNQ1 Expressions as Potential Predictors of Hearing Loss

The premature SAMP8 senescence causing early presbycusis was linked to altered levels of antioxidant enzymes and decreased activity of complexes I, II, and IV, which in turn lead to chronic inflammation and triggering of apoptotic cell death pathways (Menardo et al., 2012). Before the premature onset of hearing loss, SAMP8 cochleae already displayed an early increase in ROS levels and downregulation of antioxidant enzymes (Menardo et al., 2012; Benkafadar et al., 2019). The levels of prooxidant molecules increased concomitantly with the degradation of hearing in SAMP8, while the deficit in antioxidants remained relatively stable until 6 months of age (Benkafadar et al., 2019). Given that an age-related progression of OHC loss was observed in the SAMP8 mice, we hypothesized that the threshold variability in SAMP8 mice might be due to a different progression of OHC loss in this subgroup thus creating this observed bifurcation of SAMP8 mice with ABR thresholds allocated to the lower or upper quartiles in each age group. Surprisingly, we could not observe differences in OHC loss between the two SAMP8 subgroups (see **Figure 6B**). Although our results indicated OHC loss as one predictor for ABR threshold increase over age, it does not appear to explain the variability of threshold progression between these subgroups.

The survival of OHCs is dependent on the hair cell conductance current which is carried by K^+ (Spicer and Schulte, 1991, 1996; Schulte and Steel, 1994). This current drives the electromotility of OHCs (Ashmore and Gale, 2004) with KCNQ4 maintaining the OHC receptor potential (Kubisch et al., 1999a,b; Beisel et al., 2000; Kharkovets et al., 2000; Nouvian et al., 2003; Oliver et al., 2003; Holt et al., 2007). The ultrafast electromechanical gating of KCNQ4 in murine cochlear OHCs have been shown to develop with hearing as channel density in the basal pole of OHCs (Perez-Flores et al., 2020), while impaired membrane expression of KCNQ4 lead to progressive hearing loss (Jentsch, 2000a,b; Kharkovets et al., 2006; Gao et al., 2013; Carignano et al., 2019). In particular, the loss of KCNQ4 in the membrane of OHCs has been linked to a chronic depolarization, possibly increasing Ca^{2+} influx and causing the subsequent degeneration of OHCs due to chronic cellular stress (Ruttiger et al., 2004). Carignano et al. (2019) showed in a KCNQ4 knock-out (KO) mouse that

the number of OHCs slowly decreased at a young age with increasing cell loss up to complete degeneration at oldest ages. Based on these previous observations, we hypothesized that diminished levels of KCNQ4 expression in OHCs could be an underlying cause of the observed ABR threshold variability in SAMP8 mice. KCNQ4 membrane expression averaged over three cochlear turns appeared to be reduced in mice with ABR thresholds allocated to the upper quartile (see **Figure 8A**). The persistent and increasing differences found between the lower and upper quartiles in KCNQ4 expression over age in the middle and midbasal turns, respectively (see **Figure 9A**), was further found to be congruent with the persistent ABR threshold difference observed over age between these groups, with larger differences in the high-frequency range (see **Figure 6A**).

Another essential component for maintaining auditory function is the recycling of K^+ from OHCs to the endolymph. To facilitate the electromotility of OHCs, a high K^+ concentration in the endolymph has to be maintained (Nin et al., 2016). One major component of the K^+ recycling circuit is the voltage-dependent K^+ channel KCNQ1, which is located in the marginal cells of the SV. KCNQ1 is responsible for the secretion of K^+ to the endolymph and thereby generating and maintaining the EP (Wangemann et al., 1995; Wangemann, 2006). Loss-of-function mutations have been shown to impair K^+ secretion into the endolymph leading to a defect in endolymph production accompanied by a collapse of Reissner's membrane (Casimiro et al., 2001). Another study could observe a decrease in KCNQ1 causing SV atrophy in aged C57BL6/J with notable hearing loss (Yang et al., 2013). We thus hypothesized that diminished levels of KCNQ1 expression in the SV could be another underlying cause of the observed ABR threshold variability in SAMP8 mice. While mice allocated to either quartile generally did not show a correlation between KCNQ1 expression and age, a persistent difference over age may be interpreted between the lower and upper quartiles in the midbasal turn (see **Figure 9B**).

KCNQ4 and KCNQ1 as K^+ channels generally possess high energy requirements for continuous recycling processes to enable a proper membrane expression, suggesting them as one of the primary targets of ROS accumulations (Peixoto Pinheiro et al., 2020). Furthermore, ROS-mediated modification of K^+ channels can induce alterations of the activity of signaling mechanisms causing changes in channel activity or channel gene expression (Ruppersberg et al., 1991; Matalon et al., 2003; Cai and Sesti, 2009). As mentioned above, the premature senescence of SAMP8 mice causing early presbycusis was previously linked to altered levels of antioxidant enzymes and an accumulation of ROS. An impaired membrane expression and a disrupted KCNQ4 conductance causes progressive sensorineural hearing loss (Gao et al., 2013). Furthermore, cells in the SV have been shown to contain large numbers of mitochondria, predisposing them to an increased vulnerability to oxidative stress (Nakazawa et al., 1995; Spicer and Schulte, 2002). Consequently, reduced membrane expressions of KCNQ4 and KCNQ1 caused by ROS accumulation are suggested as potential predictors of the observed ABR threshold variability in SAMP8 mice, feasibly preceding OHC loss over age.

Other Potential Phenotypic Predictors of Hearing Loss

Although OHC and IHC loss have been demonstrated as the most important histologic predictors of human ARHL in both high- and low-frequency regions, there remain age-related effects that have not been identified in the cytohistological analysis of the human cochlea (Wu et al., 2020). These uncaptured effects may be found in the phenotype of surviving sensory hair cells or other functionally relevant structures such as the SV. As the loss of sensory hair cells and reduction in hearing function was not influenced by a single cause, we cannot exclude other cellular or phenotypic predictors that could have an effect on the progression of the ABR threshold variability in SAMP8 mice (Wangemann et al., 1995; Vetter et al., 1996).

The degeneration of SGNs can be observed both in humans and animal models of ARHL (Keithley and Feldmann, 1979; Makary et al., 2011; Viana et al., 2015). Previous studies have shown that the neuronal loss precedes the degeneration of IHCs (Viana et al., 2015; Wu et al., 2019). However, the loss of neurons did not lead to elevated ABR thresholds (Schuknecht and Woellner, 1955; Kujawa and Liberman, 2009). While Menardo et al. (2012) have observed an SGN loss of about 20% by 6 months of age in SAMP8 mice (here we describe mice up to 7 months of age), it was previously reported that even a significant loss of 50% SGN did not affect ABR thresholds in mice and guinea pigs (Kujawa and Liberman, 2009; Lin et al., 2011b). Therefore, loss of SGNs appears to play a minor role in the prediction of threshold elevation, but very likely contributes to significant decrease in speech discrimination, especially in noisy environments (Schuknecht and Woellner, 1955; Kujawa and Liberman, 2009; Wu et al., 2019).

Another potential predictor is the OHC motor protein prestin. Liberman et al. (2002) observed an increase of ABR thresholds in prestin KO animals compared with wild type. In addition, the absence of OHC electromotility due to prestin KO resulted in a loss of cochlear sensitivity of approximately 40–60 dB (Liberman et al., 2002). In the F344 rat, a disruption of prestin has been reported in aged OHCs and it was thus suggested that ROS accumulation during aging may affect prestin through protein oxidation (Chen et al., 2009; Syka, 2010). However, it remains unclear to which degree the disruption of prestin relates to OHC somatic electromotility and motor function sensitivity (Cheatham et al., 2005).

CONCLUSION

The present study supported our initial hypothesis that the large variability of threshold loss over time could be explained by a bifurcation into two subgroups, where these SAMP8 mice constituted the lower and upper quartiles of the threshold distribution, respectively. Surprisingly, the progression of threshold variability could not be linked to a parallel ongoing loss of OHCs. By contrast, OHC loss appeared to be preceded by an altered phenotype of OHCs linked to KCNQ4 membrane

expression and possibly an altered phenotype of the SV linked to KCNQ1, which appeared to be decreased in mice with ABR thresholds allocated to the upper quartile with higher ABR thresholds when compared to age-matched mice in the lower quartile. We suggest that the integrity of KCNQ4 and KCNQ1 channels has to be considered as a possibly decisive step for elevated hearing loss in SAMP8 mice that precedes OHC loss. The observed phenotypic change may underlie age-related effects of ARHL in SAMP8 mice preceding irreversible OHC loss due to accumulated metabolic challenges with age. Considering this, increase of antioxidant activity, decrease of ROS production, or pharmaceutical targeting of K^+ channels could be promising approaches to decelerate or prevent ARHL before the inevitable progression of hair cell loss.

DATA AVAILABILITY STATEMENT

The raw data supporting the conclusions of this article will be made available by the authors, without undue reservation, to any qualified researcher.

ETHICS STATEMENT

The animal study was reviewed and approved by the veterinary care unit of the University of Tübingen and by the regional Animal Care and Ethics Committee (Regierungspräsidium Tübingen).

AUTHOR CONTRIBUTIONS

BP, YA, MK, and HL contributed to conceptualization and writing. BP and YA conducted the experiments and performed statistical analysis. YA, MK, MM, and HL contributed to supervision and interpretation of data. All authors contributed to revision, editing and approved the final version of the manuscript.

FUNDING

BP was supported by a scholarship for the promotion of young scientists from the Episcopal Foundation "Cusanuswerk" (Bonn, Germany).

ACKNOWLEDGMENTS

We would like to thank Karina Gültig, Andrea Müller, and Karin Rohbock for their excellent technical assistance. This publication is dedicated to the memory of our dear colleague, mentor, and friend MM, who suddenly passed away during the course of the project.

SUPPLEMENTARY MATERIAL

The Supplementary Material for this article can be found online at: https://www.frontiersin.org/articles/10.3389/fnagi.2021.708190/full#supplementary-material

REFERENCES

Akiguchi, I., Pallàs, M., Budka, H., Akiyama, H., Ueno, M., Han, J., et al. (2017). SAMP8 mice as a neuropathological model of accelerated brain aging and dementia: toshio takeda's legacy and future directions. *Neuropathology* 37, 293–305. doi: 10.1111/neup.12373

Ashmore, J., and Gale, J. (2004). The cochlear amplifier. *Curr. Biol.* 14, 403–404. doi: 10.1016/j.cub.2004.05.025

Badri, R., Siegel, J. H., and Wright, B. A. (2011). Auditory filter shapes and high-frequency hearing in adults who have impaired speech in noise performance despite clinically normal audiograms. *J. Acoust. Soc. Am.* 129, 852–863. doi: 10.1121/1.3523476

Baker, K., and Staecker, H. (2012). Low dose oxidative stress induces mitochondrial damage in hair cells. *Anat. Rec. (Hoboken)* 295, 1868–1876. doi: 10.1002/ar.22594

Balaban, R. S., Nemoto, S., and Finkel, T. (2005). Mitochondria, oxidants, and aging. *Cell* 120, 483–495. doi: 10.1016/j.cell.2005.02.001

Barhanin, J., Lesage, F., Guillemare, E., Fink, M., Lazdunski, M., and Romey, G. (1996). KvLQTl and lsK (minK) proteins associate to form the IKs cardiac potassium current. *Nature* 384, 78–80.

Beckman, K. B., and Ames, B. N. (1998). The free radical theory of aging matures. *Physiol. Rev.* 78, 547–581. doi: 10.1152/physrev.1998.78.2.547

Beisel, K. W., Nelson, N. C., Delimont, D. C., and Fritzsch, B. (2000). Longitudinal gradients of KCNQ4 expression in spiral ganglion and cochlear hair cells correlate with progressive hearing loss in DFNA2. *Brain Res. Mol. Brain Res.* 82, 137–149.

Benkafadar, N., Francois, F., Affortit, C., Casas, F., Ceccato, J. C., Menardo, J., et al. (2019). ROS-induced activation of DNA damage responses drives senescence-like state in postmitotic cochlear cells: implication for hearing preservation. *Mol. Neurobiol.* 56, 5950–5969. doi: 10.1007/s12035-019-1493-6

Bowl, M. R., and Dawson, S. J. (2019). Age-related hearing loss. *Cold Spring Harb Perspect. Med.* 9:a033217. doi: 10.1101/cshperspect.a033217

Bredberg, G. (1968). Cellular pattern and nerve supply of the human organ of Corti. *Acta Otolaryngol.* 236 (Suppl.), 1–135.

Cai, S. Q., and Sesti, F. (2009). Oxidation of a potassium channel causes progressive sensory function loss during aging. *Nat. Neurosci.* 12, 611–617. doi: 10.1038/nn.2291

Carignano, C., Barila, E. P., Rias, E. I., Dionisio, L., Aztiria, E., and Spitzmaul, G. (2019). Inner hair cell and neuron degeneration contribute to hearing loss in a DFNA2-like mouse model. *Neuroscience* 410, 202–216. doi: 10.1016/j.neuroscience.2019.05.012

Casimiro, M. C., Knollmann, B. C., Ebert, S. N., Vary, J. C. Jr., Greene, A. E., Franz, M. R., et al. (2001). Targeted disruption of the Kcnq1 gene produces a mouse model of Jervell and Lange-Nielsen Syndrome. *Proc. Natl. Acad. Sci. U.S.A.* 98, 2526–2531. doi: 10.1073/pnas.041398998

Cheatham, M. A., Zheng, J., Huynh, K. H., Du, G. G., Gao, J., Zuo, J., et al. (2005). Cochlear function in mice with only one copy of the prestin gene. *J. Physiol.* 569(Pt. 1), 229–241. doi: 10.1113/jphysiol.2005.093518

Chen, G. D., Li, M., Tanaka, C., Bielefeld, E. C., Hu, B. H., Kermany, M. H., et al. (2009). Aging outer hair cells (OHCs) in the fischer 344 rat cochlea: function and morphology. *Hear. Res.* 248, 39–47. doi: 10.1016/j.heares.2008.11.010

Chen, G. D., Tanaka, C., and Henderson, D. (2008). Relation between outer hair cell loss and hearing loss in rats exposed to styrene. *Hear. Res.* 243, 28–34. doi: 10.1016/j.heares.2008.05.008

Dallos, P. (2008). Cochlear amplification, outer hair cells and prestin. *Curr. Opin. Neurobiol.* 18, 370–376. doi: 10.1016/j.conb.2008.08.016

El-Badry, M. M., and McFadden, S. L. (2007). Electrophysiological correlates of progressive sensorineural pathology in carboplatin-treated chinchillas. *Brain Res.* 1134, 122–130.

El-Badry, M. M., and McFadden, S. L. (2009). Evaluation of inner hair cell and nerve fiber loss as sufficient pathologies underlying auditory neuropathy. *Hear. Res.* 255, 84–90. doi: 10.1016/j.heares.2009.06.003

Engström, H., Ades, H. W., and Andersson, A. (1966). *Structural Pattern of the Organ of Corti: A Systematic Mapping of Sensory Cells and Neural Elements*. Stockholm: Almqvist & Wiksell.

Fetoni, A. R., Picciotti, P. M., Paludetti, G., and Troiani, D. (2011). Pathogenesis of presbycusis in animal models: a review. *Exp. Gerontol.* 46, 413–425. doi: 10.1016/j.exger.2010.12.003

Fetoni, A. R., Ralli, M., Sergi, B., Parilla, C., Troiani, D., and Paludetti, G. (2009). Protective effects of N-acetylcysteine on noise-induced hearing loss in guinea pigs. *Acta Otorhinolaryngol. Ital.* 29, 70–75.

Folch, J., Busquets, O., Ettcheto, M., Sanchez-Lopez, E., Pallas, M., Beas-Zarate, C., et al. (2018). Experimental models for aging and their potential for novel drug discovery. *Curr. Neuropharmacol.* 16, 1466–1483. doi: 10.2174/1570159X15666170707155345

Frisina, D. R. (2001). Subcortical neural coding mechanisms for auditory temporal processing. *Hear. Res.* 158, 1–27. doi: 10.1016/s0378-5955(01)00296-9

Frisina, D. R., and Frisina, R. D. (1997). Speech recognition in noise and presbycusis: relations to possible neural mechanisms. *Hear. Res.* 106, 95–104. doi: 10.1016/s0378-5955(97)00006-3

Frisina, R. D., and Zhu, X. (2010). Auditory sensitivity and the outer hair cell system in the CBA mouse model of age-related hearing loss. *Open Access. Anim. Physiol.* 2, 9–16. doi: 10.2147/OAAP.S7202

Fuchs, P. A., and Murrow, B. W. (1992). Cholinergic inhibition of short (outer) hair cells of the chick's cochlea. *J. Neurosci.* 12, 800–809. doi: 10.1523/JNEUROSCI.12-03-00800.1992

Fujimoto, C., and Yamasoba, T. (2014). Oxidative stresses and mitochondrial dysfunction in age-related hearing loss. *Oxid. Med. Cell. Longev.* 2014:582849. doi: 10.1155/2014/582849

Fujimoto, C., and Yamasoba, T. (2019). Mitochondria-targeted antioxidants for treatment of hearing loss: a systematic review. *Antioxidants (Basel)* 8:109. doi: 10.3390/antiox8040109

Gao, Y., Yechikov, S., Vazquez, A. E., Chen, D., and Nie, L. (2013). Impaired surface expression and conductance of the KCNQ4 channel lead to sensorineural hearing loss. *J. Cell. Mol. Med.* 17, 889–900. doi: 10.1111/jcmm.12080

Gates, G. A., and Mills, J. H. (2005). Presbycusis. *Lancet* 366, 1111–1120. doi: 10.1016/s0140-6736(05)67423-5

GBD Hearing Loss Collaborators (2021). Hearing loss prevalence and years lived with disability, 1990-2019: findings from the global burden of disease study 2019. *Lancet* 397, 996–1009. doi: 10.1016/S0140-6736(21)00516-X

Goman, A. M., and Lin, F. R. (2018). Hearing loss in older adultsfrom epidemiological insights to national initiatives. *Hear. Res.* 369, 29–32. doi: 10.1016/j.heares.2018.03.031

Gordon-Salant, S. (2005). Hearing loss and aging: new research findings and clinical implications. *J. Rehabil. Res. Dev.* 42(Suppl. 2), 9–24. doi: 10.1682/jrrd.2005.01.0006

Goycoolea, M. V., Goycoolea, H. G., Farfan, C. R., Rodriguez, L. G., Martinez, G. C., and Vidal, R. (1986). Effect of life in industrialized societies on hearing in natives of Easter Island. *Laryngoscope* 96, 1391–1396. doi: 10.1288/00005537-198612000-00015

Grinan-Ferre, C., Corpas, R., Puigoriol-Illamola, D., Palomera-Avalos, V., Sanfeliu, C., and Pallas, M. (2018). Understanding epigenetics in the neurodegeneration of Alzheimer's disease: SAMP8 mouse model. *J. Alzheimers Dis.* 62, 943–963. doi: 10.3233/JAD-170664

Halliwell, B. (1992). Reactive oxygen species and the central nervous system. *J. Neurochem.* 49, 1609–1623.

Hamernik, R. P., Qiu, W., and Davis, B. (2008). The effectiveness of N-acetyl-L-cysteine (L-NAC) in the prevention of severe noise-induced hearing loss. *Hear. Res.* 239, 99–106. doi: 10.1016/j.heares.2008.02.001

Han, C., and Someya, S. (2013). Mouse models of age-related mitochondrial neurosensory hearing loss. *Mol. Cell. Neurosci.* 55, 95–100. doi: 10.1016/j.mcn.2012.07.004

Harman, D. (1956). Aging: a theory based on free radical and radiation chemistry. *J. Gerontol.* 11, 298–300.

Henderson, D., Bielefeld, E. C., Harris, K. C., and Hu, B. H. (2006). The role of oxidative stress in noise-induced hearing loss. *Ear. Hear.* 27, 1–19. doi: 10.1097/01.aud.0000191942.36672.f3

Hequembourg, S., and Liberman, M. C. (2001). Spiral ligament pathology: a major aspect of age-related cochlear degeneration in C57BL/6 mice. *J. Assoc. Res. Otolaryngol.* 2, 118–129. doi: 10.1007/s101620010075

Hilke, H., and Plester, D. (1955). Forschungsreise in das land der präniloten im südost-sudan 1954/55. *Zeitschrift für Ethnol.* 80, 178–186.

Holt, J. R., Stauffer, E. A., Abraham, D., and Geleoc, G. S. (2007). Dominant-negative inhibition of M-like potassium conductances in hair cells of the mouse inner ear. *J. Neurosci.* 27, 8940–8951. doi: 10.1523/JNEUROSCI.2085-07.2007

Housley, G. D., and Ashmore, J. F. (1992). Ionic currents of outer hair cells isolated from the guinea-pig cochlea. *J. Physiol.* 448, 73–98.

Ison, J. R., Allen, P. D., and O'Neill, W. E. (2007). Age-related hearing loss in C57BL/6J mice has both frequency-specific and non-frequency-specific components that produce a hyperacusis-like exaggeration of the acoustic startle reflex. *J. Assoc. Res. Otolaryngol.* 8, 539–550. doi: 10.1007/s10162-007-0098-3

Jentsch, T. J. (2000a). Neuronal KCNQ potassium channelsphysiology and role in disease. *Nat. Neurosci.* 1, 21–30. doi: 10.1038/35036198

Jentsch, T. J. (2000b). Neuronal KCNQ potassium channelsphysiology and role in disease. *Nat. Neurosci.* 1, 21–30.

Jock, B. M., Hamernik, R. P., Aldrich, L. G., Ahroon, W. A., Petriello, K.-L., and Johnson, A. R. (1996). Evoked-potential thresholds and cubic distortion product otoacoustic emissionsin the chinchilla following carboplatin treatment and noise exposure. *Hear. Res.* 96, 179–190.

Kamil, R. J., Betz, J., Powers, B. B., Pratt, S., Kritchevsky, S., Ayonayon, H. N., et al. (2016). Association of hearing impairment with incident frailty and falls in older adults. *J. Aging Health* 28, 644–660. doi: 10.1177/0898264315608730

Karuppagounder, V., Arumugam, S., Babu, S. S., Palaniyandi, S. S., Watanabe, K., Cooke, J. P., et al. (2017). The senescence accelerated mouse prone 8 (SAMP8): a novel murine model for cardiac aging. *Ageing Res. Rev.* 35, 291–296. doi: 10.1016/j.arr.2016.10.006

Keithley, E. M., Canto, C., Zheng, Q. Y., Fischel-Ghodsian, N., and Johnson, K. R. (2004). Age-related hearing loss and the ahl locus in mice. *Hear. Res.* 188, 21–28. doi: 10.1016/s0378-5955(03)00365-4

Keithley, E. M., and Feldmann, M. (1979). Spiral ganglion cell counts in an age-graded series of rat cochleas. *J. Comput. Neurosci.* 188, 429–442.

Kharkovets, T., Dedek, K., Maier, H., Schweizer, M., Khimich, D., Nouvian, R., et al. (2006). Mice with altered KCNQ4 K+ channels implicate sensory outer hair cells in human progressive deafness. *EMBO J.* 25, 642–652. doi: 10.1038/

Kharkovets, T., Hardelin, J.-P., Safieddine, S., Schweizer, M., El-Amraoui, A., Petit, C., et al. (2000). KCNQ4, a K+ channel mutated in a form of dominant deafness, is expressed in the inner ear and the central auditory pathway. *PNAS* 97, 4333–4338.

Kros, C. J., Ruppersberg, J. P., and Rüsch, A. (1998). Expression of a potassium current in inner hair cells during development of hearing in mice. *Nature* 394, 291–294. doi: 10.1038/28401

Kubisch, C., Schroeder, B. C., El-Amraoui, A., Marlin, S., Petit, C., and Jentsch, T. J. (1999a). KCNQ4, a novel potassium channel expressed in sensory outer hair cells, is mutated in dominant deafness. *Cell Press* 96, 437–446. doi: 10.1016/S0092-8674(00)80556-5

Kubisch, C., Schroeder, B. C., El-Amraoui, A., Marlin, S., Petit, C., and Jentsch, T. J. (1999b). KCNQ4, a novel potassium channel expressed in sensory outer hair cells, is mutated in dominant deafness. *Cell Press* 96, 437–446.

Kujawa, S. G., and Liberman, M. C. (2009). Adding insult to injury: cochlear nerve degeneration after "temporary" noise-induced hearing loss. *J. Neurosci.* 29, 14077–14085. doi: 10.1523/JNEUROSCI.2845-09.2009

Li, H.-S., and Borg, E. (1991). Age-related loss of auditory sensitivity in two mouse genotypes. *Acta Oto Laryngol.* 111, 827–834. doi: 10.3109/00016489109138418

Liberman, M. C., and Beil, D. G. (1979). Hair cell condition and auditory nerve response in normal and noise-damaged cochleas. *Acta Otolaryngol.* 88, 161–176. doi: 10.3109/00016487909137156

Liberman, M. C., Gao, J., He, D. Z., Wu, X., Jia, S., and Zuo, J. (2002). Prestin is required for electromotility of the outer hair cell and for the cochlear amplifier. *Nature* 419, 300–304. doi: 10.1038/nature01059

Liberman, M. C., and Kiang, N. Y. (1978). Acoustic trauma in cats. cochlear pathology and auditory-nerve activity. *Acta Otolaryngol.* 358, 1–63.

Lin, F. R., Ferrucci, L., Metter, E. J., An, Y., Zonderman, A. B., and Resnick, S. M. (2011a). Hearing loss and cognition in the baltimore longitudinal study of aging. *Neuropsychology* 25, 763–770. doi: 10.1037/a0024238

Lin, F. R., Yaffe, K., Xia, J., Xue, Q. L., Harris, T. B., Purchase-Helzner, E., et al. (2013). Hearing loss and cognitive decline in older adults. *JAMA Intern. Med.* 173, 293–299. doi: 10.1001/jamainternmed.2013.1868

Lin, H. W., Furman, A. C., Kujawa, S. G., and Liberman, M. C. (2011b). Primary neural degeneration in the Guinea pig cochlea after reversible noise-induced threshold shift. *J. Assoc. Res. Otolaryngol.* 12, 605–616. doi: 10.1007/s10162-011-0277-0

Lin, M. T., and Beal, M. F. (2006). Mitochondrial dysfunction and oxidative stress in neurodegenerative diseases. *Nature* 443, 787–795. doi: 10.1038/nature05292

Lobarinas, E., Salvi, R., and Ding, D. (2013). Insensitivity of the audiogram to carboplatin induced inner hair cell loss in chinchillas. *Hear. Res.* 302, 113–120. doi: 10.1016/j.heares.2013.03.012

Makary, C. A., Shin, J., Kujawa, S. G., Liberman, M. C., and Merchant, S. N. (2011). Age-related primary cochlear neuronal degeneration in human temporal bones. *J. Assoc. Res. Otolaryngol.* 12, 711–717. doi: 10.1007/s10162-011-0283-2

Marie, A., Larroze-Chicot, P., Cosnier-Pucheu, S., and Gonzalez-Gonzalez, S. (2017). Senescence-accelerated mouse prone 8 (SAMP8) as a model of age-related hearing loss. *Neurosci. Lett.* 656, 138–143. doi: 10.1016/j.neulet.2017.07.037

Matalon, S., Hardimann, K. M., Jain, L., Eaton, D. C., Kotlikoff, M., Eu, J. P., et al. (2003). Regulation of ion channel structure and function by reactive oxygen-nitrogen species. *Am. J. Physiol. Lung. Cell Mol. Physiol.* 285, 1184–1189.

Melcher, J. R., and Kiang, N. Y. (1996). Generators of the brainstem auditory evoked potential in cat III: identified cell populations. *Hear. Res.* 93, 52–71. doi: 10.1016/0378-5955(95)00200-6

Menardo, J., Tang, Y., Ladrech, S., Lenoir, M., Casas, F., Michel, C., et al. (2012). Oxidative stress, inflammation, and autophagic stress as the key mechanisms of premature age-related hearing loss in SAMP8 mouse Cochlea. *Antioxid Redox Signal* 16, 263–274. doi: 10.1089/ars.2011.4037

Merchant, S. N., and Nadol, J. B. (2010). *Schuknecht's Pathology of the Ear*, 3rd Edn. Shelton, CT: People's Medical Publishing House-USA.

Müller, M., von Hunerbein, K., Hoidis, S., and Smolders, J. W. (2005). A physiological place-frequency map of the cochlea in the CBA/J mouse. *Hear. Res.* 202, 63–73. doi: 10.1016/j.heares.2004.08.011

Nakazawa, K., Spicer, S. S., and Schulte, B. A. (1995). Ultrastructural localization of Na,K-ATPase in the gerbil cochlea. *J. Histochem. Cytochem.* 43, 981–991. doi: 10.1177/43.10.7560888

Neyroud, N., Tesson, F., Denjoy, I., Leibovici, M., Donger, C., Barhanin, J., et al. (1997). A novel mutation in the potassium channel gene KVLQT1 causes the jervell and lange-nielsen cardioauditory syndrome. *Nat. Genet.* 15, 186–189. doi: 10.1038/ng0297-186

Nin, F., Yoshida, T., Sawamura, S., Ogata, G., Ota, T., Higuchi, T., et al. (2016). The unique electrical properties in an extracellular fluid of the mammalian cochlea; their functional roles, homeostatic processes, and pathological significance. *Pflugers Arch.* 468, 1637–1649. doi: 10.1007/s00424-016-1871-0

Noben-Trauth, K., Zheng, Q. Y., and Johnson, K. R. (2003). Association of cadherin 23 with polygenic inheritance and genetic modification of sensorineural hearing loss. *Nat. Genet.* 35, 21–23. doi: 10.1038/ng1226

Nouvian, R., Ruel, J., Wang, J., Guitton, M. J., Pujol, R., and Puel, J.-L. (2003). Degeneration of sensory outer hair cells following pharmacological blockade of cochlear KCNQ channels in the adult guinea pig. *Eur. J. Neurosci.* 17, 2553–2562. doi: 10.1046/j.1460-9568.2003.02715.x

Ohinata, Y., Miller, J. M., and Schacht, J. (2003). Protection from noise-induced lipid peroxidation and hair cell loss in the cochlea. *Brain Res.* 966, 265–273. doi: 10.1016/s0006-8993(02)04205-1

Ohlemiller, K. K. (2004). Age-related hearing loss: the status of Schuknecht's typology. *Curr. Opin. Otolaryngol. Head Neck Surg.* 12, 439–443.

Ohlemiller, K. K., Dahl, A. R., and Gagnon, P. M. (2010). Divergent aging characteristics in CBA/J and CBA/CaJ mouse cochleae. *J. Assoc. Res. Otolaryngol.* 11, 605–623. doi: 10.1007/s10162-010-0228-1

Oliver, D., Klöcker, N., Baukrowitz, T., Ruppersberg, J. P., and Fakler, B. (2000). Gating of Ca2+-activated K+ channels controls fast inhibitory synaptic transmission at auditory outer hair cells. *Neuron* 26, 595–601. doi: 10.1016/s0896-6273(00)81197-6

Oliver, D., Knipper, M., Derst, C., and Fakler, B. (2003). Resting potential and submembrane calcium concentration of inner hair cells in the isolated mouse cochlea are set by KCNQ-type potassium channels. *J. Neurosci.* 23, 2141–2149.

Peixoto Pinheiro, B., Vona, B., Lowenheim, H., Ruttiger, L., Knipper, M., and Adel, Y. (2020). Age-related hearing loss pertaining to potassium ion channels in the cochlea and auditory pathway. *Pflugers Arch.* 473, 823–840. doi: 10.1007/s00424-020-02496-w

Perez-Flores, M. C., Lee, J. H., Park, S., Zhang, X.-D., Sihn, C.-R., Ledford, H. A., et al. (2020). Cooperativity of Kv7.4 channels confers ultrafast electromechanical sensitivity and emergent properties in cochlear outer hair cells. *Sci. Adv.* 6:eaba1104. doi: 10.1126/sciadv.aba1104

Rosen, S., Bergman, M., Plester, D., El-Mofty, A., and Satti, M. H. (1962). Presbycusis study of a relatively noise-free population in the Sudan. *Ann. Otol. Rhinol. Laryngol.* 71, 727–743. doi: 10.1177/000348946207100313

Rosen, S., Plester, D., El-Mofty, A., and Rosen, H. V. (1964). High frequency audiometry in presbycusis. *Arch Otolaryngol.* 79, 18–32.

Ruppersberg, J. P., Stocker, M., Pongs, O., Heinemann, S. H., Frank, R., and Koenen, M. (1991). Regulation of fast inactivation of cloned mammalian IK(A) channels by cysteine oxidation. *Nature* 352, 711–714. doi: 10.1038/352711a0

Rutherford, B. R., Brewster, K., Golub, J. S., Kim, A. H., and Roose, S. P. (2018). Sensation and psychiatry: linking age-related hearing loss to late-life depression and cognitive decline. *Am. J. Psychiatry* 175, 215–224. doi: 10.1176/appi.ajp.2017.17040423

Ruttiger, L., Sausbier, M., Zimmermann, U., Winter, H., Braig, C., Engel, J., et al. (2004). Deletion of the Ca2+-activated potassium (BK) alpha-subunit but not the BKbeta1-subunit leads to progressive hearing loss. *Proc. Natl. Acad. Sci. U.S.A.* 101, 12922–12927. doi: 10.1073/pnas.0402660101

Sanguinetti, M. C., Curran, M. E., Zou, A., Shen, J., Spector, P. S., Atkinson, D. L., et al. (1996). Coassembly of KvLQT1 and minK (lsK) proteins to form cardiac fKs potassium channel. *Nature* 384, 80–83.

Santos-Sacchi, J. (1993). Voltage-dependent ionic conductances of type I spiral ganglion cells from the guinea pig inner ear. *J. Neurosci.* 13, 3599–3611. doi: 10.1523/JNEUROSCI.13-08-03599.1993

Schuknecht, H. F. (1955). Presbycusis. *Laryngoscope* 65, 402–419.

Schuknecht, H. F. (1964). Further observations on the pathology of presbycusis. *Arch Otolaryngol.* 80, 369–382. doi: 10.1001/archotol.1964.00750040381003

Schuknecht, H. F. (1974). *Pathology of the Ear*. Cambridge: Harvard University Press.

Schuknecht, H. F. (1993). *Pathology of the Ear*. Philadelphia: Lea & Febiger.

Schuknecht, H. F., and Gacek, M. R. (1993). Cochlear pathology in presbycusis. *Ann. Otol. Rhinol. Laryngol.* 102, 1–16.

Schuknecht, H. F., and Woellner, R. C. (1955). An experimental and clinical study of deafness from lesions of the cochlear nerve. *J. Laryngol. Otol.* 69, 75–97. doi: 10.1017/s0022215100050465

Schulte, B. A., and Steel, K. P. (1994). Expression of a! and p subunit isoforms of Na,K-ATPase in the mouse inner ear and changeswith mutations at the WV or Sld loci. *Hear. Res.* 78, 65–76.

Sergeyenko, Y., Lall, K., Liberman, M. C., and Kujawa, S. G. (2013). Age-related cochlear synaptopathy: an early-onset contributor to auditory functional decline. *J. Neurosci.* 33, 13686–13694. doi: 10.1523/JNEUROSCI.1783-13.2013

Serrano, F., and Klann, E. (2004). Reactive oxygen species and synaptic plasticity in the aging hippocampus. *Ageing Res. Rev.* 3, 431–443. doi: 10.1016/j.arr.2004.05.002

Shen, Z., and Marcus, D. C. (1998). Divalent cations inhibit IsK/KvLQT1 channels in excised membrane patches of strial marginal cells. *Hear. Res.* 123, 157–167. doi: 10.1016/s0378-5955(98)00110-5

Someya, S., and Prolla, T. A. (2010). Mitochondrial oxidative damage and apoptosis in age-related hearing loss. *Mech Ageing Dev.* 131, 480–486. doi: 10.1016/j.mad.2010.04.006

Spicer, S. S., and Schulte, B. A. (1991). Differentiation of inner ear fibrocytes according to their ion transport related activity. *Hear. Res.* 56, 53–64.

Spicer, S. S., and Schulte, B. A. (1996). The fine structure of spiral ligament cells relates to ion return to the stria and varies with place-frequency. *Hear. Res.* 100, 80–100.

Spicer, S. S., and Schulte, B. A. (2002). Spiral ligament pathology in quiet-aged gerbils. *Hear. Res.* 172, 172–185. doi: 10.1016/s0378-5955(02)00581-6

Stamataki, S., Francis, H. W., Lehar, M., May, B. J., and Ryugo, D. K. (2006). Synaptic alterations at inner hair cells precede spiral ganglion cell loss in

aging C57BL/6J mice. *Hear. Res.* 221, 104–118. doi: 10.1016/j.heares.2006.07.014

Syka, J. (2010). The fischer 344 rat as a model of presbycusis. *Hear. Res.* 264, 70–78. doi: 10.1016/j.heares.2009.11.003

Takeda, T., Hosokawa, M., Takeshita, S., Irino, M., Higuchi, K., Matsushita, T., et al. (1981). A new murine model of accelerated senescence. *Mech Ageing Dev.* 17, 183–194. doi: 10.1016/0047-6374(81)90084-1

Van Eyken, E., Van Camp, G., and Van Laer, L. (2007). The complexity of age-related hearing impairment: contributing environmental and genetic factors. *Audiol. Neurootol.* 12, 345–358. doi: 10.1159/000106478

Vermiglio, A. J., Soli, S. D., Freed, D. J., and Fisher, L. M. (2012). The relationship between high-frequency pure-tone hearing loss, hearing in noise test (HINT) thresholds, and the articulation index. *J. Am. Acad. Audiol.* 23, 779–788. doi: 10.3766/jaaa.23.10.4

Vetter, D. E., Mann, J. R., Wangemann, P., Liu, J., McLaughlin, K. J., Lesage, F., et al. (1996). Inner ear defects induced by null mutation of the isk gene. *Neuron* 17, 1251–1264. doi: 10.1016/s0896-6273(00)80255-x

Viana, L. M., O'Malley, J. T., Burgess, B. J., Jones, D. D., Oliveira, C. A., Santos, F., et al. (2015). Cochlear neuropathy in human presbycusis: confocal analysis of hidden hearing loss in post-mortem tissue. *Hear. Res.* 327, 78–88. doi: 10.1016/j.heares.2015.04.014

Viberg, A., and Canlon, B. (2004). The guide to plotting a cochleogram. *Hear. Res.* 197, 1–10. doi: 10.1016/j.heares.2004.04.016

Vuckovic, D., Mezzavilla, M., Cocca, M., Morgan, A., Brumat, M., Catamo, E., et al. (2018). Whole-genome sequencing reveals new insights into age-related hearing loss: cumulative effects, pleiotropy and the role of selection. *Eur. J. Hum. Genet.* 26, 1167–1179. doi: 10.1038/s41431-018-0126-2

Wang, S., Lai, X., Deng, Y., and Song, Y. (2020). Correlation between mouse age and human age in anti-tumor research: Significance and method establishment. *Life Sci.* 242:117242. doi: 10.1016/j.lfs.2019.117242

Wang, Y., Hirose, K., and Liberman, M. C. (2002). Dynamics of noise-induced cellular injury and repair in the mouse cochlea. *J. Assoc. Res. Otolaryngol.* 3, 248–268. doi: 10.1007/s101620020028

Wangemann, P. (2002). K+ cycling and the endocochlear potential. *Hear. Res.* 165, 1–9.

Wangemann, P. (2006). Supporting sensory transduction: cochlear fluid homeostasis and the endocochlear potential. *J. Physiol.* 576(Pt. 1), 11–21. doi: 10.1113/jphysiol.2006.112888

Wangemann, P., Liu, J., and Marcus, D. C. (1995). Ion transport mechanisms responsible for K+ secretion and the transepithelial voltage across marginal cells of stria vascularis in vitro. *Hear. Res.* 84, 19–29. doi: 10.1016/0378-5955(95)00009-S

Wu, P. Z., Liberman, L. D., Bennett, K., de Gruttola, V., O'Malley, J. T., and Liberman, M. C. (2019). Primary neural degeneration in the human cochlea: evidence for hidden hearing loss in the aging ear. *Neuroscience* 407, 8–20. doi: 10.1016/j.neuroscience.2018.07.053

Wu, P. Z., O'Malley, J. T., de Gruttola, V., and Liberman, M. C. (2020). Age-related hearing loss is dominated by damage to inner ear sensory cells. Not the Cellular Battery That Powers Them. *J. Neurosci.* 40, 6357–6366. doi: 10.1523/JNEUROSCI.0937-20.2020

Yang, H., Xiong, H., Huang, Q., Pang, J., Zheng, X., Chen, L., et al. (2013). Compromised potassium recycling in the cochlea contributes to conservation of endocochlear potential in a mouse model of age-related hearing loss. *Neurosci. Lett.* 555, 97–101. doi: 10.1016/j.neulet.2013.09.028

Zheng, Q. Y., Johnson, K. R., and Erway, L. C. (1999). Assessment of hearing in 80 inbred strains of mice by ABR threshold analyses. *Hear. Res.* 130, 94–107.

Conflict of Interest: HL is Scientific Founder and a member of the board of directors of Acousia Therapeutics (Tübingen, Germany).

The remaining authors declare that the research was conducted in the absence of any commercial or financial relationships that could be construed as a potential conflict of interest.

Publisher's Note: All claims expressed in this article are solely those of the authors and do not necessarily represent those of their affiliated organizations, or those of the publisher, the editors and the reviewers. Any product that may be evaluated in this article, or claim that may be made by its manufacturer, is not guaranteed or endorsed by the publisher.

CDDpress

www.nature.com/cddis

ARTICLE OPEN

A potassium channel agonist protects hearing function and promotes outer hair cell survival in a mouse model for age-related hearing loss

Barbara Peixoto Pinheiro[1✉], Marcus Müller[1,5], Michael Bös[2,5], Jamil Guezguez[3], Michael Burnet[3], Mara Tornincasa[4], Riccardo Rizzetto[4], Jean-Francois Rolland[4], Chiara Liberati[4], Stefan Lohmer[4], Youssef Adel[1,6] and Hubert Löwenheim[1,6✉]

Age-related hearing loss (ARHL) is the most common sensory impairment mainly caused by degeneration of sensory hair cells in the cochlea with no causal medical treatment available. Auditory function and sensory hair cell survival critically depend on the Kv7.4 (KCNQ4) channel, a voltage-gated potassium channel expressed in outer hair cells (OHCs), with its impaired function or reduced activity previously associated with ARHL. Here, we investigated the effect of a potent small-molecule Kv7.4 agonist on ARHL in the senescence-accelerated mouse prone 8 (SAMP8) model. For the first time in vivo, we show that Kv7.4 activation can significantly reduce age-related threshold shifts of auditory brainstem responses as well as OHC loss in the SAMP8 model. Pharmacological activation of Kv7.4 thus holds great potential as a therapeutic approach for ARHL as well as other hearing impairments related to Kv7.4 function.

Cell Death and Disease (2022)13:595 ; https://doi.org/10.1038/s41419-022-04915-5

INTRODUCTION

According to recent data from the WHO, hearing loss affects 20.3% of the world's population [1–3]. Age-related hearing loss (ARHL), or presbycusis, has emerged as the leading cause of years lived with disability in people over 70 years of age worldwide, compared to all other disease categories [1, 3]. Although this condition is not considered life-threatening, it can significantly degrade the quality of life and is associated with multiple comorbidities, including social isolation, depression, and cognitive decline [3–5]. Hearing loss has also been suggested as a modifiable risk factor for dementia [6, 7]. Taken together, it is evident that the functional, social, and mental impact, the extraordinary prevalence and burden of disease creates an immense medical need for a causal treatment of ARHL.

In humans, ARHL typically presents as a symmetrical decline in hearing ability over age that is more pronounced in the high frequencies [8, 9]. A recent analysis of human temporal bones showed that the degree of ARHL can be best predicted by the loss of outer hair cells (OHCs) and inner hair cells (IHCs), strongly suggesting sensory presbycusis as the predominant type of ARHL [10]. OHCs provide fast electromechanical amplification of sound and require fast repolarization of the receptor potential in order to respond to the large dynamic range and speed of sound [11]. The modulation of potassium ion (K^+) channels and potassium circulation in the cochlea maintains this demanding signal transduction process [12, 13]. Specifically, the potassium voltage-gated channel subfamily q member 4 (K_V7.4 or KCNQ4), which is expressed at the basal pole of OHCs, is involved in K^+ efflux and generation of the predominant K^+ conductance current of OHCs, $I_{K,n}$ [14–16].

Impaired surface expression or reduced activity of the K_V7.4 channel leads to functional impairment and has been associated with age-related [17–21], noise-induced [20, 22–25], ototoxic hearing loss [26], and genetic hearing loss in human hereditary deafness DFNA2 [27–29]. The central role of the K_V7.4 channel for OHC function and survival has been demonstrated by genetic ablation in *Kcnq4*$^{-/-}$ mice and loss-of-function mutations leading to progressive hearing loss and slow degeneration of OHCs [30, 31]. The loss of the K_V7.4 in OHCs can result in chronic depolarization, which can consequently lead to their degeneration due to chronic cellular stress [32]. Notably, pharmacological inhibition of K_V7.4 by linopirdine in an adult guinea pig model has been shown to cause acute hearing loss through compromised function and severe OHC degeneration in the basal turn, which corresponds to the high-frequency range of the cochlea [33]. These various findings lead to the hypothesis that pharmacological activation of K_V7.4 may preserve hearing function and prevent OHC loss in ARHL, and possibly other forms of hearing loss related to compromised K_V7.4 function.

For over a decade, K_V7.4 has been suggested as a drug target for small-molecule activators [20, 26, 34–36]. As a proof of principle, Leitner et al. [36] showed in vitro that synthetic channel openers, such as retigabine (RTG) and zinc pyrithione (ZnP), could potentiate and stabilize the K_V7.4-mediated $I_{K,n}$ conductance in

[1]Translational Hearing Research, Tübingen Hearing Research Center, Department of Otolaryngology, Head & Neck Surgery, University of Tübingen, 72076 Tübingen, Germany. [2]Acousia Therapeutics, 72070 Tübingen, Germany. [3]Synovo, 72076 Tübingen, Germany. [4]Axxam, Bresso, 20091 Milan, Italy. [5]Deceased: Marcus Müller, Michael Bös. [6]These authors contributed equally: Youssef Adel, Hubert Löwenheim. ✉email: barbara.peixoto-pinheiro@uni-tuebingen.de; hubert.loewenheim@uni-tuebingen.de

Edited by Professor Massimiliano Agostini

Received: 7 February 2022 Revised: 29 April 2022 Accepted: 4 May 2022
Published online: 11 July 2022

OHCs with DFNA2-causing mutations in the $K_V7.4$ channel. Moreover, they observed an enhancement of the native $K_V7.4$-mediated $I_{K,n}$ conductance in OHCs [36]. However, the applicability of small-molecule $K_V7.4$ activation as a treatment approach has thus far not been demonstrated in an in vivo model.

In the present study, we investigated the effect of a novel, potent small-molecule $K_V7.4$ agonist ACOU085 [37] on ARHL in the senescence-accelerated mouse prone strain 8 (SAMP8) mouse model [38]. The SAMP8 mouse model shows an early progressive, age-related increase in auditory brainstem response (ABR) thresholds as well as loss of OHCs, predominantly in the high-frequency range [18]. The cochlear exposure of ACOU085 from a formulation administered via transtympanic injection was determined in a pharmacokinetic study by analyzing cochlear tissue and perilymph. In an electrophysiology study, the effect of repeated ACOU085 administrations on ARHL was investigated in a within-subject design, with mice receiving unilateral administrations of ACOU085 and contralateral vehicle as control. The magnitude of hearing loss was determined by measuring ABR threshold shifts and showed reduced age-related functional decline in treated ears when compared with vehicle controls. After termination, morphological analysis of cochlear whole-mounts confirmed a concomitant reduction in OHC loss in the high-frequency range of the cochlea. Thus, pharmacological activation of $K_V7.4$ appears as an attainable therapeutic approach for ARHL and potentially other hearing impairments related to compromised $K_V7.4$ function.

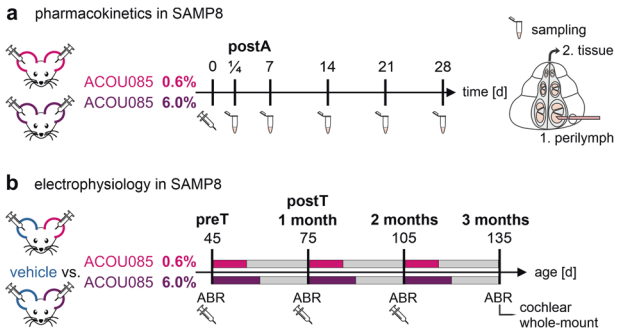

Fig. 1 Schematic representation of the pharmacokinetic and electrophysiology study design. a Schematic representation of the pharmacokinetic study design. Cochlear perilymph and tissue were sampled after a single administration of 0.6% or 6.0% w/v ACOU085 formulation via transtympanic injection into both ears of SAMP8 mice. Samples were collected for the timepoints 0.25, 7, 14, 21, and 28 days post-administration (postA). Concentrations of ACOU085 in cochlear perilymph and tissue were determined by liquid chromatography and mass spectrometry. **b** Schematic representation of the electrophysiology study design. The effect of repeated unilateral administrations via transtympanic injection of ACOU085 versus contralateral vehicle control was investigated in the SAMP8 mouse model for two dose groups, 0.6% or 6.0% w/v ACOU085, in a within-subject design. Auditory function was assessed at 1-month intervals from the age of 45 days (pre-treatment, preT) to 135 days (3-months post-treatment, postT) by determining auditory brainstem response (ABR) thresholds. After termination, mice were sacrificed and their cochleae were extracted for cochlear whole-mount analysis.

METHODS

Animals

Female SAMP8/TaHsd mice were acquired from Envigo (Horst, Netherlands) at an age of 30 days and were housed in groups of up to five animals in a standard macrolon polycarbonate cage under a 12-h light-dark cycle with ad libitum access to food and water. Animal care, treatments, and procedures were performed according to the German (TierSchG) and European Union (directive 2010/63/EU) guidelines for the protection of animals used for experimental purposes, following revision and approval by the veterinary care unit of the University of Tübingen and the regional animal care and ethics committee (Regierungspräsidium Tübingen, approval no. HN3/17).

Drug preparation and administration

ACOU085 (Acousia Therapeutics, Tübingen, Germany) is a novel small-molecule agonist of the $K_V7.4$ (KCNQ4) voltage-gated potassium channel with higher potency than ML-213 in the nanomolar range [37] (see Fig. S1). The compound was provided in an injectable formulation which contained proprietary lipid-based gel formulation. In this study, ACOU085 was administered at 0.6% w/v or 6.0% w/v concentrations, with the formulation alone serving as a vehicle control. The formulations were stored at 4 °C and warmed in a water bath to 40 °C before administration.

Transtympanic injection was accomplished by placing the mice in a lateral decubitus position on a custom-made heating pad. The tympanic membrane (TM) was visualized using a surgical microscope (OPMI-1, Zeiss, Oberkochen, Germany). ACOU085 or vehicle formulations were administered into the middle ear until they emerged back through the needle perforation, indicating that the entire middle ear cavity was filled. The applicability of the formulation varied with ACOU085 concentrations; therefore, the 0.6% w/v concentration or the vehicle alone were administered using a 1-ml syringe (B. Braun SE, Melsungen, Germany) and a 20-µl microloader tip (Eppendorf, Wesseling-Berzdorf, Germany). The 6.0% w/v concentration was administered with a 1-ml syringe and a 22 G needle (Epican Paed caudal, Braun, Melsungen, Hessen). For a given mouse, the injection volume was 5–15 µl per ear depending on individual constraints, e.g., anatomical variations, age, and the number of previous transtympanic injections.

Pharmacokinetics

Experimental design. To determine the drug distribution from the middle ear cavity into the cochlea, perilymph and cochlear tissue samples were collected from SAMP8 mice at different timepoints after a single administration via transtympanic injection in each ear of ACOU085 in 0.6% w/v ($n = 14$) or 6.0% w/v ($n = 24$) concentrations. Sampling timepoints were ¼ (6 h), 7, 14, 21, and 28 days (see Fig. 1a). Sample sizes varied between timepoints due to insufficient sampling volumes or contamination. After collection, perilymph and tissue samples were delivered for liquid chromatography with tandem mass spectrometry (LC-MS/MS) analysis.

Perilymph and tissue sampling. At the respective timepoint of sample collection, mice were exposed to a gradually increasing amount of CO_2 until complete cessation of breathing was observed for a minimum of 2 min, followed by decapitation. Temporal bones were extracted from the skull and cochleae were then isolated and dried with a cotton swab prior to sampling to ensure that remnant formulation was not carried into the cochlea during sampling. The perilymph was sampled through the round window by puncturing the membrane with a 20-µl microloader tip (Eppendorf) and collecting a perilymph volume of approximately 2 µl. For tissue sampling, the cochlear apex was perforated with a 27 G needle, then fine forceps were used to widen the opening and collect cochlear tissue. Samples were immediately transferred into PCR tubes (Eppendorf), which were calibrated for weight, after collection. They were stored at 4 °C for a maximum of 2 h before being delivered for LC-MS/MS analysis.

Liquid chromatography with tandem mass spectrometry analysis. ACOU085 concentrations in perilymph and cochlear tissue samples were analyzed using LC-MS/MS by Synovo (Tübingen, Germany). Tissue samples were first weighed then approximately five volumes of water were added (generally to a final sample size of 10 mg or 10 µl) followed by a 5-min sonication step as initial preparation. To each perilymph or tissue sample, 6 volumes of acetonitrile (generally 60 µl, Th. Geyer, Renningen, Germany) was added containing the internal injection volume (terbuthylazine). After centrifugation for 5 min at 20,000 RCF, each supernatant was transferred into a glass auto-sampler vial. Dilution of the perilymph or tissue samples was required due to excessive concentration or low sample volume. The dilution factor was considered for data collection and calculations. The processed samples were stored at 4 °C before LC-MS/MS analysis.

All solvents used as mobile phase and for sample preparation were of analytical grade or better. Calibration curves and quality controls were obtained by preparing a stock solution of ACOU085 in DMSO with a final concentration of 10 mM followed by a serial dilution in threefold steps in mouse plasma or artificial perilymph. The calibration curve ranged from 5 to 100,000 nM in final concentration and quality controls had a

concentration of 100, 1000, and 10,000 nM. Sample separation was performed using using an Agilent 1260 Binary Pump (Agilent Technologies, Santa Clara, CA, USA), CTC PAL Autosampler (CTC Analytics, Zwingen, Switzerland), and Agilent 1260 thermostatted column compartment (Agilent Technologies). The system was coupled to an API 4500 triple quadrupole mass spectrometer (AB Sciex, Framingham, MA, USA). Data acquisition and processing were performed using Analyst Instrument Control and Data Processing Software (version 1.6.2, AB Sciex).

Electrophysiology

Experimental design. To determine the effect of repeated administrations of a $K_V7.4$ agonist ACOU085 on ARHL in the SAMP8 model, two groups of mice received unilateral transtympanic injections of ACOU085 in the right ear in either 0.6% w/v ($n = 10$) or 6.0% w/v ($n = 10$) doses, referred to as the 0.6% or 6.0% groups, respectively. In the contralateral left ears, an equivalent volume of the vehicle formulation was administered as a control. The 0.6% and 6.0% groups were tested independently in consecutive experimental series. At the age of 45 days, preT ABR measurements were conducted, followed by initial treatment via transtympanic injection of ACOU085 or vehicle. Due to asymmetrical hearing loss in preT ABR measurements, two mice of the group treated with 6.0% ACOU085 had to be excluded, yielding a sample size of $n = 8$ for this group. Two subsequent administrations followed in 1-month intervals, i.e., at 75 and 105 days of age. Follow-up ABR measurements were conducted at 1-month, 2-months, and 3-months post-treatment timepoints (Fig. 1b). After the last follow-up ABR measurement at 3-months post-treatment (age of 135 days), cochleae were extracted for immunohistochemical cochlear whole-mount analysis.

Auditory brainstem response. ABR was recorded in response to click (100-µs square pulse) or tonebursts at frequencies 2.0–45.2 kHz in two steps per octave, with a duration of 3 ms and 1 ms rise and fall times. Stimuli were presented at 10–100 dB SPL in 3 dB steps with alternating condensation and rarefaction polarities. To generate the stimuli and record the ABR signal, a multi-function I/O-card (National Instruments, Austin, Texas, USA) was used. Acoustic stimuli were delivered in a calibrated open-field system using a dynamic loudspeaker placed lateral to the respective auricle of the mouse. The sound pressure level was calibrated before each block of measurements with a microphone probe (Brüel & Kjær Types 4939 and 2670, Nærum, Denmark) placed near the entrance of the external auditory canal in line with the loudspeaker at an angle of 90°. A differential amplifier recorded the ABR signal between silver wire electrodes inserted subcutaneously at the back (ground), the vertex (positive terminal), and at the mastoid of each ear (negative terminal) with 80 dB gain. Signals were filtered between 100 Hz and 5 kHz using sixth-order Butterworth low- and high-pass filters and then processed by the Audiology Lab software (Otoconsult, Frankfurt am Main, Germany) after analog-to-digital conversion at 50 kHz sampling frequency. ABR measurements were conducted in a soundproof chamber (IAC Acoustics, Niederkrüchten, Germany). An ABR threshold was defined as the sound pressure level at which a stimulus-related response was clearly identified by visual inspection of the ABR signal averaged from 128 stimulus repetitions for each polarity.

All animals were anesthetized during ABR measurements by intraperitoneal injection of 0.05 mg/kg fentanyl (Fentadon, Dechra, Aulendorf, Germany), 0.5 mg/kg medetomidine hydrochloride (Dormilan, alfavet, Neumünster, Germany) and 2.5 mg/kg midazolam (Hameln Pharma, Hameln, Germany). To preserve eye moisture, an ointment (Bepanthen, Bayer AG, Leverkusen, Germany) was administered. Over the course of the measurements, the animals were placed in the prone position, electrocardiography was monitored, and a heating blanket maintained their body temperature at ~37 °C.

Cochlear whole-mount analysis. Following ABR measurement at 3 months post-treatment (135 days of age), pre-anesthetized mice from both experimental groups were sacrificed by intracardiac injection of 600 mg/kg pentobarbital sodium (Narcoren, Boehringer Ingelheim, Ingelheim am Rhein, Germany), followed by decapitation. Temporal bones were extracted, dissected on ice, perfused with 4% formaldehyde, and decalcified in 0.2 M EDTA for 27 h at 4 °C. Once decalcification was completed, the cochlear sensory epithelium, i.e., the Organ of Corti (OC), was dissected under a stereo microscope (Zeiss Stemi 200-C). OC extraction was performed by removing the bony labyrinth, detaching the stria vascularis (SV), then separating the OC from the spiral ganglion. The OC was then divided into three segments: apical, middle, or basal. For each cochlea, the three OC segments were finally transferred into one well of a 48-well plate filled with 500 µl of PBS.

For fluorescence and immunofluorescence labeling, whole-mount preparations were first permeabilized with 0.2% Triton X-100 in PBS for 20 min and immersed in a blocking buffer containing 0.2% Triton X-100 in PBS and 1% normal donkey serum for 30 min at room temperature. Visualization was achieved by incubation with anti-myosin VIIa (1:400, rabbit, Proteus Biosciences Inc., Waltham, MA, USA), followed by detection with an Alexa 488-conjugated anti-rabbit secondary antibody (1:400, Invitrogen, Paisley, UK). Each antibody was diluted in PBS supplemented with 0.2% Triton X-100 and 0.5% normal donkey serum. All samples were incubated for 20 min at room temperature in DAPI (1:100, Sigma-Aldrich, St. Louis, MO, USA) and phalloidin 568 (1:400, Invitrogen) for nuclear and F-actin fluorescence staining, respectively, then coverslipped using FluorSave mounting medium (Calbiochem, Merck, Darmstadt, Germany). Imaging of the immunolabelled whole-mount preparations was conducted with 10x magnification using an epifluorescence microscope (Zeiss Axioplan 2 with an ApoTome.2 unit).

Data analysis

Cytocochleograms. Images of OC whole-mount preparations were analyzed using ImageJ (NIH, Bethesda, MD, USA) and cell counting was carried out manually by assigning different counting markers stored with their coordinates using the plug-in "Cellcounter". The length of each OC whole-mount segment (apical, middle, or basal) was measured along the clearly defined junction connecting the outer pillar cells and the first row of OHCs. Along the longitudinal axis of the OC, this line was traced and concatenated across all three segments to determine the total spiral length. OHCs and IHCs were counted as present if co-staining of three cellular markers were evident, i.e., the nucleus (DAPI), the stereocilia bundle (phalloidin), and the cytoplasm (myosin VIIa). If any of these cellular markers were absent, hair cells were counted as missing. For each counting marker (present or missing OHCs and IHCs), the nearest point on the spiral of the OC was assigned by calculating the minimum Euclidean distance. The total spiral length was normalized to 100% and the number of present or missing OHCs and IHCs, respectively, was calculated as a function of the relative distance from the apex subdivided into 5% bins. This approach was used to determine the extent and pattern of cell loss along the cochlear length mapped as a "cytocochleogram" [18, 39, 40].

Statistics. Data are presented as means with standard deviations (SD), with standard error of the mean (SEM), or as box plots. Sample distributions were tested for normality by the Shapiro-Wilk test. Within-subject differences were compared for statistical significance using the two-sided paired-samples *t*-test for two samples, or two-way repeated-measures analysis of variance (ANOVA) for more than two samples to determine the main effect of treatment. A *p*-value of less than 0.05 was considered statistically significant and, if applicable, was adjusted for multiple comparisons using the Bonferroni correction. Statistical analysis was performed using IBM SPSS Statistics 27 (IBM Corporation, Armonk, NY, USA).

RESULTS

ACOU085 readily diffuses into the cochlea from the middle ear cavity

To determine the diffusion of the $K_V7.4$ activator ACOU085 from the formulation administered into the middle ear cavity into the targeted cochlea, the concentration of ACOU085 was sampled in cochlear perilymph and tissue for the timepoints ¼ (6 h), 7, 14, 21, and 28 days after a single transtympanic injection of 0.6% w/v ($n = 14$) or 6.0% w/v ($n = 24$) formulations in SAMP8 mice (Fig. 1a). For each mouse, ACOU085 concentrations obtained by LC-MS/MS for either perilymph or tissue samples were averaged, respectively, across both ears. The lower limit of quantification (LLOQ) was averaged from individual LLOQs that were calculated for each timepoint taking dilution factors into account, with the mean LLOQ over all timepoints shown in gray shading (Fig. 2a and b). For the 0.6% w/v ACOU085 formulation, the mean concentration measured in perilymph at ¼ days post-administration (postA) was 5.20 ± 4.54 µM, whereas the concentration in cochlear tissue reached more than thrice that level with a mean concentration

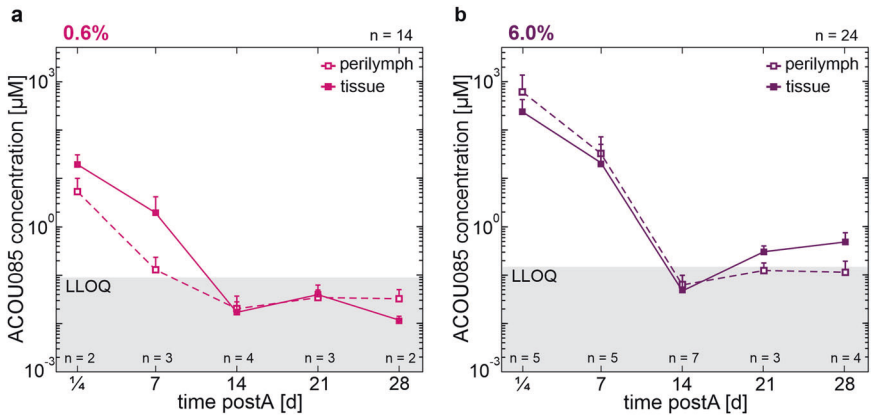

Fig. 2 Distribution of ACOU085 in the cochlea of SAMP8 mice after a single administration. Concentrations of ACOU085 in cochlear perilymph and tissue were determined by liquid chromatography with tandem mass spectrometry (LC-MS/MS). Mean and standard deviation of ACOU085 concentrations are shown for perilymph (open squares) and tissue (closed squares) sampling after a single administration of the 0.6% (**a**) or 6.0% (**b**) w/v ACOU085 formulation. The lower limit of quantification (LLOQ) was calculated for each timepoint taking dilution factors into account, with the mean LLOQ over all timepoints shown (gray shading).

of 18.86 ± 11.03 µM (Fig. 2a). At 7 days postA, the concentration decreased to 0.13 ± 0.10 µM in perilymph and to 1.89 ± 2.16 µM in tissue. At 14 days and beyond, concentrations in both sample types were found below LLOQ. For the 6.0% w/v formulation, at ¼ days postA a mean ACOU085 concentration of 621.45 ± 754.15 µM was found in the perilymph, and 247.25 ± 181.34 µM in tissue (Fig. 2b). These concentrations are at least an order of magnitude higher than for the 0.6% w/v formulation, which is consistent with a dose-dependent exposure [41]. At 7 days postA, mean ACOU085 concentration in the perilymph remained relatively high at 32.72 ± 39.77 µM, and in the tissue, it was 21.12 ± 29.58 µM. Similar to the 0.6% w/v formulation, ACOU085 concentrations at 14 days and beyond were generally below or at LLOQ for the 6.0% w/v formulation. However, tissue concentrations appeared to increase slightly at 21 days and 28 days postA (Fig. 2b). This may be due to variability between mice given that sampling was terminal and not continuous within subjects. In summary, this pharmacokinetic study demonstrated that ACOU085 readily diffused into the cochlear perilymph and tissue from the middle ear cavity in a dose-dependent fashion. Given an EC_{50} in the nanomolar range [37] (Fig. S1), therapeutically relevant concentrations of ACOU085 are estimated to be available in the cochlea for 7–14 days after a single administration, with higher concentrations and a presumably longer time window for the 6.0% w/v dose.

K_V7.4 agonist reduces age-related ABR threshold shifts in SAMP8 mice

The pharmacodynamic effect of cochlear K_V7.4 enhancement on ARHL in the SAMP8 model was investigated in two groups of mice that received three consecutive, unilateral transtympanic injections of ACOU085 in 0.6% w/v ($n = 10$) or 6.0% w/v ($n = 8$) doses, hereafter referred to as the 0.6% or 6.0% group, respectively. In contralateral ears, equivalent volumes of the vehicle formulation were administered as a control. For each group, the baseline measurement, i.e., pre-treatment (preT) ABR thresholds, was conducted at the age of 45 days followed by initial administration via transtympanic injection of ACOU085 or vehicle. Two subsequent administrations followed in 1-month intervals, i.e., at 75 and 105 days of age. Based on the pharmacokinetic study, we estimate that at least half the 1-month administration interval had sub-EC_{50} concentrations of ACOU085 in the target tissue for either group, suggesting that effects were obtained without sustained target engagement. Follow-up ABR measurements were conducted at 1-month, 2-months, and 3-months post-treatment (postT) intervals (Fig. 1b). At preT, toneburst- (Fig. 3a, b) and click-evoked (Fig. 3c, d) ABR thresholds showed no statistically significant differences between ears selected for treatment with ACOU085 or vehicle in either group. ABR threshold shifts were calculated as the difference between individual thresholds (for each ear) and the population mean at preT ($n = 36$, two ears per mouse). In general, the 6.0% group showed a more rapid progression of hearing loss compared with the 0.6% group (Fig. 3c, d); when comparing click-evoked threshold shifts of vehicle-treated ears between these groups at 3-months postT, the mean threshold shift for the 0.6% group was 21.0 ± 11.6 dB in contrast to a 37.9 ± 8.1 dB threshold shift for the 6.0% group. These significantly different threshold shifts ($p = 0.0048$) between vehicle-treated ears may be traced back to the variability of age-related threshold loss in SAMP8 mice [18]. However, this does not affect within-subject comparisons in either dose group. Within-subject comparisons of click-evoked ABR threshold shifts in the 0.6% group showed no significant effect of treatment for any postT interval, but a trend of decreased threshold shifts for ACOU085- compared with vehicle-treated ears can be observed (Fig. 3c). In the 6.0% group, a similar trend was observed and significant within-subject differences between ACOU085- and vehicle-treated ears were evident at 3-months postT ($p = 0.029$, Fig. 3d). Tone-burst evoked ABR also showed similar trends for both dose groups (see Fig. S2); the main effect of treatment (ACOU085 vs. vehicle) at 3-months postT was statistically significant in the 0.6% group, $F(1,9) = 11.76$, $p = 0.008$, and was just above significance level in the 6.0% group, $F(1,6) = 5.596$, $p = 0.056$. Altogether, the reduced ABR threshold shifts demonstrate that repeated treatments with the K_V7.4 agonist protected hearing function from the age-related decline in SAMP8 mice.

K_V7.4 agonist reduces age-related OHC loss in SAMP8 mice

To determine the effect of treatment on the degree of hair cell survival, cochleae were extracted for immunohistochemical analysis after the final follow-up ABR measurement at 3-months postT. Cytocochleograms were generated from OC whole-mount preparations stained for the nucleus (DAPI), the stereocilia bundle (phalloidin), and the cytoplasm (myosin VIIa). Illustrative examples of OC whole-mount analysis are shown in Fig. 4a. Both present and absent OHCs and IHCs were respectively counted and divided into 5% bins along the normalized spiral length of the OC as previously described [18]. Cytocochleograms visualize the percentage of hair cell loss in each bin based on the ratio of absent hair cells to the sum of present and absent hair cells (Fig. 4b). In both the 0.6% and 6.0% groups, IHC loss remained negligible below 7% for either treatment. This finding is consistent with previous

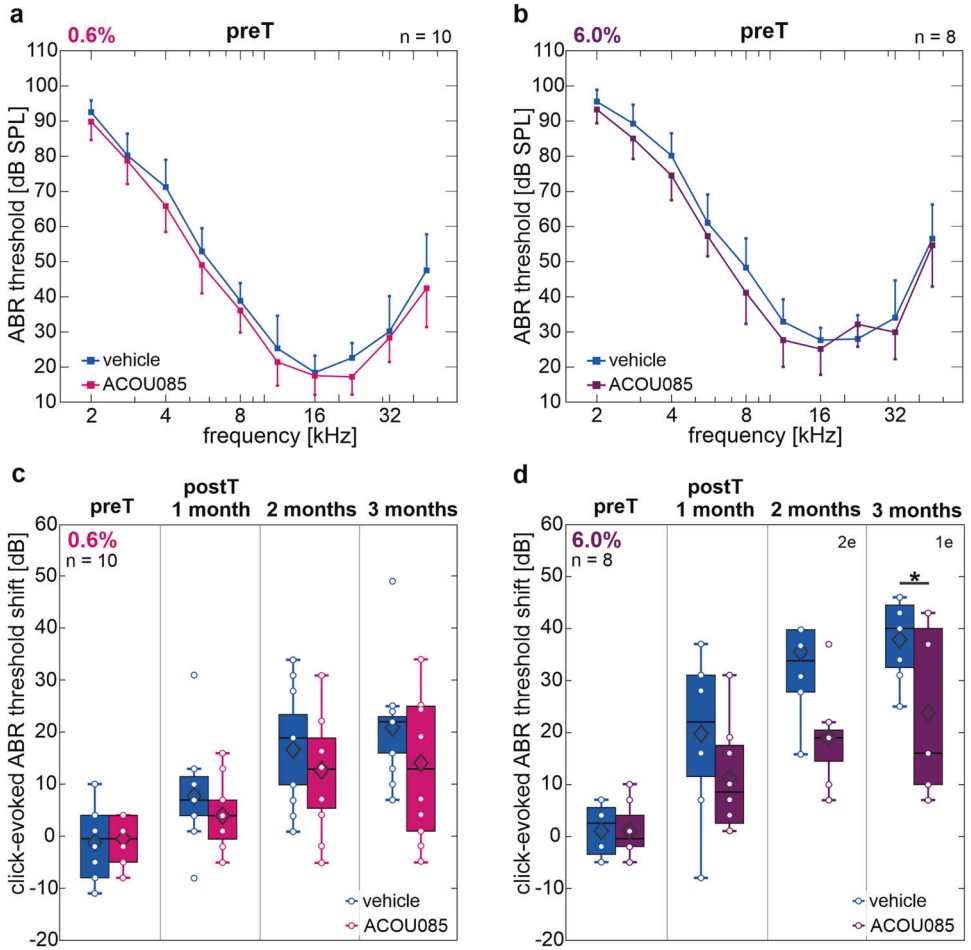

Fig. 3 ABR thresholds of SAMP8 mice before treatment and click-evoked ABR threshold shifts of SAMP8 mice treated with ACOU085 and vehicle control. a, **b** Mean and standard deviation of ABR thresholds are shown for SAMP8 mice at the age of 45 days before treatment with ACOU085 at 0.6% (**a**) or 6.0% (**b**) w/v dose or contralateral vehicle control. **c**, **d** Means (diamonds), box plots, and individual (circles) click-evoked auditory brainstem response (ABR) threshold shifts are shown for SAMP8 mice treated unilaterally with either 0.6% (**c**) or 6.0% (**d**) w/v ACOU085 and contralateral vehicle control measured at different timepoints: pre-treatment (preT), and 1-, 2-, 3-months post-treatment (postT). Threshold shifts were calculated as the difference between individual thresholds and the population mean at preT. Significant pairwise comparisons (paired-samples *t*-Test) are indicated by asterisks (*$p < 0.05$). Note that due to technical issues resulting in data loss, two mice had to be excluded at the 2-months and 1 mouse at the 3-months postT intervals, respectively, in the 6.0% group. This is denoted by "1e" and "2e", i.e., 1 ear and 2 ears excluded, respectively.

histological data on age-related IHC loss in SAMP8 mice [18, 42]. As is also expected from previous data, mean OHC loss of up to 36% was observed in the high-frequency range of vehicle-treated ears, starting at a distance of 30–40% from the apex. OHC loss showed no relevant differences between ACOU085- and vehicle-treated ears in the 0.6% group. By contrast, OHC loss in the 6.0% group was generally reduced up to 14% in ACOU085-treated ears. Given that cytocochleogram bins without valid hair cell counting markers for a given cochlea had to be excluded from the analysis (see Methods), statistical comparisons between treatments were not possible for each bin. A mouse place-frequency map was implemented to convert the relative distance from apex to corresponding center frequencies [39], which facilitates a more direct comparison with ABR data. According to the previously shown progressive OHC loss in SAMP8 mice in the middle and basal regions (>40% distance from apex) in contrast to the apical region, the place-frequency map was used to divide cytocochleograms into low- (≤8 kHz) and high-frequency (>8 kHz) ranges. OHC loss was then averaged over each frequency range. Correspondingly, toneburst-evoked ABR threshold shifts at 3-months postT were averaged over the same frequency ranges (low or high), for each treatment and group to allow frequency range-specific comparisons with OHC loss. The 0.6% group showed a significant main effect of treatment on ABR threshold shifts with $F(1,9) = 11.76$, $p = 0.008$ (Fig. 5a), which is consistent with the analysis for each frequency at 3-months postT (c.f. Fig. S2a). However, no significant differences were evident in OHC loss. The main effect of treatment on ABR threshold shifts in the 6.0% group was just above significance level, $F(1,6) = 5.60$, $p = 0.056$, which is also consistent with the analysis for each frequency (c.f. Fig. S2b). While no significant main effect of treatment was found on OHC loss, a significant interaction effect of treatment and frequency range was found, $F(1,6) = 8.43$, $p = 0.027$ (Fig. 5b). Post-hoc testing correspondingly showed a significant reduction of OHC loss in ACOU085- compared with vehicle-treated ears in the high-frequency range ($p = 0.00063$). This frequency range-specific effect of treatment with reduced OHC loss is consistent with the significant reduction in click-evoked ABR threshold shifts at 3-months postT (Fig. 3d). In summary, repeated administration of the $K_V7.4$ agonist in the 6.0% group over a period of three months was shown to significantly reduce age-related OHC loss in the high-frequency range. This increased morphological preservation of OHCs correlated with the functional protection of ABR thresholds in this group.

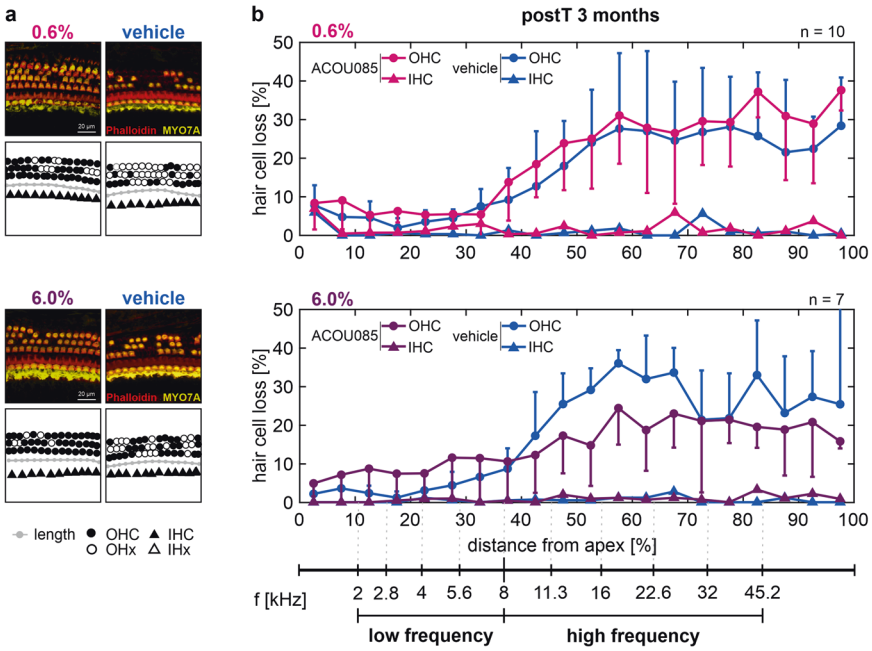

Fig. 4 Quantification of outer and inner hair cell loss in SAMP8 mice treated with ACOU085 and vehicle control. The effect of repeated unilateral administrations via transtympanic injection of ACOU085 versus contralateral vehicle control was investigated in the SAMP8 mouse model in a within-subject design. After the last follow-up measurement at 3-months post-treatment (postT, age of 135 days, see Fig. 1b), cochleae were extracted for immunohistochemical analysis to determine the degree of outer and inner hair cell (OHC and IHC, respectively) loss for either 0.6% or 6.0% w/v ACOU085 and corresponding vehicle control. **a** Illustrative examples are shown for cochlear segments (scale bar, 20 µm) stained with myosin VIIa (MYO7A, yellow) for cytoplasm and phalloidin (red) for stereocilia of SAMP8 mice treated with either 0.6% or 6.0% w/v ACOU085 and vehicle control. **b** Cytocochleograms show mean and standard error of the mean OHC and IHC loss in percent, respectively, which are calculated as the ratio of absent hair cells to the sum of present and absent hair cells within 5% bins of distance from apex, for the 0.6% ($n = 10$) or the 6.0% group ($n = 7$, due to 1 exclusion at 3-months postT). A mouse place-frequency map [39, 40, 55] was then used to divide the cytocochleograms into low- (≤8 kHz) and high-frequency (>8 kHz) ranges. For reference, a frequency (*f*) axis is depicted with respect to the relative distance from apex.

DISCUSSION

Hearing impairment is the third most common sensory deficit in humans, with ARHL constituting the leading cause in the population older than 70 years [3]. Causal and effective medical treatments for ARHL constitute a significant unmet need in the elderly. Dysfunctional $K_V7.4$ has been previously associated with genetic, noise-induced, and age-related hearing loss [19, 22, 24]. Therefore, maintaining $K_V7.4$ expression in OHCs was suggested as a promising therapeutic approach for hearing loss. In the present study, we examined a treatment principle for ARHL by $K_V7.4$ channel activation, which has a central role for OHC function and survival [30, 31]. A potent small-molecule $K_V7.4$ agonist (ACOU085 [37]) was shown to diffuse from a transtympanically injected formulation into the cochlea, and had a protective effect on age-related ABR threshold shifts and OHC loss in the SAMP8 mouse model of ARHL.

We confirmed in a pharmacokinetic study that ACOU085 administered in a sustained release formulation via transtympanic injection readily diffused from the middle ear cavity into the cochlea. After a single administration of ACOU085 in 0.6% or 6.0% w/v dose, drug levels well above the nanomolar range [37] were reached in cochlear perilymph and tissue. This presumably allowed target engagement within an estimated, therapeutically relevant dose-dependent exposure lasting from 7 to 14 days (c.f. Fig. 2a, b). The administration of a drug formulation through the TM into the middle ear allows drugs to reach the cochlea and has a long-standing clinical application [41]. Transtympanic drug delivery primarily relies on diffusion through the round window membrane (RWM) for drug entry into the cochlea. Although this method presents major challenges for drug delivery, such as presumably unequal distribution over the cochlear spiral or the amount of drug elimination via multiple routes, transtympanic injection as a method for cochlear drug delivery allows for rapid and high local target exposure. Another limitation of transtympanic injection involves the perforation of the TM which can cause scarring that leads to conductive hearing loss. Thus, an administration interval of 1 month was adopted in the electrophysiology study to minimize the effect of TM scarring [43, 44]. Consequently, the therapeutic time window estimated within a time frame of 7–14 days was less than or equal to half of the 1-month treatment interval. This pharmacokinetic restriction posed an additional challenge to the investigated effects of $K_V7.4$ activation on age-related decline in the SAMP8 model.

Despite this limited therapeutic time window in the electrophysiology study, a significant protective effect was detected for treatments with ACOU085 in the 6.0% w/v dose at the functional as well as morphological level. In this group, ACOU085 significantly reduced click-evoked ABR threshold shifts when compared with vehicle-treated ears (c.f. Fig. 3d). Auditory thresholds are known to be a sensitive measure of OHC function, as they play an essential role in the lower dynamic range of the cochlear amplifier [45]. The OHC conductance current carried by K^+ drives their electromotility [46], with $K_V7.4$ maintaining the OHC receptor potential and K^+ homeostasis [14, 15, 33, 47]. A preliminary analysis of the ABR input-output functions of the present study showed no additional suprathreshold effects on wave latency or slope, but only differences in threshold. This suggests that OHCs were the main target of ACOU085 treatment in this model, appearing to have maintained their function and increased their survival rate over age. In line with this assertion, cytocochleograms of the 6.0% group showed significantly reduced OHC loss for ACOU085- compared with vehicle-treated ears in the high-frequency range (>8 kHz, c.f. Fig. 5b), which corresponds to a protective benefit of 29.4%. Although we have not measured the drug distribution along the cochlear length, these data suggest a precedence for protective effects in the basal turn.

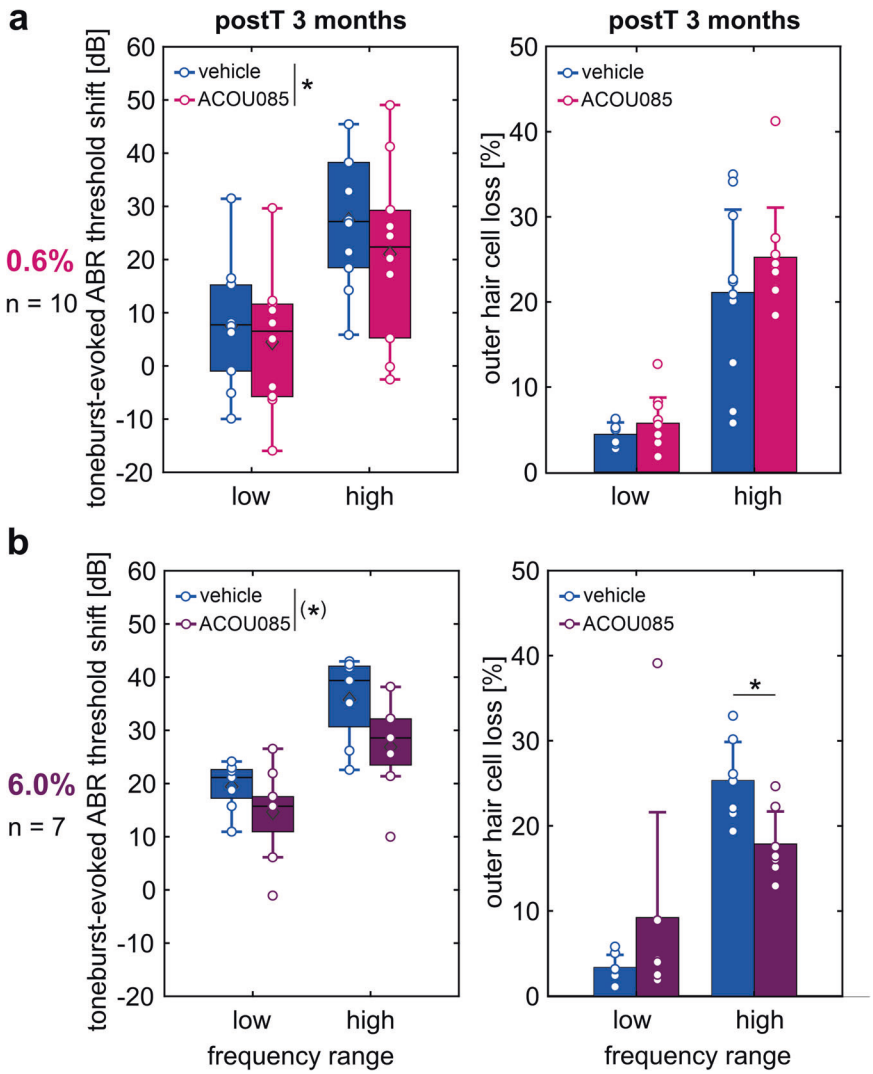

Fig. 5 Repeated treatments with $K_V7.4$ agonist reduced age-related decline of toneburst-evoked ABR threshold shifts and age-related OHC loss in the high-frequency range. Following the final follow-up measurement at 3-months post-treatment (postT, age of 135 days, see Fig. 1b), cochleae were extracted for immunohistochemical analysis to generate cytocochleograms. A mouse place-frequency map was used to divide the cytocochleograms into low- (≤8 kHz) and high-frequency (>8 kHz) ranges (see Fig. 4b), then outer hair cell (OHC) loss was averaged over each frequency range. Correspondingly, toneburst-evoked auditory brainstem response (ABR) threshold shifts at 3-months postT were averaged over each frequency range, for each mouse and treatment. Means (diamonds), box plots, and individual (circles) toneburst-evoked ABR threshold shifts are compared with mean and standard deviation of OHC loss of SAMP8 mice treated unilaterally with ACOU085 at 0.6% (**a**, $n = 10$) or 6.0% w/v dose (**b**, $n = 7$, due to 1 exclusion at 3-months postT) and contralateral vehicle control. A significant main effect of treatment (ACOU085 vs. vehicle, two-way repeated-measures ANOVA) and significant pairwise comparisons (two-tailed paired-samples *t*-test with Bonferroni correction for multiple comparisons) are indicated by asterisks (*$p < 0.05$). The main effect of treatment just above the significance level ($p = 0.056$) is indicated by an asterisk within parentheses.

The protective effect on the age-related functional decline in SAMP8 was, however, only significant for click-evoked ABR at 3-months postT, but just above significance level for toneburst-evoked ABR in the 6.0% group (see Fig. 3d and Fig. S2b). Acoustic click stimuli generally have a broader spectral spread than transient toneburst stimuli [48], thereby evoking a broader neural population. We have previously observed a large variability between SAMP8 mice in the progression of age-related toneburst-evoked ABR threshold shifts [18]. Thus, the relatively narrow spectral spread and the large variability between mice could have impeded the detection of the protective effects on the local level by toneburst-evoked ABR in the 6.0% group. The opposite observation in the 0.6% group, where ABR threshold shifts evoked by tonebursts were significantly reduced but not for click (see Figs. 3c and 5a), could be traced back to a protective effect dominated by the high-frequency range (≥16 kHz). This is suggested by significant differences in pairwise comparisons for toneburst-evoked ABR at 16 and 32 kHz before adjustment of the significance level for multiple comparisons. Since click stimuli have reduced spectral energy in the region beyond 10 kHz, they would be limited in detecting an effect localized at the frequency range beyond 16 kHz. However, while the functional protection observed in the 6.0% group was in concordance with significantly reduced OHC loss, this was not the case in the 0.6% group. The observed large variability between SAMP8 mice in the progression of age-related threshold decline could previously not be explained by OHC loss alone [18]. Therefore, the protective effect observed in the 0.6% group without reduction of OHC loss can arguably be attributed to a protective effect against the functional sensory degeneration primarily linked to oxidative stress in SAMP8 mice [42, 49, 50].

The survival of OHCs is dependent on the functional K^+ recycling circuit, which facilitates OHC electromotiliy [51]. An

essential component for maintaining K^+ cycling is the voltage-dependent K^+ channel $K_V7.1$ (KCNQ1), which is expressed in the SV and is responsible for K^+ secretion to the endolymph. A decrease in $K_V7.1$ has been previously observed to cause SV atrophy with notable hearing loss [52]. However, Peixoto Pinheiro et al. [18] have found no consistent correlations between $K_V7.1$ membrane expression decline and age in SAMP8 mice. By contrast, relevant linear regressions and negative correlations were found between $K_V7.4$ membrane expression in OHCs and age, especially in middle and midbasal turns. This is consistent with the protection of OHC function in both dose groups, as well as OHC survival in the higher dose group. Considering the pharmacokinetic restriction reducing drug exposure to half or less than half of the experimental time and the large variability in age-related auditory decline of the SAMP8 mouse model, the observed protective effects appear very encouraging and have considerable potential for further improvement, e.g., by increased dosing, frequency of treatment, or potentially a different formulation allowing prolonged release of the drug.

Small-molecule $K_V7.4$ agonists have been in research for over a decade as a strategy to treat hearing impairments [20, 34]. One of the most characterized $K_V7.4$ channel activators is RTG, which causes a shift in the hyperpolarizing direction of the channel's voltage-dependence [53]. Leitner et al. [36] were the first to show in vitro that a combined administration of ZnP and RTG can functionally rescue $K_V7.4$-mediated currents from deafness-causing mutations and, furthermore, this drug combination was able to enhance the native $K_V7.4$-mediated $I_{K,n}$ current. An in-vivo study involving $K_V7.4$ agonists has only been performed in a rat model of tinnitus, whereby treatment with RTG was able to reverse reduced compound action potential amplitudes at low and high frequencies, respectively [54]. However, RTG failed to reverse reduced distortion-product otoacoustic emissions, suggesting that protection was most probably not mediated at the OHC level. Although the application of $K_V7.4$ activators as a treatment modality for ARHL appeared logical from previous $K_V7.4$ activation studies [20], the variability of ARHL models and the necessary long-term application have complicated a potential in vivo experimental design to investigate their protective effect. We have demonstrated for the first time in vivo that a novel small-molecule $K_V7.4$ agonist can functionally and morphologically protect OHCs in a mouse model of ARHL. These findings suggest that pharmacological $K_V7.4$ activation holds great potential as a novel therapeutic approach for ARHL by preventing or decelerating age-related decline of auditory function and morphological loss of OHCs, as well as for other hearing impairments related to compromised $K_V7.4$ function.

Reporting summary

Further information on research design is available in the Nature Research Reporting Summary linked to this article.

DATA AVAILABILITY

The data supporting the findings of this study are available from the corresponding authors BP and HL upon reasonable request. Restrictions apply to details, analytics, and formulations of ACOU085 as well as the in-vitro pharmacodynamic data (Fig. S1), which are subject to a non-disclosure agreement with Acousia Therapeutics (Tübingen, Germany). These data can, however, be made available from the corresponding authors upon reasonable request and with permission by Acousia Therapeutics.

REFERENCES

1. World Health Organization. World report on hearing. Geneva 2021: World Health Organization; 2021.
2. Wilson BS, Tucci DL. Addressing the global burden of hearing loss. Lancet 2021;397:945–7.
3. Hearing GBD. Loss Collaborators. Hearing loss prevalence and years lived with disability, 1990-2019: findings from the Global Burden of Disease Study 2019. Lancet. 2021;397:996–1009.
4. Bowl MR, Dawson SJ. Age-related hearing loss. Cold Spring Harb Perspect Med. 2019;9:a033217.
5. Rutherford BR, Brewster K, Golub JS, Kim AH, Roose SP. Sensation and psychiatry: linking age-related hearing loss to late-life depression and cognitive decline. Am J Psychiatry. 2018;175:215–24.
6. Livingston G, Huntley J, Sommerlad A, Ames D, Ballard C, Banerjee S, et al. Dementia prevention, intervention, and care: 2020 report of the Lancet Commission. Lancet. 2020;396:413–46.
7. Livingston G, Sommerlad A, Orgeta V, Costafreda SG, Huntley J, Ames D, et al. Dementia prevention, intervention, and care. Lancet. 2017;390:2673–734.
8. Frisina RD. Age-related hearing loss: ear and brain mechanisms. Ann N Y Acad Sci. 2009;1170:708–17.
9. Frisina RD, Frisina DR. Physiological and neurobiological bases of age-related hearing loss: biotherapeutic implications. Am J Audiol. 2013;22:299–302.
10. Wu PZ, O'Malley JT, de Gruttola V, Liberman MC. Age-related hearing loss is dominated by damage to inner ear sensory cells, not the cellular battery that powers them. J Neurosci. 2020;40:6357–66.
11. Dallos P. Cochlear amplification, outer hair cells and prestin. Curr Opin Neurobiol. 2008;18:370–6.
12. Hibino H, Kurachi Y. Molecular and physiological bases of the K+ circulation in the mammalian inner ear. Physiology. 2006;21:336–45.
13. Zdebik AA, Wangemann P, Jentsch TJ. Potassium ion movement in the inner ear: insights from genetic disease and mouse models. Physiology. 2009;24:307–16.
14. Kharkovets T, Hardelin J-P, Safieddine S, Schweizer M, El-Amraoui A, Petit C, et al. KCNQ4, a K+ channel mutated in a form of dominant deafness, is expressed in the inner ear and the central auditory pathway. Proc Natl Acad Sci USA. 2000;97:4333–8.
15. Holt JR, Stauffer EA, Abraham D, Geleoc GS. Dominant-negative inhibition of M-like potassium conductances in hair cells of the mouse inner ear. J Neurosci. 2007;27:8940–51.
16. Housley GD, Ashmore JF. Ionic currents of outer hair cells isolated from the guinea-pig cochlea. J Physiol. 1992;448:73–98.
17. Peixoto Pinheiro B, Vona B, Lowenheim H, Ruttiger L, Knipper M, Adel Y. Age-related hearing loss pertaining to potassium ion channels in the cochlea and auditory pathway. Pflugers Arch. 2021;473:823–40.
18. Peixoto Pinheiro B, Adel Y, Knipper M, Muller M, Lowenheim H. Auditory threshold variability in the SAMP8 mouse model of age-related hearing loss: functional loss and phenotypic change precede outer hair cell loss. Front Aging Neurosci. 2021;13:708190.
19. Van Eyken E, Van Laer L, Fransen E, Topsakal V, Lemkens N, Laureys W, et al. KCNQ4: a gene for age-related hearing impairment? Hum Mutat. 2006;27:1007–16.
20. Rim JH, Choi JY, Jung J, Gee HY. Activation of KCNQ4 as a therapeutic strategy to treat hearing loss. Int J Mol Sci. 2021;22:2510.
21. Van Eyken E, Van Camp G, Van Laer L. The complexity of age-related hearing impairment: contributing environmental and genetic factors. Audio Neurootol. 2007;12:345–58.
22. Wang Q, Li W, Cai C, Hu P, Lai R. miR-153/KCNQ4 axis contributes to noise-induced hearing loss in a mouse model. J Physiol Sci. 2021;71:28.
23. Van Laer L, Carlsson PI, Ottschytsch N, Bondeson ML, Konings A, Vandevelde A, et al. The contribution of genes involved in potassium-recycling in the inner ear to noise-induced hearing loss. Hum Mutat. 2006;27:786–95.
24. Marchetta P, Mohrle D, Eckert P, Reimann K, Wolter S, Tolone A, et al. Guanylyl cyclase A/cGMP signaling slows hidden, age- and acoustic trauma-induced hearing loss. Front Aging Neurosci. 2020;12:83.
25. Jaumann M, Dettling J, Gubelt M, Zimmermann U, Gerling A, Paquet-Durand F, et al. cGMP-Prkg1 signaling and Pde5 inhibition shelter cochlear hair cells and hearing function. Nat Med. 2012;18:252–9.
26. Leitner MG, Halaszovich CR, Oliver D. Aminoglycosides inhibit KCNQ4 channels in cochlear outer hair cells via depletion of phosphatidylinositol(4,5)bisphosphate. Mol Pharm. 2011;79:51–60.
27. Coucke PJ, Van Hauwe P, Kelley PM, Kunst H, Schatteman I, Van Velzen D, et al. Mutations in the KCNQ4 gene are responsible for autosomal dominant deafness in four DFNA2 families. Hum Mol Genet. 1999;8:1321–8.
28. Van Hauwe P, Coucke PJ, Ensink RJ, Huygen P, Cremers CW, Van Camp G. Mutations in the KCNQ4 K+ channel gene, responsible for autosomal dominant hearing loss, cluster in the channel pore region. Am J Med Genet. 2000;93:184–7.
29. Kubisch C, Schroeder BC, Friedrich T, Lutjohann B, El-Amraoui A, Marlin S, et al. KCNQ4, a novel potassium channel expressed in sensory outer hair cells, is mutated in dominant deafness. Cell. 1999;96:437–46.

30. Carignano C, Barila EP, Rias EI, Dionisio L, Aztiria E, Spitzmaul G. Inner hair cell and neuron degeneration contribute to hearing loss in a DFNA2-like mouse model. Neuroscience. 2019;410:202–16.
31. Kharkovets T, Dedek K, Maier H, Schweizer M, Khimich D, Nouvian R, et al. Mice with altered KCNQ4 K+ channels implicate sensory outer hair cells in human progressive deafness. EMBO J. 2006;25:642–52.
32. Ruttiger L, Sausbier M, Zimmermann U, Winter H, Braig C, Engel J, et al. Deletion of the Ca2+-activated potassium (BK) alpha-subunit but not the BKbeta1-subunit leads to progressive hearing loss. Proc Natl Acad Sci USA. 2004;101:12922–7.
33. Nouvian R, Ruel J, Wang J, Guitton MJ, Pujol R, Puel J-L. Degeneration of sensory outer hair cells following pharmacological blockade of cochlear KCNQ channels in the adult guinea pig. Eur J Neurosci. 2003;17:2553–62.
34. Wulff H, Castle NA, Pardo LA. Voltage-gated potassium channels as therapeutic targets. Nat Rev Drug Discov. 2009;8:982–1001.
35. Borgini M, Mondal P, Liu R, Wipf P. Chemical modulation of Kv7 potassium channels. RSC Med Chem. 2021;12:483–537.
36. Leitner MG, Feuer A, Ebers O, Schreiber DN, Halaszovich CR, Oliver D. Restoration of ion channel function in deafness-causing KCNQ4 mutants by synthetic channel openers. Br J Pharm. 2012;165:2244–59.
37. Bös M. Cyclic amides as potassium channel openers (EP3484863B1), European Patent Office. 2020.
38. Takeda T, Hosokawa M, Takeshita S, Irino M, Higuchi K, Matsushita T, et al. A new murine model of accelerated senescence. Mech Ageing Dev. 1981;17:183–94.
39. Viberg A, Canlon B. The guide to plotting a cochleogram. Hear Res. 2004;197:1–10.
40. Muller M, von Hunerbein K, Hoidis S, Smolders JW. A physiological place-frequency map of the cochlea in the CBA/J mouse. Hear Res. 2005;202:63–73.
41. Salt AN, Plontke SK. Pharmacokinetic principles in the inner ear: Influence of drug properties on intratympanic applications. Hear Res. 2018;368:28–40.
42. Menardo J, Tang Y, Ladrech S, Lenoir M, Casas F, Michel C, et al. Oxidative stress, inflammation, and autophagic stress as the key mechanisms of premature age-related hearing loss in SAMP8 mouse Cochlea. Antioxid Redox Signal. 2012;16:263–74.
43. Gupta S, Harshvardhan R, Samdani S. To study the association of the size and site of tympanic membrane perforation with the degree of hearing loss. Indian J Otolaryngol Head Neck Surg. 2019;71(Suppl 2):1047–52.
44. Pannu KK, Chadha S, Kumar D, Preeti. Evaluation of hearing loss in tympanic membrane perforation. Indian J Otolaryngol Head Neck Surg. 2011;63:208–13.
45. Liberman MC, Kiang NY. Acoustic trauma in cats. Cochlear pathology and auditory-nerve activity. Acta Otolaryngol Suppl. 1978;358:1–63.
46. Ashmore J, Gale J. The cochlear amplifier. Curr Biol. 2004;14:403–4.
47. Kubisch C, Schroeder BC, El-Amraoui A, Marlin S, Petit C, Jentsch TJ. KCNQ4, a novel potassium channel expressed in sensory outer hair cells, is mutated in dominant deafness. Cell Press. 1999;96:437–46.
48. Burkard R. Calibration of acoustic transients. Brain Res. 2006;1091:27–31.
49. Benkafadar N, Francois F, Affortit C, Casas F, Ceccato JC, Menardo J, et al. ROS-induced activation of DNA damage responses drives senescence-like state in postmitotic cochlear cells: implication for hearing preservation. Mol Neurobiol. 2019;56:5950–69.
50. Fujimoto C, Yamasoba T. Oxidative stresses and mitochondrial dysfunction in age-related hearing loss. Oxid Med Cell Longev. 2014;2014:582849.
51. Nin F, Yoshida T, Sawamura S, Ogata G, Ota T, Higuchi T, et al. The unique electrical properties in an extracellular fluid of the mammalian cochlea; their functional roles, homeostatic processes, and pathological significance. Pflug Arch. 2016;468:1637–49.
52. Yang H, Xiong H, Huang Q, Pang J, Zheng X, Chen L, et al. Compromised potassium recycling in the cochlea contributes to conservation of endocochlear potential in a mouse model of age-related hearing loss. Neurosci Lett. 2013;555:97–101.
53. Miceli F, Soldovieri MV, Martire M, Taglialatela M. Molecular pharmacology and therapeutic potential of neuronal Kv7-modulating drugs. Curr Opin Pharm. 2008;8:65–74.
54. Sheppard AM, Chen GD, Salvi R. Potassium ion channel openers, Maxipost and Retigabine, protect against peripheral salicylate ototoxicity in rats. Hear Res. 2015;327:1–8.
55. Wang Y, Hirose K, Liberman MC. Dynamics of noise-induced cellular injury and repair in the mouse cochlea. J Assoc Res Otolaryngol. 2002;3:248–68.

ACKNOWLEDGEMENTS

We would like to thank Karina Gültig and Andrea Müller for their excellent technical assistance. We would also like to thank Stefan Fink and Lukas Rüttiger for their valuable time and great help with the data analysis. BP was supported by a scholarship for the promotion of young scientists from the Episcopal Foundation 'Cusanuswerk' (Bonn, Germany). Acousia Therapeutics (Tübingen, Germany) provided the compound ACOU085, which is an agonist of the $K_V7.4$ (KCNQ4) channel, in an injectable formulation. This publication is dedicated to the memory of our dear colleagues and friends Marcus Müller and Michael Bös, who both suddenly passed away during the course of the project.

AUTHOR CONTRIBUTIONS

BP, CL, SL, YA, and HL contributed to conceptualization and writing. BP, MM, and YA conducted the experiments and performed data and statistical analyses. JG and M Burnet conducted the LC-MS/MS analysis in the pharmacokinetic study. MT, RR, and JFR conducted the in-vitro pharmacodynamic experiments and performed data analysis. MM, M Bös, YA, and HL contributed to the supervision and interpretation of data. All authors (except MM and M Bös) contributed to the revision, editing, and approved the final version of the manuscript.

FUNDING

Open Access funding enabled and organized by Projekt DEAL.

ETHICAL APPROVAL

Animal care, treatments, and procedures were performed according to the German (TierSchG) and European Union (directive 2010/63/EU) guidelines for the protection of animals used for experimental purposes, following revision and approval by the veterinary care unit of the University of Tübingen and the regional animal care and ethics committee (Regierungspräsidium Tübingen, approval no. HN3/17).

COMPETING INTERESTS

M Bös (deceased) was the former Chief Scientific Officer of Acousia Therapeutics (Tübingen, Germany) and inventor of the composition of matter and use of ACOU085 and related compounds, filed and assigned to Acousia Therapeutics [37]. SL is shareholder and member of the board of directors, and HL is scientific founder, shareholder, and member of the board of directors of Acousia Therapeutics. This study and the salary of BP were in part financed under a master service agreement between the University of Tübingen Medical Center (Universitätsklinikum Tübingen, Tübingen, Germany) and Acousia Therapeutics. All other authors declare that the research was conducted in the absence of any commercial or financial relationships that could be construed as a potential conflict of interest.

ADDITIONAL INFORMATION

Supplementary information The online version contains supplementary material available at https://doi.org/10.1038/s41419-022-04915-5.

Correspondence and requests for materials should be addressed to Barbara Peixoto Pinheiro or Hubert Löwenheim.

Reprints and permission information is available at http://www.nature.com/reprints

Publisher's note Springer Nature remains neutral with regard to jurisdictional claims in published maps and institutional affiliations.